



# Durham E-Theses

---

## *Synthesis, characterisation and properties of novel dendrimers*

Stoddart, Alison

### How to cite:

---

Stoddart, Alison (2002) *Synthesis, characterisation and properties of novel dendrimers*, Durham theses, Durham University. Available at Durham E-Theses Online: <http://etheses.dur.ac.uk/4153/>

### Use policy

---

The full-text may be used and/or reproduced, and given to third parties in any format or medium, without prior permission or charge, for personal research or study, educational, or not-for-profit purposes provided that:

- a full bibliographic reference is made to the original source
- a [link](#) is made to the metadata record in Durham E-Theses
- the full-text is not changed in any way

The full-text must not be sold in any format or medium without the formal permission of the copyright holders.

Please consult the [full Durham E-Theses policy](#) for further details.

# **SYNTHESIS, CHARACTERISATION AND PROPERTIES OF NOVEL DENDRIMERS**

The copyright of this thesis rests with the author.  
No quotation from it should be published without  
his prior written consent and information derived  
from it should be acknowledged.

A thesis submitted for the degree of

**DOCTOR OF PHILOSOPHY**

by

**Alison Stoddart**

Interdisciplinary Research Centre in Polymer Science and Technology  
Department of Chemistry  
University of Durham

September 2002



**25 MAR 2003**

## Abstract

A new family of aliphatic, polyurethane dendritic macromolecules has been designed, synthesised and characterised. The convergent route to dendrimers and the reactions of the selective coupling agent, carbonyl diimidazole (CDI) were employed. The method was successful in the preparation of first, second and third generation dendrimers and dendrons of the first to fourth generations. The structure of the termini of these branched macromolecules was varied to consist of *t*-butyl, benzhydryl, cyclohexyl or 4-heptyl groups. The dendrons were also coupled to a trifunctional aromatic core unit to create another series of dendrimers with an innermost layer of ester functions. The compounds prepared were soluble in most common organic solvents and insoluble in water. The physical state of the materials ranged from sticky oils to hard, amorphous solids depending on the nature of the end groups and the molecular weight of the macromolecules.

The synthesis of the second generation dendrimer with *t*-butyl end groups was adapted to make a series of six codendrimers with differing arrangements of concentric layers of urethane and carbonate functions as well as the polycarbonate analogue. These second generation dendrimers varied in their physical state from oils of low viscosity to hard amorphous solids depending on the proportion of carbonate and urethane functions in the molecule.

The hydrogen bonding interactions in solution of some of the dendritic compounds were investigated by <sup>1</sup>H NMR and Infrared spectroscopy. From the analysis it was concluded that the hydrogen bonding was intramolecular rather than intermolecular in nature and that the degree of hydrogen bonding was dependent on the generation and the terminal groups of the structures. In addition, the degree of hydrogen bonding of the urethane functions was observed to be dependent on the location of the urethane layers in the second generation poly(urethane-carbonate) codendrimers.

The thermal properties of the dendrimers were investigated and the materials observed to have a single glass transition. The glass transition temperatures of the dendritic families with different termini were found to be dependent on the composition of the end group and the molecular weight of the molecule. The glass transition temperatures of the codendrimers were dependent on the proportion of urethane and carbonate links in the structure and also the relative location of the layers. In a preliminary study, it was shown that blends of two different dendrimers were characterised by only one glass transition.

## Contents

<b>Chapter One: Introduction</b>	<b>1</b>
1.1 Overview	1
1.2 Dendrimers	2
1.2.1 Dendritic Macromolecules	2
1.2.2 Synthesis of Dendrimers	3
1.2.3 Some Unique Properties of Dendrimers	7
1.2.3.1 Intrinsic Viscosity	7
1.2.3.2 Solubility	8
1.3 Polyurethane Dendrimers	9
1.3.1 Introduction	9
1.3.2 Linear Polyurethanes	9
1.3.3 Other Urethane Syntheses	10
1.3.3.1 Method 1	10
1.3.3.2 Method 2	11
1.3.4 Polyurethane Dendrimers and Hyperbranched Polymers	11
1.3.5 Conclusions	14
1.4 1,1'-Carbonyl Diimidazole (CDI)	15
1.4.1 Introduction	15
1.4.2 Selective Reactions of CDI and Adducts	16
1.4.2.1 Carbonate Synthesis	16
1.4.2.2 Urethane Synthesis	18
1.4.2.3 Amide Synthesis	19
1.4.2.4 Selective Reactions of Molecules with Mixed Functionality	19
1.4.3 Use of CDI in Polymer Synthesis	20
1.4.3.1 Linear and Hyperbranched Polymers	20
1.4.4 Conclusions	22
1.5 References	23
 <b>Chapter Two: Synthesis and Characterisation of Novel Polyurethane Dendrimers</b>	 <b>25</b>
2.1 Introduction	25
2.2 Description of Polyurethane Dendrimers	26
2.3 Nomenclature of Dendrimers	27
2.3.1 Background	27
2.4 Synthesis and Characterisation of Polyurethane Dendrons	31
2.4.1 First Generation Dendron	31
2.4.2 Branching Unit or AEAP	35
2.4.3 Second Generation Dendron	36

2.4.4	Third Generation Dendron	43
2.4.5	Fourth Generation Dendron	47
2.4.6	Polyurethane Dendrimers	50
2.4.7	Dendrimers with Aromatic-Ester Core Unit	64
2.5	Conclusions	70
2.6	References	71
<b>Chapter Three:</b>	<b>Synthesis and Characterisation of Codendrimers</b>	<b>73</b>
3.1	Introduction	73
3.2	Background	74
3.2.1	Overview of Codendrimers	74
3.2.2	Segment-block Codendrimers	75
3.2.3	Layer-block Codendrimers	76
3.2.4	Surface Codendrimers	76
3.3	Synthesis of Layer Codendrimers	79
3.3.1	Introduction	79
3.3.2	Structure of Second Generation Codendrimers	79
3.3.3	Synthesis of Dendrons	81
3.3.4	Synthesis of Codendrimers and a Polycarbonate Dendrimer	84
3.4	Characterisation of Codendrons and Codendrimers	87
3.4.1	<sup>13</sup> C NMR Spectroscopy	87
3.4.2	<sup>1</sup> H NMR Spectroscopy	89
3.4.3	Gel Permeation Chromatography	94
3.4.4	Mass Spectrometry	95
3.5	Conclusions	96
3.6	References	96
<b>Chapter Four:</b>	<b>Thermal Properties of Dendritic Systems</b>	<b>98</b>
4.1	Introduction	98
4.2	The Glass Transition Temperature	99
4.2.1	Background	99
4.2.2	Factors that affect the T <sub>g</sub> of a Linear Polymer	99
4.3	The Glass Transition Temperature of Dendrimers and Hyperbranched Polymers	102
4.3.1	Relationship between T <sub>g</sub> and Molecular Weight	103
4.3.2	Derivation of Equations for Dendritic System	104
4.3.3	Application of Derived Equations	105
4.3.4	Dendritic Macromolecules with Different Terminal Groups	108
4.3.5	Dendrimers with Different Branching Units	109
4.3.6	Codendrimers	109

4.4	Thermal Properties of Polyurethane Dendrons and Dendrimers	111
4.4.1	Experimental Measurement of $T_g$	111
4.4.2	Effect of Molecular Weight and End Group on the $T_g$ of the Polyurethane Dendrons	112
4.4.3	Determination of $T_{g\infty}$ for Polyurethane Dendrons	113
4.4.4	Determination of $T_{g\infty}$ for Polyurethane Dendrimers	115
4.4.5	Comparison of Dendrons and Dendrimers	116
4.4.6	Dendrimers and Aromatic-ester Core	117
4.4.7	Layer Codendrimers	118
4.4.8	$T_g$ of Dendrimer Blends	125
4.5	Conclusions	126
4.6	References	127
	<b>Chapter Five: Experimental</b>	<b>128</b>
5.1	General Information	128
5.1.1	Chemicals	128
5.1.2	Characterisation	128
5.2	Procedures for the Synthesis of the First to Fourth Generation Polyurethane Dendrons	130
5.3	Procedures for the Synthesis of the Second Generation Dendrons	137
5.4	Procedures for the Synthesis of Third and Fourth Generation Dendrons	141
5.5	General Procedure for the Synthesis of First Generation Dendrimers with Amine core units	143
5.6	General Procedure for the Synthesis of First and Second Generation Dendrimers with Aromatic-ester core units	145
5.7	General Procedure for the Synthesis of Second Generation Dendrimers with Amine core units	148
5.7.1	Polyurethane Homodendrimers	148
5.7.2	Layer Codendrimers and Polycarbonate Homodendrimer	149
5.8	General Procedure for the Synthesis of Third Generation Dendrimers with Amine core unit	153
5.9	General Procedure for the Synthesis of Third Generation Dendrimers with Aromatic-ester core unit	154
5.10	Reference	154
	<b>Appendix</b>	<b>155</b>

### **Declaration**

The work reported in this PhD thesis has been carried out at the Interdisciplinary Research Centre in Polymer Science and Technology, Department of Chemistry, University of Durham from October 1999 to September 2002. This work has not been previously submitted for a degree at the University of Durham or elsewhere and, unless stated otherwise, is the original work of the author

### **Statement of Copyright**

The copyright of this thesis rests with the author. No quotation from it should be published without prior written consent and information derived from it should be acknowledged.

## Acknowledgements

The first words of thanks go to Jim for his encouragement, guidance and kindness over the course of my PhD and for giving me the opportunity to carry out this research. I would also like to thank Steve, for his continuous creative insight into the project as well as his much appreciated enthusiasm.

Within the Department of Chemistry at Durham there are many colleagues it is a pleasure to thank for their advice and expertise in various spectroscopic and analytical techniques. Firstly, my thanks go to all the members of the first class NMR team of Alan, Catherine and Ian; the welcoming environment they have offered and their efficiency is greatly appreciated. For mass spectrometry data, I would like to thank Mike and Lara, who have shown great perseverance with the electrospray method in particular. For MALDI-TOF (Voyager) mass spectrometry data and for his insight in to the world of dendritic molecules I am extremely grateful to Dave. For running a friendly and efficient elemental analysis service I would like to thank Jaroslava. Last but not least, I would like to thank Doug for running all the TGA, DSC and GPC and consequently for his patience (!) and for providing entertainment.

Over the last three years there are many people I would like to thank for their help and friendship. First and foremost, I would like to thank all the members of the IRC, both past and present, for generating a fun and stimulating working environment. In particular, I am indebted to Stuart for his assistance with all computing matters in recent months. For their special friendships and senses of humour I would like to thank Lorna, Ian and Steph. Also, others outside the PhD sphere who I would like to mention are Jenny and Graham.

Finally, I would like to thank Fiona, for allowing me a share of the chemistry gene (!), her empathy throughout the last months and for being a great, favourite sister. I am also very grateful to Quentin for his advice about the world of chemistry and for all the other help he has offered. To my Mum and Dad, I would like to say thank you for giving me the best opportunities and for being inspirations to me.



## Abbreviations

AcOH	glacial acetic acid
AEAP	1-[N,N-bis(2-aminoethyl)amino]-2-propanol
approx.	approximate or approximately
br	broad
BOC	<i>t</i> -butoxycarbonyl
CDCl <sub>3</sub>	deuterated chloroform
CDI	1,1' Carbonyl diimidazole
CD <sub>3</sub> OD	deuterated methanol
(CD <sub>3</sub> ) <sub>2</sub> SO	deuterated dimethylsulfoxide
<i>cf.</i>	compare
CH <sub>2</sub> Cl <sub>2</sub>	dichloromethane
d	doublet
dd	doublet of doublets
δ	chemical shift
Da	Daltons
DCC	dicyclohexylcarbodiimide
DMAP	4-dimethylaminopyridine
DPPA	diphenylphosphoryl azide
DPTS	dimethylaminopyridinium toluene- <i>p</i> -sulfonate
DSC	differential scanning calorimetry
<i>e.g.</i>	for example
ES	electrospray
EtOAc	ethyl acetate
g	gram
G	generation
GC, CI	gas chromatography, chemical ionisation (MS data)
GC, EI	gas chromatography, electron ionisation (MS data)
GPC	gel permeation chromatography
HEAP	1-[N,N-bis(2-hydroxyethyl)amino]-2-propanol
hrs	hours
Hz	Hertz

<i>i.e.</i>	that is
IR	infrared
J	coupling constant
KOH	potassium hydroxide
L	litre
NMR	nuclear magnetic resonance
m	multiplet
M	molar
MALDI-TOF	matrix-assisted laser-desorption ionisation – time of flight
MeOH	methanol
mg	milligram
mL	millilitre
mM	millimolar
MS	mass spectrometry
$M_w$	molecular weight
$m/z$	mass to charge ratio
PAMAM	polyamidoamine
Pd	polydispersity
PPI	poly(propyleneimine)
ppm	parts per million
q	quartet
qn	quintet
$r$	correlation coefficient
s	singlet
t	triplet
TAEA	tris(2-aminoethyl)amine
TEA	triethanolamine
$T_g$	glass transition temperature
TGA	thermogravimetric analysis
$T_m$	melting temperature

# Chapter 1

## Introduction

### 1.1 Overview

This introductory chapter will begin with a description of the branched structure of dendrimers and an explanation of the established routes for their synthesis. An investigation into examples of polyurethane dendritic macromolecules in the literature will follow with a particular focus on the possible reasons for the relatively slow development of research into such structures. In the final section, the selectivity of reactions involving 1,1'-carbonyl diimidazole (CDI), a coupling agent capable of introducing urethane functions, will be outlined together with examples of the use of CDI in dendritic synthesis to date.

It is intended that these sections will contain sufficient information to provide a background to the synthetic project outlined in this thesis; however, the area of dendrimer science is highly developed and several excellent and comprehensive reviews are recommended to the reader on the general topic of dendrimers.<sup>1-4</sup>

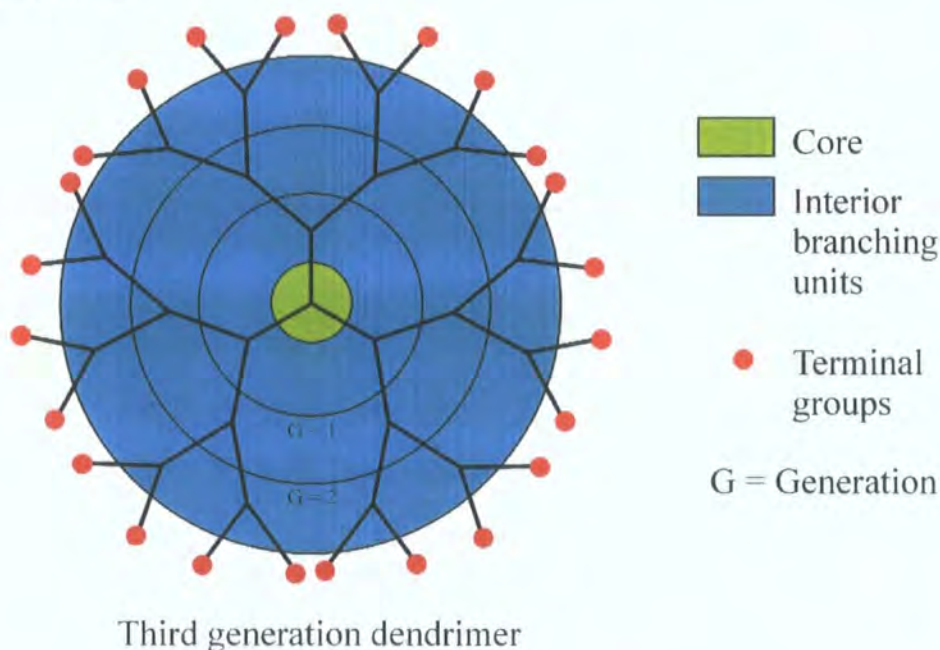


## 1.2 Dendrimers

### 1.2.1 Dendritic Macromolecules

The evolution of synthetic dendritic polymers has resulted in the formation of two classes of branched macromolecules, namely dendrimers and hyperbranched polymers.<sup>2</sup> Dendrimers are usually defined as *perfectly* branched, monodisperse macromolecules and have also been termed arborols, starburst<sup>TM</sup> or cascade polymers.<sup>4</sup> The other class, hyperbranched polymers, are *irregularly* branched structures that have varying degrees of branching and are polydisperse in size and structure.<sup>5</sup> The syntheses to form these structures differ in their approach but both involve the use of  $AB_x$  monomers, where  $x$  is greater than or equal to two. Dendrimers are typically synthesised by a stepwise, repetitive sequence of a few reactions, often coupled with purification procedures, whereas their irregularly branched counterparts are prepared by a one-step polymerisation of an  $AB_x$  monomer. The more complicated synthetic route required for dendrimers compared with their hyperbranched analogues is rewarded as the former macromolecules often exhibit unique properties and can be created with predetermined, specific structures.<sup>6-8</sup>

A dendrimer can be considered as comprising of three distinct regions – the core, the interior branching units and the terminal or end groups – and these are depicted in the two-dimensional schematic of *Figure 1.1*. The number of layers within a dendrimer is commonly described as the generation ( $G$ ) of the structure; for example, the dendrimer in *Figure 1.1* is of the third generation.



*Figure 1.1 Schematic of a dendrimer*

### 1.2.2 Synthesis of Dendrimers

Dendrimers are usually synthesised using a repetitive sequence of two reactions, which comprise the addition of the monomer, corresponding to a structural increase of one generation, and another step involving the deprotection/activation of a function or functions. In turn, the activation of the group(s) enables repetition of the two reactions resulting in the synthesis of dendritic molecules of the next generation.

Two main synthetic strategies have been extensively employed in the synthesis of dendrimers over the past three decades. These methods differ in the direction in which the molecules are constructed and are termed accordingly as either the divergent route or the convergent route.<sup>1,2</sup> The *divergent route* builds up the dendrimer, layer by layer, starting from a multifunctional core molecule diverging out towards the periphery (Figure 1.2). In the first step, an  $AB_x$  monomer ( $x = 2$  in this case) containing protected B groups ( $B_p$ ) reacts with a trifunctional core to yield a first generation dendrimer with an unreactive periphery. Branch points may also be introduced by multiple reactions at the appropriate sites of the core molecule (see Figure 1.3, overleaf). In the second step, deprotection or activation of these end groups forms a first generation dendrimer that is able to add the next layer. Repetition of these two steps results in the preparation of a second generation dendrimer with activated end groups.

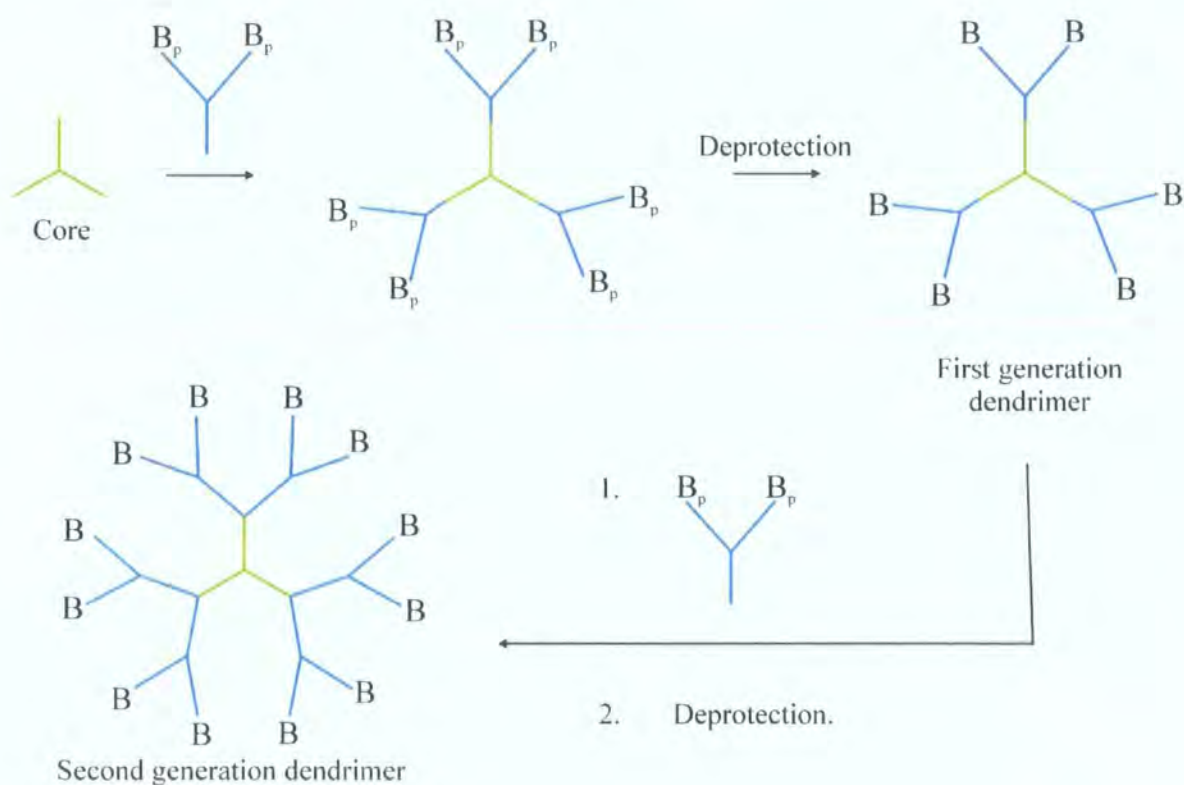


Figure 1.2 Schematic of the divergent route



The earliest example in the literature of the repetitive concept of dendrimer synthesis was reported by Vögtle *et al.* and was achieved using the divergent route (Figure 1.3).<sup>9</sup> The first reaction in the procedure, resulting in the introduction of a branch point, was effected by the Michael addition of a primary amine function to acrylonitrile. The next stage activated the terminal groups towards further reaction by reduction of the nitrile groups to primary amine functions. The repetition of this sequence of reactions yielded a structure of the second generation, however, the development of the series was hindered because of problems encountered during the reduction steps. Since this literature report, the problems with the reduction have been solved by other researchers within the field of dendrimer chemistry and structures, termed poly(propylene imine) (PPI) dendrimers, are now commercially available up to the fifth generation having 64 amine end groups (for the structure of second generation PPI dendrimer, see page 28).<sup>10-12</sup> Another well-known series of dendrimers, which are commercially available and synthesised divergently, are the polyamidoamine dendrimers (PAMAMs).<sup>13</sup>

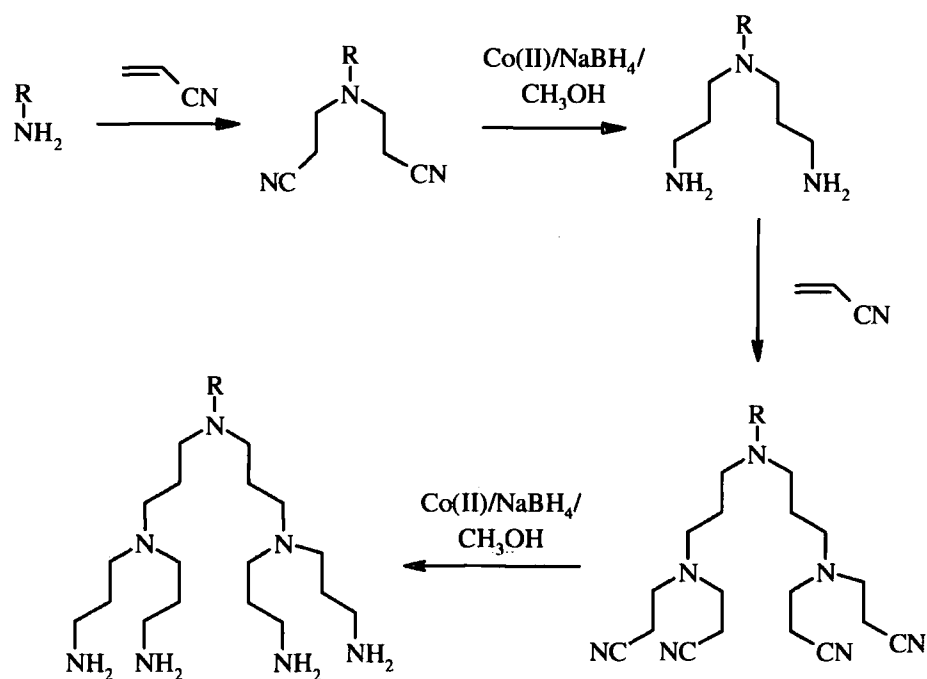
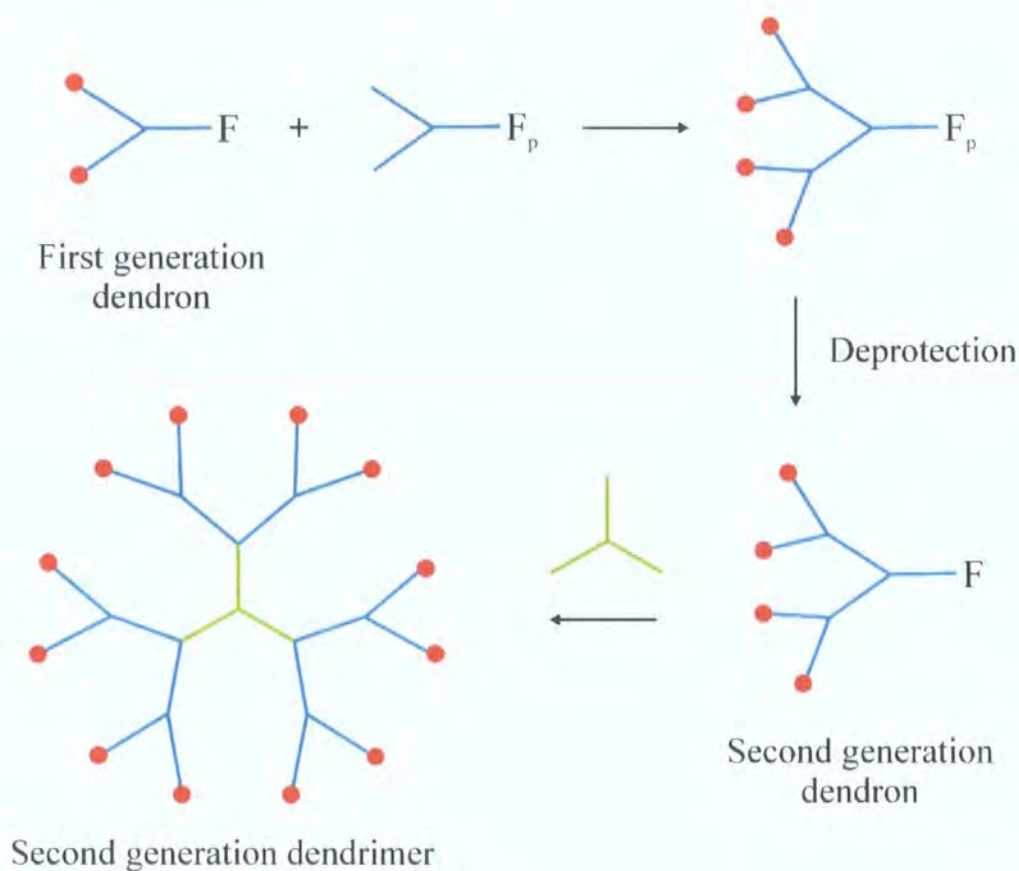


Figure 1.3 First repetitive, divergent synthesis of a dendritic molecule<sup>9</sup>

The employment of the divergent route has enabled dendrimers of high generations to be prepared, for example, the synthesis of the PAMAM series has reportedly been successful up to the tenth generation dendrimer; the ideal structure of which contains 3072 terminal groups.<sup>14</sup> However, the number of reactions required to occur on each molecule increases exponentially for successive generations in the divergent route and, as a consequence, at high

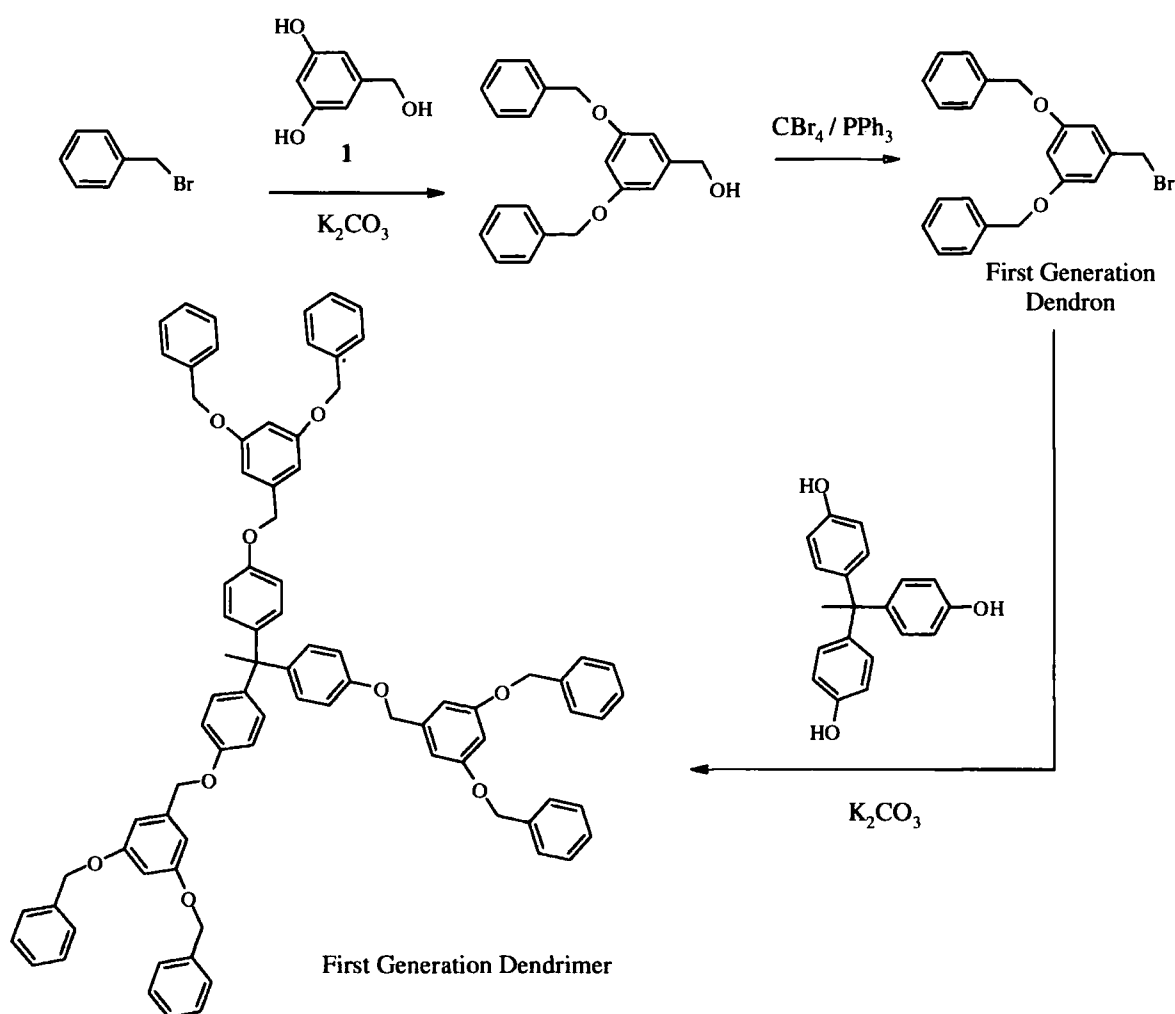
generations the incomplete formation of the branches is a problem. These imperfect macromolecules and other impurities resulting from side reactions are, in general, impossible to remove because of their similarity to the desired perfectly branched dendrimer. Therefore, dendrimers of high generations are likely to contain defects and have some degree of polydispersity.

In contrast to the previous method, the *convergent* route to dendrimer synthesis assembles the macromolecule by starting at the periphery of the structure and moving inwards to the core. This is achieved by the construction of dendrons or dendritic wedges, which can be coupled to a multifunctional core molecule to produce dendrimers of differing generations. The convergent procedure is outlined schematically for the synthesis of a second generation dendrimer in *Figure 1.4*. The apex of a dendron is often referred to as the ‘focal point’ and the function at this position can be either protected ( $F_p$ ) or reactive ( $F$ ) depending on the stage in the procedure. The first step in the scheme represents the addition of the branched monomer, which contains a protected focal point ( $F_p$ ) to the first generation dendron with a reactive focal point ( $F$ ). This yields a second generation structure with a protected focal point and after deprotection, the dendron can be coupled to a multifunctional core to produce a second generation dendrimer.



*Figure 1.4 Schematic of the convergent route*

The convergent method was first introduced by Hawker and Fréchet who reported a series of poly(benzyl ether) dendrimers, the synthesis of the first generation is outlined in *Figure 1.5*.<sup>15,16</sup> The molecule 3,5-dihydroxybenzyl alcohol **1** was used as an AB<sub>2</sub> monomer in the assembly of the dendrons. The first step was a Williamson ether synthesis of benzyl bromide reacting with the phenolic hydroxyl groups. The primary alcohol function at the focal point of the branched molecule was then activated by conversion to a benzyl bromide function. These two steps were repeated to prepare higher generation dendrons (up to G = 6), or as shown in *Figure 1.5*, coupled to multifunctional core molecule to yield the first generation dendrimer.



*Figure 1.5* Synthesis of a first generation poly(benzyl ether) dendrimer

A similar series of poly(benzyl ester) dendrimers were also synthesised using the convergent route and the isolation of dendrimers of both series up to the fifth generation has been achieved.<sup>7</sup> The major drawback of this method has been the difficulty in synthesising higher generation structures, which has been attributed to the steric demands involved in



coupling two (or more) large molecules to functions in close proximity on the same branching unit or core. However, the small number of reactions required for each generational increase and the ability to remove any impurities by chromatographic techniques has enabled the isolation of dendrimers, which are more precisely monodisperse than those isolated via the divergent route. In addition, the convergent method has offered a high degree of control over the structure and precise location of functions within the dendrimer<sup>7,8</sup> – a theme which is investigated in Chapter 3 of this thesis.

Modifications of the convergent route and its combination with the divergent route have resulted in dendrimers being synthesised using methods that reduce the number of steps required for high generation structures.<sup>17-20</sup> These have been termed ‘accelerated syntheses’ and include the branched monomer approach<sup>18</sup>, in which an AB<sub>4</sub> monomer rather than an AB<sub>2</sub> monomer is used and an orthogonal approach.<sup>19</sup> This latter method incorporates two different monomer units with two pairs of complimentary coupling units; however, each pair must react under conditions in which the other functional groups are inert. As a consequence the need for the deprotection or activation step is circumvented, hence greatly reducing the number of steps to yield high generations.

### 1.2.3 Some Unique Properties of Dendrimers

#### 1.2.3.1 Intrinsic Viscosity

Intrinsic viscosity is the solution viscosity at infinite dilution<sup>21</sup> and, as a consequence, is proportional to the volume of the polymer divided by its mass. It is well established that for linear polymers the intrinsic viscosity increases with molecular weight, as indicated on the schematic graph in *Figure 1.6*. However, for several series of dendrimers it has been observed that a generation is reached at which the intrinsic viscosity begins to decrease with increasing molecular weight (*Figure 1.6*).<sup>6</sup> This may be explained by considering how the volume and mass change as the generation number of the dendrimer, which is assumed to adopt a spherical conformation, increases. The volume of the dendrimer is proportional to the cube of its radius and grows with each additional generation whereas the mass doubles for each generational increase. Therefore, at high generations the mass term dominates which results in a decrease in the intrinsic viscosity. In the study of the poly(benzyl ether) dendrimer series (*Figure 1.5*) the maximum in the graph was coincident with the third generation and the dendrimer of the next generation was observed to have a lower intrinsic viscosity.<sup>6</sup>

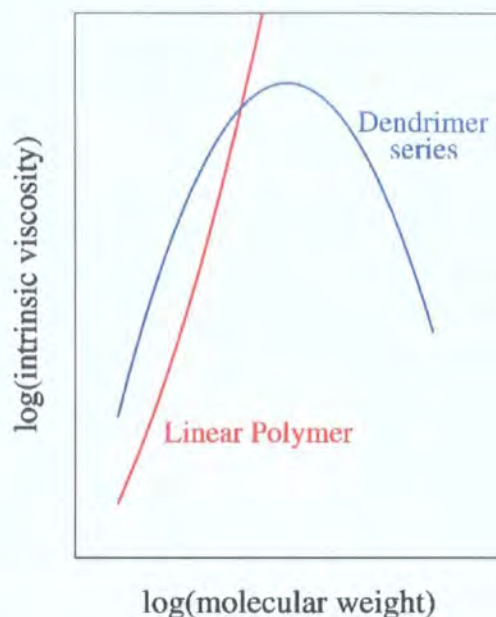


Figure 1.6 Schematic graph of log (intrinsic viscosity) versus molecular weight<sup>1</sup>

### 1.2.3.2 Solubility

In a study of polyester branched and linear macromolecules with comparable structures, the solubility of a dendrimer ( $1.05 \text{ g mol}^{-1}$ ) was found to be significantly greater than for its linear analogue ( $0.05 \text{ g mol}^{-1}$ ) in tetrahydrofuran (Figure 1.7).<sup>22</sup> A hyperbranched polymer constructed using the same aromatic building block also had an enhanced solubility ( $0.70 \text{ g mol}^{-1}$ ) compared with the linear polyester but was less soluble than the dendrimer. The highly branched and spherical topology of a dendrimer and the large number of chain ends per molecule were believed to be the factors that caused this difference in solubility.

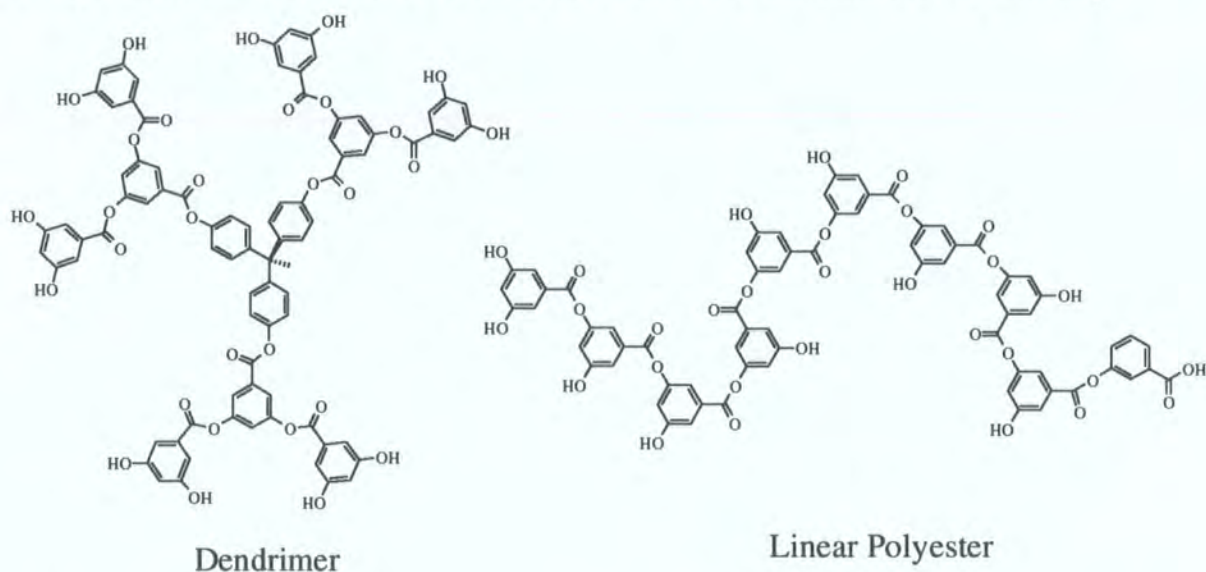


Figure 1.7 Representative structures of the dendrimers and linear polymers for which solubilities have been compared

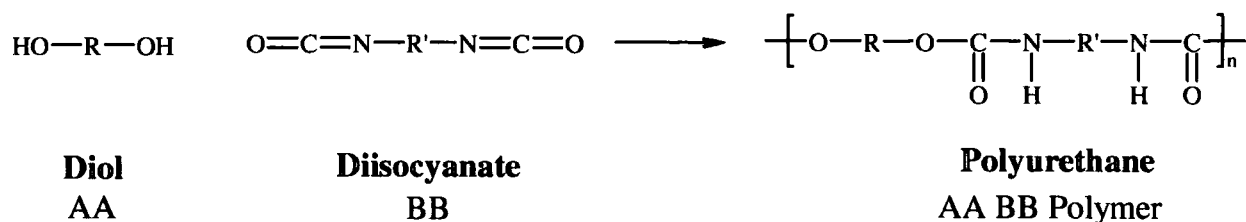
## 1.3 Polyurethane Dendrimers

### 1.3.1 Introduction

There are few accounts of polyurethane dendrimers<sup>23-26</sup> and hyperbranched polymers<sup>27</sup> in the literature whereas the synthesis, properties and potential application of dendritic structures incorporating other functional groups, for example amide<sup>13</sup> and ester<sup>7</sup>, are widely reported. Problems involved in the synthesis and storage of an AB<sub>x</sub> monomer from which polyurethane dendritic macromolecules can be prepared have been the main factors hindering their development. In general, AB<sub>x</sub> monomers for other dendritic systems have been adapted from the chemistry used in the synthesis of an appropriate linear polymer, *i.e.* from an AB monomer, or using knowledge of small molecule coupling reactions. However, urethane-linked structures are more challenging because formation of the functional group is limited to a few known routes which have proved difficult to adapt to the synthesis of dendrimers. In the following sections some of the existing methods for preparing urethane-links in a linear polymer and in small molecule syntheses are outlined. Subsequently, the modification of a few procedures to create dendrimers and hyperbranched polymers that include urethane functions will be summarised.

### 1.3.2 Linear Polyurethanes

The most common synthesis of linear polyurethanes uses the coupling of isocyanate and alcohol functions.<sup>28</sup> The reactive nature of the isocyanate group makes it difficult to synthesise and isolate an AB monomer with both isocyanate and alcohol functions on the same molecule. Therefore, the AA and BB monomer approach, which involves the polymerisation of two different monomers, generally is used to synthesise linear polyurethanes. The two types of monomers involved are a diol and a diisocyanate and step-growth polymerisation occurs without the loss of a small molecule (*Figure 1.8*).



*Figure 1.8 Synthesis of linear polyurethane using AA and BB monomers*

Despite its inherent difficulty, several research groups have reported examples of AB type polymerisation, using a monomer containing an isocyanate and an alcohol function on the same molecule.<sup>29,32</sup> Usually the highly reactive monomer was not isolated before polymerisation, an exception being the synthesis developed by Thiem *et al.*<sup>31</sup> The majority of these methods were complex and inappropriate for use in branched dendritic systems. However, a procedure recently developed by Meijer *et al.*, using an *in situ* polymerisation of an AB monomer, was subsequently modified for use in dendrimer synthesis.<sup>26,32</sup> This method involved the conversion of an asymmetric molecule **2**, with alcohol and amine functions at opposite ends, to the isocyanato alcohol **4** using the selective reagent di-*tert*-butyltricarboxylate **3** (Figure 1.9). Polymerisation of the AB monomer **4** was achieved *in situ* under catalytic conditions and gave polyurethane **5**, subsequent to removal of cyclic impurities by filtration. An advantage of this route is the absence of phosgene in the preparation of the isocyanate group.

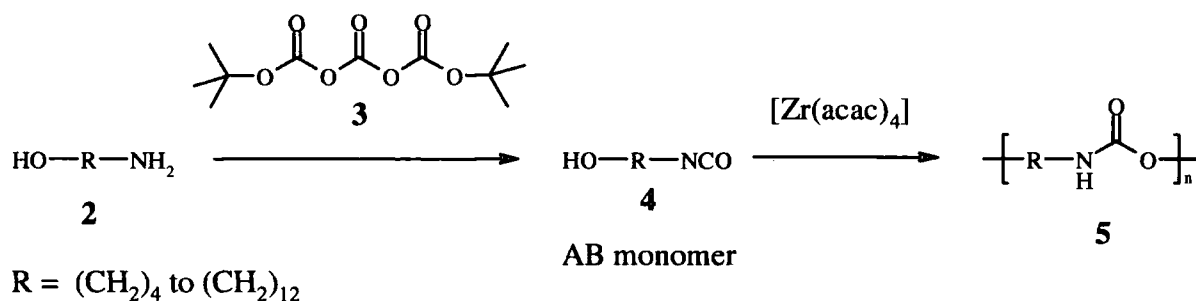


Figure 1.9 Synthesis of linear polyurethane using an AB monomer

### 1.3.3 Other Urethane Syntheses

#### 1.3.3.1 Method 1

In small molecule chemistry McGhee *et al.* have demonstrated the preparation of a urethane function via a procedure excluding the use of isocyanates.<sup>33,34</sup> Reaction of a secondary amine with carbon dioxide, in the presence of a strong organic base, generates a urethane anion **6** which reacts with an alkyl chloride or alkyl sulfonate to give a urethane group (Figure 1.10).

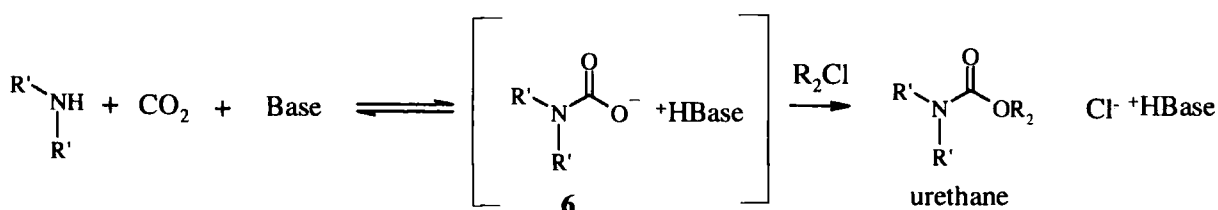
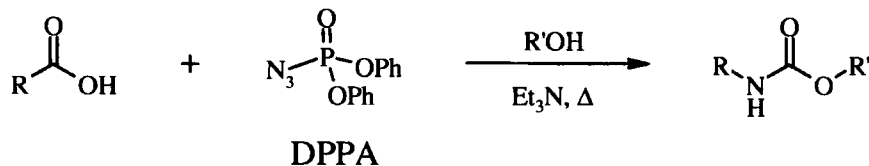


Figure 1.10 Synthesis of a urethane group developed by McGhee *et al.*

### 1.3.3.2 Method 2

Urethane synthesis is also possible via a procedure known as the Curtius reaction.<sup>35</sup> The Curtius reaction was modified by Yamada *et al.* resulting in the preparation of a urethane group from a carboxylic acid, diphenylphosphoryl azide (DPPA) and an alcohol (*Figure 1.11*).



*Figure 1.11 Urethane synthesis via modified Curtius reaction*

### 1.3.4 Polyurethane Dendrimers and Hyperbranched Polymers

#### *Example 1*

Spindler and Fréchet were the first to report the synthesis of a polyurethane dendritic structure.<sup>27</sup> The procedure involved the generation of a monomer containing two isocyanate functions and an alcohol function **8**, which was polymerised *in situ* to give the aromatic hyperbranched polyurethane **9** (*Figure 1.12*, overleaf). The activated AB<sub>2</sub> monomer **8** was formed from the thermal deprotection of the precursor compound **7**, in which the two isocyanate functions were 'blocked'. At high concentrations the increasing occurrence of unwanted side reactions resulted in crosslinking of the polymer whereas at lower concentrations this was not a problem and molecular weights in excess of 30 000 Da were achieved.

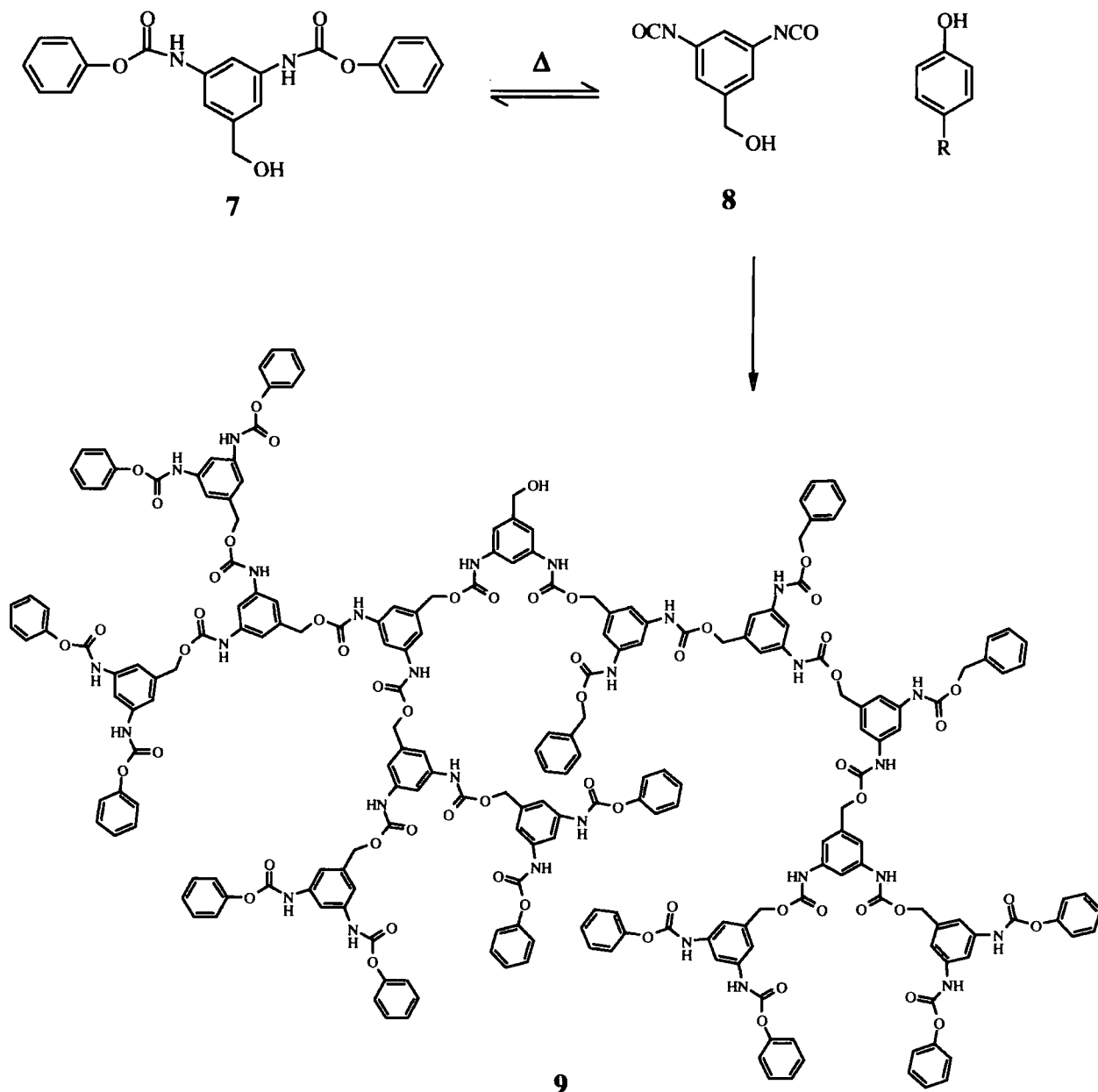
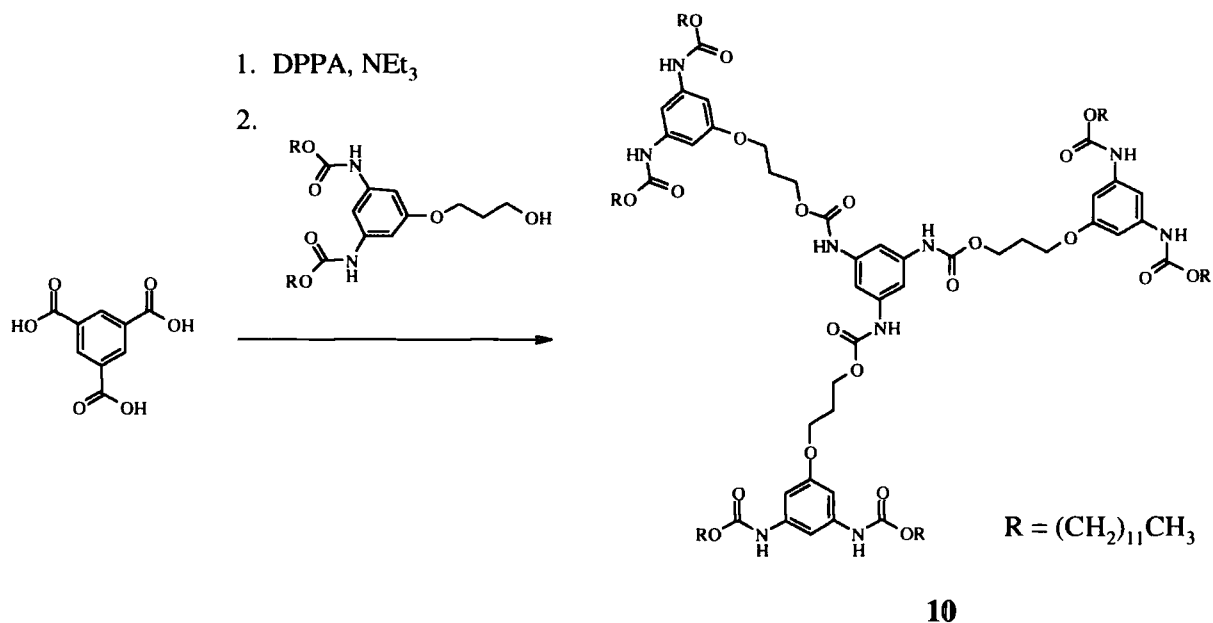


Figure 1.12 Synthesis of hyperbranched polyurethane using a protected AB<sub>2</sub> monomer

### Example 2

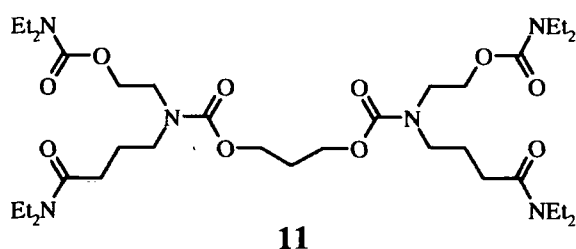
The most successful synthesis of a polyurethane dendrimer was achieved by R. T. Taylor and Puapaboon.<sup>23,24</sup> Modification of the Curtius reaction outlined above in **Method 2** (page 11) was used to prepare a series of macromolecules and the synthesis of the first generation dendrimer **10** is shown overleaf (*Figure 1.13*). The structures contain urethane links at each layer, aromatic branching groups and aliphatic spacer and end groups. The molecular weight of the largest dendritic structure obtained was 9588 Da.



*Figure 1.13 First generation polyurethane dendrimer synthesised by R. T. Taylor and Puapaboorn*

### Example 3

A first generation aliphatic urethane dendrimer **11** has been synthesised by modification of **Method 1** (*Figure 1.14*).<sup>25</sup> This is the only route, known to the author, for synthesising a dendrimer series containing urethane groups in each layer and with an entirely aliphatic composition.



*Figure 1.14 First generation aliphatic dendrimer*

### Example 4

Meijer *et al.* adapted the procedure described above for the linear polyurethane (page 10) and were successful in synthesising high generation aliphatic dendrimers containing alternating urethane and urea layers (*Figure 1.15*).<sup>26</sup> The two isocyanate functions of branching unit **12** are attached to a primary or secondary carbon centre of which only the former will react with an alcohol function, resulting in a urethane link. The isocyanate

function connected to the secondary carbon centre subsequently reacts with an amine to produce a urea link and with repetition of these steps the dendrimer is constructed divergently.

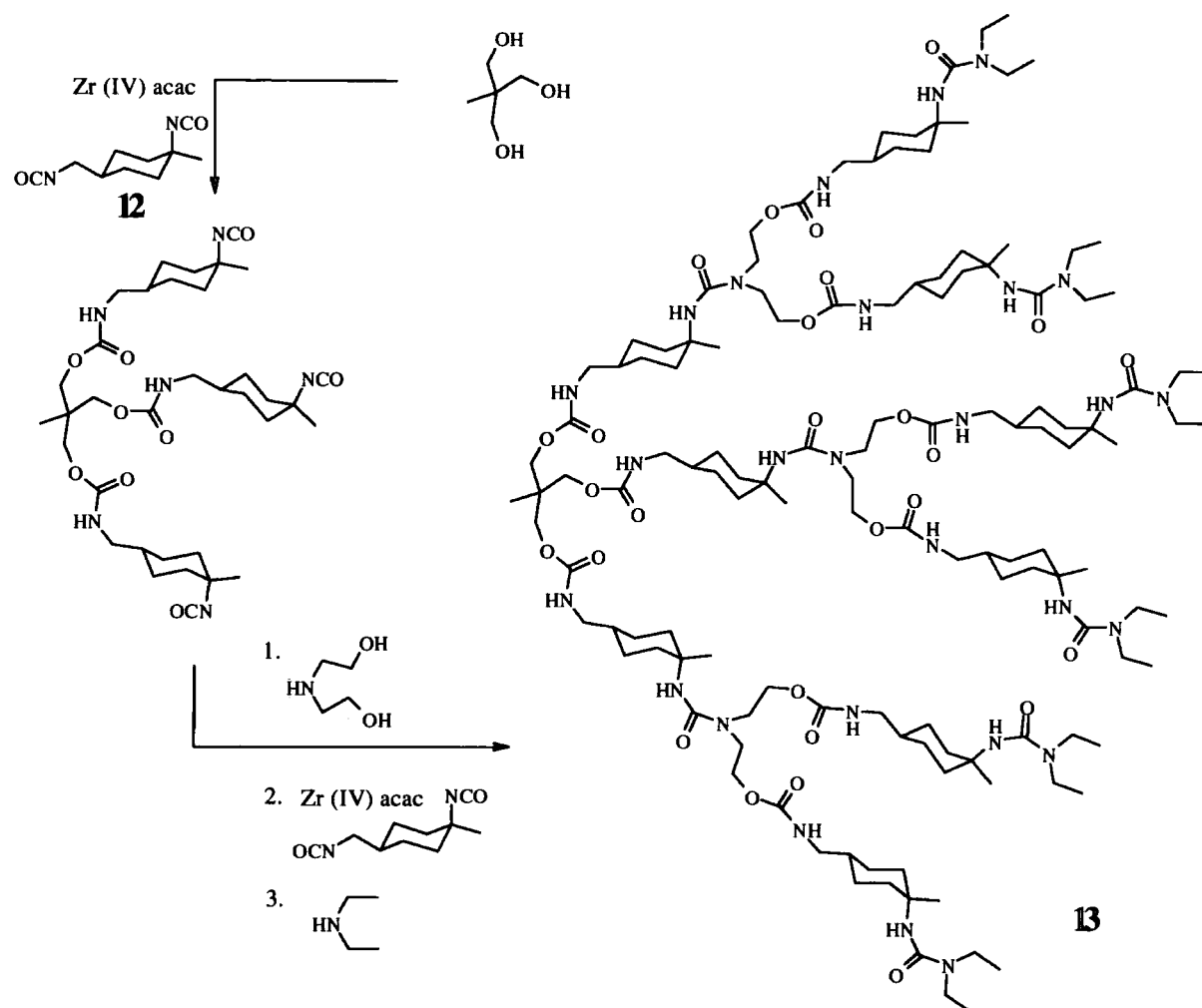


Figure 1.15 Synthesis of second generation poly(urethane-urea) dendrimer

### 1.3.5 Conclusions

The problems associated with the synthesis of an AB<sub>x</sub> monomer and the limited number of literature precedents for polyurethane dendritic structures demonstrate the need for new procedures to be developed to establish this area of polymer chemistry. The existing methods, which often include synthetically challenging procedures using highly reactive and toxic reagents, have been difficult to apply to the preparation of dendrimers and the only example of high generation polyurethane homodendrimers was achieved by R. T. Taylor and Puapaboon.<sup>23,24</sup> However, the work of Rannard and Davis using the coupling agent 1,1'-Carbonyl Diimidazole (CDI), is an attractive method for the selective introduction of a urethane group into a dendritic structure. The chemistry of this molecule is the next topic of this introduction.



## 1.4 1,1'-Carbonyl Diimidazole (CDI)

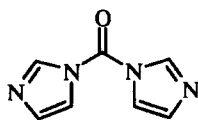


Figure 1.16 CDI

### 1.4.1 Introduction

In 1962, Staab reported the chemistry of CDI in a review outlining the role of heterocyclic amides in synthesis.<sup>36</sup> Since then the principal use of the molecule has been as a coupling agent in the formation of peptides and in small molecule synthesis.<sup>37</sup> As a reagent CDI was shown to have practical advantages compared to its considerably more toxic analogue, phosgene. For example, CDI is a white crystalline solid and phosgene is a gas, so the former can be handled more conveniently. Also, the by-product of CDI reactions is imidazole, a crystalline solid, which can be easily removed by filtration and/or aqueous work-up, compared to the generation of toxic hydrogen chloride gas in equivalent phosgene experiments.

The versatility of CDI is demonstrated by its ability to react with a combination of various acids, alcohols and amines in a two-stage reaction to create five different functional groups (*Figure 1.17*).

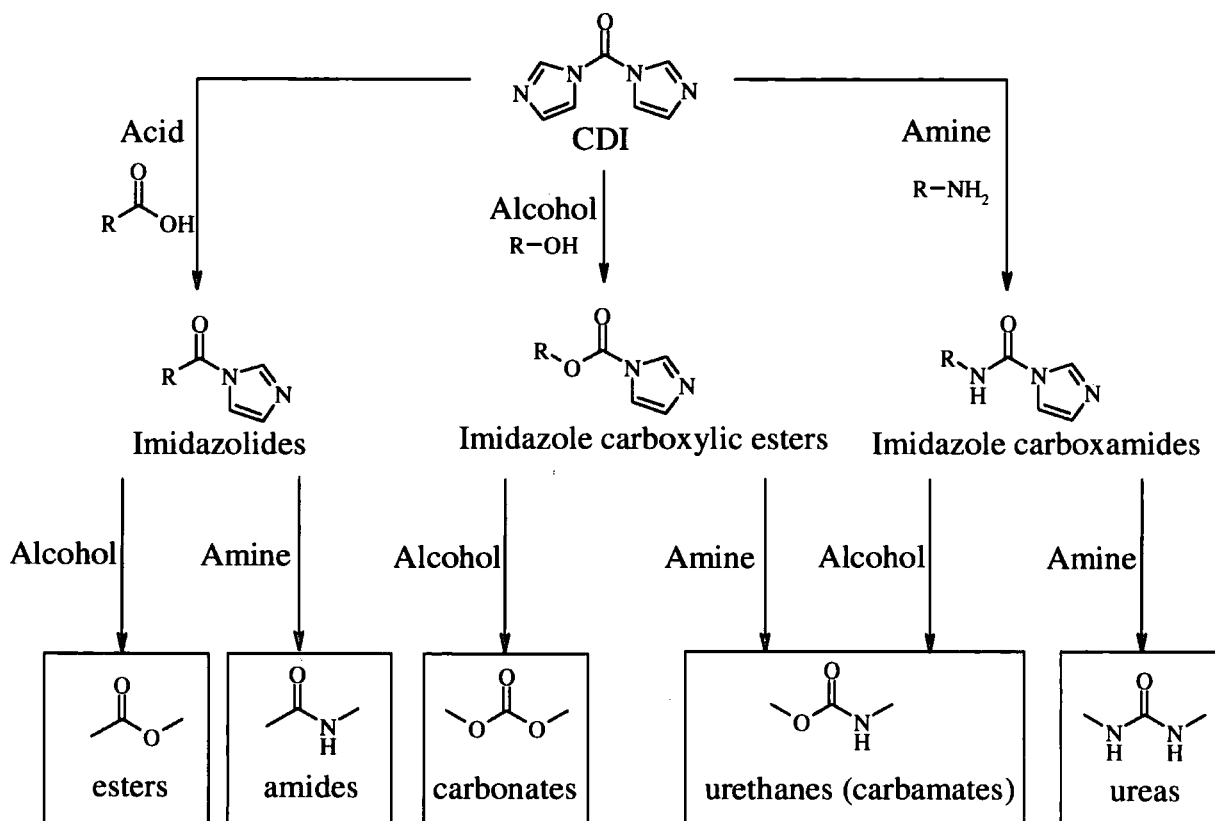


Figure 1.17 The potential reactions of CDI with acids, alcohols and amines.

Imidazolides, imidazole carboxylic esters and imidazole carboxamides are the monosubstituted intermediates, formed after the first stage of the reaction, in which only one of the imidazoles of CDI has been replaced. In this thesis, these intermediates will often be referred to as 'CDI adducts' or 'adducts'. Staab, using the term 'two-in-one reactions', recognised it was unnecessary to separate these intermediates from the imidazole produced and used them *in situ* but did not report any evidence of these intermediates reacting selectively with alcohols and amines.<sup>36</sup> However, recent investigations have shown that the success of the second reaction in the formation of the desired functional group (ester, amide etc.) is dependent on whether the acids, alcohols or amines used in both stages are of a primary (1°), secondary (2°) or tertiary (3°) nature.<sup>38-41</sup>

#### 1.4.2 Selective Reactions of CDI and Adducts

The ability of CDI to control the structure of a final product was described first by Rannard and Davis in the synthesis of polycarbonate and polyamide dendrons.<sup>38</sup> The regioselectivity of the reactions was also noted by Bertolini *et al.* and used to synthesise asymmetric carbonates.<sup>42</sup> An account of model reactions by Rannard and Davis, which demonstrated the selective formation of carbonates, amide and urethane groups, appeared subsequently.<sup>40,41</sup>

##### 1.4.2.1 Carbonate Synthesis

The 'selection rules' for the carbonate case are presented below and illustrated overleaf in *Figure 1.18*.

- Under certain reaction conditions a primary alcohol undergoes a disubstitution reaction with CDI, resulting in the formation of a symmetrical carbonate **17**. However, if an excess of CDI is used, at room temperature and no base is present, the intermediate adduct **14** rather than the symmetrical carbonate **17** is isolated in a yield of 94%.
- Secondary and tertiary alcohols react with CDI in a 1:1 ratio to give the corresponding adducts, **15** and **16** respectively. Even if the alcohols are used as the reaction solvent, no second addition is observed.
- Adducts of primary, secondary and tertiary alcohols, **14**, **15** and **16**, react selectively with primary alcohols, under base catalysis and at a reaction temperature of 60°C, to give **17**, **18**, and **19** respectively.
- No reaction is observed between all three adducts and secondary and tertiary alcohols.

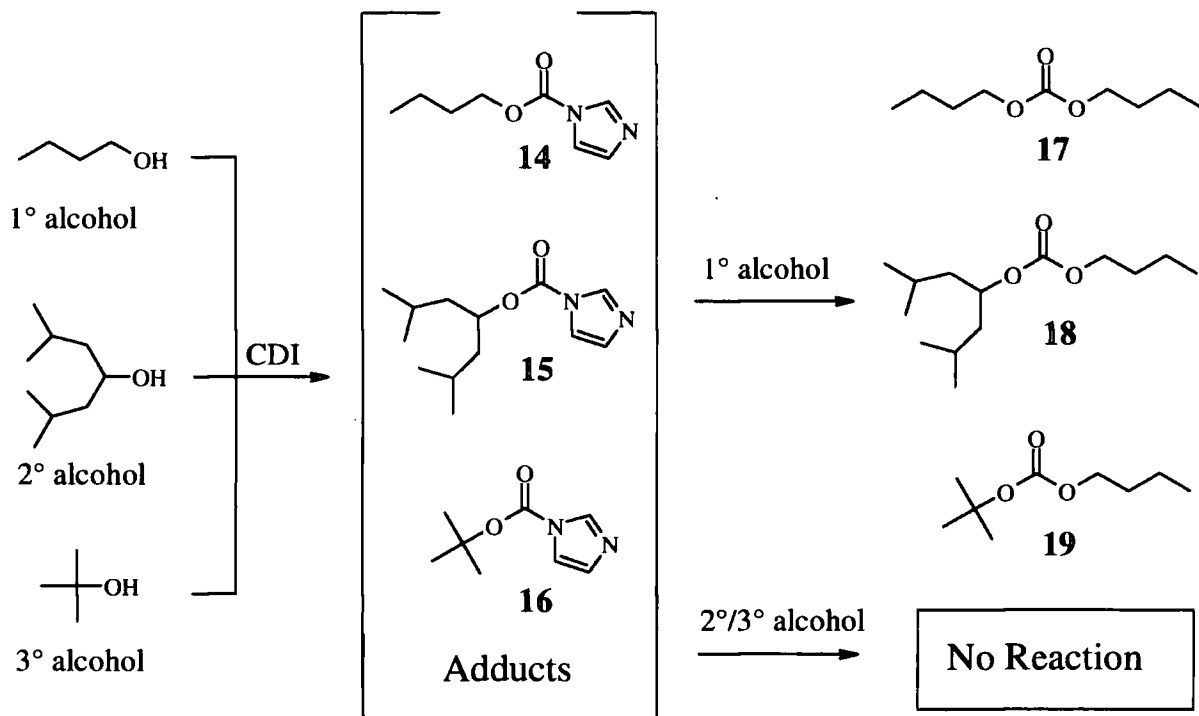


Figure 1.18 Selective reactions of CDI and CDI adducts with alcohols

Some exceptions have been found to the selection rules described above. For example, CDI adducts of secondary alcohols (e.g. **15**), react with 1,4-pentanediol to give predominantly carbonate **20**, formed by reaction at the primary site of the diol but there was evidence of 20% reaction occurring at the secondary site (Figure 1.19). However, reaction of tertiary alcohol adduct **16** with 1,4-pentanediol follows the rules and there was no evidence of reaction at the secondary site.

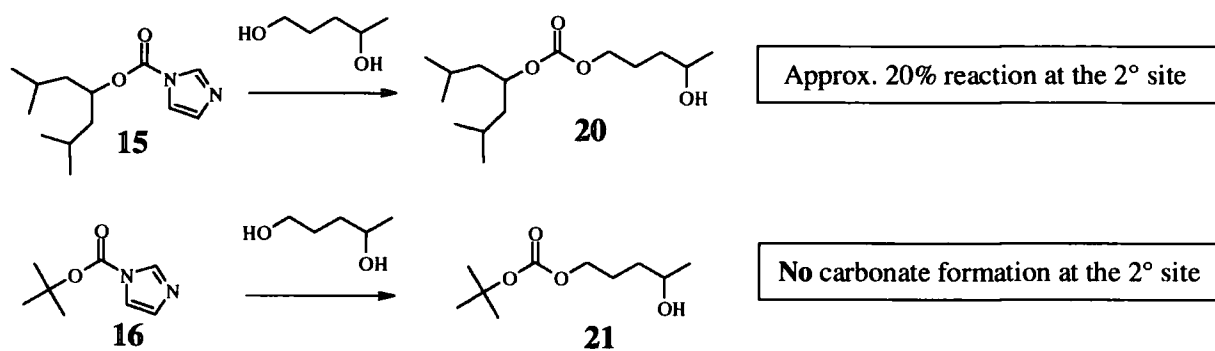


Figure 1.19 Carbonate formation not following the selection rules

Bertolini *et al.* noted similar selectivity during the preparation of asymmetric carbonates (Figure 1.20).<sup>42</sup> The 'one-pot' experiments (equivalent of Staab's 'two-in-one' reaction) involved the addition of CDI to an equimolar mixture of a primary and a secondary

alcohol, **22** and **23**, followed by addition of a different primary alcohol **26**, under base catalysis.

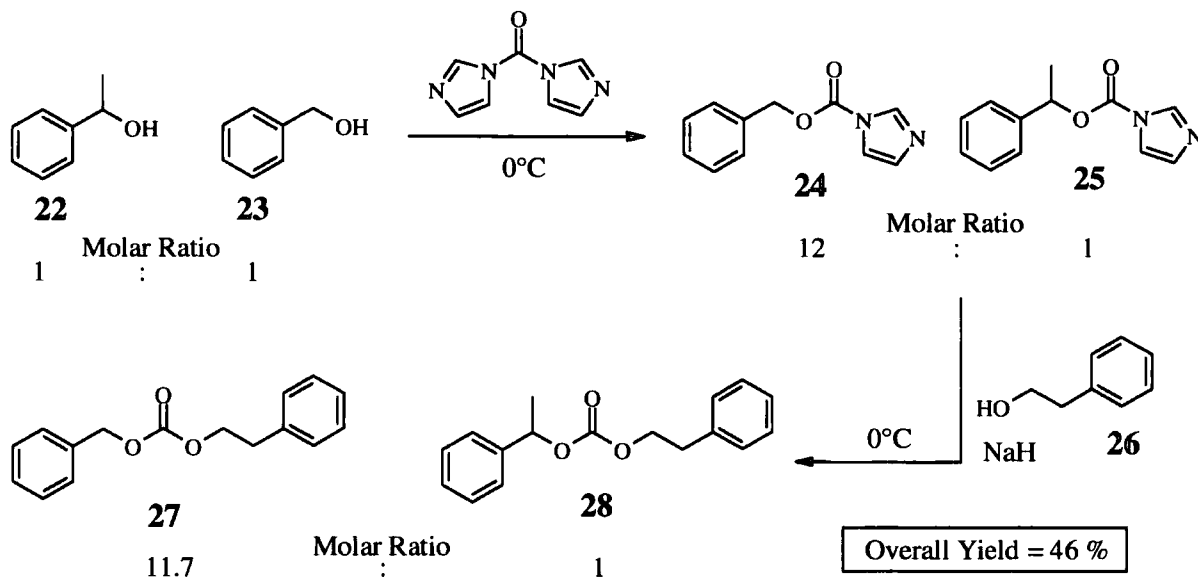


Figure 1.20 Synthesis of asymmetric carbonates by Bertolini et al.

In the first stage, the primary alcohol adduct **24** was formed preferentially over the secondary alcohol adduct **25**, in a ratio 12: 1. Subsequent addition of a different primary alcohol **26** and base (NaH) to the mixture, produced predominantly carbonate **27**, rather than carbonate **28**. Compound **27** is formed from reaction of **26** with the adduct of a primary alcohol whereas **28** arises from reaction with the adduct of a secondary alcohol (ratio of products of 11.7: 1). The yield of the reaction was improved when intermediates **24** and **25** were isolated, because any residual amount of alcohols **22** and **23** was removed, thus preventing the synthesis of carbonates **29** and **30** (Figure 1.21).

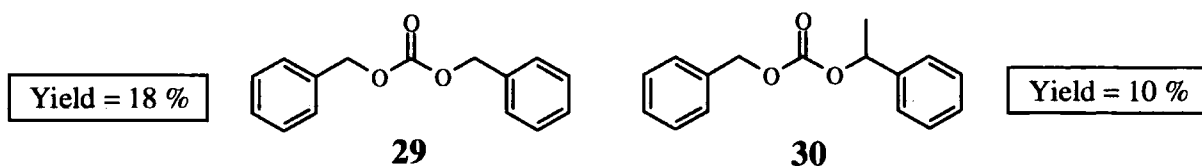
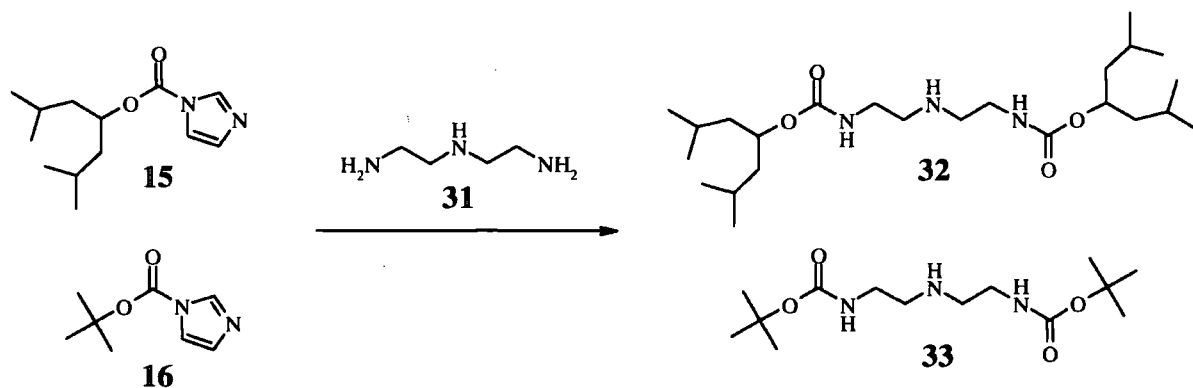


Figure 1.21 Side products isolated in the one-pot reaction of Figure 1.19

#### 1.4.2.2 Urethane Synthesis

The two-stage synthesis of a urethane link consists of the reaction of an alcohol with CDI, followed by reaction of the intermediate produced with an amine. Urethane formation follows selection rules similar to those for carbonates; for example, primary amines will react with the adducts of primary, secondary and tertiary alcohols. However, secondary or tertiary amines will not react with adducts formed from secondary and tertiary alcohols, intermediates **15** or **16**, whereas in carbonate synthesis the equivalent reaction occurs in some cases. This

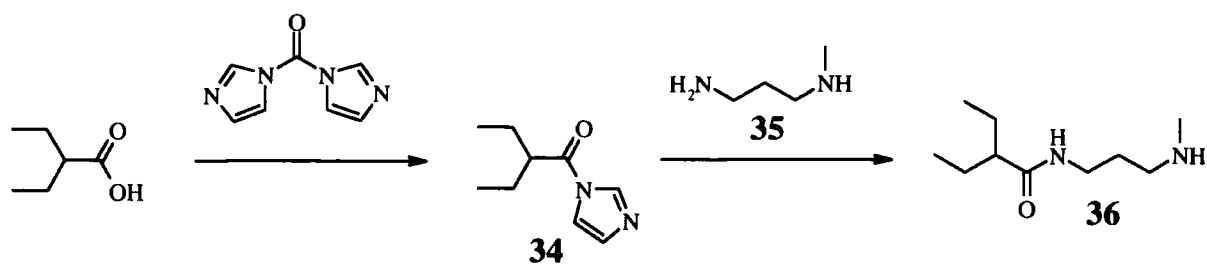
regioselective urethane formation can be demonstrated by the reaction of triamine **31** with adducts **15** or **16**, as reaction only occurs at the primary sites, to give **32** and **33**, and there is no evidence of reaction at the secondary site (*Figure 1.22*).



*Figure 1.22 Regioselective reactions of CDI adducts with a multifunctional amine*

#### 1.4.2.3 Amide Synthesis

The synthesis of amides is achieved by the reaction of CDI with a carboxylic acid, followed by addition of an amine (*Figure 1.23*).<sup>41,43</sup> On addition of CDI to the carboxylic acid, the reaction mixture effervesces, because of the evolution of carbon dioxide. The CDI adducts of acids, *i.e.* imidazolides, are generally used *in situ* because of their short hydrolytic half lives, but isolation is possible if required.<sup>36</sup> The selection rules are similar to those described previously for carbonates and urethanes, for example, a secondary carboxylic acid adduct **34** will react with the primary site of diamine **35**, to give **36** as the only product.



*Figure 1.23 Selective amidation reaction*

#### 1.4.2.4 Selective Reactions of Molecules with Mixed Functionality

Staab noted that CDI would react preferentially with acids in the presence of alcohols.<sup>36</sup> Similarly, because the reaction of primary amines with CDI adducts will occur at room temperature whereas alcohols require heat and base catalysis, the regioselective formation of amide **37** is possible (*Figure 1.24, overleaf*).<sup>44</sup>

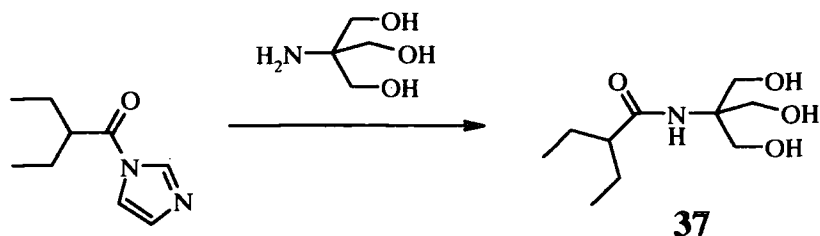


Figure 1.24 Regioselective amidation in the presence of primary alcohol groups

The use of CDI chemistry in this amidation circumvents the need for protection of the primary alcohols and therefore reduces the synthetic pathway by two extra steps (protection and deprotection are unnecessary). It is the effectiveness of these regioselective reactions, which makes it possible to create controlled structures, such as dendrimers. The use of CDI replaces the need to protect and deprotect at each generation growth stage.

### 1.4.3 Use of CDI in Polymer Synthesis

#### 1.4.3.1 Linear and Hyperbranched Polymers

Fréchet *et al.* have prepared various linear tertiary polycarbonates **39** by polymerisation of monomer unit **38** with different diols (Figure 1.25).<sup>45</sup> The polycondensation reaction of these AA and BB monomers was achieved by using the technique of phase-transfer catalysis to give polycarbonates with a molecular weight in the region of  $15 \times 10^3$  Da and polydispersities of around 1.5, depending on the diol used.

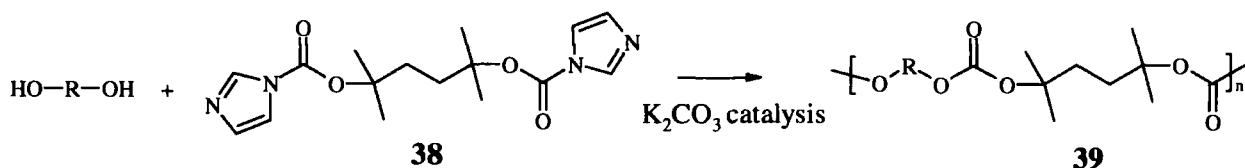
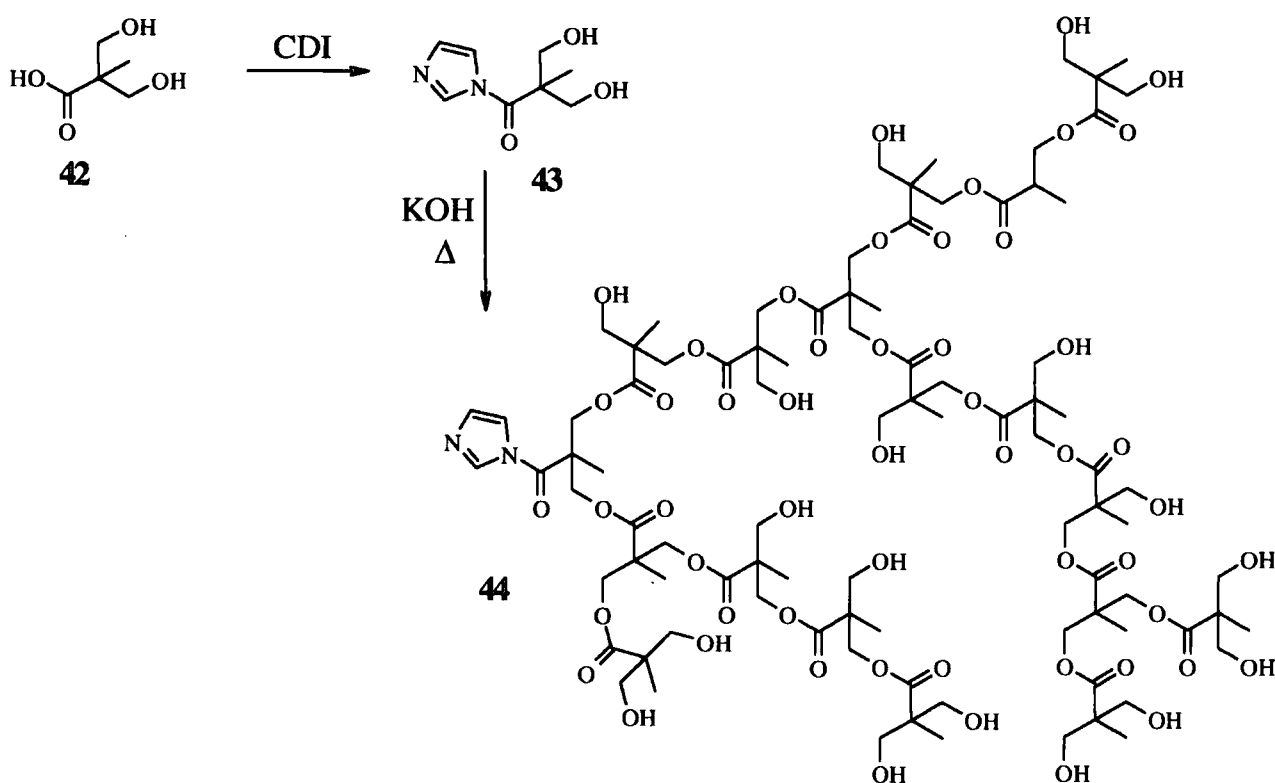


Figure 1.25 Polycondensation reaction of a bis(imidazole carboxylic ester)

Wooley and Bolton have made a different linear aliphatic polycarbonate using an AB monomer **40** (Figure 1.26, overleaf).<sup>46</sup> The monomer is composed of 1,4-cyclohexanediol, one alcohol function of which has been protected with a silyl group and the other activated as a CDI adduct. Removal of the protecting group with cesium fluoride yields the alkoxide anion, which reacts by nucleophilic attack on a CDI adduct to yield the polycarbonate **41**. As this methodology utilises the polymerisation of an AB monomer, the synthesis has been

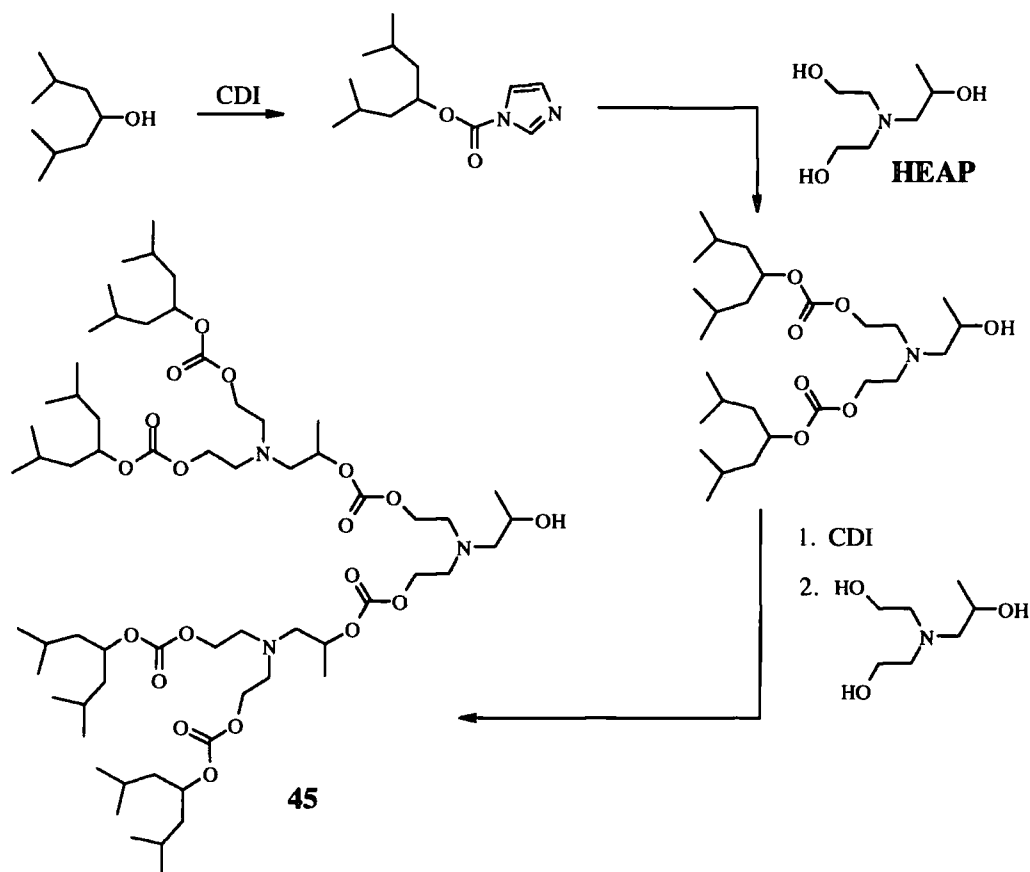
However, instead of using protecting group chemistry, Rannard and Davis have exploited the regioselectivity of CDI reactions in the synthesis of hyperbranched aliphatic polyurethanes, aliphatic polyesters and aromatic polyesters (*Figure 1.27*).<sup>48</sup> The carboxylic acid of the multifunctional molecule **42** reacts with CDI to form the activated monomer **43**, which is polymerised under basic conditions to give water-soluble polyester **44**. Using a combination of different monomers, copolyesters (aliphatic/aromatic) and polyurethane/polyester copolymers of differing composition were also prepared. Both liquid and solid hyperbranched polymers could be synthesised by varying the ratio of aliphatic and aromatic monomers used in the preparation of the polyesters.



21

## b) Dendrimers

Rannard and Davis synthesised polycarbonate dendrimers by exploiting the selective reactions of CDI.<sup>38</sup> The commercially available branching unit bis-hydroxyethylamino-2-propanol (**HEAP**) was used and the synthesis of the second generation dendron **45** is outlined in *Figure 1.28*. Polyamide dendrimers were also prepared, the largest being a third generation structure with a molecular weight of 3999 Da.<sup>43</sup>



*Figure 1.28 Synthesis of a second generation polycarbonate dendron*

### 1.4.4 Conclusions

The regioselective reactions of CDI have been shown to be effective in the synthesis of small molecules and macromolecules, circumventing the need for the use of protecting groups. This attribute, together with the relatively high yielding nature of the reactions, makes CDI an attractive choice of coupling agent in the synthesis of dendrimers.

The dendritic structures, synthesised to date are almost all included in the above account and represent only a small amount of the infinite number of structures that can be made. In this thesis, the design, synthesis and properties of some new polyurethane dendrimers and some codendrimers (polyurethane/polycarbonate) will be reported.



## 1.5 References

- (1) Matthews, O. A.; Shipway, A. N.; Stoddart, J. F. *Prog. Polym. Sci.* **1998**, 23, 1.
- (2) Fréchet, J. M. J.; Hawker, C. J. *Synthesis and Properties of Dendrimers and Hyperbranched Polymers*, in *Comprehensive Polymer Science*, 2<sup>nd</sup> Suppl., 1996, p 71.
- (3) Bosman, A. W.; Janssen, H. M.; Meijer, E. W. *Chem. Rev.* **1999**, 99, 1665.
- (4) Newkome, G. R.; Moorefield, C. N.; Vögtle, F. *Dendritic Molecules: Concepts, Syntheses and Perspectives*; VCH: Weinheim, 1996.
- (5) Hult, A.; Johansson, M.; Malmstrom, E. *Adv. Polym. Sci.* **1999**, 143, 1.
- (6) Mourey, T. M.; Turner, S. R.; Rubinstein, M.; Fréchet, J. M. J.; Hawker, C. J.; Wooley, K. L. *Macromolecules* **1992**, 25, 2401.
- (7) Hawker, C. J.; Fréchet, J. M. J. *J. Am. Chem. Soc.* **1992**, 114, 8405.
- (8) Wooley, K. L.; Hawker, C. J.; Fréchet, J. M. J. *J. Chem. Soc. Perkin Trans. 1* **1991**, 1059.
- (9) Vögtle, F.; Wehner, W.; Buhleier, E. *Synthesis* **1978**, 155.
- (10) Worner, C.; Mullhaupt, R. *Angew. Chem. Int. Ed.* **1993**, 32, 1306.
- (11) de Brabander-van den Berg, E. M. M.; Meijer, E. W. *Angew. Chem. Int. Ed. Engl.* **1993**, 32, 1308.
- (12) van Genderen, M. H. P.; Meijer, E. W. In *Supramolecular Technology*; Reinhoudt, D. N., Ed.; John Wiley & Sons Ltd., 1999; p 47.
- (13) Tomalia, D. A.; Baker, H.; Dewald, J.; Hall, M.; Kallos, G.; Martin, S.; Roeck, J.; Ryder, J.; Smith, P. *Poly. Jour.* **1985**, 17, 117.
- (14) Tomalia, D. A.; Naylor, A. M.; Goddard, W. A. *Angew. Chem. Int. Ed. Engl.* **1990**, 29, 138.
- (15) Hawker, C. J.; Fréchet, J. M. J. *J. Am. Chem. Soc.* **1990**, 112, 7638.
- (16) Hawker, C. J.; Fréchet, J. M. J. *J. Chem. Soc., Chem. Commun.* **1990**, 15, 1010.
- (17) Spindler, R.; Fréchet, J. M. J. *J. Chem. Soc. Perkin Trans. 1* **1993**, 913.
- (18) Wooley, K. L.; Hawker, C. J.; Fréchet, J. M. J. *Angew. Chem. Int. Ed. Engl.* **1994**, 33, 82.
- (19) Zeng, F.; Zimmermann, S. C. *J. Am. Chem. Soc.* **1996**, 118, 5326.
- (20) Kawaguchi, T.; Walker, K. L.; Wilkins, C. L.; Moore, J. S. *J. Am. Chem. Soc.* **1995**, 117, 2159.
- (21) Strobl, G. *The Physics of Polymers*, 1 ed.; Springer: Berlin, 1996.
- (22) Wooley, K. L.; Fréchet, J. M. J.; Hawker, C. J. *Polymer* **1994**, 35, 4489.
- (23) Taylor, R. T.; Puapaboon, U. *Tet. Lett.* **1998**, 39, 8005.

- (24) Puapaiboon, U.; Taylor, R. T. *Rapid Comm. in Mass Spec.* **1999**, *13*, 508.
- (25) Clark, A. J.; Echenique, J.; Haddleton, D. M.; Straw, T. A.; Taylor, P. C. *J. Org. Chem.* **2001**, *66*, 8687.
- (26) Peerlings, H. W. I.; van Benthem, R. A. T. M.; Meijer, E. W. *J. Polym. Sci., Part A: Polym. Chem.* **2001**, *39*, 3112.
- (27) Spindler, R.; Fréchet, J. M. J. *Macromolecules* **1993**, *26*, 4809.
- (28) Cowie, J. M. G. *Polymers: Chemistry and Physics of Modern Materials*, 2nd ed.; Blackie A & P: London, 1997.
- (29) Kinstle, J. F.; Sepulveda, L. E. *J. Polym. Sci. Polym. Lett. Ed.* **1977**, *15*, 467.
- (30) Ghatge, N. D.; Y., J. J. *J. Polym. Sci. Polym. Chem.* **1983**, *21*, 1941.
- (31) Bachmann, F.; Reimer, J.; Ruppenstein, M.; Thiem, J. *Macromol. Rapid. Commun.* **1998**, *19*, 21.
- (32) Versteegen, R. M.; Sijbesma, R. P.; Meijer, E. W. *Angew. Chem. Int. Ed.* **1999**, *38*, 2917.
- (33) McGhee, W. D.; Pan, Y.; Riley, D. P. *Chem. Comm.* **1994**, 699.
- (34) McGhee, W.; Riley, D.; Christ, K.; Pan, Y.; Parnas, B. *J. Org. Chem.* **1995**, *60*, 2820.
- (35) March, J. *Advanced Organic Chemistry*, 4th ed.; Wiley & Sons: New York, 1992.
- (36) Staab, H. A. *Angew. Chem. Int. Ed. Engl.* **1962**, *1*, 351.
- (37) Breuilles, P.; Kaspar, K.; Uguen, D. *Tet. Lett.* **1995**, *36*, 8011.
- (38) Rannard, S.; Davis, N. *Abstr. Pap. Am. Chem. Soc. 214* **1997**, *144-PMSE Part 2*, 63.
- (39) Rannard, S. P.; Davis, M. J.; Courtaulds Corporate Technology, 2000; p 2.
- (40) Rannard, S. P.; Davis, N. J. *Org. Lett.* **1999**, *6*, 933.
- (41) Rannard, S. P.; Davis, N. J. *Org. Lett.* **2000**, *2*, 2117.
- (42) Bertolini, G.; Pavich, G.; Vergani, B. *J. Org. Chem.* **1998**, *63*, 6031.
- (43) Rannard, S. P.; Davis, N.; McFarland, H. *Polym. Int.* **2000**, *39*, 1002.
- (44) Rannard, S. P., *Personal Communication*, **1999**.
- (45) Houlihan, F. M.; Bouchard, F.; Fréchet, J. M. J. *Macromolecules* **1986**, *19*, 13.
- (46) Bolton, D. H.; Wooley, K. L. *J. Polym. Sci., Part A: Polym. Chem.* **1996**, *35*, 1133.
- (47) Bolton, D. H.; Wooley, K. L. *Macromolecules* **1997**, *30*, 1890.
- (48) Davis, N.; Rannard, S. *Abstr. Pap. Am. Chem. Soc.* **1997**, *214*, 158.

## **Chapter 2**

# **Synthesis and Characterisation of Novel Polyurethane Dendrimers**

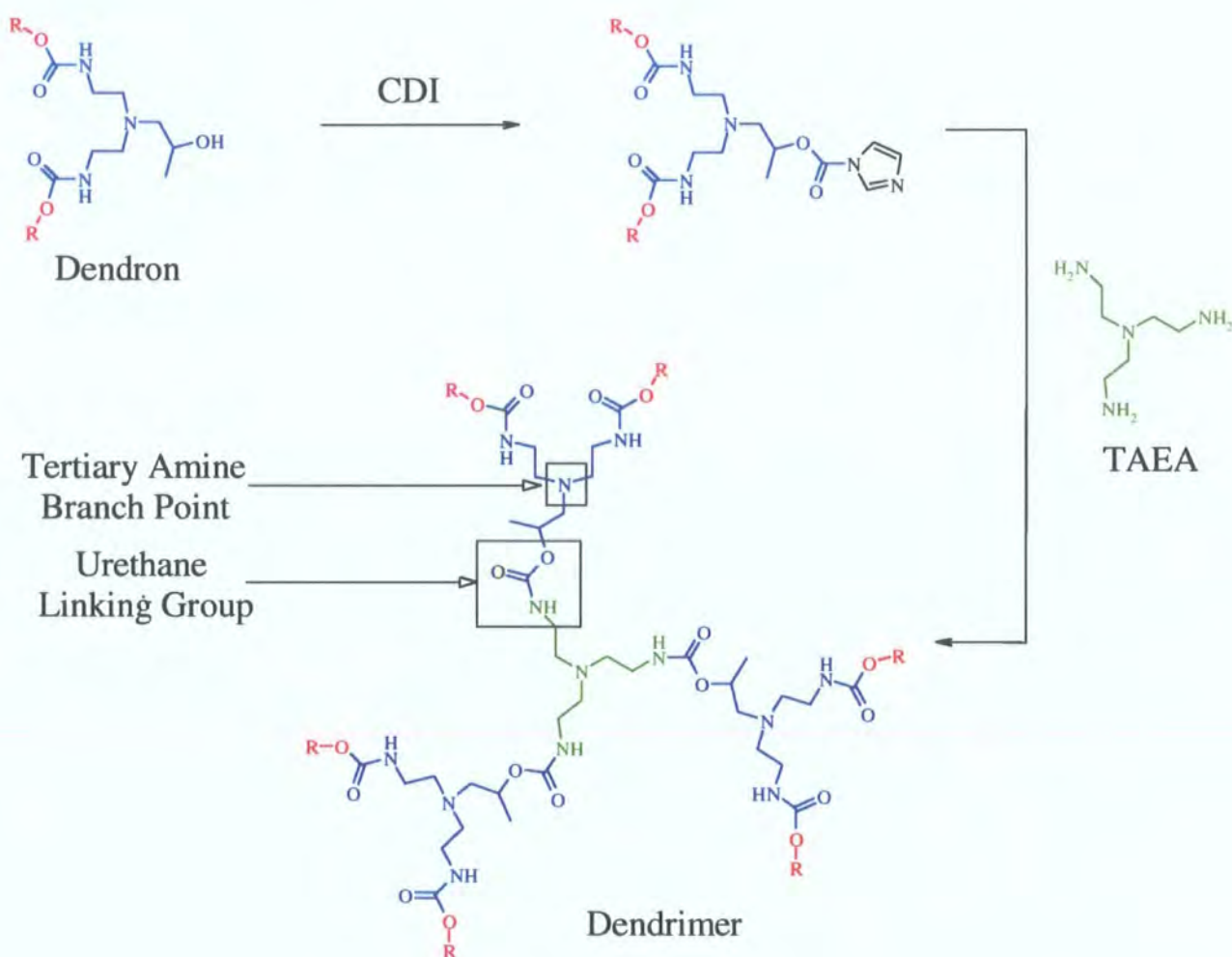
### **2.1 Introduction**

The aim of the project was to ascertain how differences in the three main structural areas of a dendrimer, *i.e.* the terminal or end groups, the branching units and the cores, affect its properties. Therefore, the first task was to synthesise a range of dendrimers with subtle variations in these three areas. This was achieved by using the versatility of both the convergent route to dendrimer synthesis and the selective reactions of the coupling agent, carbonyl diimidazole (CDI).

The design, synthesis and characterisation of a novel series of polyurethane dendrons, with different end groups and their attachment to two different cores will be described in this chapter. The issue of nomenclature for dendrimers will be introduced and a code by which the dendrimers and dendrons are to be identified will be explained. The variation of the branching group of the dendrimer will not be tackled in this chapter, but will be addressed under the heading of 'codendrimers' in Chapter 3.

## 2.2 Description of Polyurethane Dendrimers

The homodendrimers consist of urethane bonds between the branching units of successive layers and between the dendron and the core unit (*Figure 2.1*). They are also characterised by the location of tertiary amines at each branch point and at the centre of the core. The dendrons used in the synthesis of the polyurethane dendrimers have a secondary alcohol function at the focal point, which is activated with CDI allowing the subsequent reaction with the trifunctional core molecule, Tris(2-AminoEthyl)Amine (TAEA). In this thesis the colour scheme shown in *Figure 2.1* will be used, in which red represents the end or terminal groups, blue represents the interior branching units and green corresponds to the core.



*Figure 2.1 Synthesis of a polyurethane dendrimer*

Dendrimers with the four different end groups, *t*-butyl, 4-heptyl, cyclohexyl and benzhydryl have been synthesised (*Figure 2.2*, overleaf).

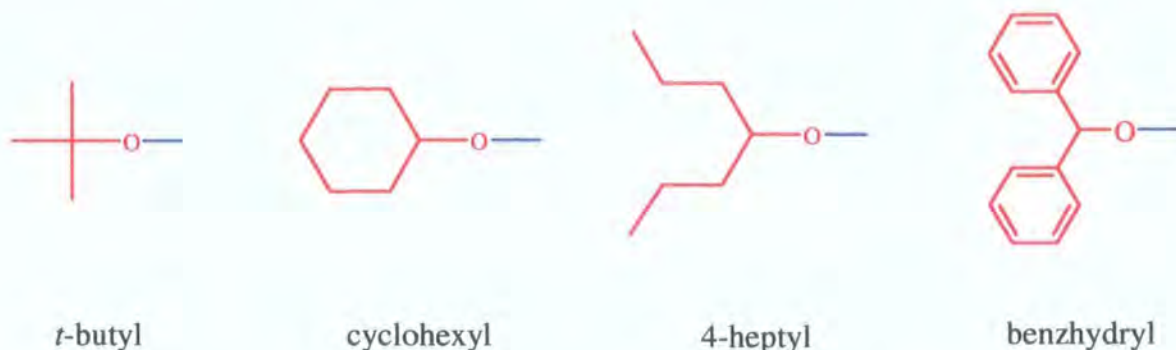


Figure 2.2 The four different end groups for the polyurethane dendrimers

Using some of these end groups, the syntheses and purifications of structures as large as the fourth generation dendron and third generation dendrimer have been successful. However, before the synthesis, purification and characterisation of the dendrons and dendrimers is explained in detail, a code that will be applied to the macromolecules in order to simplify their identification will be introduced.

## 2.3 Nomenclature of Dendrimers

### 2.3.1 Background

The well-defined and symmetric shape of dendrimers may lead a chemist to imagine that the naming of these macromolecules is straightforward. In reality, the process has proved to be rather complicated and those working in the field have yet to adopt a common naming system, even although some have been suggested.<sup>1-4</sup> Newkome *et al.* illustrated the lengthy and inefficient process of applying traditional nomenclature to dendrimers and then proceeded to propose a simplified naming system for the polymers (Figure 2.3).<sup>2</sup>

$$\text{Z - cascade: } \begin{array}{c} \text{Core} \\ \text{Unit} \end{array} [\text{N}_c]: \left( \begin{array}{c} \text{Intermediate} \\ \text{repeat unit} \end{array} \right)^l: \begin{array}{c} \text{terminal} \\ \text{unit} \end{array}$$

$\text{Z}$  = number of terminal groups  
 $\text{N}_c$  = multiplicity of branching at core  
 $l$  = number of layers of repeat units (generations)

Figure 2.3 Dendrimer nomenclature suggested by Newkome *et al.*

The word cascade is included to signify that the molecules are ‘cascade polymers’ (*i.e.* dendrimers) and the core, repeat and terminal units are each described by their chemical composition. The advantage of this system is that at first glance, useful structural information

about the dendrimer can be gleaned, for example, the number of terminal groups ( $Z$ ), the number of layers/generations ( $I$ ) and the multiplicity of the core unit ( $N_c$ ). Using this method, the name given to the second generation poly(propylene imine) dendrimer, with 12 terminal groups and a trifunctional core is: 12-cascade:ammonia [3]:(1-azapropylidene)<sup>2</sup>:ethylamine (Figure 2.4).

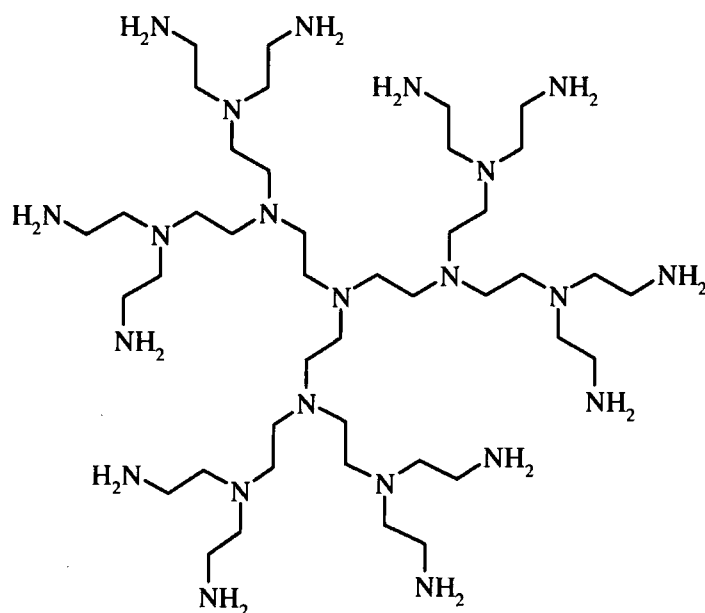


Figure 2.4 12-Cascade:ammonia [3]:(1-azopropylidene)<sup>2</sup>:ethylamine.

Mendenhall suggested a different method based on fractal notation, which simplifies the name into a more mathematical form.<sup>4</sup> Despite the rational approach of both systems, they are not used in the literature so for the purposes of this report, the dendrimers and dendrons synthesised and discussed, will be described by a code created by the author. This idea is similar to one introduced by Seebach *et al.* in an attempt to simplify the identification of a series of chiral polyether dendrimers.<sup>5</sup>

### 2.3.2 Code for Polyurethane Dendrimers with Amine and Aromatic-ester Core Units

The code used to identify the homodendrimers and dendrons synthesised in this project consists of three parts. The first part describes the nature of the terminal groups, the second part indicates the number of layers or generations and the third signifies whether the dendritic molecule is a dendrimer or dendron (Figure 2.5, overleaf). Information relating to the core of the dendrimer and the functionality of the focal point of the dendron can be deduced from this final part of the code.




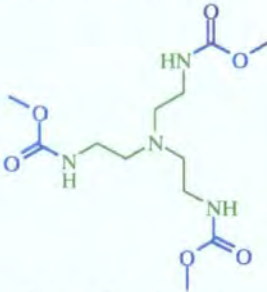

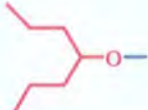
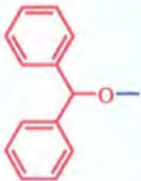
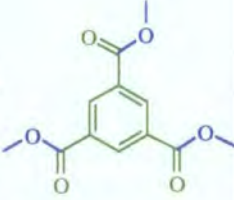
Dendrimer Code		
Terminal Groups	Generation	Dendrimer Core
 <i>t-Butyl</i> <b>B</b>	<b>G<sub>x</sub></b> $x = 1, 2, 3..$  Since all examples in this work have a trifunctional core, G <sub>x</sub> gives the number of terminal groups, e.g. when $x = 1, 2$ and $3$ the no. of terminal groups is 6, 12 and 24 respectively.	<b>D</b>  <i>Polyurethane Dendrimer</i>
 <i>Cyclohexyl</i> <b>C</b>		
 <i>4-Heptyl</i> <b>H</b>		
 <i>BenzHyderyl</i> <b>BH</b>		
		<b>DAC</b>  <i>Dendrimer with Aromatic-ester Core</i>

Figure 2.5 Identification code for different dendrimers

Firstly, the four different terminal groups are represented by the following letters; *t*-Butyl (**B**), Cyclohexyl (**C**), 4-Heptyl (**H**), BenzHyderyl (**BH**) (see Figure 2.2, page 27). The second part indicates the generation of the structure with the term **G<sub>x</sub>**, where  $x$  is the number of the generations (*i.e.* 1, 2, 3 *etc.*). Thirdly, the letter **D** follows the generation number to signify that the structure is a dendrimer, rather than a dendron. The use of the triamine core resulting in the formation of polyurethane homodendrimers, is represented simply by the letter **D**; however, dendrimers that have an Aromatic-ester Core unit are represented by the letters **DAC**. For example, the corresponding codes for two different first generation dendrimers with 4-heptyl end groups, one with an amine core and the other with an aromatic-ester core are **HG1D** and **HG1DAC** respectively (Figure 2.6, overleaf).

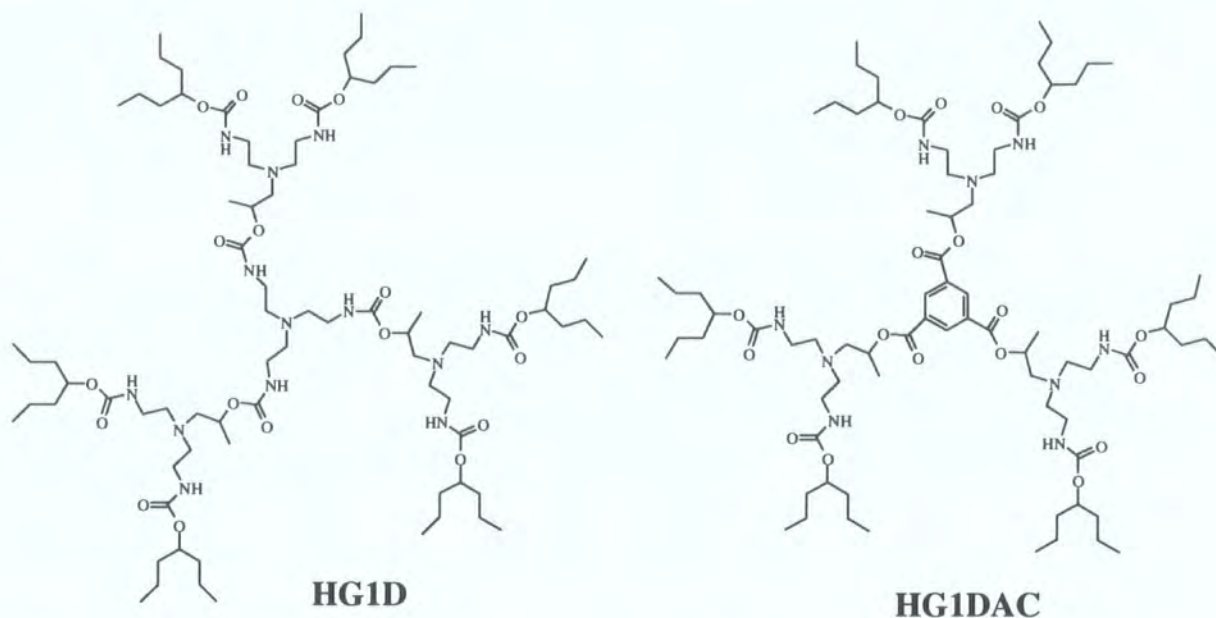


Figure 2.6 Codes for two different first generation dendrimers

The dendrons, used as building blocks for the preparation of the dendrimers, are described by a code similar to that used for the dendrimers (Figure 2.7).

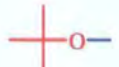

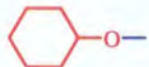
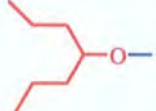
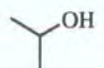
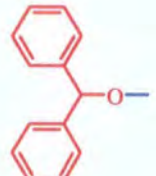
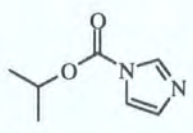
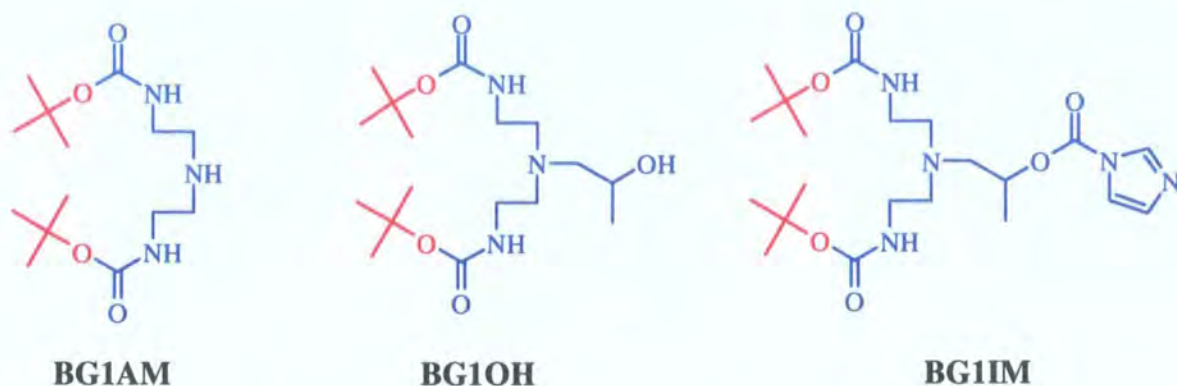
Dendron Code		
Terminal Groups	Generation	Focal Point of Dendron
 <i>t-Butyl</i> <b>B</b>	<b>G<sub>x</sub></b>  $x = 1, 2, 3..$	<b>AM</b>  Secondary <b>AM</b> ine
 <i>Cyclohexyl</i> <b>C</b>		
 <i>4-Heptyl</i> <b>H</b>		<b>OH</b>  Secondary alc <b>OH</b> ol
 <i>BenzHydryl</i> <b>BH</b>		<b>IM</b>  <b>IM</b> idazole Carboxylic Ester

Figure 2.7 Identification code for polyurethane dendrons

The only variation is that the third part, previously used to represent the core of the dendrimer, is used to identify the functional group at the focal point. These three different



functionalities are a secondary **AM**ine function (**AM**), a secondary alc**OH**ol function (**OH**) and an **IM**idazole carboxylic ester group (**IM**). Three first generation dendrons showing all these different functionalities at the focal point and the corresponding codes for the structures are shown below (*Figure 2.8*).



*Figure 2.8 First generation dendrons with different functions as the focal points*

Now the code has been established it will be used throughout this thesis in order to identify the dendrimers or dendrons being discussed and can also be found on the inserted bookmark.

## 2.4 Synthesis and Characterisation of Polyurethane Dendrons

The first, second, third and fourth generation structures in a series of novel polyurethane dendrons have been successfully synthesised, purified and characterised. The syntheses of dendrons with different terminal groups are similar, so the procedure will be described using the *t*-butyl terminated dendrons as an example. Any crucial variations from the reported method, which were applied in the synthesis of dendrons with the three other end groups will be stated.

### 2.4.1 First Generation Dendron

#### a) Synthesis

The three-step reaction scheme adopted for the synthesis of the first generation dendron uses the selective chemistry of CDI in the first two steps, followed by the regiospecific ring opening of propylene oxide in the final stage (*Figure 2.9, overleaf*).

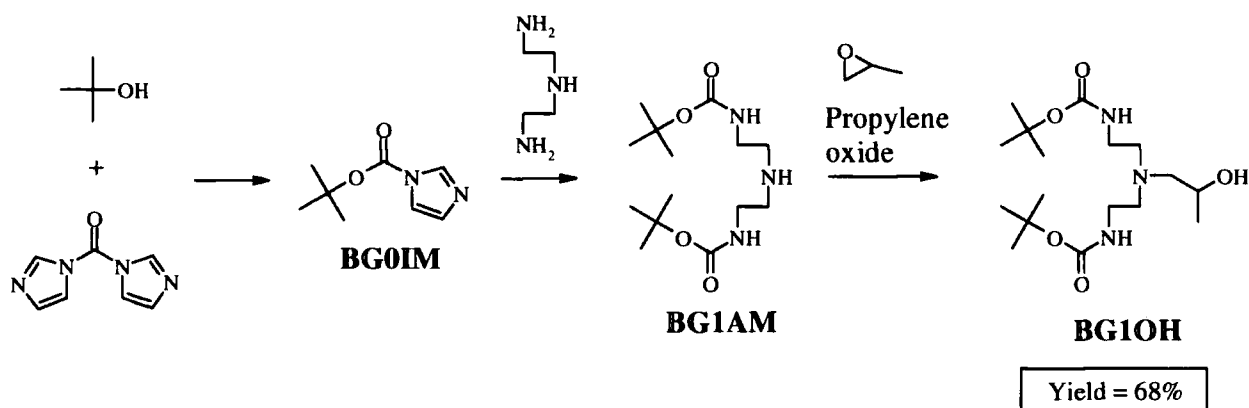
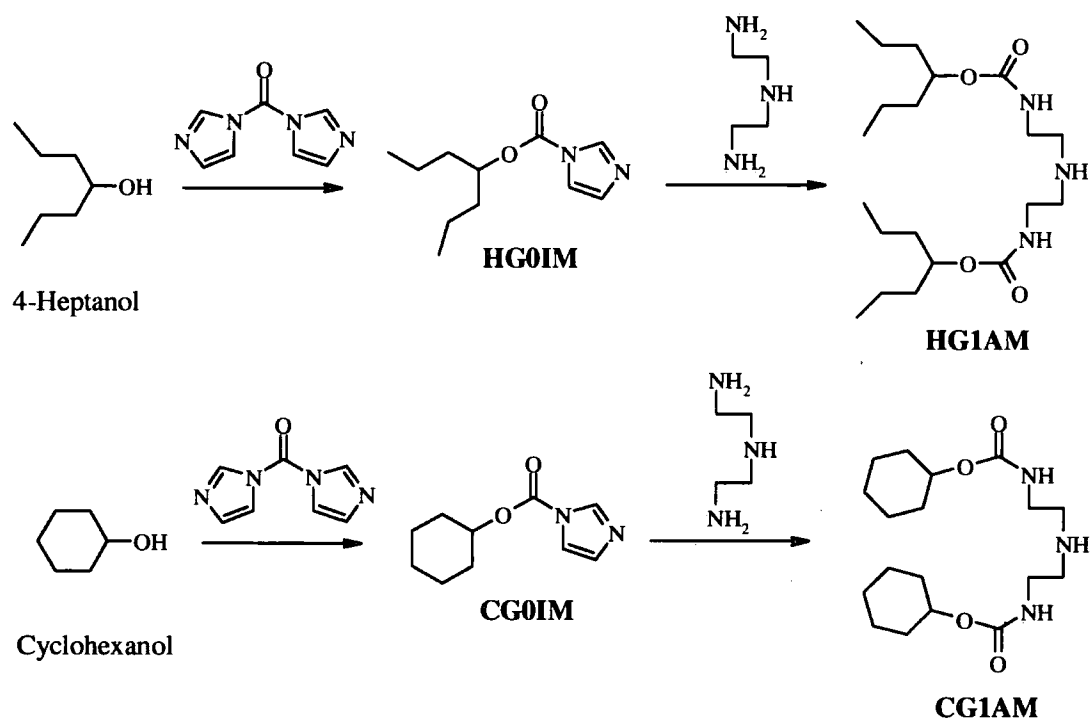


Figure 2.9 Synthesis of first generation dendron **BG1OH**

In the first step, despite presence of the alcohol in excess, *t*-butanol reacted in an equimolar ratio with CDI, to give the adduct **BG0IM**. The isolation of **BG0IM** was unnecessary because an excess of *t*-butanol guaranteed the absence of CDI in the second step of the reaction. It was essential that all CDI had been removed, as any residual CDI would create side products on addition of the triamine. This second step involved the dropwise addition of diethylenetriamine, a reagent containing two primary amine functions and one secondary amine function, to the mixture. The adduct **BG0IM** reacted exclusively at the primary sites of the triamine and after aqueous work-up of the mixture, the di-substituted amine **BG1AM** was isolated as a white crystalline solid. The mono-substituted amine and imidazole, which were the side products of this one-pot reaction, are water soluble and were removed via aqueous work-up. A slight stoichiometric excess of the triamine was necessary, to ensure no **BG0IM** remained, as the CDI adduct could not be removed by the work-up process. The final step in the reaction scheme was the ring opening of propylene oxide by the secondary amine function of the di-substituted amine **BG1AM** (Figure 2.9). The method, which was adapted from a literature procedure for a similar reaction, involved the addition of a three-fold excess of propylene oxide to a stirred solution of **BG1AM** in ethanol at 30°C.<sup>6</sup> After the removal of the solvent, the oil obtained was purified by silica gel chromatography to give **BG1OH** as a white crystalline solid (68% overall). In this final step, the asymmetric epoxide undergoes regiospecific, nucleophilic attack from the amine at the least hindered carbon to give the first generation dendron, which has a secondary alcohol function at the focal point. There was no spectroscopic evidence to indicate attack had occurred on the more hindered side of the epoxide. The use of propylene oxide as a racemate, introduces a chiral centre into the molecule and results in the formation of the first generation dendron as an equimolar mixture of enantiomers.

## b) Other Terminal Groups

The synthesis of first generation dendrons with either 4-heptyl (**H**) or cyclohexyl (**C**) end groups differed slightly from this procedure. The one-pot reactions to prepare **HG1AM** and **CG1AM** were successful but excess 4-heptanol and cyclohexanol could not be removed by aqueous work-up or under vacuum (*Figure 2.10*). To overcome this problem, CDI was used in excess in the first step and intermediates **HG0IM** and **CG0IM** were isolated before reaction with diethylenetriamine. With the benefit of hindsight this extra step could probably be avoided since CDI does not have a long enough lifetime under the reaction conditions for an excess of the reagent to become a problem.



*Figure 2.10 Reaction scheme for **HG1AM** and **CG1AM***

Attempts to recrystallise the first generation dendrons with aliphatic terminal groups were unsuccessful as the compounds 'oiled out' of solution. Therefore, to try and promote crystallisation, structures with symmetrical aromatic terminal groups, were prepared. The synthesis of the first generation dendron with these aromatic benzhydryl (**BH**) end groups followed a similar procedure to the method described for **HG1OH** and **CG1OH** (*Figure 2.11*). At the final stage, recrystallisation in ethanol gave **BHG1OH** as a white crystalline solid, but it was necessary to purify **BHG1AM** by filtration through silica. Therefore, there was little synthetic advantage in using this terminal group but because of its varied structure compared to the aliphatic groups higher generation structures were prepared.

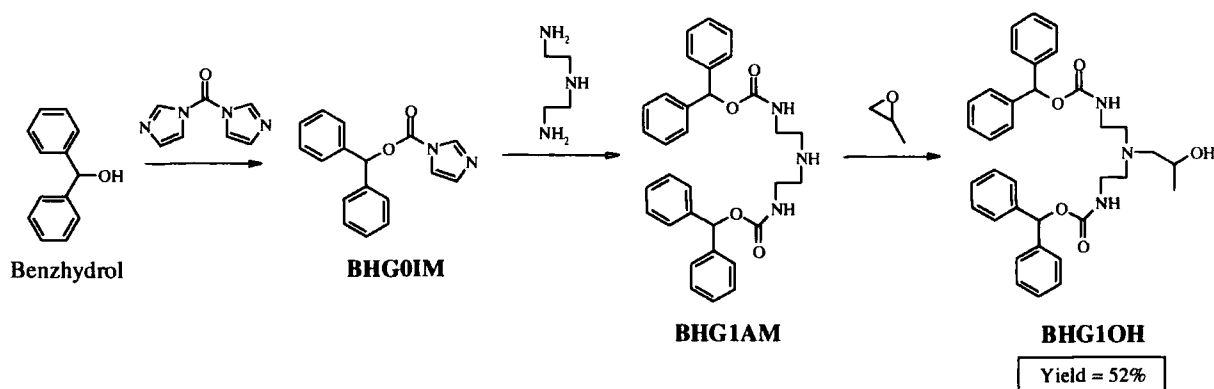


Figure 2.11 Synthesis of first generation dendron with benzhydryl end groups

### c) Characterisation

The  $^{13}\text{C}$  NMR spectra of the first generation dendrons with *t*-butyl, 4-heptyl and cyclohexyl terminal groups were uncomplicated, containing the correct number of resonances corresponding to the number of distinct carbon environments. For example, **BG1OH** contains 8 different carbon environments and 8 resonances were observed in the spectrum (Appendix, page I). However, the presence of a chiral centre together with methylene groups in the dendrons results in more complex  $^1\text{H}$  NMR spectra for the molecules. The two hydrogens of these methylene groups are diastereotopic and it is well established that the chemical environments of the hydrogens differ within the molecule.<sup>7</sup> Since they are not identical the resonances for the diastereotopic hydrogens can appear at different chemical shifts and have the ability to couple to each other. In general, the closer the pair of hydrogens to the stereocentre, the greater the observed effect for the corresponding resonances in the  $^1\text{H}$  NMR spectrum. In the first generation dendrons there are three sets of diastereotopic hydrogens, one pair adjacent to the chiral centre ( $\text{H}_\alpha$  and  $\text{H}_\beta$  in Figure 2.12 overleaf) and two pairs between the urethane groups and tertiary amine function. In the  $^1\text{H}$  NMR spectrum of **BG1OH** the coupling pattern of the pair adjacent to the chiral centre cannot be well resolved but there is evidence of the presence of diastereotopic hydrogens (Appendix, page I). However, the difference in chemical shift is greater for the equivalent pair of hydrogens in the  $^1\text{H}$  NMR spectra of **CG1OH** and **HG1OH** and an interesting coupling pattern is observed. For example, in the spectrum of **HG1OH** the methylene hydrogens  $\text{H}_\alpha$  and  $\text{H}_\beta$  are represented by two doublets of doublets as they couple to each other ( $^2J$  or geminal coupling) and to the hydrogen attached to the chiral centre ( $^3J$  or vicinal coupling) (Figure 2.12). The difference in the  $^3J$  coupling constant for the two hydrogens is discussed in more detail in Chapter 3 (pages 89-91). The difference in resonance frequency for hydrogens  $\text{H}_\alpha$  and  $\text{H}_\beta$  of **HG1OH** is 0.11 ppm and the corresponding difference is 0.09 ppm in cyclohexyl-terminated **CG1OH**. The

diastereotopic hydrogens of the methylenes between the tertiary amine function and the urethane groups of **HG1OH** can be provisionally assigned by analogy with the methylene shifts and multiplicities of **HG1AM**. Those nearest to the tertiary amine appear to be split into two triplets and the same pattern is observed in the  $^1\text{H}$  NMR spectra of the other first generation dendrons. However, this pseudo simplicity is probably misleading and the observed multiplicity arises from a complex non-first order interaction of all four hydrogens.

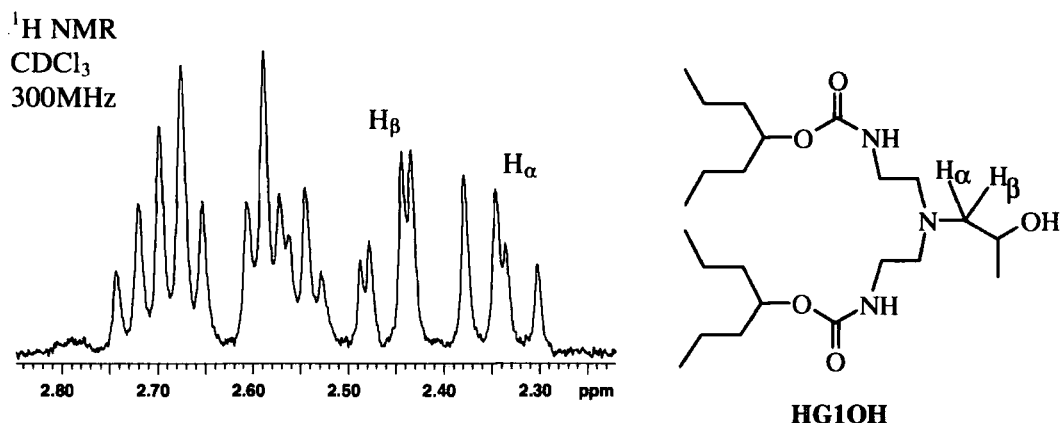


Figure 2.12  $^1\text{H}$  NMR spectrum of **HG1OH** demonstrating coupling of diastereotopic hydrogens

In addition to characterisation by NMR spectroscopy, the first generation structures were confirmed by mass spectrometry and elemental analysis (see experimental section).

## 2.4.2 Branching Unit or AEAP

### a) Synthesis

The branching unit for this series of dendrons, 1-[N,N-bis(2-AminoEthyl)Amino-2-Propanol or **AEAP**, was prepared from the first generation dendron with *t*-butyl terminal groups **BG1OH** (Figure 2.13). The *t*-BOC groups of **BG1OH** were removed by acid deprotection to give a tris-ammonium salt, which was then transformed to the free amine by ion exchange. The ion exchange process was achieved by stirring a solution of the salt in distilled water with Amberlite® ion exchange beads. This replaced the chloride ions of the salt with hydroxide ions to give the branching unit and water. The subsequent removal of water *in vacuo* and purification by vacuum distillation gave the branching unit **AEAP** as a colourless oil (64%). The structure of **AEAP** was confirmed by the characterisation techniques of NMR spectroscopy and mass spectrometry (Appendix, page II).

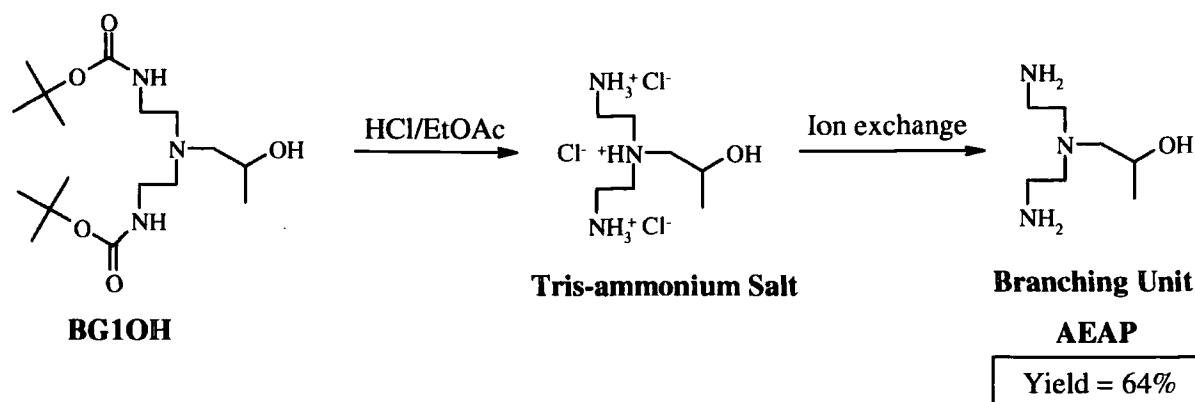


Figure 2.13 Branching unit, **AEAP**, used to synthesise second, third and fourth generation dendrons

The synthesised branching unit was used in the preparation of higher generation dendrons thus reducing the number of steps required for each generational increase from three to two.

### 2.4.3 Second Generation Dendron

#### a) Synthesis

The second generation dendron was prepared in a one-pot synthesis involving the activation of the focal point of the first generation dendron, followed by reaction with the branching unit **AEAP** (Figure 2.14). The selectivity of CDI reactions was exploited in both steps of the scheme. In the first step, CDI reacted in a 1:1 ratio with the first generation dendron **BG1OH**, to give the intermediate **BG1IM**. The reaction mixture was analysed by  $^1\text{H}$  NMR spectroscopy to confirm complete conversion of the secondary alcohol to the imidazole ester, prior to the next step. This was achieved by monitoring the resonance of the hydrogen attached to the chiral centre, which experiences a downfield shift from 3.76 ppm to 5.20 ppm in the  $^1\text{H}$  NMR spectrum. If complete conversion was observed, the branching unit **AEAP** was added but if some **BG1OH** remained, an approximately sufficient amount of CDI was added and the reaction continued for 2 hours before addition of the branching unit. In the second step, **BG1IM** reacted preferentially with the primary amine functions rather than the secondary alcohol function of the branching unit. There was no spectroscopic evidence of reaction at the secondary alcohol function of **AEAP**. The crude product was purified by column chromatography (silica gel, eluent EtOAc) to give the second generation dendron as a colourless amorphous solid (50%). The loss of some product during the purification step, rather than the efficiency of the reaction, is the probable explanation for the low yield.

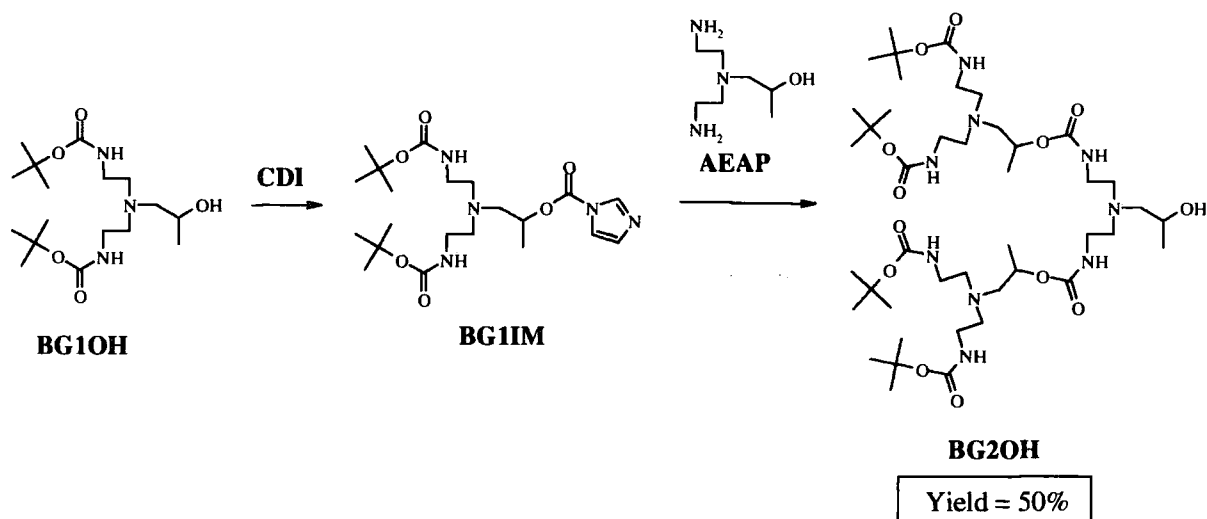


Figure 2.14 Synthesis of second generation dendron **BG2OH**

### b) Other Terminal Groups

The procedure outlined above was used to synthesise the second generation dendrons with 4-heptyl and cyclohexyl end groups, *i.e.* **HG2OH** and **CG2OH** (Figure 2.15). The dendron with the 4-heptyl end groups was isolated as a sticky colourless oil and **CG2OH** as a colourless amorphous solid. The only variant in the experimental method was the polarity of the solvent ratio used for the column chromatography step.

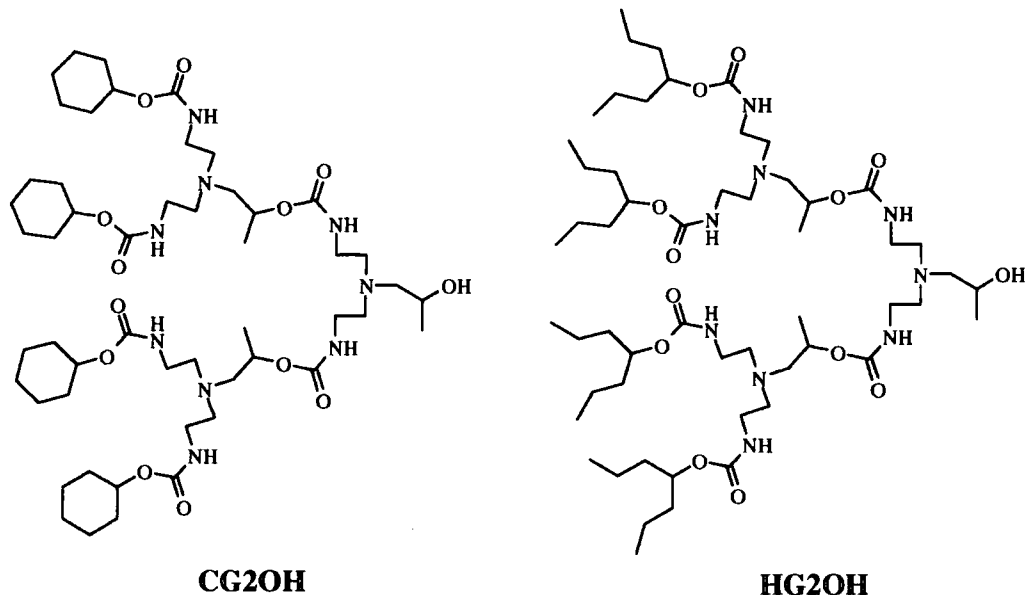


Figure 2.15 Second generation dendrons **CG2OH** and **HG2OH**

### c) Characterisation

#### NMR Spectroscopy

For the second generation dendrons the use of deuterated chloroform as an NMR solvent resulted in spectra with broad signals that were difficult to assign. Therefore, a protic



NMR solvent was used to break up, to some degree, the hydrogen bonding causing the reduced mobility of the molecules and consequently the broadening of resonances. The solvent chosen was deuterated methanol ( $\text{CD}_3\text{OD}$ ) and resolution of the NMR spectra improved and peak assignment was possible. The  $^{13}\text{C}$  NMR spectra of the second generation dendron with *t*-butyl end groups **BG2OH** has 14 resonances corresponding to the 14 different carbon environments in the molecule (for spectrum and assignment of resonances see Appendix, page III). The  $^{13}\text{C}$  NMR spectrum of **HG2OH** also contains the expected number of carbon resonances; however, two signals are coincident in the spectrum of **CG2OH**. One feature in the  $^{13}\text{C}$  NMR spectra of all second generation dendrons is the splitting of the carbon resonance corresponding to the chiral centre at the focal point (\*) into three peaks (Figure 2.16). The resonances corresponding to the carbons adjacent to this chiral centre also show some splitting but the peaks are not well resolved. After deconvolution of the three peaks in the  $^{13}\text{C}$  NMR spectrum of **BG2OH** the ratio of their areas was found to be approximately 2.0:4.0:1.6. The carbon resonance for the two symmetrically equivalent chiral centres in the outer layer of the dendron (•) is seen as one peak in the  $^{13}\text{C}$  NMR spectrum (Figure 2.16). However, the peak is broad and therefore may mask the presence of a splitting pattern.

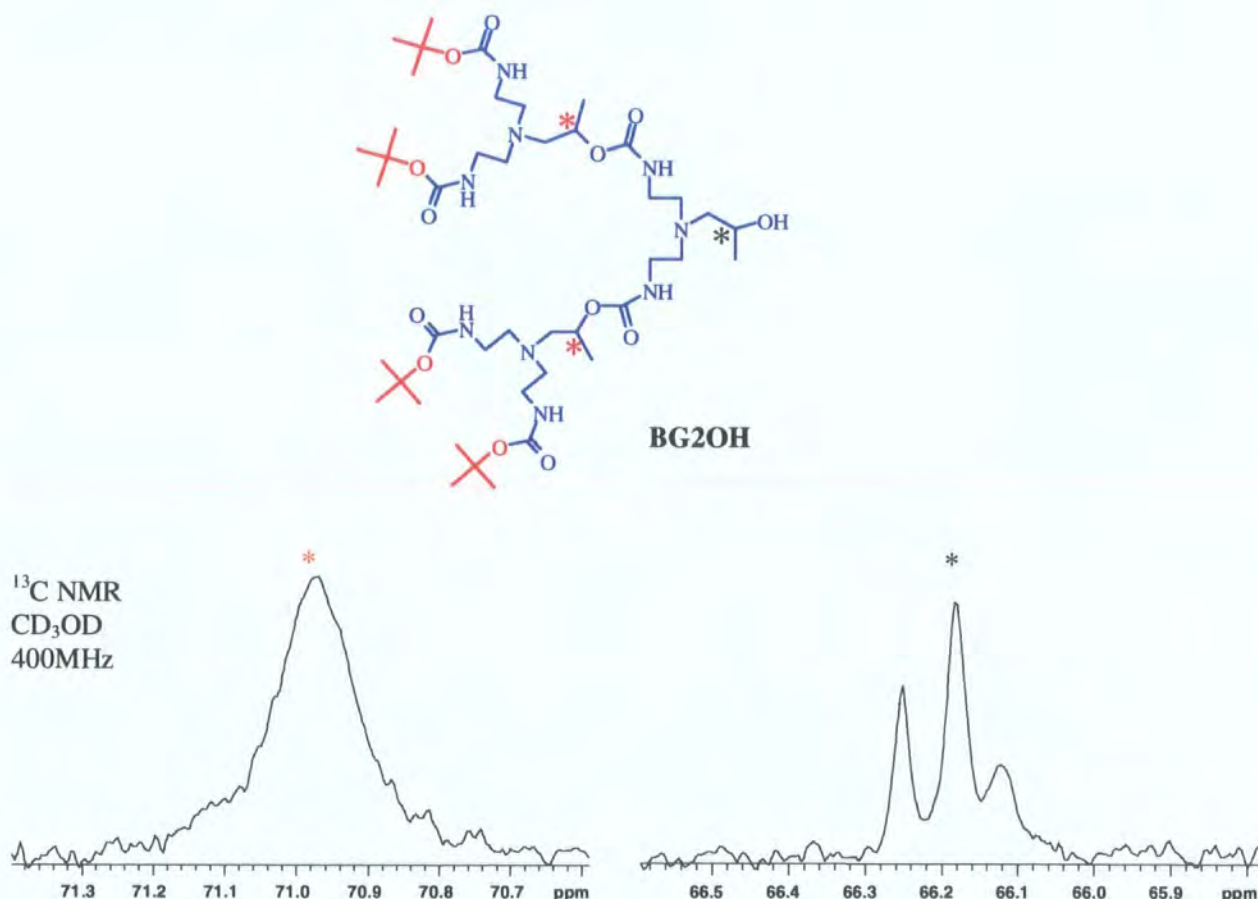


Figure 2.16 Resonances of the chiral centres (•) and (\*) in the  $^{13}\text{C}$  NMR spectrum



A possible explanation for the splitting of the carbon resonance into three peaks is the presence of different isomers of the compound. The racemic nature of the reagents used in the synthesis of the second generation dendron results in its formation as a mixture of stereoisomers. In contrast to the first generation, this mixture of stereoisomers for the second generation dendrons includes diastereoisomers which may not have identical  $^{13}\text{C}$  NMR spectra. The number of possible stereoisomers (**I**) can be deduced from the number of chiral centres (**n**) in the molecule using Equation (1).

$$2^n = \mathbf{I} \quad (1)$$

There are three chiral centres in the second generation dendron so, in theory, there should be eight stereoisomers, *i.e.* *A* to *H* (Figure 2.17). However, two pairs of the eight combinations of chiral centres are identical subsequent to rotation by  $180^\circ$  and inversion at the tertiary amine site near the focal point. The equivalence of the molecules (*B* and *D*) and (*F* and *H*) reduces the number of different stereoisomers from eight to six. Of these stereoisomers there are three sets of enantiomers, which have identical NMR spectra *i.e.* (*A* and *G*), (*B/D* and *F/H*) and (*C* and *E*). The relationship between all three enantiomeric pairs is diastereomeric. The formation of a statistical distribution of diastereoisomers is expected, resulting in the presence of the different isomers in the ratio of 2:4:2.

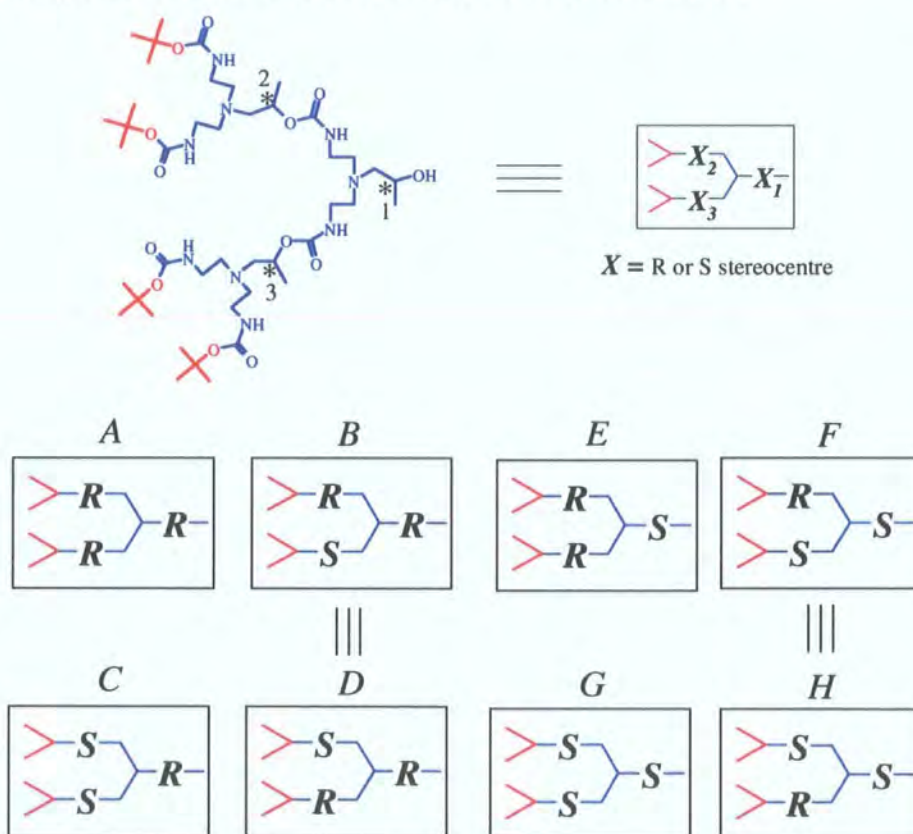
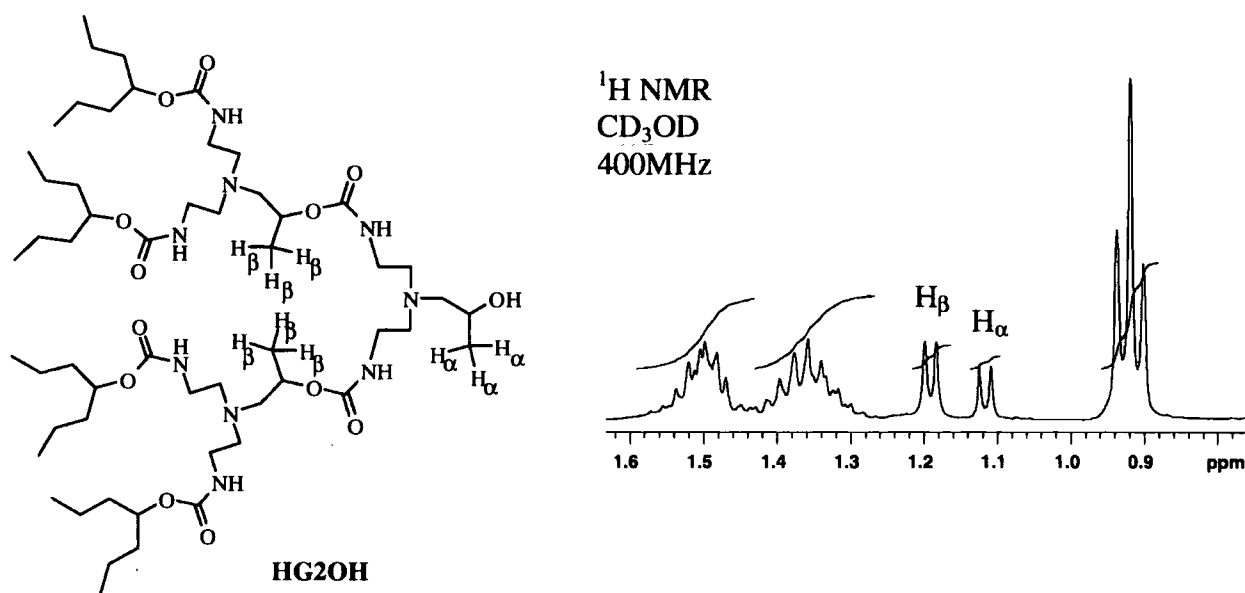


Figure 2.17 Eight combinations of the three chiral centres

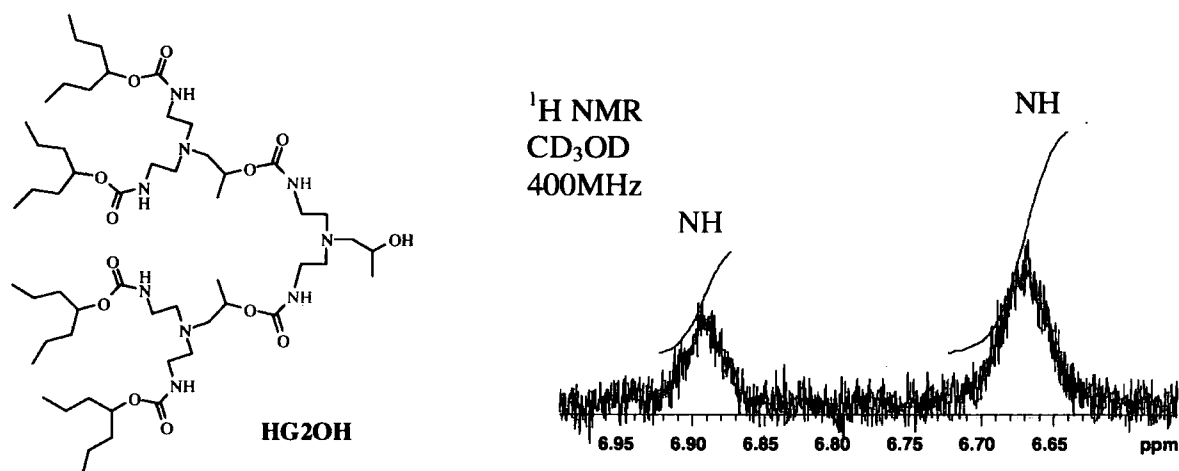
The presence of three diastereomeric forms of the second generation dendron is a proposed explanation for the observed splitting of a carbon resonance into three peaks. Also, the integration of the peaks approximately coincides with the expected statistical ratio of isomers present. The difference in chemical shift of equivalent carbons in the three diastereoisomers should be most pronounced close to the chiral centres of the molecule. This is observed as the chiral centre near the focal point (\*) is split into three peaks whereas the adjacent carbons are split but not well resolved and the resonances of the carbons further away show no splitting effect. For the chiral centres (\*), in the outer layer of the dendron, the resonance is broad so the presence of different diastereoisomers is masked. The broadening of the peak probably results from the reduced mobility of the outer chiral centres. This is unsurprising as these chiral centres are located within a 'chain' and have restricted movement compared to the 'chain ends' at the focal point of the dendrons. The  $^{13}\text{C}$  NMR experiment was repeated at an elevated temperature of  $50^\circ\text{C}$  and at a higher field (500MHz) but the number of resonances and their splitting pattern was not observed to vary. Further evidence in support of this analysis occurred during codendrimer synthesis (see Chapter 3, pages 87-88).

$^1\text{H}$  NMR spectroscopy was a useful technique in the characterisation of second generation dendrons **HG2OH**, **BG2OH** and **CG2OH** and the  $^1\text{H}$  NMR spectrum of the 4-heptyl terminated structure is included in the Appendix (page III). A distinctive feature of the spectra is the presence of two doublets at approximately 1.2 ppm in the integrated ratio of 1:2 (*Figure 2.18*). These two doublets correspond to the methyl group hydrogens  $\text{H}_\alpha$  and  $\text{H}_\beta$  and are present in the second generation dendrons in the ratio 1:2.



*Figure 2.18 Methyl group hydrogens of **HG2OH***

Another interesting feature of the  $^1\text{H}$  NMR spectra is the chemical shift dependency of the two urethane N-H resonances on the nature of the dendrons' end groups. In the spectrum of **HG2OH** the two N-H resonances occur at 6.67 ppm and 6.89 ppm and integration of the peaks suggests the signals correspond to the N-H resonances of the outer and inner urethanes respectively (*Figure 2.19*).



*Figure 2.19 Urethane N-H resonances of HG2OH*

The chemical shifts of N-H resonances for **HG2OH** and the other second generation dendrons are listed in *Table 2.1*. For all three dendrons the chemical shift of the inner urethane is approx. 6.88 ppm and can be considered identical within experimental error. However, the resonance of the outer urethanes shifts downfield for the sequence of dendrons **BG2OH**, **CG2OH**, and **HG2OH**, implying the degree of hydrogen bonding for the outer urethane groups increases in this order. This result suggests the presence of bulk and sterically demanding groups *i.e.* *t*-butyl hinders the formation of hydrogen bonds by the urethane groups near the termini. In contrast, the flexible 4-heptyl units allow closer proximity of the end groups and therefore increased hydrogen bonding.

Dendron	N-H resonance of urethane (ppm) in $\text{CD}_3\text{OD}^a$	
	Inner	Outer
<b>HG2OH</b>	6.89	6.67
<b>CG2OH</b>	6.88	6.61
<b>BG2OH</b>	6.88	6.43

<sup>a</sup> The chemical shifts of the N-H resonances were constant with different concentrations

*Table 2.1 Urethane N-H resonances of second generation dendrons*

The dendrons were also analysed by electrospray (ES) mass spectrometry, gel permeation chromatography (Appendix, page IV) and elemental analysis. The ES mass spectrum of **HG2OH**, with a calculated mass of 1104, is shown below (Figure 2.20). The protonated molecular ion  $[M+H]^+$  and those cationised by sodium and potassium,  $[M+Na]^+$  and  $[M+K]^+$ , are observed in the spectrum at  $m/z$  values of 1105, 1127 and 1143. Some doubly cationised species are also present at  $m/z$  values of 553, 564 and 575 corresponding to  $[M+2H]^{2+}$  and  $[M+H+Na]^{2+}$  and  $[M+2Na]^{2+}$  respectively.

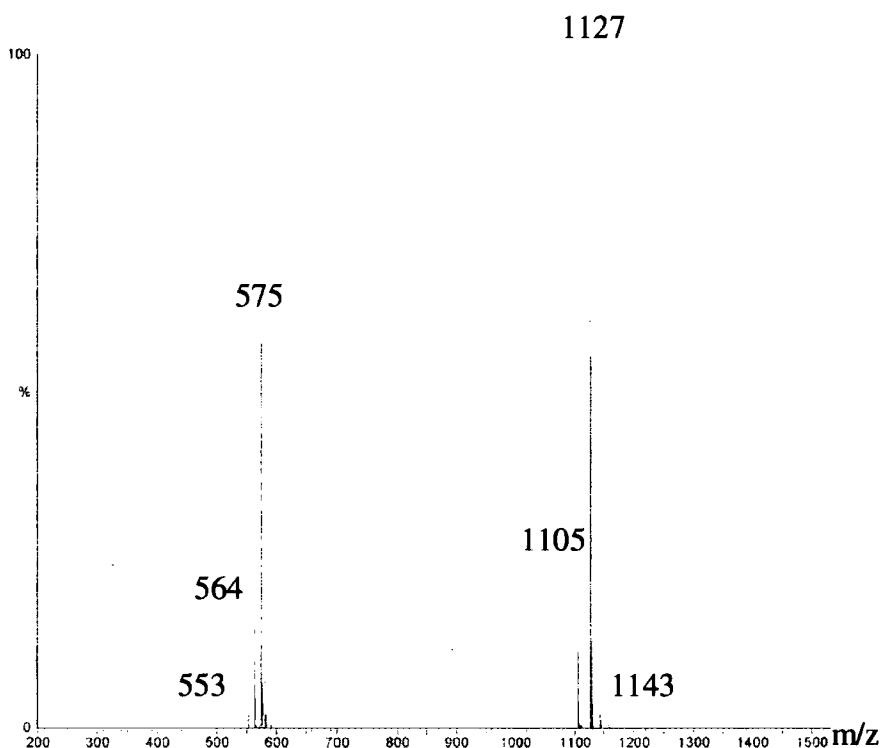


Figure 2.20 Electrospray mass spectrum of **HG2OH**

The second generation dendron with *t*-butyl end groups, **BG2OH**, was characterised by electrospray and MALDI-TOF (Voyager) mass spectrometry. In the second method (Figure 2.21, overleaf), mass peaks corresponding to the protonated molecular ion,  $[M+H]^+$ , and those cationised with sodium and potassium,  $[M+Na]^+$  and  $[M+K]^+$ , were present, together with a similar pattern of peaks at successive intervals of 100 mass units below these signals. The intensities of the peaks at lower  $m/z$  were observed to increase slightly with increasing laser power. This phenomenon only occurs for the dendron with *t*-butyl termini and these 'fragmentation' peaks are not evident in the mass spectra of the other second generation dendrons. This observation, and the increments of 100 suggest the *t*-BOC groups are labile under the conditions used for mass analysis with the MALDI-TOF (Voyager) mass spectrometer, (*i.e.* 100 mass units corresponds to the loss of isoprene and carbon dioxide). A



similar pattern was observed in the MALDI-TOF (Voyager) mass spectra of the codendrons, which also have *t*-butyl end groups (structures depicted in Chapter 3, page 81). An enlargement of the appropriate region in the ES mass spectrum of a codendron is included in the Appendix (page XVII). The fragmentation of these lower molecular weight compounds with *t*-butyl end groups may explain the problems that arose during the mass analysis of the higher molecular weight dendrons and dendrimers (with *t*-butyl end groups) synthesised in this project.

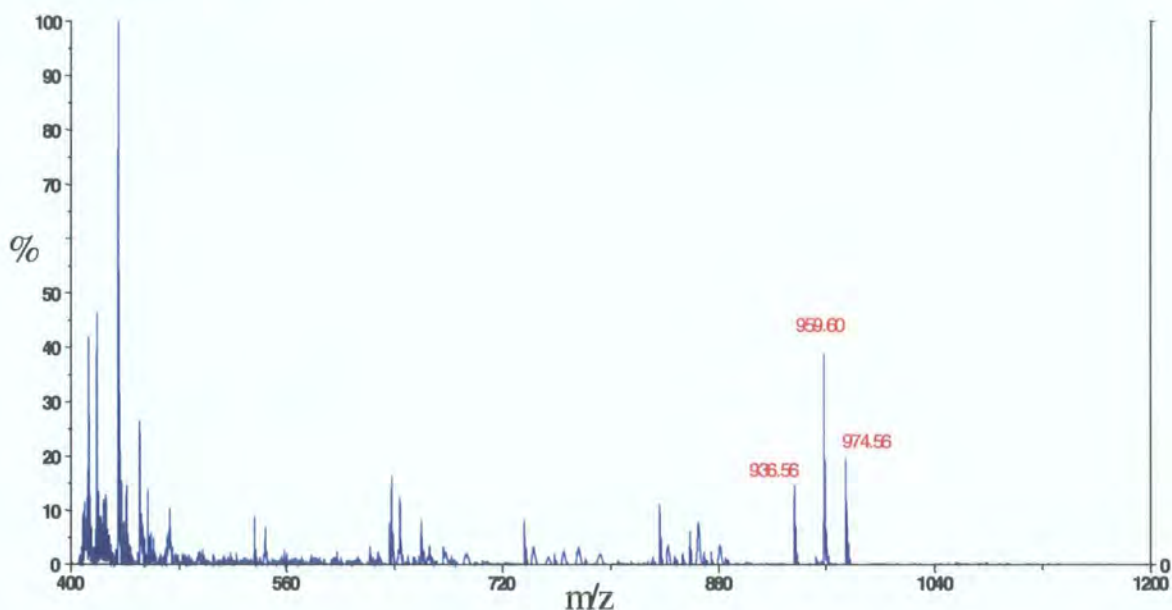


Figure 2.21 MALDI-TOF (Voyager) mass spectrum of **BG2OH**

## 2.4.4 Third Generation Dendron

### a) Synthesis

The third generation dendron was synthesised from the second generation dendron, using the one-pot reaction involving the consecutive addition of CDI and the branching unit **AEAP** (Figure 2.22, overleaf). The experimental procedure was similar to the method described for the second generation dendron. However, in some cases a residual amount of second generation dendron was present after purification by silica gel chromatography and it was necessary to purify the dendron using preparative gel permeation chromatography (GPC) or Bio-Beads (Bio-Rad, S-X1 Bio-Beads; using toluene as the solvent and gravity flow). The medium involved in the second purification method separates the compounds in the mixture with respect to their hydrodynamic volumes. Therefore, the first molecule to be eluted from the column was the third generation dendron, followed by the lower molecular weight impurity, *i.e.* the second generation dendron. After the two purification procedures, the third generation dendron **BG3OH** was isolated as a white amorphous solid (48%).

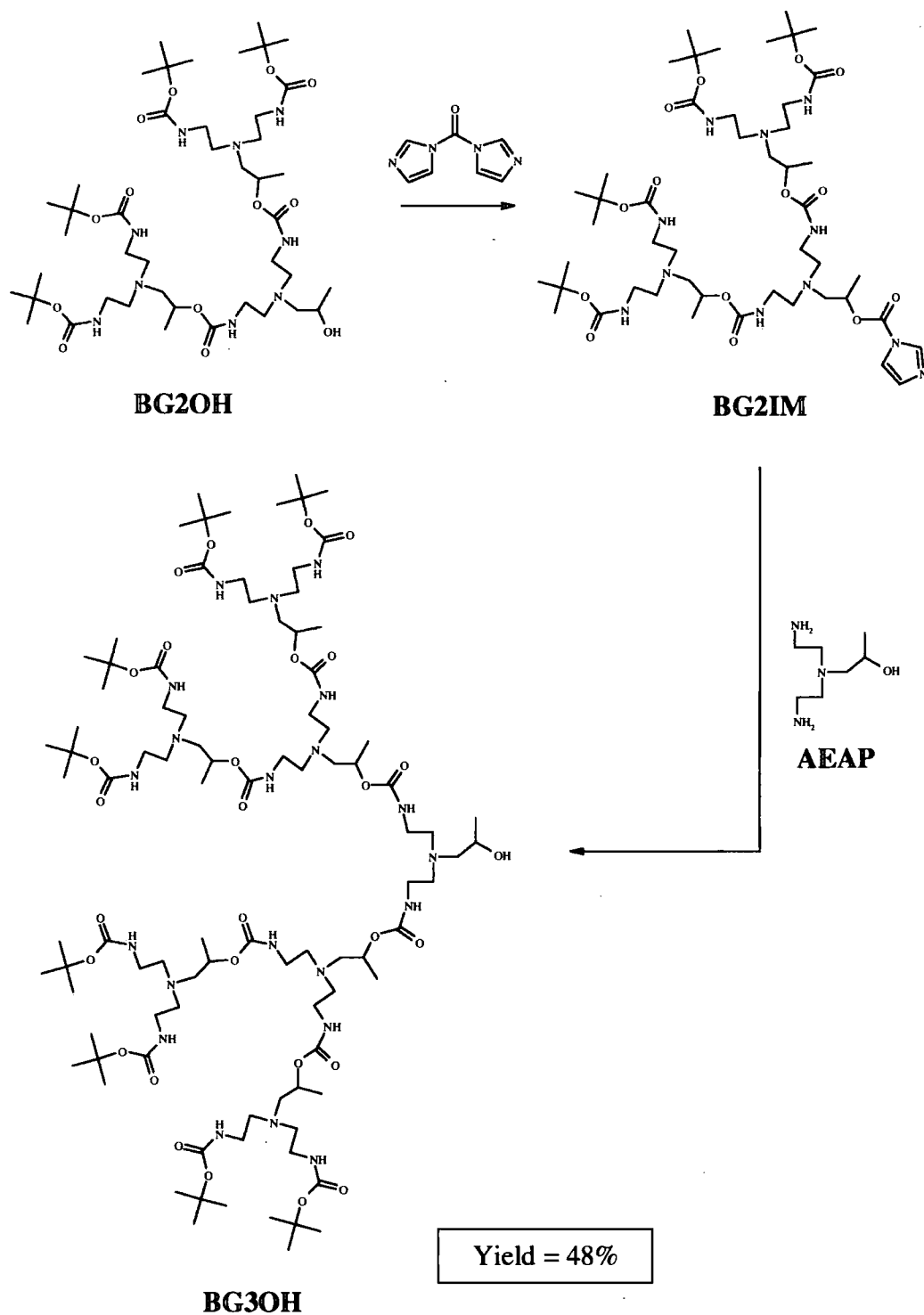


Figure 2.22 Synthesis of a third generation dendron

#### b) Other Terminal Groups

The third generation dendrons with 4-heptyl and cyclohexyl terminal groups, **HG3OH** and **CG3OH** were synthesised using the same procedure as above (Figure 2.23, overleaf). The cyclohexyl-terminated dendron was isolated as a colourless amorphous solid and the equivalent 4-heptyl structure as a sticky colourless oil.

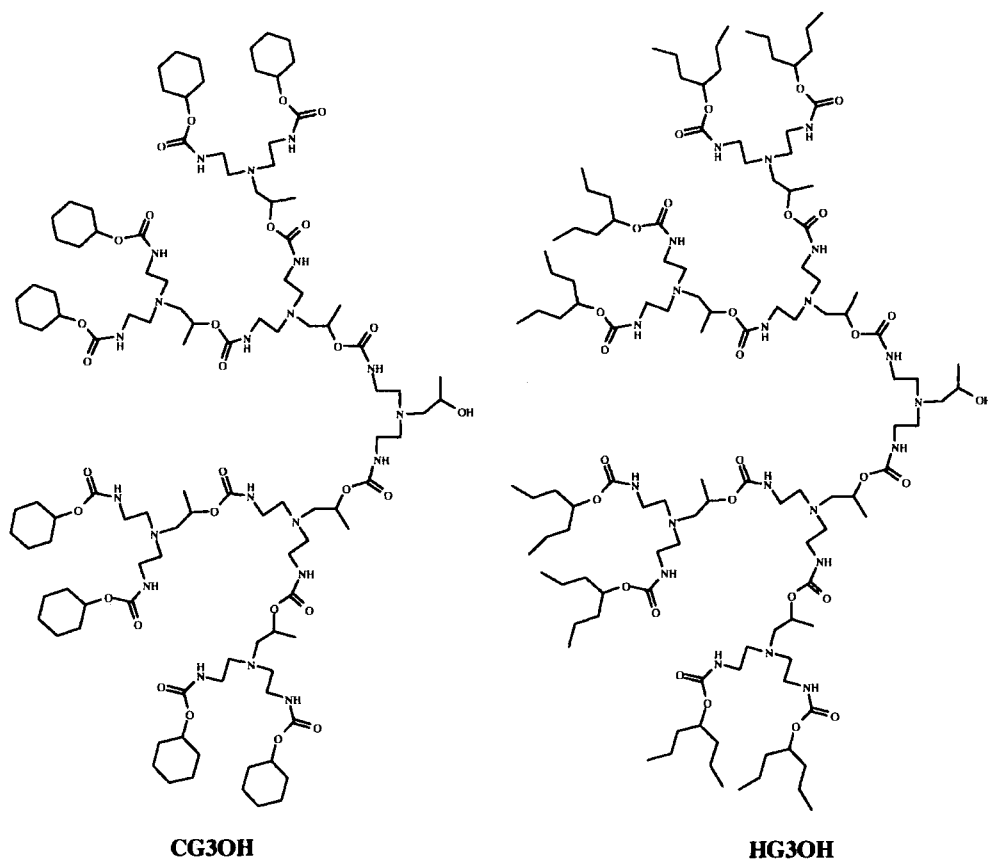


Figure 2.23 Third generation dendrons with 4-heptyl and cyclohexyl terminal groups

### c) Characterisation

The number of observed resonances in the  $^{13}\text{C}$  NMR spectra of the third generation dendrons was lower than expected because of the overlap of signals corresponding to carbons in equivalent positions in successive layers of the structure. For example, the spectrum of **BG3OH** contains 15 distinct carbon signals but there are 20 different carbon environments in the macromolecule (Appendix, page IV). The carbonyl regions of the spectra for dendrons **BG3OH** and **CG3OH** contain three resonances, *e.g* in the *t*-butyl terminated dendron the carbon signals are at 158.3 ppm, 158.7 ppm and 158.8 ppm (Figure 2.24). The closer the carbonyl group is to the focal point of the dendron the greater the downfield shift of the resonance. The  $^{13}\text{C}$  NMR spectrum of the 4-heptyl terminated third generation dendron is also included in the Appendix (page V) and only two signals are observed in the carbonyl region in this case.

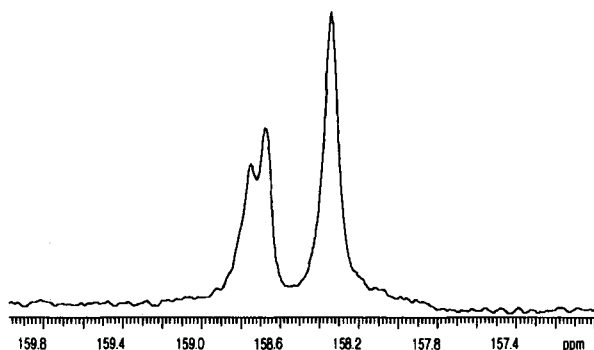


Figure 2.24 Carbonyl region of  $^{13}\text{C}$  NMR spectrum of **BG3OH**

Each of the third generation dendrons has seven stereocentres and the calculated number of different diastereoisomers is 21. Unsurprisingly, the presence of all these isomers is not evident in the  $^{13}\text{C}$  NMR spectrum. However, the carbon resonance corresponding to the chiral centre at the focal point does appear to be split but no pattern could be resolved. (Figure 2.25).

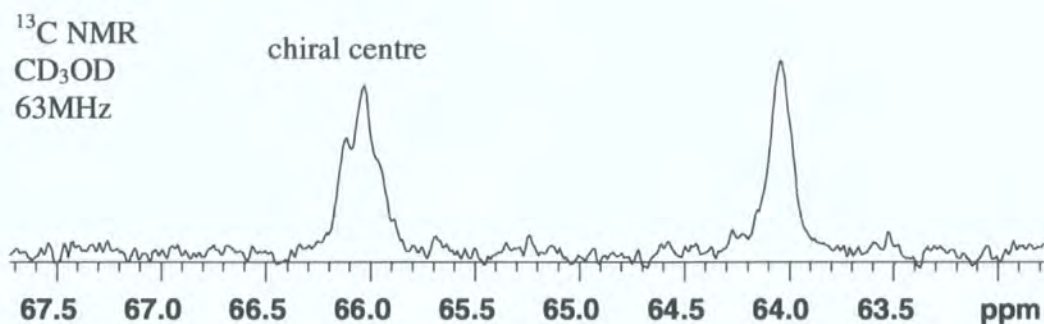


Figure 2.25 Carbon resonances at the focal point of **BG3OH**

The third generation dendrons were analysed by MALDI-TOF mass spectrometry using the Voyager and Kratos instruments. As an example, the mass spectrum (Voyager) for the dendron **HG3OH**, which has a calculated molecular weight of 2422.3 is shown below (Figure 2.26). The  $[\text{M}+\text{H}]^+$  species is observed at an  $m/z$  value of 2423.6 and the ions cationised with sodium and potassium,  $[\text{M}+\text{Na}]^+$  and  $[\text{M}+\text{K}]^+$ , are present at  $m/z$  values of 2445.2 and 2461.2.

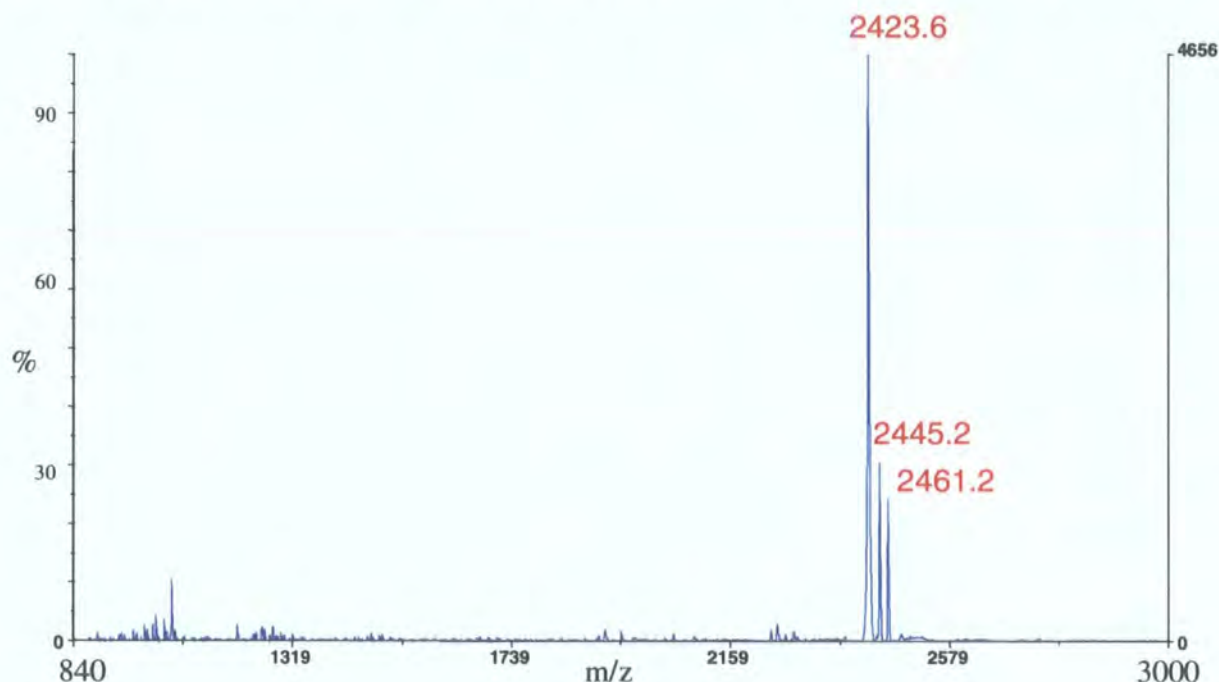


Figure 2.26 MALDI-TOF (Voyager) mass spectrum of **HG3OH**



## 2.4.5 Fourth Generation Dendron

### a) Synthesis

The fourth generation dendron with cyclohexyl end groups **CG4OH** was synthesised using a similar experimental procedure to that employed for the second and third generation dendrons. The starting material for the one-pot reaction was the third generation dendron **CG3OH** (Figure 2.26).

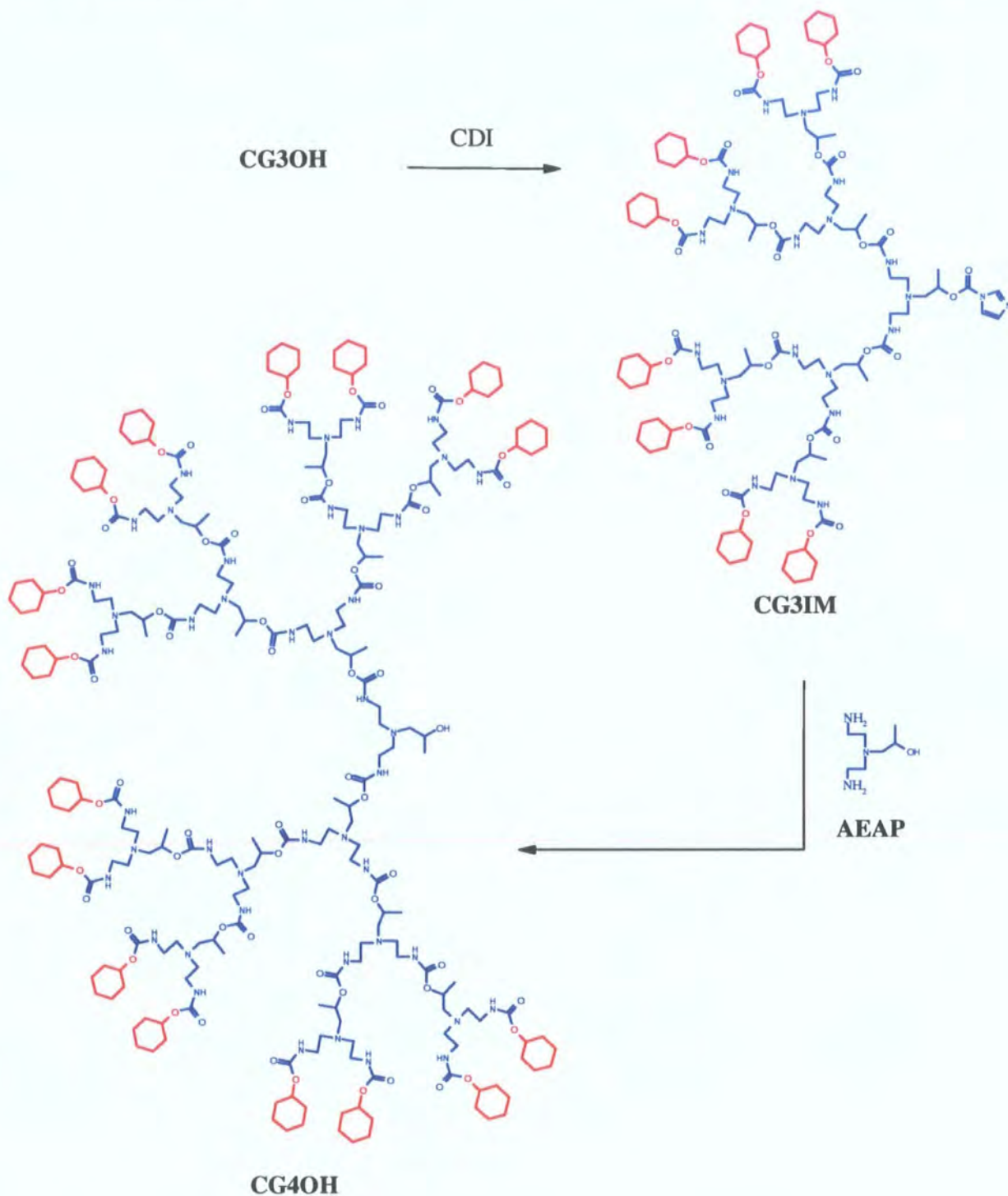


Figure 2.26 Synthesis of fourth generation dendron **CG4OH**

The crude product was analysed by GPC and the presence of two peaks in a roughly 2:1 ratio was revealed. The peak with the shorter retention time, and therefore larger hydrodynamic volume, was of lower intensity. This observation was consistent with the third generation dendron (**CG3OH**) and/or the product of mono-substitution being the predominant species being present at the end of the reaction rather than the desired di-substitution product. However, purification by silica gel chromatography and preparative GPC was successful and gave **CG4OH** as a colourless amorphous solid in a yield of 14%. There are several possible explanations for the low yield of the reaction. Firstly, the correct stoichiometric ratios of starting materials were difficult to obtain because of the inaccuracy involved in weighing the branching unit. Also, despite the reaction occurring under an atmosphere of  $N_2$  and care taken during storage of **AEAP**, the hygroscopic nature of the molecule may introduce water into the reaction causing the decomposition of the adduct **CG3IM**. Finally, the steric demands in coupling two bulky third generation wedges to the branching unit may decrease the yield.

#### b) Other Terminal Groups

The isolation of the fourth generation dendrons with *t*-butyl and 4-heptyl groups was unsuccessful because of the inability to remove lower molecular weight impurities.

#### c) Characterisation

The fourth generation dendron **CG4OH** was characterised by GPC, NMR and MALDI-TOF mass spectroscopy. The  $^1H$  and  $^{13}C$  NMR spectra are included in the appendix (pages V-VI). In the  $^1H$  NMR spectrum the resonances corresponding to three hydrogens of the methyl group near the focal point of the dendron ( $H_\alpha$ ) can still be distinguished from the methyl group hydrogens in other layers of the structure ( $H_\beta$ ) for which signals from successive layers overlap with signals from cyclohexyl hydrogens of the termini, which prevents integration (Figure 2.27).

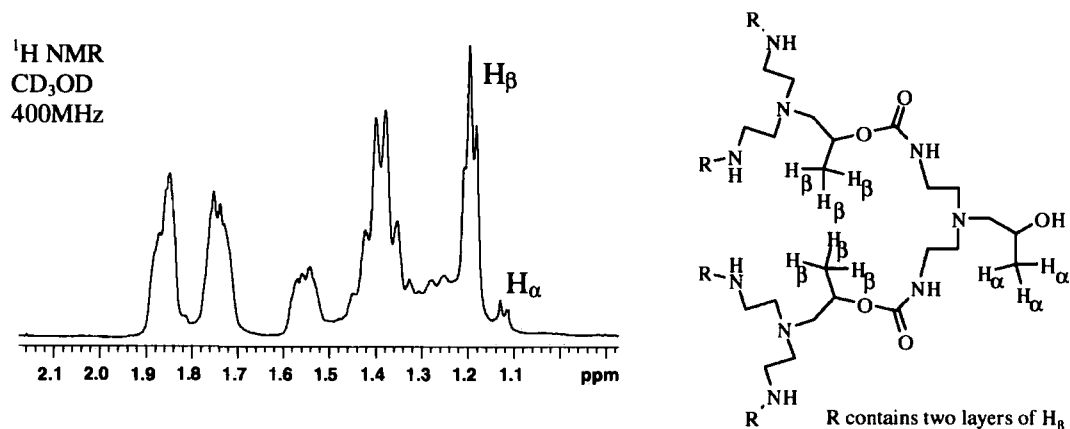
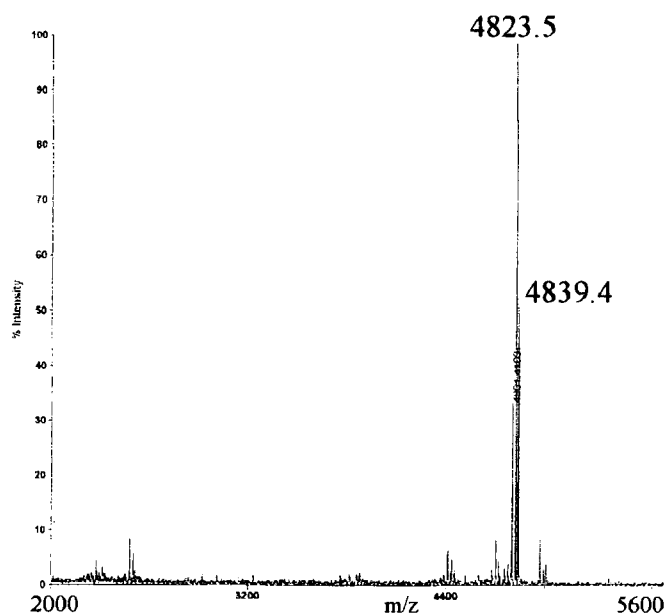


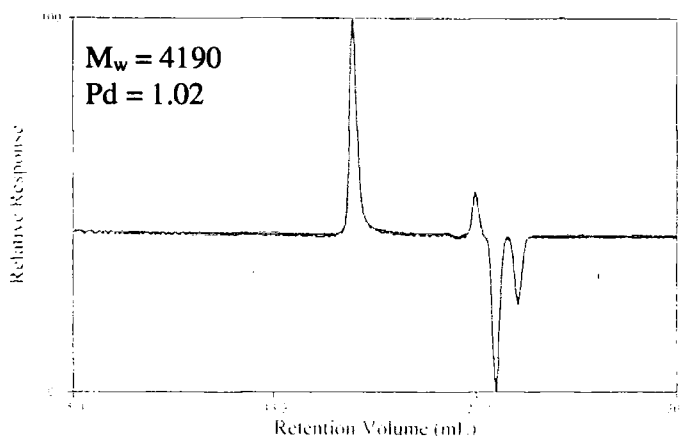
Figure 2.27 Aliphatic region of  $^1H$  NMR spectrum of **CG4OH**

The fourth generation dendron has been analysed by MALDI-TOF (Voyager) mass spectrometry and the spectrum obtained is shown below (*Figure 2.28*). The ions cationised with sodium and potassium,  $[M+Na]^+$  and  $[M+K]^+$ , are present at  $m/z$  values of 4823.5 (cf. calculated value of  $[M+Na]^+ = 4823.1$  Da) and 4839.4. A small amount of the mono-substituted dendron was detected at an  $m/z$  value of 2481.



*Figure 2.28* MALDI-TOF(Voyager) mass spectrum of fourth generation dendron **CG4OH**

The corresponding GPC trace of **CG4OH** was obtained by conventional calibration against linear polystyrene (random coil) standards (*Figure 2.29*). The  $M_w$  value (4190 Da) found from this analytical method was lower than the calculated and experimentally determined value (ca. 4800 Da) from mass spectrometry (see pages 62-63 for discussion). However, analysis of the higher generation dendrons by GPC was considered a valuable technique for structure elucidation when used in conjunction with other techniques, *i.e.* NMR and mass spectrometry, and was thought to provide a good indication of sample purity.



*Figure 2.29* GPC trace of fourth generation dendron **CG4OH**

## 2.4.6 Polyurethane Dendrimers

### a) Synthesis

A series of polyurethane dendrimers was synthesised from the first, second and third generation dendrons discussed in the previous section. In each case, the reaction scheme involved activation of the focal point followed by coupling of the reactive dendron with a trifunctional core unit. This was achieved by the consecutive addition of CDI and the trisamine core **TAEA** in a one-pot reaction. The synthesis of the *t*-butyl terminated generation dendrimer **BG1D**, which has a molecular weight of 1307 Da, is outlined below (Figure 2.30).

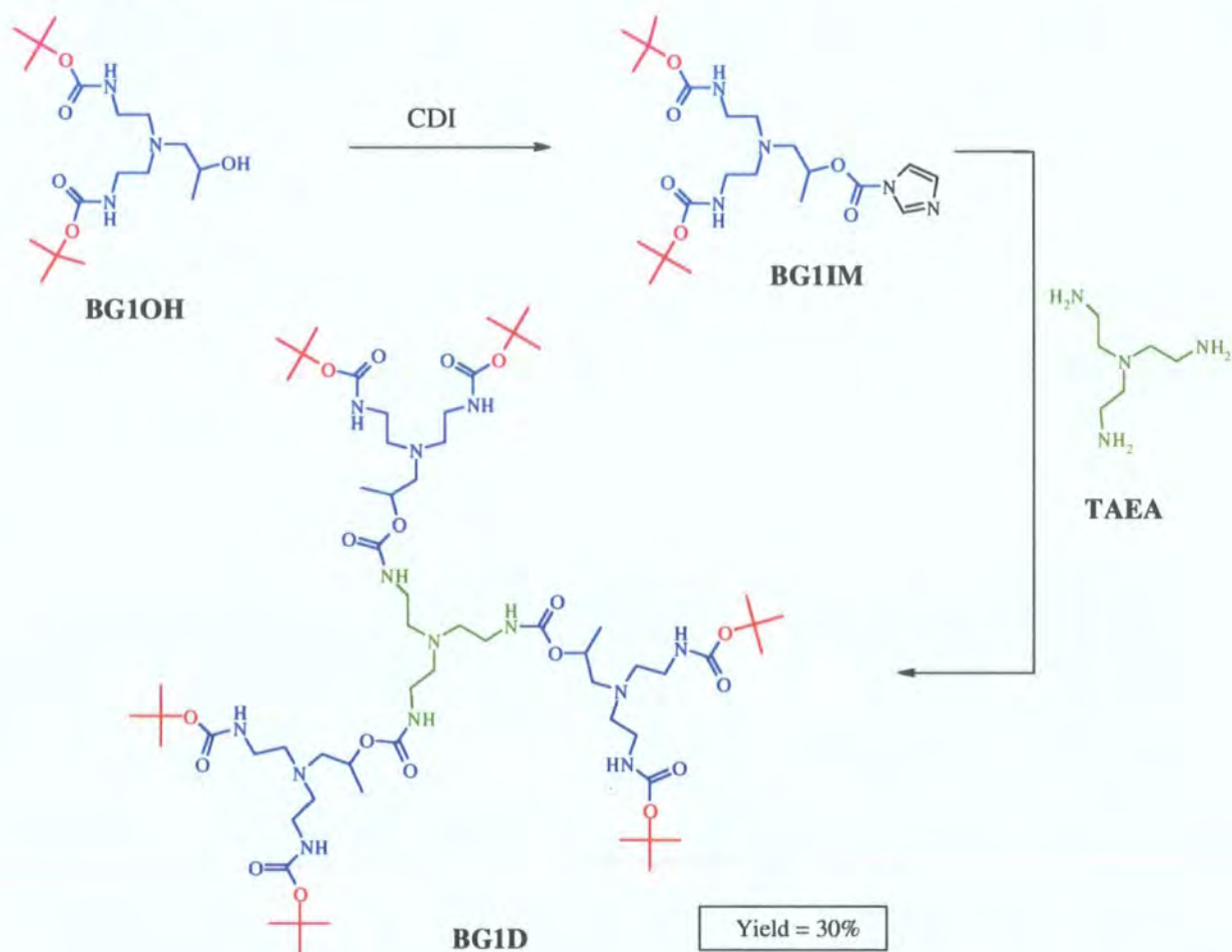


Figure 2.30 Synthesis of first generation dendrimer **BG1D**

The dendrimer **BG1D** and the corresponding cyclohexyl terminated structure **CG1D** (Figure 2.31, overleaf) were isolated as colourless amorphous solids after purification by silica gel chromatography. The equivalent dendrimer with 4-heptyl end groups, **HG1D**, was isolated as a sticky colourless oil after a similar synthetic and purification procedure (Figure 2.31, overleaf). The difference in polarity between the impurities and the first generation dendrimers resulted in somewhat easier purification compared to the dendron synthesis.



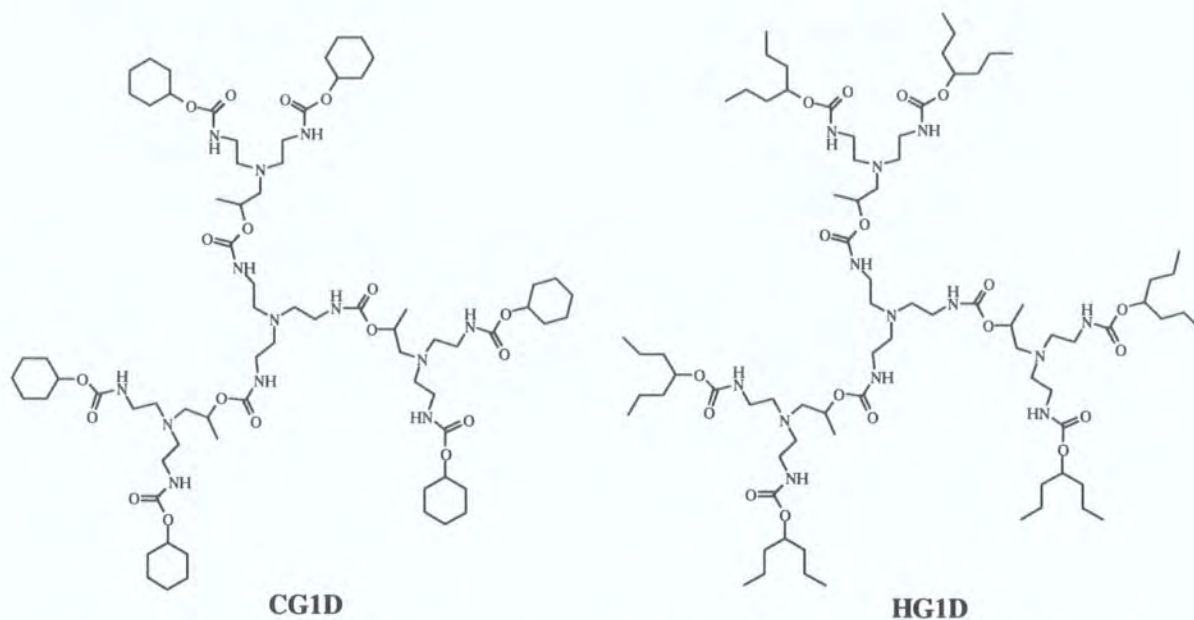


Figure 2.31 First generation dendrimers with cyclohexyl and 4-heptyl end groups

Second generation dendrimers with *t*-butyl, cyclohexyl and 4-heptyl end groups were synthesised from the appropriate second generation dendrons in yields of between 24% and 41% (e.g. **BG2D**, Figure 2.32).

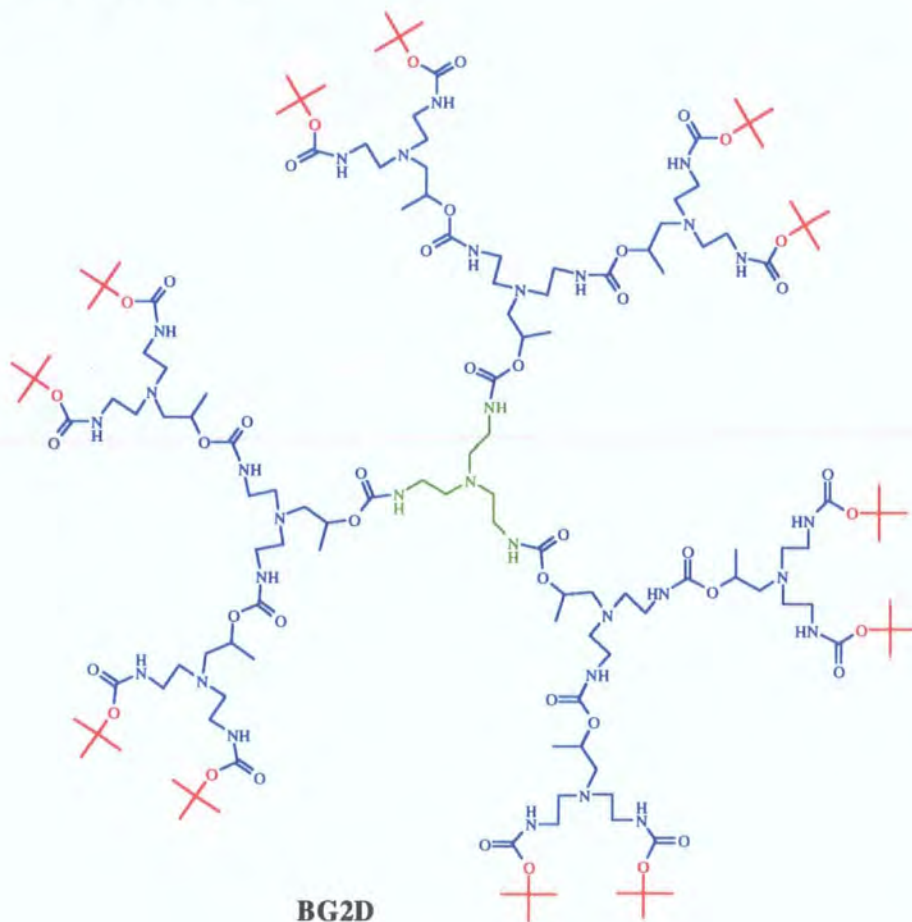


Figure 2.32 Second generation dendrimer **BG2D**

The reaction procedure for the preparation of the second generation dendrimer followed a similar method to that used in the synthesis of the first generation. However, purification was more challenging because of the smaller polarity differences between the desired macromolecule and impurities in the crude mixture. Consequently, it was necessary to purify the dendrimer by preparative GPC (Biobeads) after silica gel chromatography. The *t*-butyl and cyclohexyl terminated structures **BG2D** and **CG2D** were isolated as colourless amorphous solids and **HG2D** was isolated as a sticky colourless oil. The molecular weights of **BG2D**, **CG2D** and **HG2D** were calculated to be 3032.8, 3345.2 and 3537.7 Daltons respectively.

Two third generation dendrimers with either *t*-butyl or 4-heptyl end groups were synthesised from third generation dendrons **BG3OH** and **HG3OH** (e.g. **HG3D**, Figure 2.33).

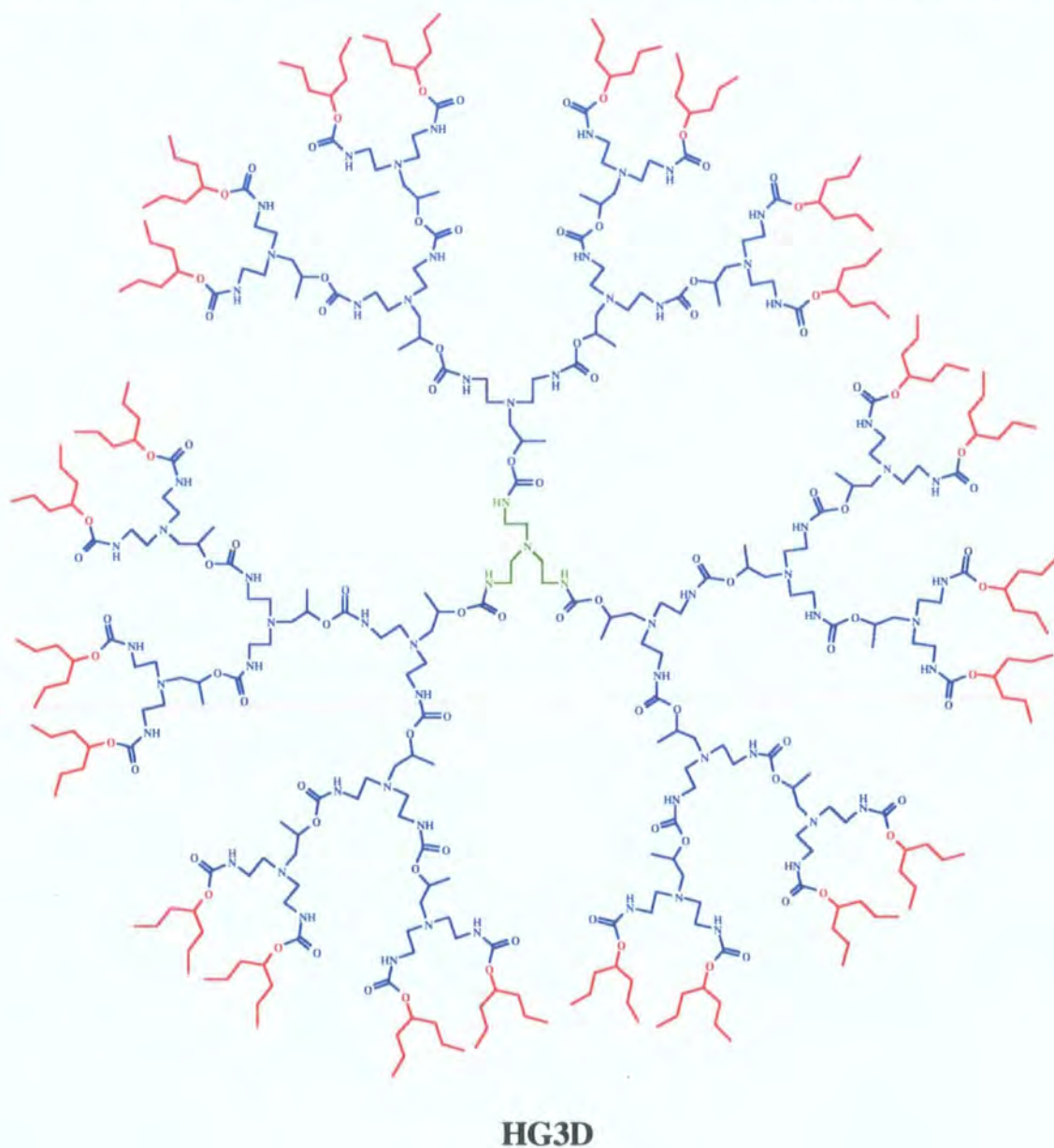


Figure 2.33 Third generation dendrimer **HG3D**

The third generation dendrimers **BG3D** and **HG3D** were isolated as colourless amorphous solids after purification by silica gel chromatography and preparative GPC (Biobeads) in yields of 20% and 10%. The dendrimers **BG3D** and **HG3D** have calculated molecular weights of 6481.05 Da and 7490.96 Da and the latter structure is the largest dendritic molecule synthesised in this study.

The first, second and third generation dendrimers synthesised were soluble in chloroform, dichloromethane, tetrahydrofuran, toluene, acetone, acetonitrile, ethyl acetate and methanol but insoluble in hexane and water. The solubility of **BG3D** in methanol was considerably less than the other dendrimers, and so when deuterated methanol was used for NMR analysis, gentle heating of the sample was required for the solute to dissolve.

## b) Characterisation

### *Introduction*

The polyurethane dendrimers were characterised by  $^{13}\text{C}$  and  $^1\text{H}$  NMR spectroscopy, electrospray (ES) and/or MALDI-TOF mass spectrometry, GPC and elemental analysis. For the second and third generations mass spectrometry and GPC were the key techniques for structure elucidation. This section summarises the characterisation methods used for analysis of the dendrimers but the complete data can be found in the experimental section (pages 143 to 153).

### *NMR Spectroscopy*

For a series of dendrimers of different generations with one type of end group the  $^{13}\text{C}$  and  $^1\text{H}$  NMR spectra are almost identical. This is caused by the high symmetry of the molecule and the overlap of resonances corresponding to nuclei in equivalent positions in successive layers. This effect is particularly noticeable in the  $^{13}\text{C}$  NMR spectra of the second and third generation dendrimers, as there are fewer resonances than expected for the number of different carbon environments in the molecules. Quantitatively, the three consecutive generations of the *t*-butyl terminated series have 11, 16 and 23 distinct carbon environments and the  $^{13}\text{C}$  NMR spectra of all three structures display only 11 resonances. The spectra of the first and second generation dendrimers, **BG1D** and **BG2D**, are included in the Appendix, (pages VI-VII) and the spectrum of **BG3D** is shown overleaf (*Figure 2.34*). A similar pattern is evident for the dendrimer series with 4-heptyl end groups and the  $^{13}\text{C}$  NMR spectrum of the third generation dendrimer is included in the Appendix (page VIII). There is no splitting effect for the resonances corresponding to the chiral centres; however, the broadness of the

peaks may mask the evidence as was observed for the outer chiral centres in the second generation dendrons (pages 38-40).

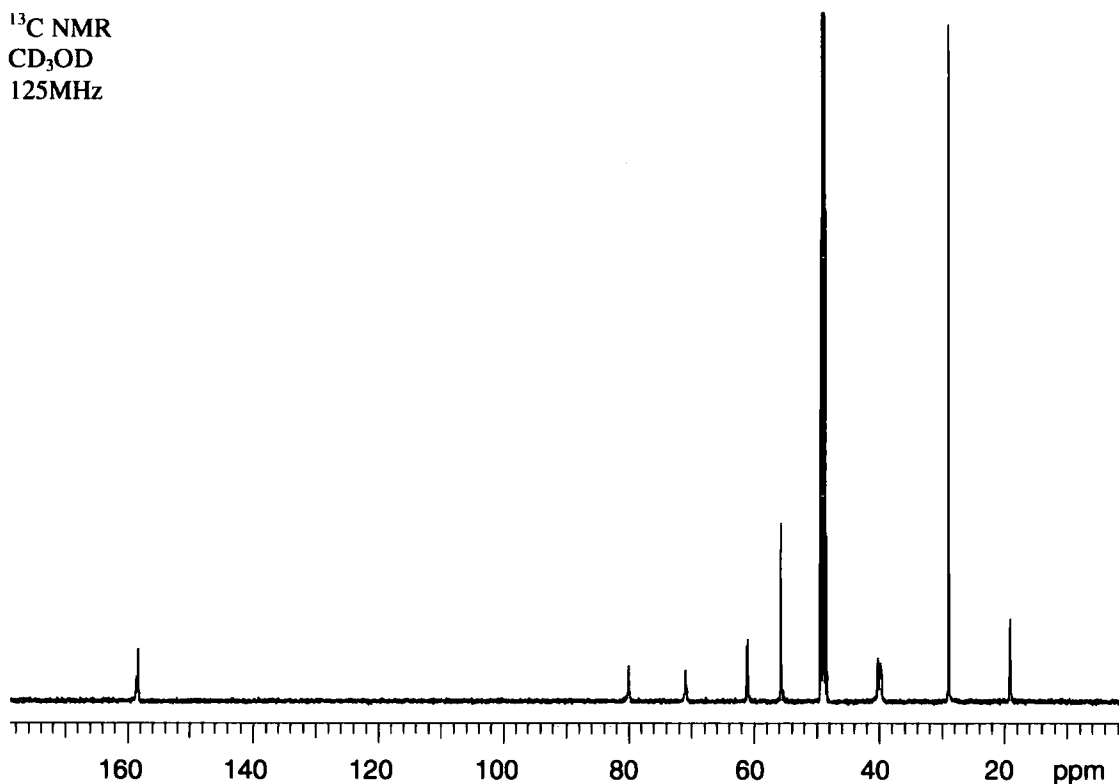


Figure 2.34 <sup>13</sup>C NMR spectrum of third generation dendrimer BG3D

The <sup>1</sup>H NMR spectra for the two dendrimer series containing either *t*-butyl or 4-heptyl end groups are included in the Appendix (pages VIII-XI). Within each series, the spectra are very similar so it becomes evident that at higher generations characterisation of the compounds by NMR spectroscopy is not very informative. However, there are a few characteristic regions of the <sup>1</sup>H NMR spectra that can be used for the rapid analysis of the dendrimer during purification. For example, in all dendrimers the methyl hydrogens, adjacent to the chiral centres in successive layers are observed as one coincident doublet (Figure 2.35).

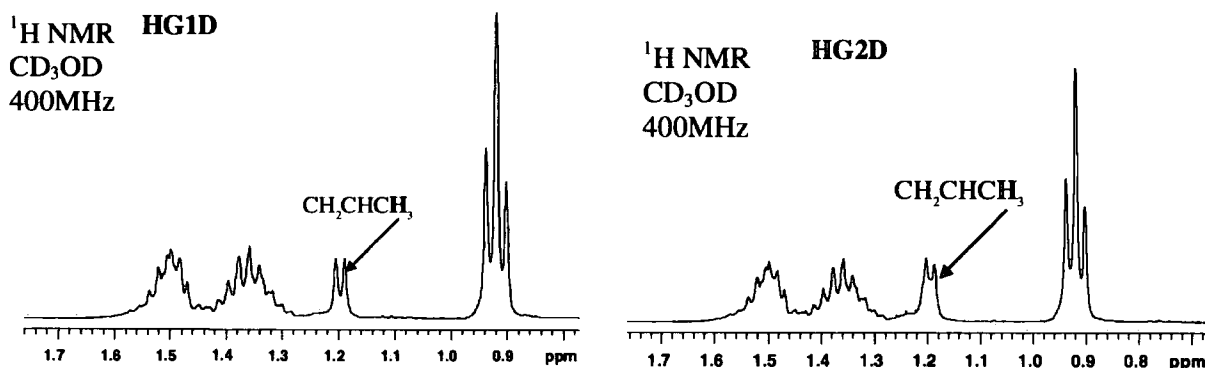


Figure 2.35 Aliphatic regions of the <sup>1</sup>H NMR spectra of HG1D and HG2D



A similar pattern to that observed for the N-H resonances of the urethane groups in the second generation dendrons is found for the first generation dendrimers with *t*-butyl, cyclohexyl and 4-heptyl end groups, as the outer N-H resonances shift downfield in the dendrimer sequence **BG1D**, **CG1D** and **HG1D** (Table 2.1). The appropriate regions of the spectra for **HG1D** and **BG1D** are shown below in which it can be observed that the chemical shifts of the N-H resonances for the inner urethane groups are roughly identical whereas the corresponding resonances for the outer urethane units vary by about 0.2 ppm (Figure 2.36).

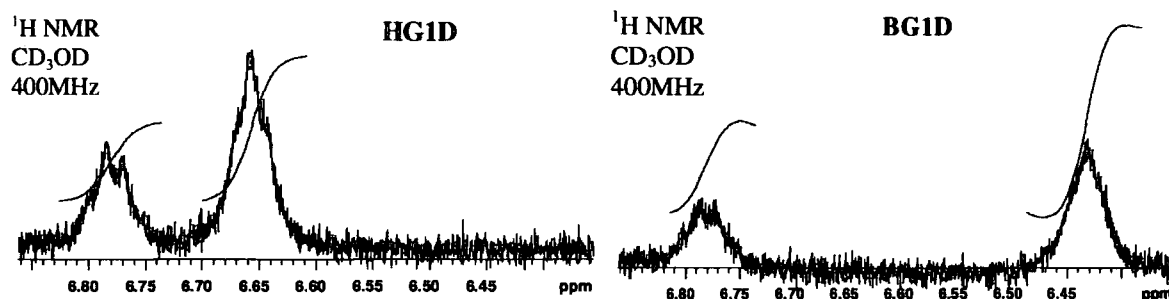


Figure 2.36 Urethane N-H resonances of **HG1D** and **BG1D**

	N-H resonance of urethane (ppm) in CD <sub>3</sub> OD <sup>a</sup>	
	Inner	Outer
<b>HG1D</b>	6.79	6.66
<b>CG1D</b>	6.77	6.60
<b>BG1D</b>	6.79	6.43

<sup>a</sup> The chemical shifts of the N-H resonances were constant with different concentrations

Table 2.1 Urethane N-H resonances for first generation dendrimers

The N-H resonances for urethanes in successive layers of higher generation dendrimers were difficult to assign because of the overlap of resonances and as a consequence it was impossible to obtain similar, reliable information. For example, in the <sup>1</sup>H NMR spectrum (CD<sub>3</sub>OD, 400 MHz) of **BG3D** two N-H resonances occur at 6.71 ppm and 6.42 ppm, but the former peak is asymmetric and broad and therefore, probably composed of overlapping resonances from urethane functions in different layers. However, it is likely that the N-H resonance at 6.42 ppm corresponds to the urethane functions in the outermost layer of the dendrimer.

The hydrogen bonding interactions for dendrimers with *t*-butyl and 4-heptyl end groups and of differing generations were investigated by solution phase infrared (IR) spectroscopy. This was possible because resonances corresponding to the N-H stretching frequencies of the non-hydrogen bonded and hydrogen bonded states can be distinguished in the spectrum.<sup>7</sup> The resonance attributed to the hydrogen bonded form is broader and occurs at lower wavenumber than the resonance for the non-hydrogen bonded form. A similar analysis to determine the location of end groups for poly(propyleneimine) dendrimers with urethane or amide termini is reported in the literature.<sup>8,9</sup> In the reported study the proportion of the non-hydrogen bonded state to the hydrogen bonded state was obtained from deconvolution of the two resonances. Analysis of the IR spectra of dendrimers from the first to fifth generation resulted in the conclusion that the amount of hydrogen bonding increased with generation. This effect was explained by the closer proximity of the end groups at high generations. The hydrogen bonding was also established to be intramolecular rather than intermolecular, as the proportion of the hydrogen bonded and non-hydrogen bonded states remained constant for different concentrations of the dendrimer solutions.

In this study the IR spectra in dichloromethane ( $\text{CH}_2\text{Cl}_2$ ) of the polyurethane dendrimers with *t*-butyl and 4-heptyl end groups were obtained and after subtraction of the pure solvent spectrum, only the resonances from the dendrimer were observed. The IR spectra of the macromolecules were performed at only one concentration for each dendrimer. However, supporting evidence from NMR data (pages 41 and 55), suggests that the hydrogen bonding in solution is intramolecular and hence the ratio of the N-H resonances from the two species should be the same at different concentrations. The concentration of the dendrimer solutions in  $\text{CH}_2\text{Cl}_2$  for **BG1D**, **HG1D**, **BG2D**, and **HG2D** was 1 mM but the concentrations of **BG3D** and **HG3D** were 0.15 mM and 0.38 mM respectively. The regions of the spectra including the N-H stretching frequencies of the hydrogen bonded and non-hydrogen bonded states were obtained and the two peaks deconvoluted in each case. As an example, this region and the deconvolution of the peaks for the first generation dendrimer **BG1D** is shown below (Figure 2.37, overleaf). The relative proportion of the non-hydrogen bonded form to the hydrogen bonded form could be calculated from the areas under the peaks and in this study this is quoted as the percentage of the hydrogen bonded state present, *i.e.* 73% for **BG1D**.

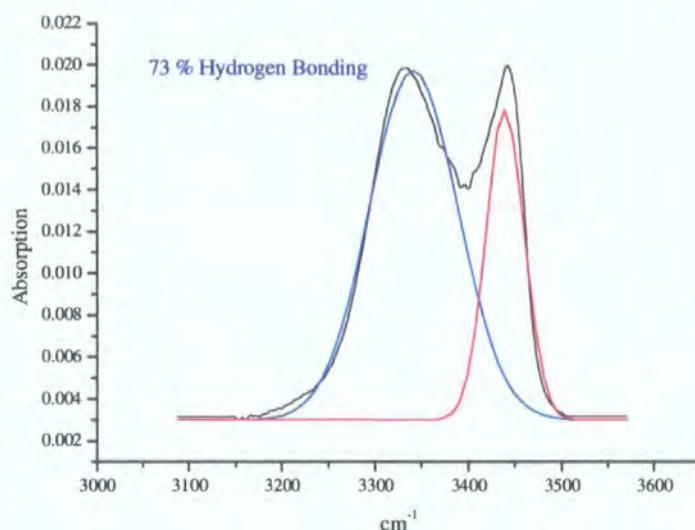


Figure 2.37 Region of IR spectrum showing resonances corresponding to hydrogen bonded and non-hydrogen bonded states and their deconvolution for **BG1D**

An analogous deconvolution procedure was carried out for the N-H resonances in the IR spectra of second and third generation dendrimers, **BG2D** and **BG3D**. Consequently, the percentage of urethane functions in the hydrogen bonded state was obtained experimentally for all three generations in the series (Table 2.2). The results indicated an increase in the percentage of urethane functions that are in a hydrogen bonded state, with an increase in generation of the dendrimer.

Dendrimer	Percentage of hydrogen bonding for urethane functions <sup>a</sup>
<b>BG1D</b>	73
<b>BG2D</b>	75
<b>BG3D</b>	80

<sup>a</sup> Deconvolution of the two peaks was repeated three times and the average percentage is quoted

Table 2.2 Percentage of hydrogen bonding for *t*-butyl-terminated dendrimers

The same experimental procedure was used to ascertain the amount of hydrogen bonding for the equivalent dendrimers with 4-heptyl end groups. The appropriate regions of the IR spectra of **HG1D**, **HG2D** and **HG3D** and the percentages of the hydrogen bonded species established by the deconvolution method, are given below (Figure 2.38 and Table 2.3, overleaf). It is evident that in contrast to the results obtained for the *t*-butyl dendrimers the hydrogen bonding for the 4-heptyl dendrimer series is constant with generation. As the number of urethane units in the dendrimer increases with generation, if the concentration of



the solutions had remained constant, a larger difference between the intensities of the peaks for the second and third generation dendrimers would have been observed.

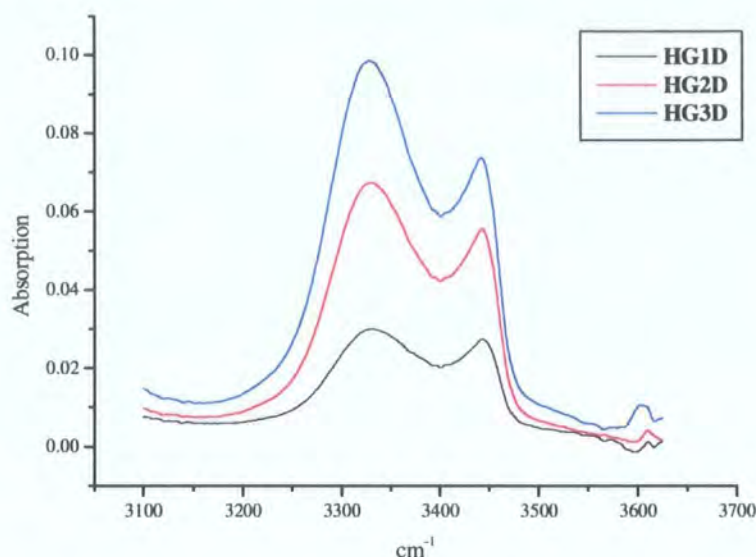


Figure 2.38 Overlaid regions of the IR spectra of 4-heptyl-terminated dendrimers

Dendrimer	Percentage of hydrogen bonding for urethane functions <sup>a</sup>
HG1D	79
HG2D	80
HG3D	80

<sup>a</sup> Deconvolution of the two peaks was repeated three times and the average percentage is quoted

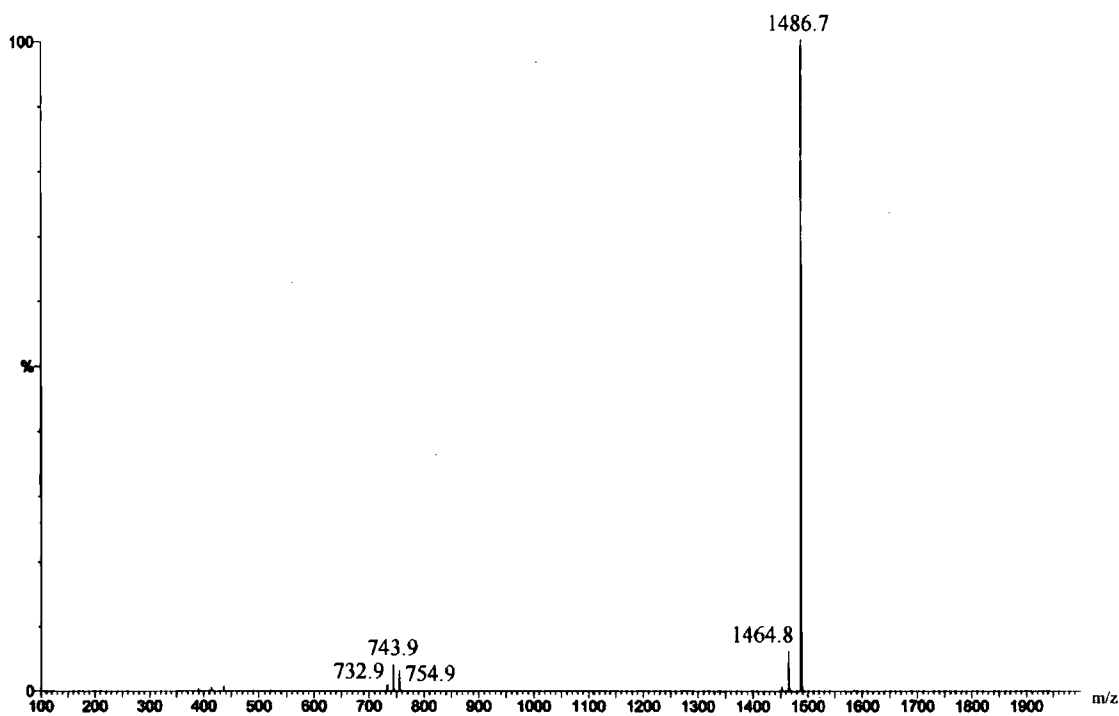
Table 2.3 Percentage of hydrogen bonding of 4-heptyl dendrimers

These results from solution phase IR spectroscopy suggest that the hydrogen bonding of the urethane groups in the first and second generation dendrimers is determined by the nature of the terminal groups. The third generation structures hydrogen bond to the same degree, *i.e.* 80%, and this percentage may be considered as a limiting, maximum value for the polyurethane dendrimers. The structures with 4-heptyl groups hydrogen bond to this maximum percentage by the first generation and an explanation is that the flexible termini do not restrict the close approach of the outermost layer of urethane functions. However, for the lower generation dendrimers with *t*-butyl termini the hydrogen bonding of the urethane functions in this outermost layer is inhibited as a consequence of the bulky and sterically demanding nature of the end groups. For the third generation dendrimer, **BG3D**, the observed maximum percentage of hydrogen bonding is reached, probably resulting from the enforced shorter distance between the urethane groups because of the denser composition of the dendrimer. The NMR data discussed previously in this chapter (page 55) suggests that the

degree of hydrogen bonding for the urethane groups near the core of **BG1D** and **HG1D** is the same whereas the outer urethane groups are hydrogen bonded to a different degree. Therefore, it is evident that the conclusions drawn from the two methods of analysing the hydrogen bonding of the dendrimers in solution are in agreement.

#### *Mass Spectrometry and Gel Permeation Chromatography (GPC)*

The first generation dendrimers were analysed by ES and MALDI-TOF mass spectrometry (Voyager and/or Kratos). In the ES mass spectra peaks corresponding to the protonated molecular ion, and ions cationised with sodium and sometimes potassium were observed, as well as some doubly cationised species. As an example, the ES mass spectrum of **CG1D**, which has a calculated molecular weight of 1463 Da, is shown overleaf (*Figure 2.39*). The mass peaks present in the spectrum are consistent with  $m/z$  values expected for  $[M+H]^+$  (1464.8),  $[M+Na]^+$  (1486.7). In addition, doubly cationised species are present at  $m/z$  values of 732.9, 743.9 and 754.9 corresponding to  $[M+2H]^{2+}$ ,  $[M+H+Na]^{2+}$  and  $[M+2Na]^{2+}$ , respectively.



*Figure 2.39 ES mass spectrum of CG1D*

For comparison with the ES mass spectrum, the MALDI-TOF (Voyager) mass spectrum of the same sample of **CG1D** is shown below (*Figure 2.40*). This implies that the array of peaks below the molecular ion is indicative of the method of analysis rather than impurities in the sample. The ES and MALDI-TOF mass spectrum of **HG1D** are included in the Appendix (pages XI-XII).

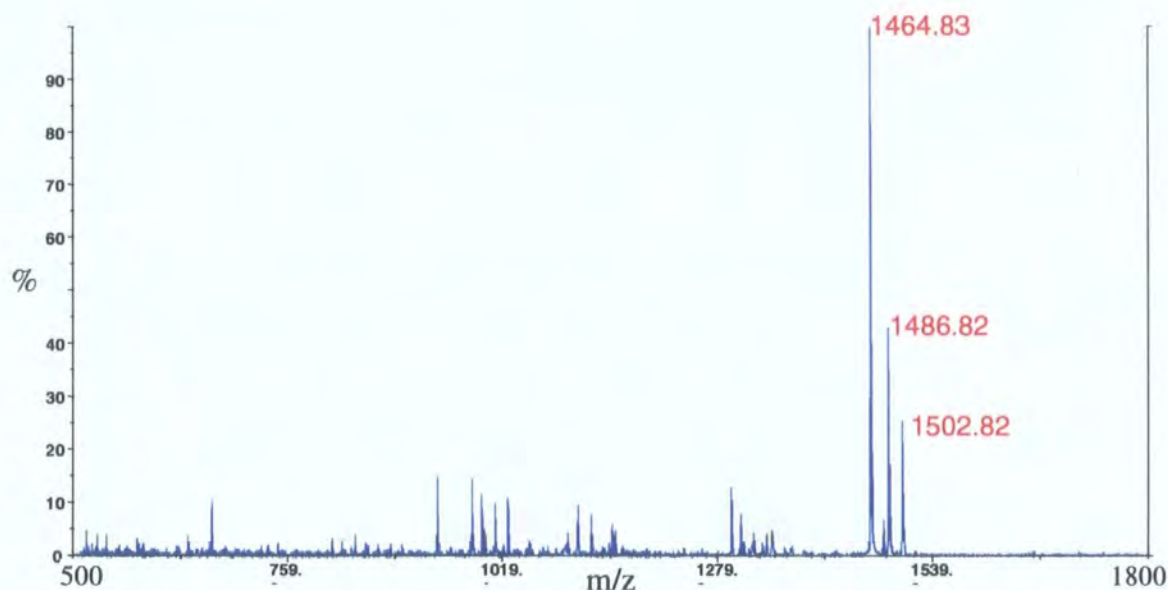


Figure 2.40 MALDI-TOF (Voyager) mass spectrum of **CG1D**

The second generation dendrimers were also analysed by ES and MALDI-TOF mass spectrometry. The ES mass spectrum of **HG2D**, which has a calculated molecular weight of 3533 Da, has peaks at  $m/z$  values of 3558.5 and 1791.7 (Figure 2.41 and full spectrum in the Appendix, page XII). It is assumed the peaks correspond to  $[M+Na]^+$  (3558.5),  $[M+2Na]^{2+}$  (1791.7), however, the results are inaccurate by a couple of mass units which is probably a consequence of the instruments' calibration.

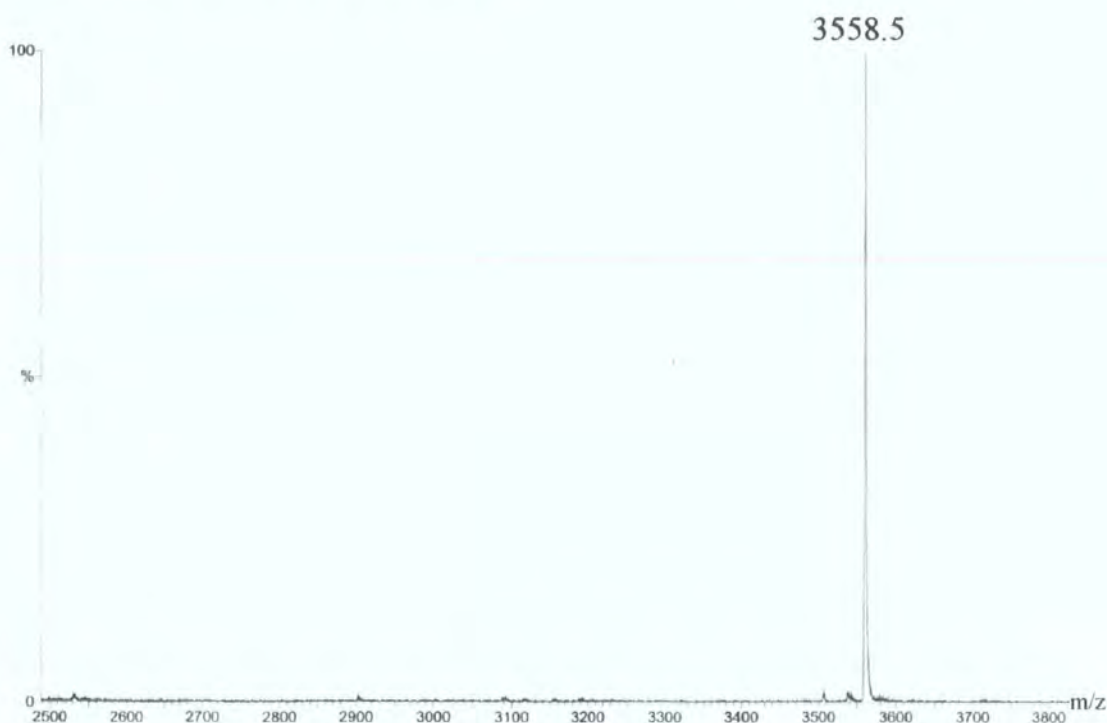
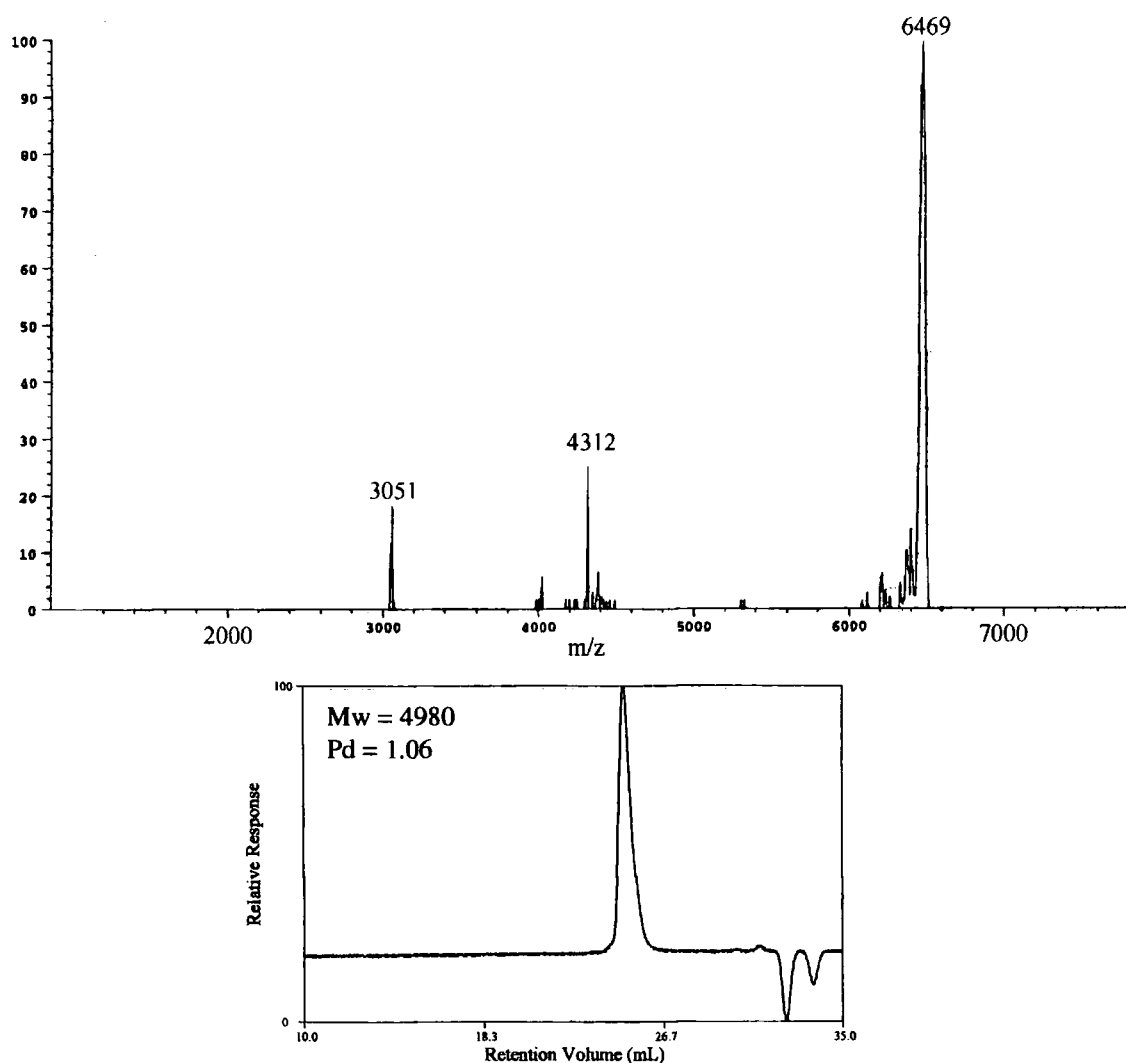


Figure 2.41 ES mass spectrum of **HG2D**

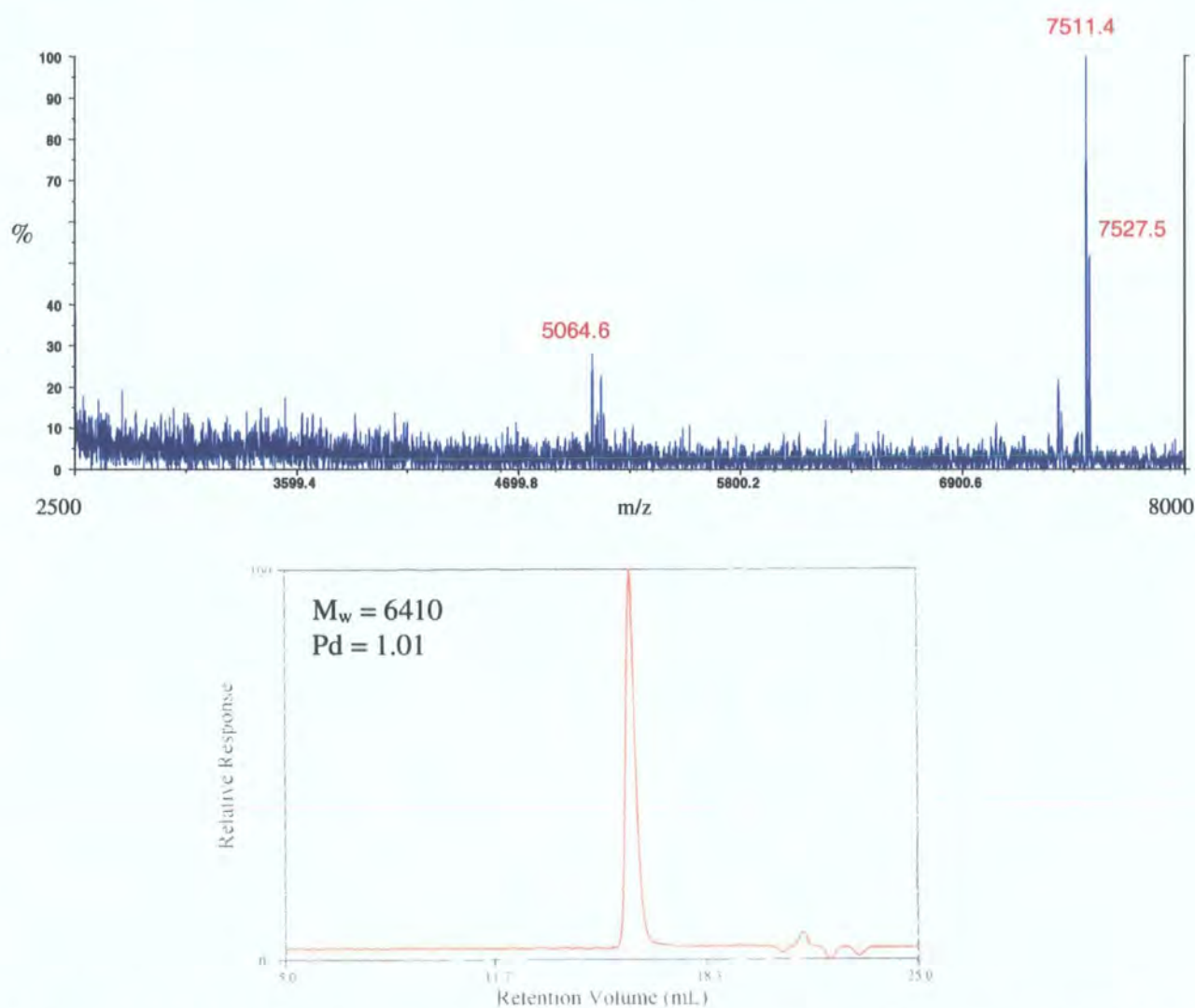
Mass spectra of good quality were difficult to obtain for the third generation dendrimers, **BG3D** and **HG3D**. For the *t*-butyl terminated dendrimer, analysis using the MALDI-TOF (Voyager) mass spectrometer did not yield any results. However, using the MALDI-TOF (Kratos) mass spectrometer it was possible to obtain an informative mass spectrum, with some perseverance (*Figure 2.42*). The calibration proved difficult in this molecular weight range and could not be relied upon. The calculated molecular weight of the **BG3D** is 6481 Da and it is thought that the peak at an  $m/z$  value of 6469 corresponds to the molecular ion  $[M+H]^+$ . The sharp peak, which occurs at an  $m/z$  value of 4312, was present in the mass spectrum of the matrix without any sample and hence is probably not to be a true mass peak. The other third peak at 3051 maybe an impurity in the sample, however this is not detected in the GPC trace of the dendrimer (*Figure 2.42*). In the ES mass spectrum of **BG3D** mass peaks were not present in the range expected, however, a series of low intensity peaks which approximately correspond to the doubly cationised species  $[M+2H]^{2+}$ ,  $[M+H+Na]^{2+}$ ,  $[M+2Na]^{2+}$  were identified at 3235.8, 3246.9 and 3257.9.



*Figure 2.42 MALDI-TOF (Kratos) mass spectrum and corresponding GPC trace of **BG3D***



The characterisation of the 4-heptyl terminated third generation dendrimer, **HG3D**, by mass spectrometry was a more straightforward process, as it was possible to obtain a MALDI-TOF (Voyager) mass spectrum of the macromolecule (*Figure 2.43*). The calculated molecular weight of the structure is 7491.0 Da and the ions cationised with sodium and potassium,  $[M+Na]^+$  and  $[M+K]^+$ , are present at  $m/z$  values of 7511.4 and 7527.5. There is also evidence of a mass peak at an  $m/z$  value of 5064.6 that corresponds approximately to the two-armed dendrimer. However, from analysis of the GPC trace of the same sample of **HG3D** (*Figure 2.43*) it is evident that the predominant species is the three-armed dendrimer.

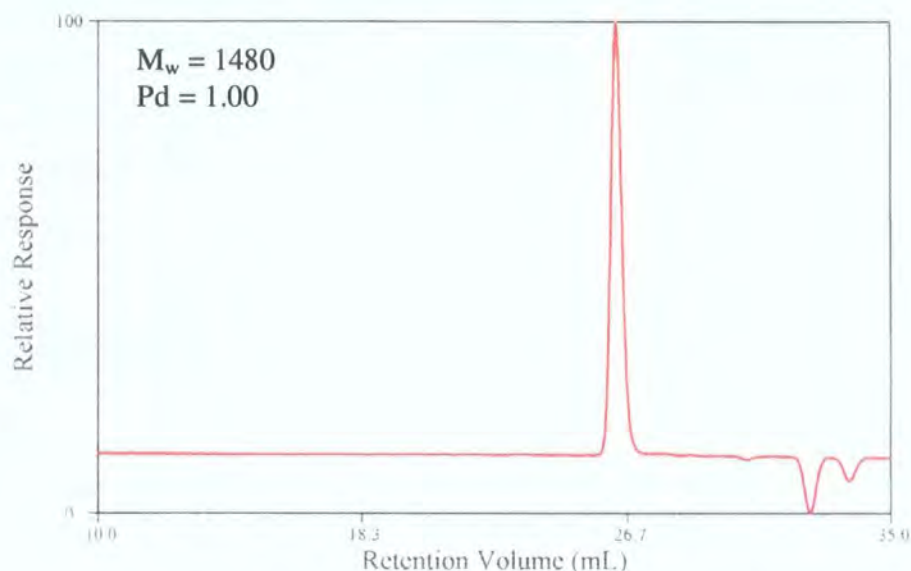


*Figure 2.43 MALDI-TOF (Voyager) mass spectrum and corresponding GPC trace of **HG3D***

The GPC traces and the corresponding  $M_w$  values shown in *Figures 2.42* and *2.43* were obtained using conventional calibration with linear polystyrene standards. For these higher generation structures the values of molecular weight obtained were *underestimated* with respect to the expected masses. This discrepancy has been reported in the literature for other



dendrimers and is explained by the higher generations adopting a denser, three-dimensional spherical conformation rendering the calibration with random coil polymers inappropriate.<sup>10,11</sup> The molecular weights obtained by GPC analysis of the first and second generation polyurethane dendrimers were reasonably accurate and, if not, were usually overestimated. For example, the GPC trace and the relevant information obtained for the first generation dendrimer, **BG1D**, with an expected molecular weight around 1300 Da is shown in *Figure 2.44*.



*Figure 2.44* GPC trace of first generation dendrimer **BG1D**

In this study, dendrimer solutions of known concentrations (4 mg/mL) were also characterised by GPC using the ‘universal calibration’ method, an approach to GPC analysis that is solely dependent on the size of the polymer in solution. From this method, the radii of gyration of the dendrimers **CG1DAC**, **CG2DAC** and **CG3DAC** were found to be 1.33 nm, 1.80 nm and 2.35 nm respectively, *i.e.* increasing with generation. These results are only considered to be qualitative because the exact values are unreliable as a consequence of the topology difference between the dendrimers and the linear, random coil polymer calibrants.

However, the principle use of GPC in the characterisation of the dendrimers (and dendrons) was in the determination of sample purity. As an explanation for this statement the GPC traces of the third generation dendrimer **HG3D** before and after purification by preparative GPC are included in the Appendix (page XIII).

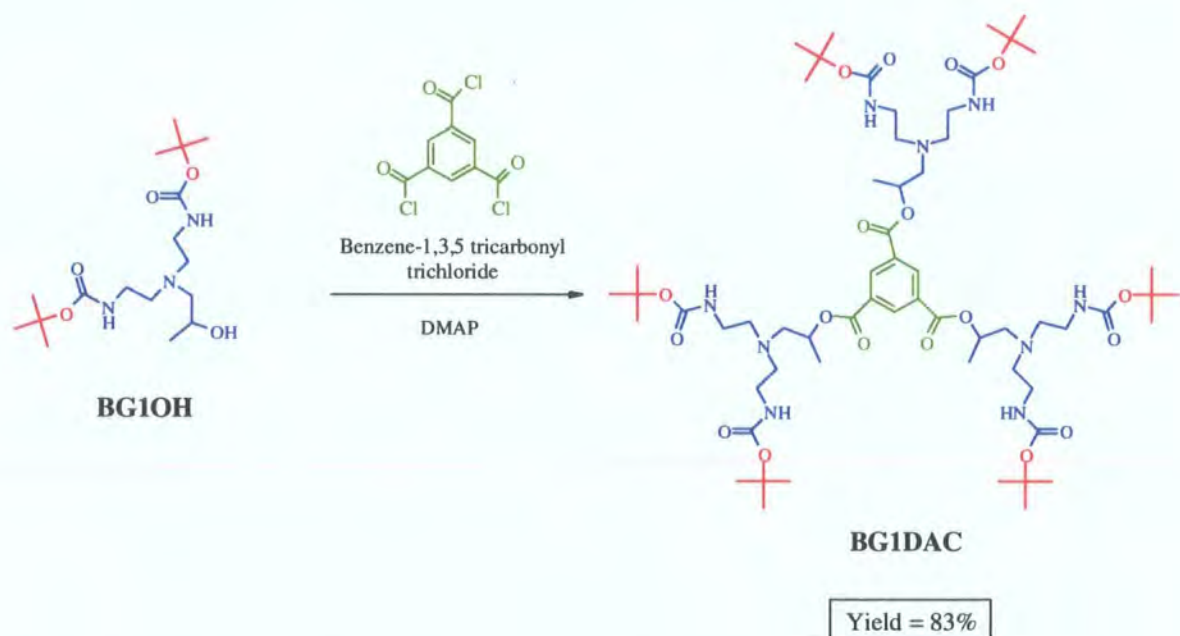
## 2.4.7 Dendrimers with Aromatic-Ester Core Unit

### a) Introduction

Another series of dendrimers was synthesised by the coupling of the first, second and third generation polyurethane dendrons to the trifunctional molecule, benzene-1,3,5 tricarboxyl trichloride (*Figure 2.45*). This trifunctional reagent has been used in several reported dendrimer syntheses to introduce either ester<sup>12-14</sup> or amide<sup>15</sup> units near the core of the dendron. In this study, the polyurethane dendrons comprise an alcohol function at this position and hence ester-linking groups are formed. The third part of the dendrimer code was modified by the substitution of the letters **DAC** for **D**, to distinguish this series of **Dendrimers with an Aromatic-ester Core** from those synthesised using the triamine molecule (see page 29).

### b) Synthesis

The method used was adapted from a literature procedure<sup>14</sup> and was similar for all three generations (see Experimental, pages 145-148 and 154). The synthesis of the first generation dendrimer with *t*-butyl terminal groups will be outlined as an example (*Figure 2.45*).

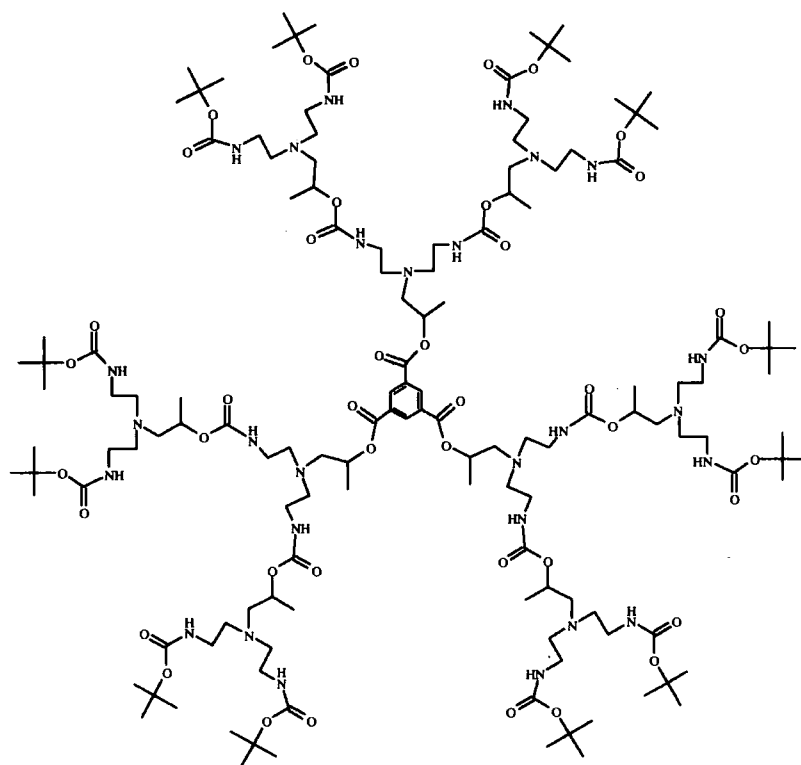


*Figure 2.45 Synthesis of a first generation dendrimer with an aromatic-ester core unit*

A solution of the first generation dendron, **BG1OH**, and 4-dimethylaminopyridine (DMAP) in benzene was refluxed for 2 hours using apparatus with a Dean-Stark trap containing molecular sieves attached. After the reaction mixture had cooled to room temperature the core unit, benzene-1,3,5 tricarboxyl trichloride, was added. The reaction mixture was stirred and heated at 40°C for four hours and was subsequently concentrated *in*

*vacuo*. The crude product was purified by silica gel chromatography, eluting with a solvent ratio of ethyl acetate:hexane 5:1, to give the first generation dendrimer **BG1DAC** as a white, amorphous solid in a yield of 83%. The high yield is probably a consequence of the unproblematic purification of the dendrimer, as the compound eluted from the column first and the polarity of impurities present in the crude mixture varied considerably. Following similar procedures, the first generation dendrimers with benzhydryl, cyclohexyl and 4-heptyl end groups, **BHG1DAC**, **CG1DAC** and **HG1DAC** were also synthesised. The dendrimers were isolated as amorphous solids with the exception of the waxy solid state of the 4-heptyl-terminated macromolecule. The calculated molecular weights of the first generation dendrimers varied from 1240.5 Da for **BG1DAC** to 1901.2 Da for **BHG1DAC**.

The second generation dendrimers with *t*-butyl, 4-heptyl and cyclohexyl end groups were synthesised from the appropriate dendrons using a similar method to that described for the first generation structures. However, a higher reaction temperature of 50°C was required and in some cases it was necessary to purify the dendrimers using preparative GPC (Biobeads) subsequent to purification by silica gel chromatography. As an example the second generation dendrimer with *t*-butyl terminal groups, **BG2DAC**, is shown in *Figure 2.46*. The dendrimers **BG2DAC** and **CG2DAC** were isolated as amorphous solids and the dendrimer **HG2DAC** as a sticky oil in yields of around 60%.



**BG2DAC**

*Figure 2.46 Second generation dendrimer with aromatic core and t-butyl end groups*



The third generation dendrimers with *t*-butyl and cyclohexyl terminal groups **BG3DAC** and **CG3DAC** (Figure 2.47) were prepared using an analogous procedure, however, a reflux temperature (80°C) was required for reaction to occur. The crude mixtures were purified by silica gel chromatography and preparative GPC (Biobeads) to give the dendrimers as amorphous solids in yields of around 45%. The 4-heptyl dendrimer, **HG3DAC**, was also synthesised but an insufficient amount of material resulted from the inability to purify the molecule to a satisfactory degree.

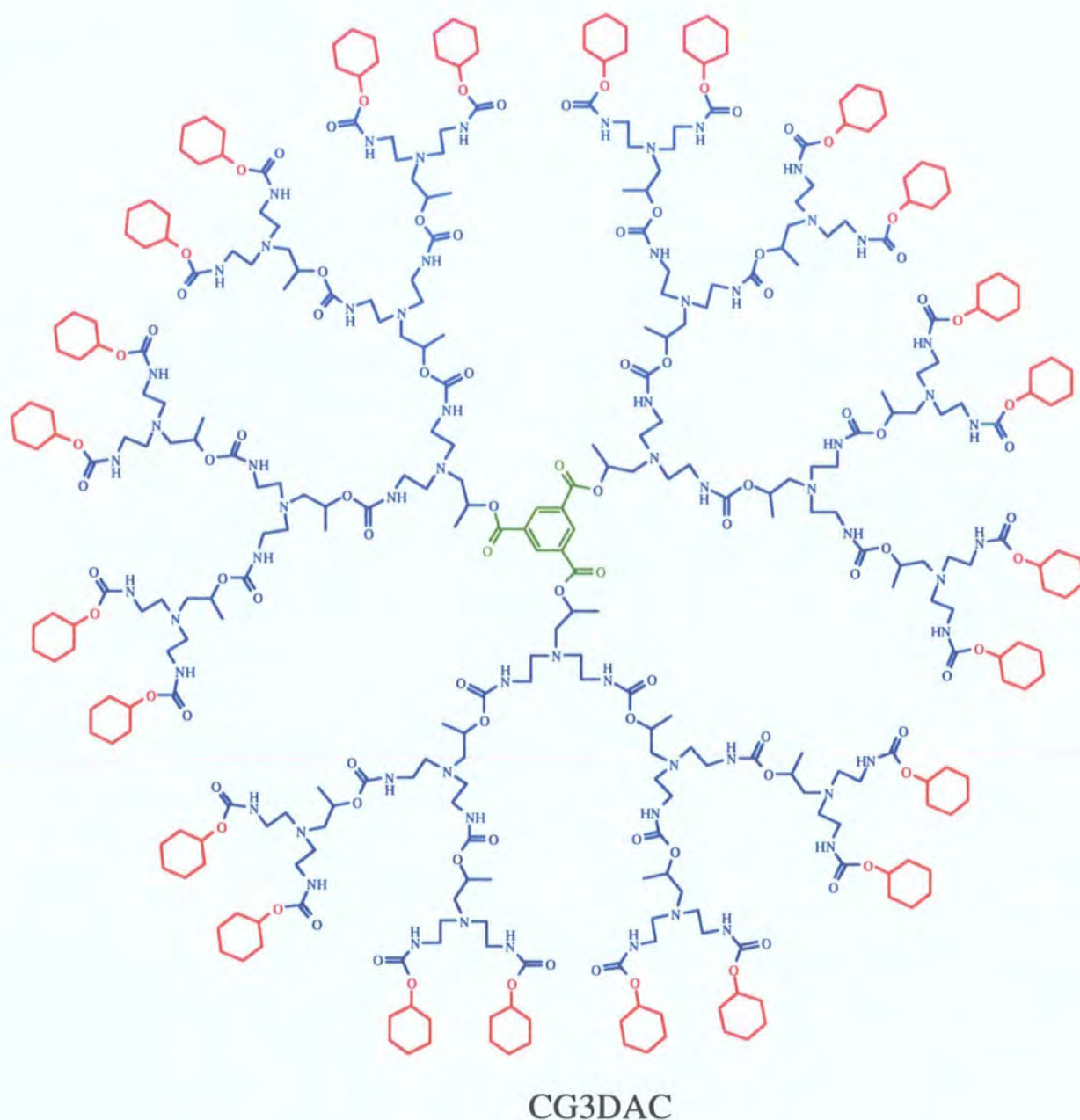
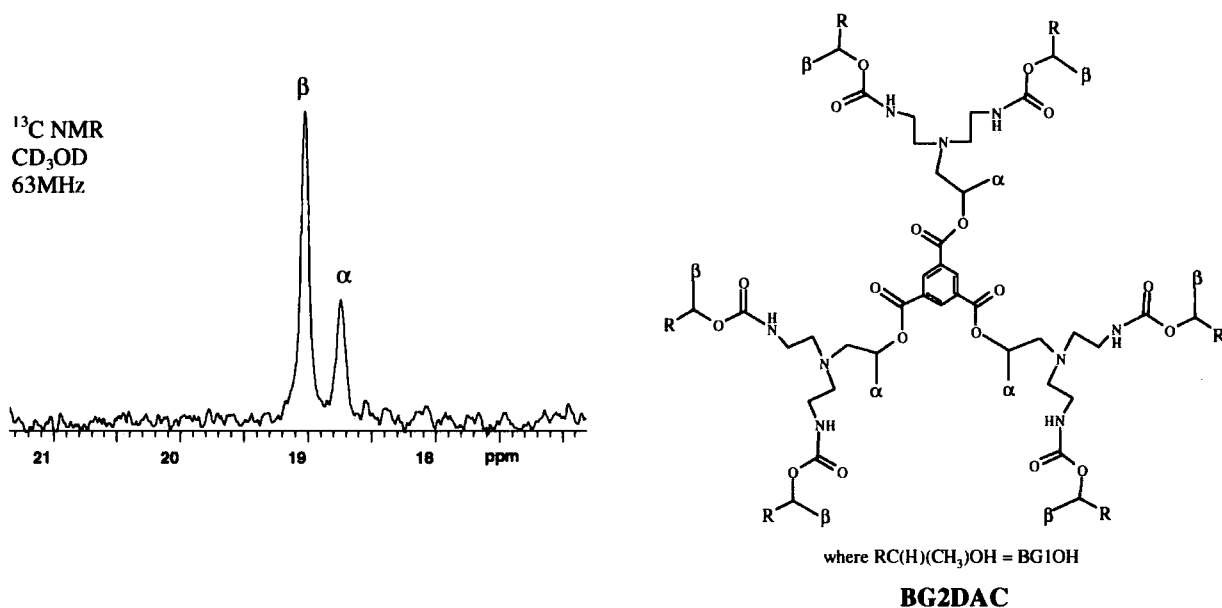


Figure 2.47 Third generation dendrimer with cyclohexyl termini and aromatic core unit

## b) Characterisation

### NMR Spectroscopy

The  $^{13}\text{C}$  and  $^1\text{H}$  NMR spectra obtained for this series of dendrimers were more informative than for the polyurethane homodendrimers as resonances corresponding to nuclei of or close to the core could be distinguished from those in the outer layers. For example, in the  $^{13}\text{C}$  NMR spectrum of **BG2DAC** the two resonances for the methyl group carbons, occur at slightly different chemical shifts whereas for the equivalent polyurethane homodendrimer, **BG2D**, only one signal was present (*Figure 2.48*).



*Figure 2.48 Resonances for the methyl group carbons in the  $^{13}\text{C}$  NMR spectrum of the second generation dendrimer **BG2DAC***

The number of resonances in the  $^{13}\text{C}$  NMR spectra for the amine-core dendrimer series did not vary with generation but in the spectra of **BG1DAC**, **BG2DAC** and **BG3DAC** an increasing number of 11, 15 and 16 resonances occurred compared with the 11, 17 and 23 distinct carbon environments in the macromolecules. The  $^{13}\text{C}$  NMR spectra of several dendrimers in this series, with either *t*-butyl or cyclohexyl termini, are included in the Appendix, pages XIV-XVI. In the downfield region of the spectra two carbon resonances from the aromatic core unit were observed together with those of the different carbonyl groups in the molecules. As an example the assignment of these peaks in the  $^{13}\text{C}$  NMR spectrum for **BG1DAC** is shown below (*Figure 2.49*, overleaf).

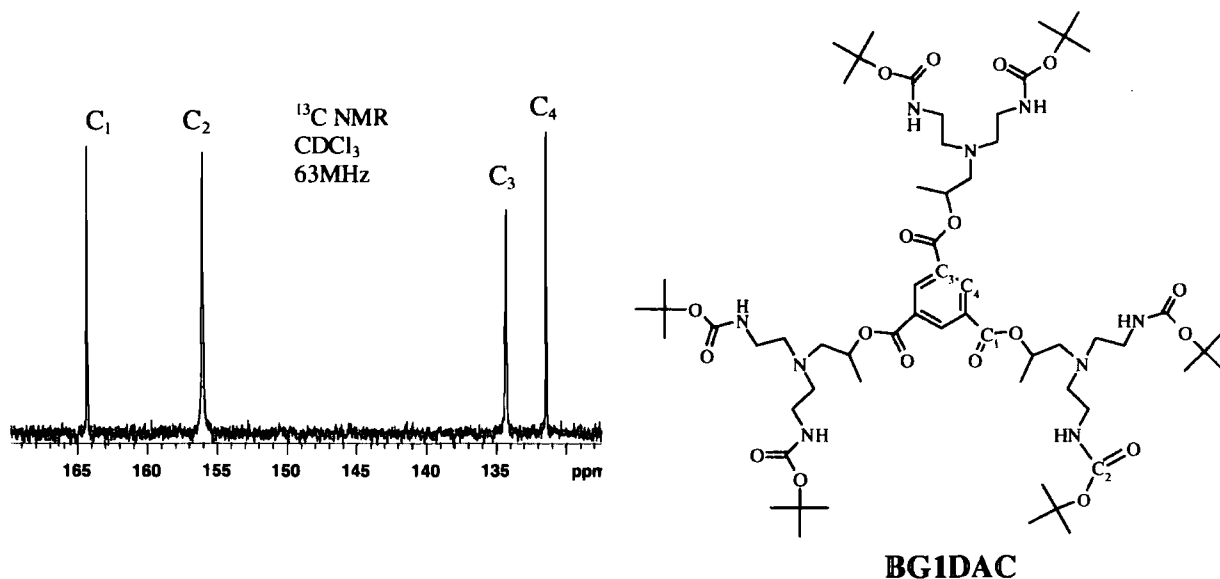


Figure 2.49 Downfield region of the  $^{13}\text{C}$  NMR spectrum of **BG1DAC**

In the  $^{13}\text{C}$  NMR spectrum of **BG3DAC** three separate signals occur at *ca.* 158 ppm corresponding to the carbonyl carbons of the different urethane groups linking successive layers of the structure (Figure 2.50). The closer the urethane group is to the centre of the dendrimer the greater the downfield shift of the carbon resonance. As expected, the carbon signal of the ester group at the core of the third generation structure, which occurs at about 166 ppm, is of a lower relative intensity than the signals from the urethane carbonyls than in the spectra for the first and second generation dendrimer.

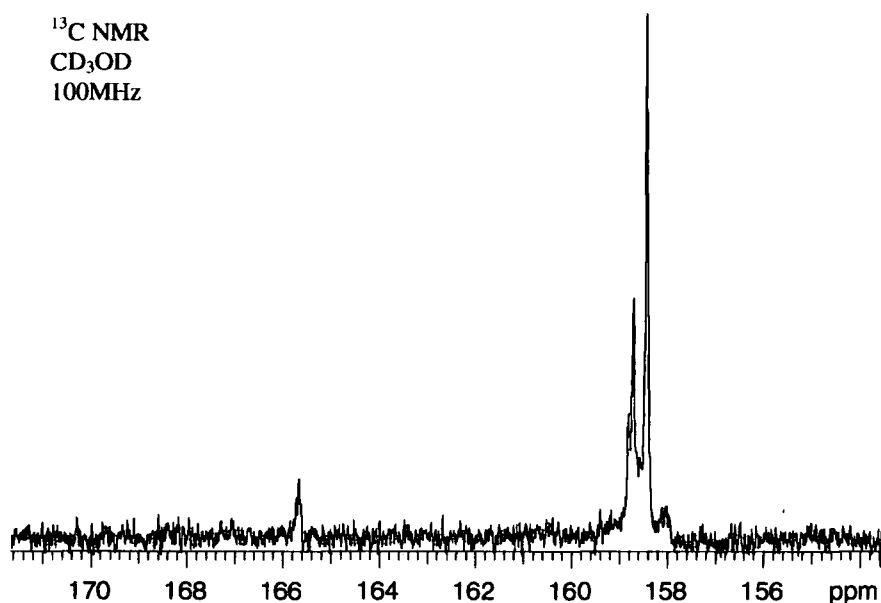
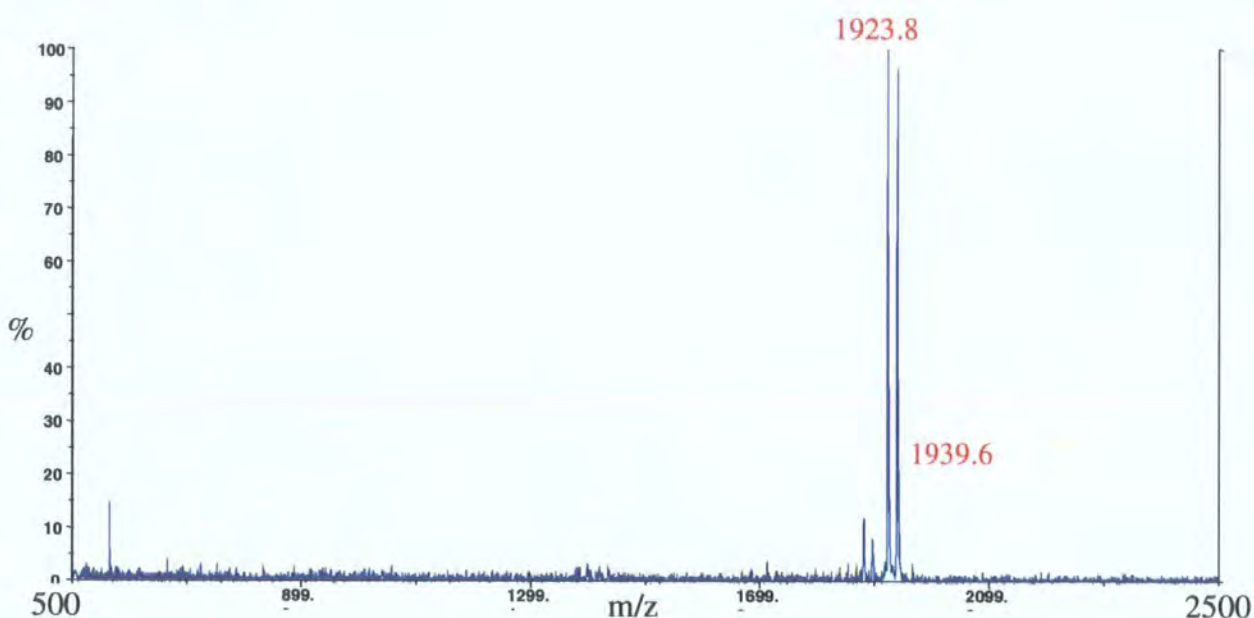


Figure 2.50 Part of the  $^{13}\text{C}$  NMR spectrum of **BG3DAC**

The  $^1\text{H}$  NMR spectra of the aromatic-core dendrimers were useful for structure elucidation during purification of the compounds as impurities resulting from incomplete reaction of the dendron with the trifunctional core unit could be easily identified. In the spectrum of the desired product or 'three-armed' dendrimer, a singlet occurs at a chemical shift of about 8.80 ppm, corresponding to the three equivalent hydrogens of the aromatic core unit. If impurities resulting from incomplete reaction with the trifunctional core, *i.e.* the mono-substituted and di-substituted products are present, a second singlet downfield from the signal associated with the tris-substituted dendrimer is observed. As an example the  $^1\text{H}$  NMR spectrum of **CC1DAC** is included in the Appendix, pages XVI.

#### *Mass Spectroscopy and Gel Permeation Chromatography*

The first and second generation dendrimers were analysed by MALDI-TOF mass spectrometry, using the Kratos and/or Voyager machine. The mass spectrum for the first generation dendrimer with the benzhydryl end groups **BHG1DAC**, with a calculated molecular weight of 1901.2 Da, is shown below (*Figure 2.51*). The molecular ions charged with sodium and potassium,  $[\text{M}+\text{Na}]^+$  and  $[\text{M}+\text{K}]^+$ , were evident at  $m/z$  values of 1923.8 and 1939.6 respectively.

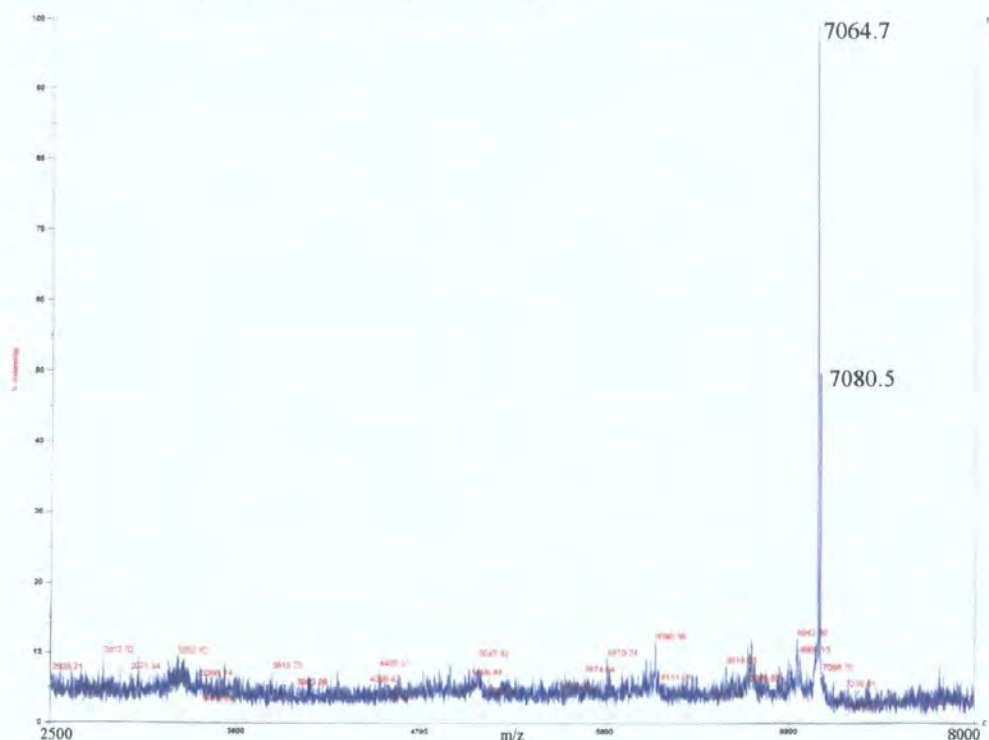


*Figure 2.51 MALDI-TOF (Voyager) mass spectrum of **BHG1DAC***

The mass analysis of the third generation dendrimer **CG3DAC** was achieved using the MALDI-TOF (Voyager) mass spectrometer and the spectrum is shown in *Figure 2.52*. The macromolecule has a calculated molecular weight of 7037.8 and ions charged with sodium



and potassium,  $[M+Na]^+$  and  $[M+K]^+$ , were observed in the mass spectrum at  $m/z$  values of 7064.7 and 7080.5. The calibration of the machine is thought to be the cause of the inaccurate correlation between the expected  $m/z$  values of 7060.8 and 7076.8 for  $[M+Na]^+$  and  $[M+K]^+$  and those obtained experimentally. The characterisation of the third generation dendrimer with *t*-butyl termini, **BG3DAC**, was attempted by MALDI-TOF mass spectrometry but no results were obtained. Two possible explanations for the difficulties experienced are that ionisation of the molecule is prohibited by the dense, aliphatic nature of the end groups and fragmentation of the molecule is occurring. Therefore, the analysis of **BG3DAC** was limited to GPC, elemental analysis and NMR spectroscopy.



another series of dendrimers with a layer of ester functions at the core. The reaction yields for the syntheses of these dendrimers with aromatic-ester core units were considerably higher than for the polyurethane homodendrimers.

The compounds prepared were soluble in most common organic solvents with the exception of hexane and were insoluble in water. The physical state of the materials ranged from sticky oils to hard, amorphous solids depending on the nature of the end groups and the molecular weight of the macromolecules. This observation is discussed in further detail in Chapter 4, when results from their thermal characterisation are considered. In addition, the structures were characterised by several spectroscopic methods, including NMR and infrared spectroscopy, mass spectrometry and gel permeation chromatography. From analysis of NMR and IR spectra it was possible to conclude that the hydrogen bonding interactions of the dendritic molecules in solution were intramolecular rather than intermolecular and that the degree of hydrogen bonding was dependent on the generation and the terminal groups of the structures.

The future development of this project would involve the synthesis and characterisation of higher generations in the dendritic sequence using procedures similar to those described for the lower generations. However, it is likely that purification and characterisation of the compounds will become more challenging with increasing molecular weight and by comparison with other families of convergent dendrimers it is improbable that structures higher than the six generation will be successfully prepared.

## 2.6 References

- (1) Newkome, G. R.; Moorefield, C. N.; Vögtle, F. *Dendritic Molecules: Concepts, Syntheses and Perspectives*; VCH: Weinheim, 1996.
- (2) Newkome, G. R.; Baker, G. R.; Young, J. K.; Traynham, J. G. *J. Polym. Sci.* **1993**, *31*, 641.
- (3) Mendenhall, G. D. In *Mesomolecules*; Mendenhall, G. D.; Greenburg, A.; Liebman, J. F., 2nd ed; Chapman & Hall: New York, 1995; p 181.
- (4) Mendenhall, G. D. *J Polym Sci, Part A: Polym. Chem.* **1998**, *36*, 2979.
- (5) Murer, P. K.; Lapierre, J.-M.; Greiveldinger, G.; Seebach, D. *Helv, Chem. Acta* **1997**, *80*, 1648.
- (6) Kimura, E.; Kodama, Y.; Koike, T.; Shiro, M. *J. Am. Chem. Soc.* **1995**, *117* (32), 8304.
- (7) Williams, D. H.; Fleming, I. *Spectroscopic Methods in Organic chemistry*, 4th ed.; McGraw-Hill: London, 1987.

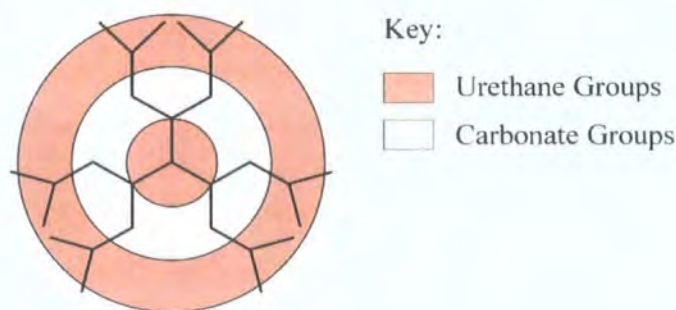
- (8) Bosman, A. W.; Bruining, M. J.; Kooijman, H.; Spek, A. L.; Janssen, R. A. J.; Meijer, E. W. *J. Am. Chem. Soc.* **1998**, *120*, 8547.
- (9) Jansen, J. F. G. A.; de Brabander-van den Berg, E. M. M.; Meijer, E. W. *Science* **1994**, *266*, 1226.
- (10) Hawker, C. J.; Fréchet, J. M. J. *J. Am. Chem. Soc.* **1990**, *112*, 7638.
- (11) Fréchet, J. M. J. *Synthesis and Properties of Dendrimers and Hyperbranched Polymers*, 1996.
- (12) Schultz, L. G.; Zhao, Y.; Zimmermann, S. C. *Angew. Chem. Int. Ed.* **2001**, *40*, 1962.
- (13) Twyman, L. J.; Beezer, A. E.; Mitchell, J. C. *J. Chem. Soc. Perkin Trans. I* **1994**, 407.
- (14) Chang, H.-T.; C.-T., C.; Kondo, T.; Siuzdak, G.; Sharpless, B. *Angew. Chem. Int. Ed.* **1996**, *35*, 182.
- (15) Ashton, P. R.; Hounsell, E. F.; Jayaraman, N.; Nilsen, T. M.; Spencer, N.; Stoddart, J. F.; Young, M. *J. Org. Chem.* **1998**, *63*, 3429.

## Chapter 3

# Synthesis and Characterisation of Codendrimers

### 3.1 Introduction

The previous chapter was focused on a new family of polyurethane dendrons and dendrimers that were comprised entirely of urethane functions so could be considered as *homodendritic* structures. The realm of this chapter is the introduction, synthesis and characterisation of *heterodendritic* macromolecules, which contain a mixture of functional groups and are given the term 'codendrimers'. In this study, the codendrimers prepared are second generation structures consisting of layers of urethane functions and carbonate functions concentrically arranged around the centre of the molecule. A schematic to indicate the compositional layering of one of the poly(urethane-carbonate) codendrimers synthesised is shown below (*Figure 3.1*). In this chapter, the synthesis and characterisation of these dendritic structures will be recounted including some interesting details of their NMR spectra.



*Figure 3.1 Schematic of second generation dendrimer consisting of concentric layers of urethane-carbonate-urethane functions*



## 3.2 Background

### 3.2.1 Overview of Codendrimers

Dendritic block copolymers or codendrimers are structures consisting of regions of differing chemical composition and are prepared by using dissimilar synthetic building blocks.<sup>1</sup> In contrast to a linear polymer, the highly branched three-dimensional topology of a dendrimer creates the potential for several distinct arrangements of the differing chemistries within the macromolecule. These arrangements can be divided into three main types of dendritic copolymers termed segmental-block, layer-block and surface-block codendrimers (Figure 3.2).<sup>1</sup> Segmental-block codendrimers are comprised of different dendritic segments or dendrons attached to a polyfunctional core.<sup>2,3</sup> Layer-block codendrimers consist of concentric layers of varying chemical composition around a central core unit.<sup>2</sup> Thirdly, surface-block codendrimers are structures that vary exclusively according to the nature of the dendrimers' surface groups.<sup>4-7</sup>

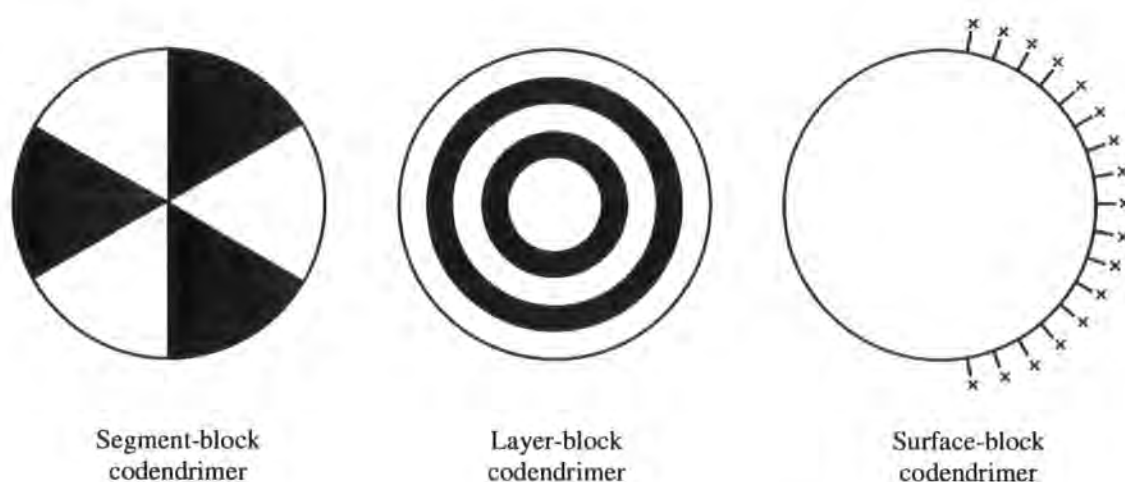
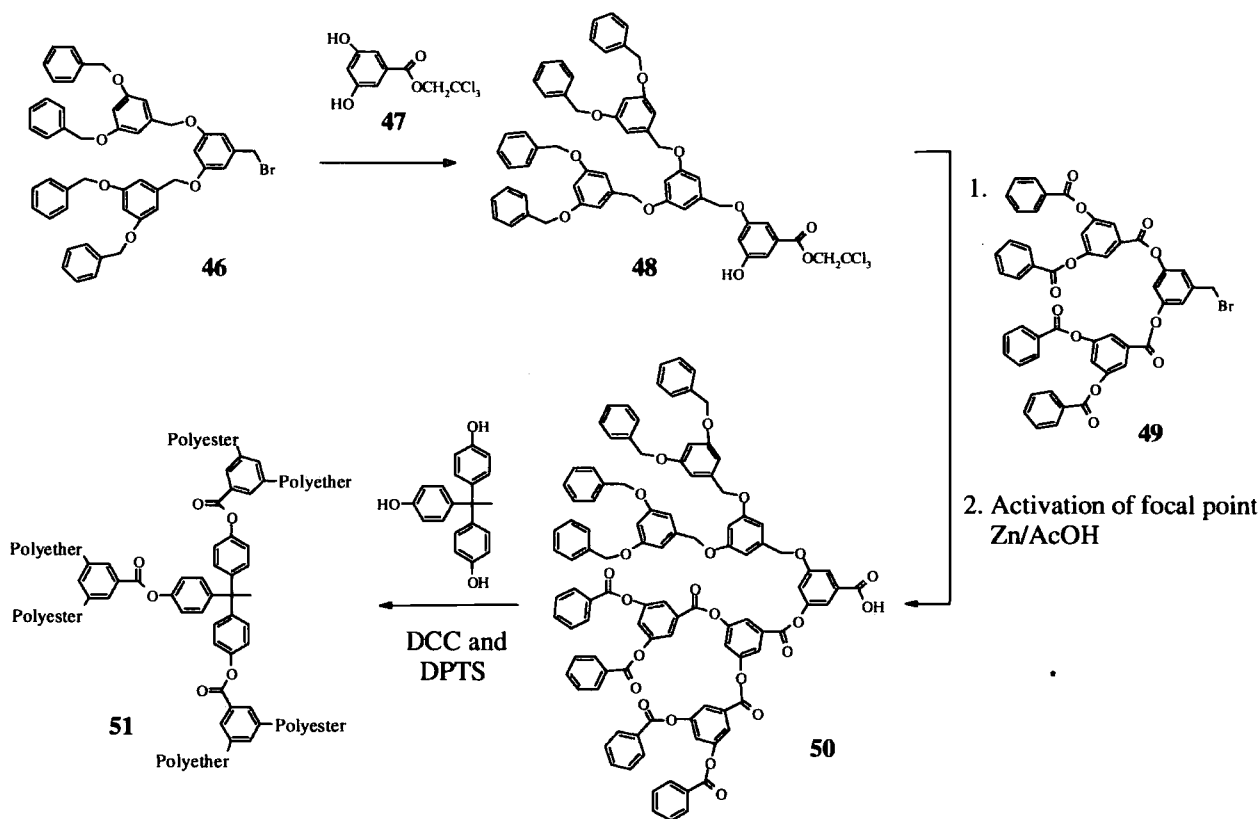


Figure 3.2 Schematic representation of the three types dendritic-block codendrimers<sup>1</sup>

A characteristic of some divergent dendrimer syntheses is the alternate addition of different reagents, which results in the formation of layer-block codendrimers.<sup>8,9</sup> However, most examples in the literature of codendrimer synthesis use the convergent route since this method enables precise control of the surface groups, generation growth and core unit.<sup>2,5</sup> The possibility of constructing dendrimers with subtle changes in their different regions was recognised and reported concurrently with the development of the convergent method and a series of publications describing the synthesis of poly(ether-ester) codendrimers and surface codendrimers followed.<sup>2,5,10</sup> Some of these hybrid macromolecules, synthesised in the research group of Fréchet, are used as examples in the following sections.

### 3.2.2 Segment-block Codendrimers

Dendrimers comprising alternate radial segments have been prepared either by the coupling of different dendrons to a monomer unit, followed by attachment to a polyfunctional core or by the coupling of different dendrons to a core.<sup>2,3</sup> The former method was used in the first reported synthesis of a segmental codendrimer and the structure prepared consisted of three segments of both ester and ether groups (*Figure 3.3*).<sup>2</sup> The ether-linked dendron **46** reacted with branched monomer **47** to give the mono-substituted dendron **48**. Addition of the corresponding ester-linked dendron **49**, followed by activation of the focal point (zinc in glacial acetic acid) gave codendrion **50** consisting of one segment of ether groups and another segment of ester groups. The codendrion was coupled to a trifunctional core to give the dendritic segment-block dendrimer **51** using the reagents dicyclohexylcarbodiimide (DCC) and 4-dimethylaminopyridinium toluene-*p*-sulfonate (DPTS).

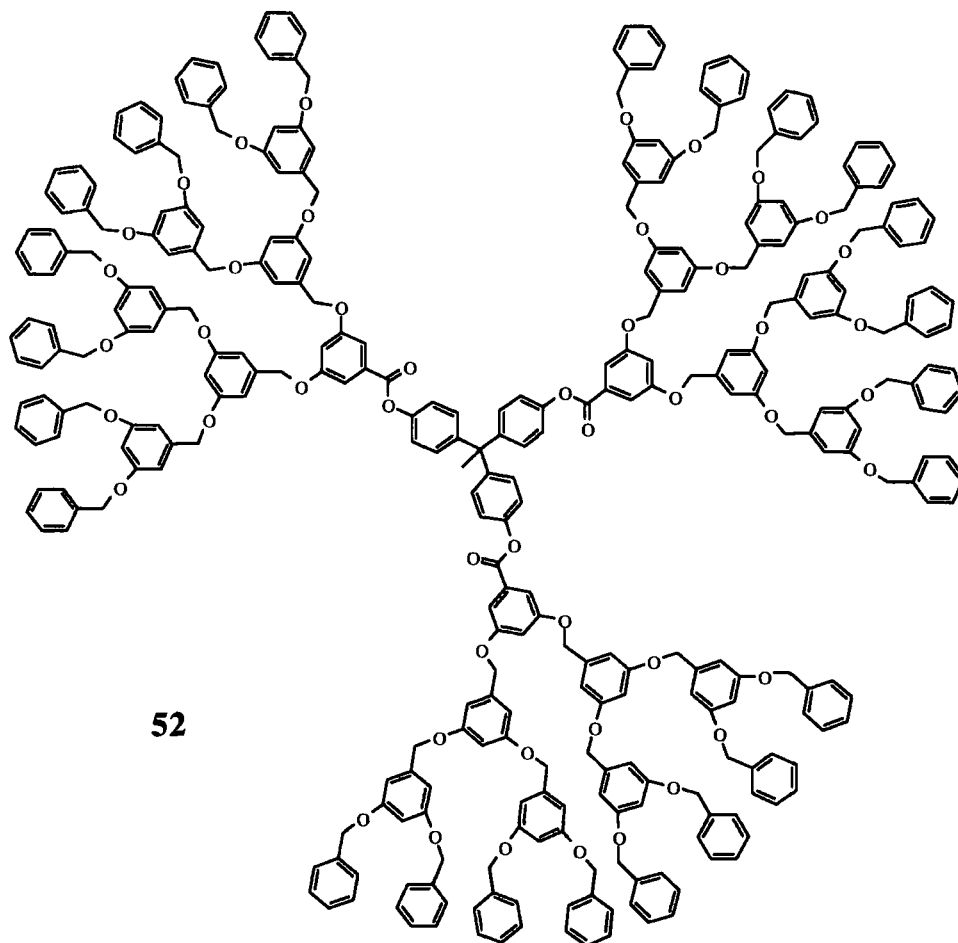


*Figure 3.3 Synthesis of segment-block codendrimer*

The only restriction in the synthetic route to segment-block codendrimers is the requirement of the different dendrons to be compatible with the reaction conditions involved in coupling the dendrons to the core. Otherwise, the possible range of structures is large as characteristics of the codendrimer, including the number and size of the segments and their chemical composition can be varied.

### 3.2.3 Layer-block Codendrimers

Poly(ester-ether) layer codendrimers could also be prepared from the same building blocks and reactions used in the synthesis of the segmental structures.<sup>2</sup> One example is macromolecule **52**, which contains three outer ether layers and one inner ester layer, but as it was possible to vary the width and sequence of the concentric layers, several different layer codendrimers were synthesised (*Figure 3.4* and *Figure 4.8*, page 110). The compatibility of the reactions involved in the introduction of the alternating layers is the only constraint on the many different synthetic possibilities.



*Figure 3.4 Layer-block codendrimer with outer ether and inner ester layers*

### 3.2.4 Surface Codendrimers

The ability to control the chain ends of dendrimers has lead to tailoring of their synthesis to create structures with different surface functionalities. These functionalities can be arranged in blocks, *i.e.* **53**, or located at predetermined individual positions on the surface, *i.e.* **54** and **55**, or in an alternating fashion, *i.e.* **56** (*Figure 3.5*, overleaf). To the knowledge of the author, examples in the literature of the alternating arrangement have been limited to dendron synthesis.<sup>7</sup>



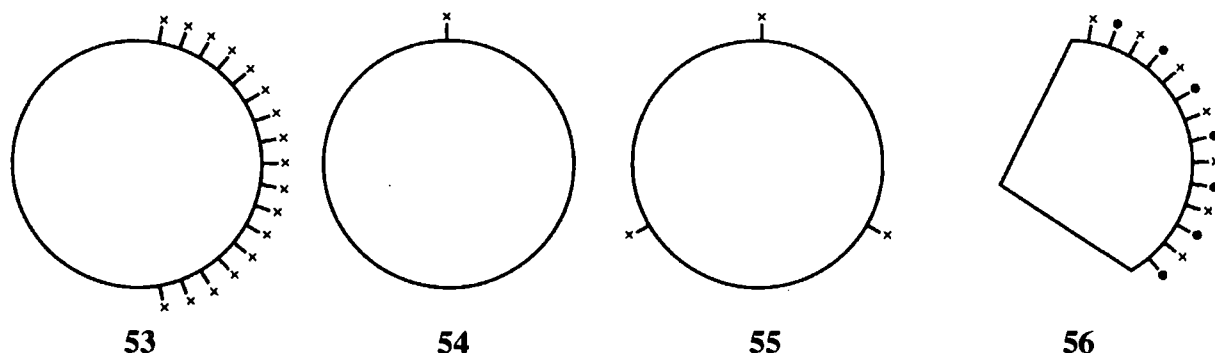


Figure 3.5 Different arrangements of functionalities for surface codendrimers

The majority of surface codendrimers synthesised and investigated are those of the block arrangement **53** because of their interesting properties.<sup>11-13</sup> For example, the unsymmetrical surface codendrimer **57**, which consists of one block of electron withdrawing cyano groups and another of electron donating benzyloxy groups (Figure 3.6), has an enhanced dipole moment compared to the equivalent entirely benzyloxy terminated structure.<sup>11</sup> The concept of this feature was suggested to be of interest in the field of nanotechnology because the structure may be considered as a globular molecular switch. Also, a similar polyether codendrimer with blocks of hydrophobic and hydrophilic surface groups has been shown to create globular amphiphiles that stabilise organic/aqueous emulsions.<sup>12</sup>

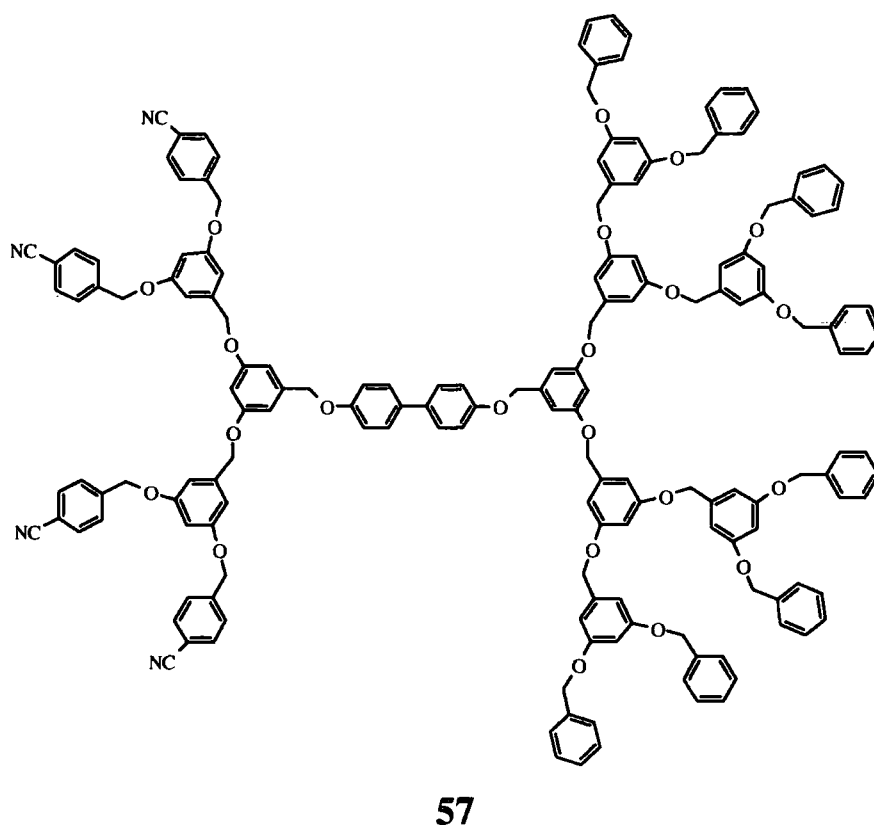
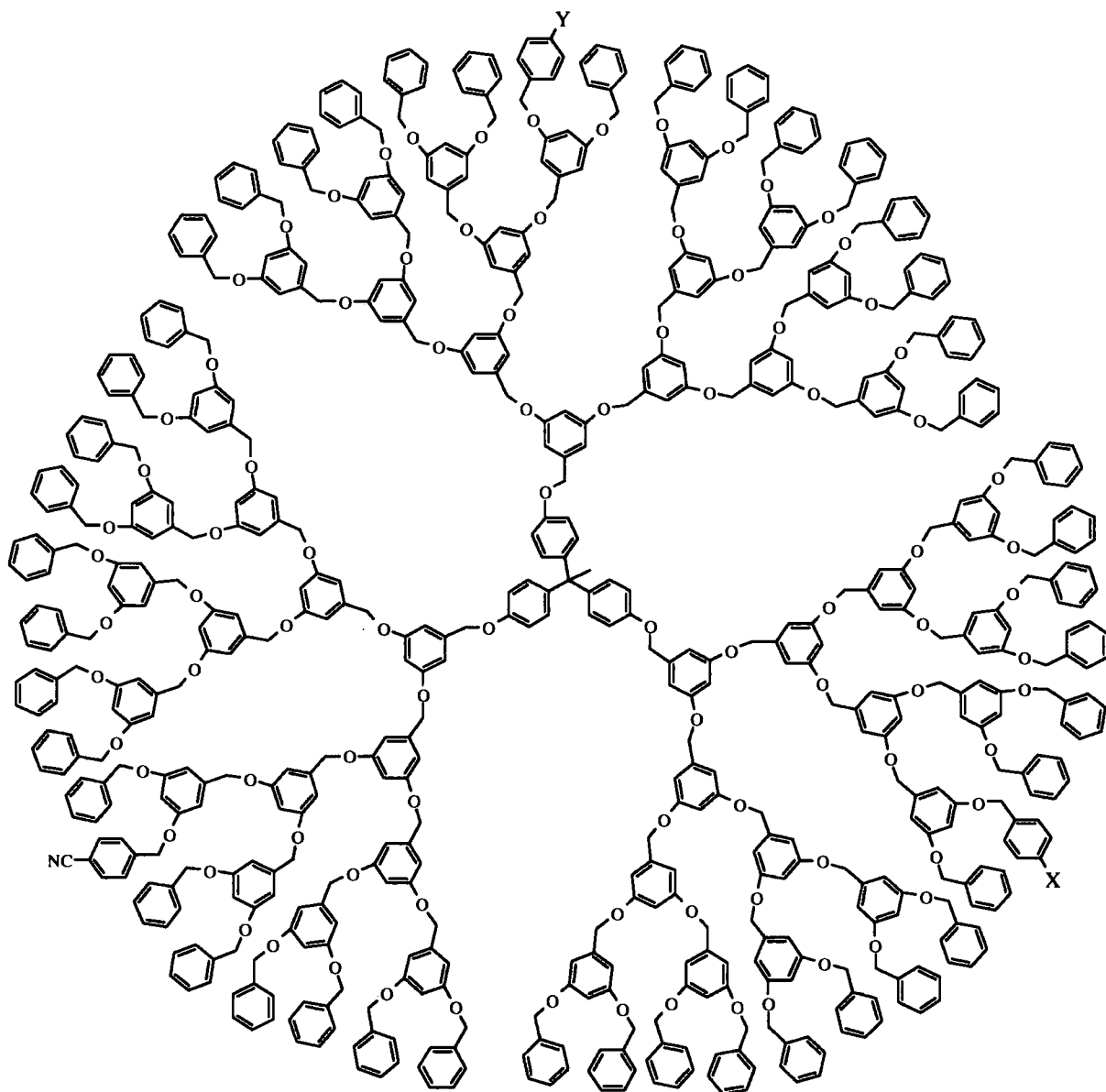


Figure 3.6 A dipolar surface-block codendrimer

Surface polyether codendrimers of the type illustrated by schematic pictures **54** and **55** on the previous page have also been synthesised. Fourth generation structures with one, two or three cyano end groups per macromolecule, *i.e.* **58**, **59** and **60**, were prepared demonstrating the high degree of architectural control using the convergent growth method (Figure 3.7).



**58** X = Y = H

**59** X = H, Y = CN

**60** X = Y = CN

Figure 3.7 Fourth generation surface codendrimers with either one, two or three cyano groups per molecule

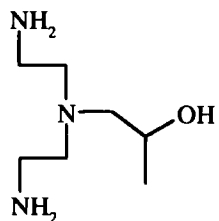
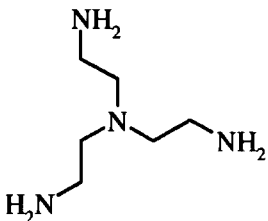
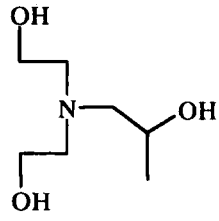
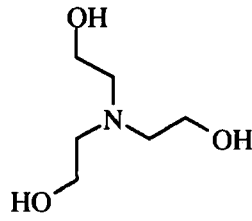
### 3.3 Synthesis of Layer Codendrimers

#### 3.3.1 Introduction

Primarily, this project has involved the synthesis of homodendritic macromolecules composed of urethane linking groups. However, the reactions of CDI are versatile and can be used to create ester, amide, urethane, carbonate and urea functional groups depending on the chemical composition and the sequence in which reagents are introduced (Chapter 1, page 15). This advantage of CDI chemistry together with the application of the convergent route to dendrimer synthesis has made it possible to construct a series of second generation layer codendrons and codendrimers. These macromolecules consist of differing proportions of urethane and carbonate groups but otherwise have identical chemical compositions as similar reagents were employed in the synthesis. Their synthesis and characterisation by NMR and mass spectroscopy will be outlined in the following sections.

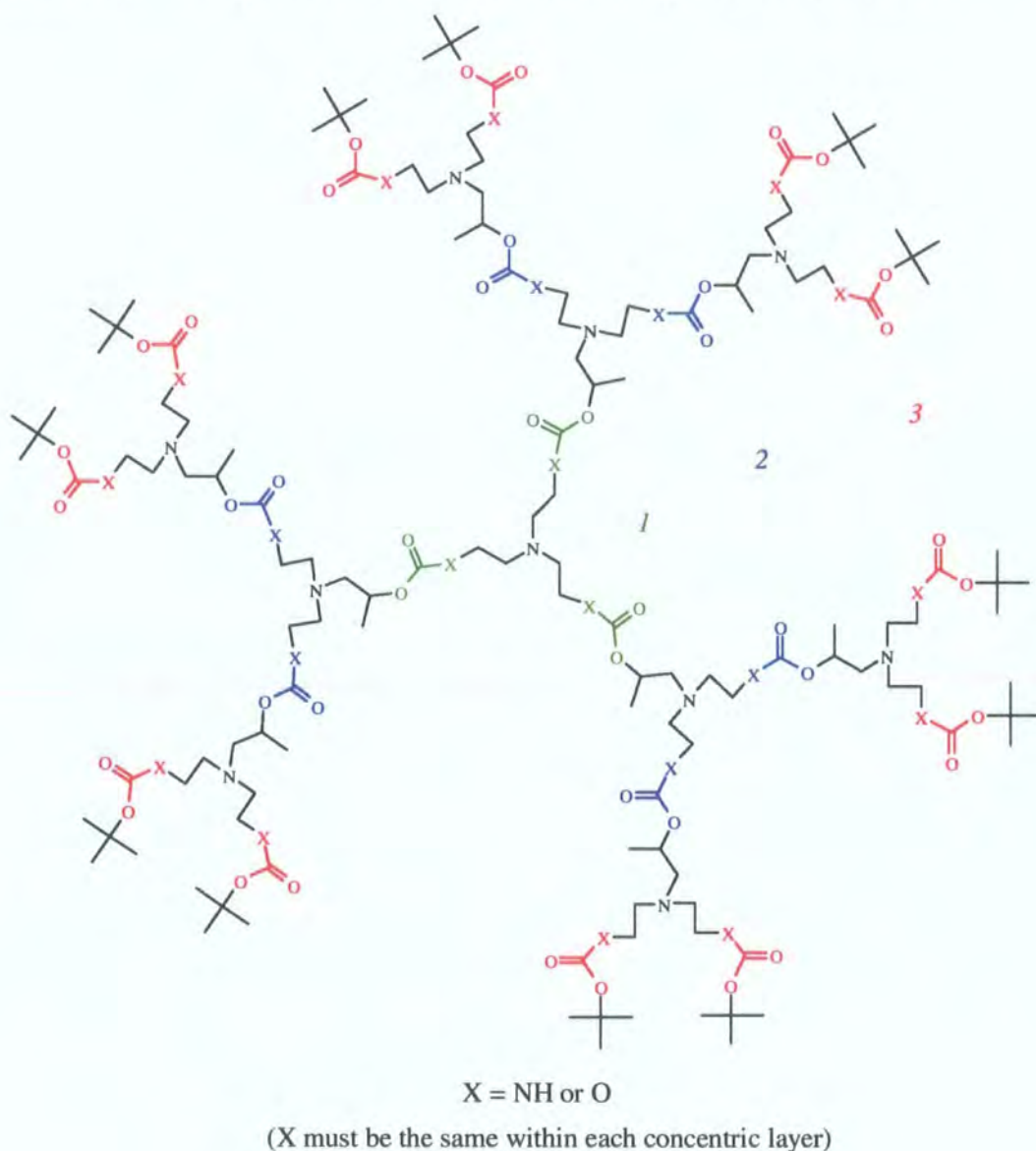
#### 3.3.2 Structure of Second Generation Codendrimers

The four building blocks used in the codendrimer synthesis are the branching units **AEAP** and 1-[N,N-bis(2-hydroxyethyl)amino]-2-propanol (**HEAP**), and the core units **TAEA** and triethanolamine (**TEA**) (*Figure 3.8*). With the exception of **AEAP**, they are all commercially available. The use of the branching unit or core with primary amine functions (**AEAP** and **TAEA**) introduces a urethane link into the structure and the use of the branching unit and core with primary alcohol functions (**HEAP** and **TEA**) leads to a carbonate link.

Branching Units		Cores
 <b>AEAP</b>	Urethane Synthesis	 <b>TAEA</b>
 <b>HEAP</b>	Carbonate Synthesis	 <b>TEA</b>

*Figure 3.8 Branching units and cores for codendrimer synthesis*

All eight possible arrangements of urethane and carbonate groups at the three concentric layers in the second generation dendrimer have been synthesised. These combinations include the two extremes, the polyurethane and polycarbonate homodendrimers. The synthesis of the polyurethane structure **BG2D** has been described in the previous chapter. The code system introduced in Chapter 2 has been adapted to indicate the different compositional layering of the second generation codendrimers (*Figure 3.9* and *Table 3.1*, overleaf). The first four characters of the code, *e.g.* **BG2D** (UCC), indicate the second generation dendrimers have *t*-butyl terminal groups and triamine core units. The following letters in brackets describe the composition of the layers, where **U** represents a urethane group and **C** a carbonate group. The sequence of the letters is also crucial so the layering is described from the innermost to the outermost layer, *i.e.* in the order 1, 2, and 3, so **BG2D** (UCC) has a urethane layer near the core and two outer layers of carbonate links.



*Figure 3.9 Schematic of second generation dendrimer*

Structure	1	2	3	Code of Dendrimer
Polycarbonate homodendrimer	C	C	C	<b>BG2D (CCC)</b>
Codendrimers	U	C	C	<b>BG2D (UCC)</b>
	C	U	C	<b>BG2D (CUC)</b>
	U	U	C	<b>BG2D (UUC)</b>
	C	C	U	<b>BG2D (CCU)</b>
	U	C	U	<b>BG2D (UCU)</b>
	C	U	U	<b>BG2D (CUU)</b>
Polyurethane homodendrimer	U	U	U	<b>BG2D</b>

Table 3.1 Codes for homo- and heterodendrimers

### 3.3.3 Synthesis of Dendrons

The eight dendrimers included in the table above were synthesised from four different second generation dendrons (*Figure 3.10*). The preparation of the entirely urethane-linked dendron, **BG2OH**, was outlined in the previous chapter. The procedures for the other structures, *i.e.* the polycarbonate dendron **BG2OH (CC)** and codendrons **BG2OH (UC)** and **BG2OH (CU)**, will be explained in this section. The coding system for the dendrons follows the principle above as the initial part **BG2OH** contains the information that the molecules are second generation dendrons with *t*-butyl end groups and a hydroxyl function at the focal point. The first letter in the bracket represents the linking group closest to the focal point whereas the last letter represents the linking group near the *t*-butyl groups.

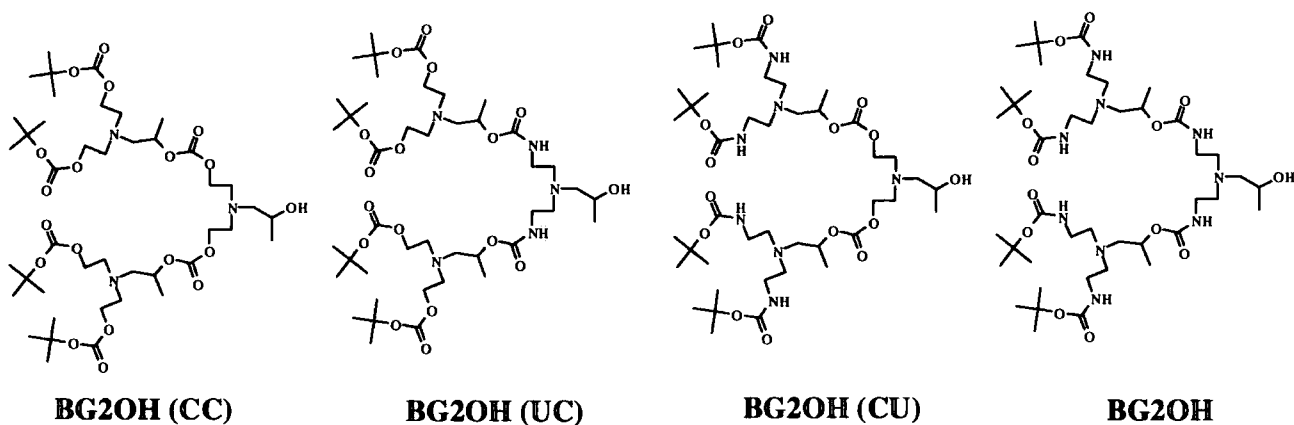
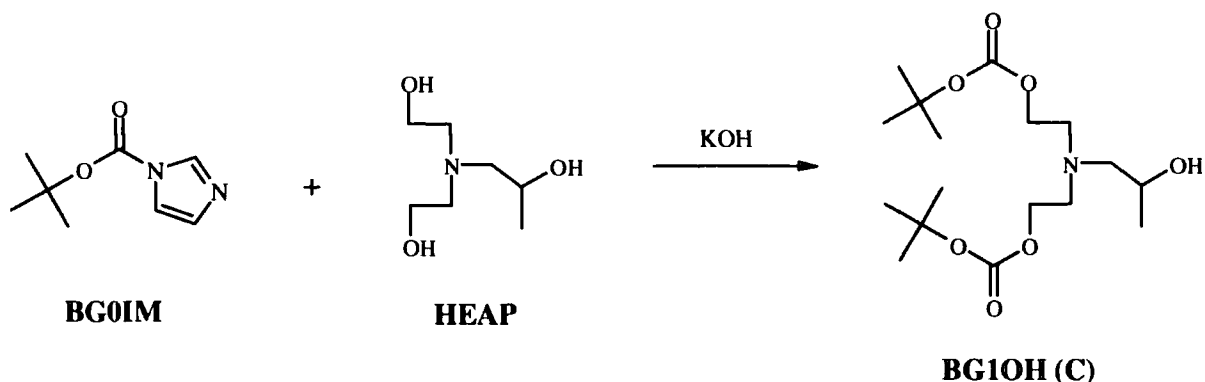


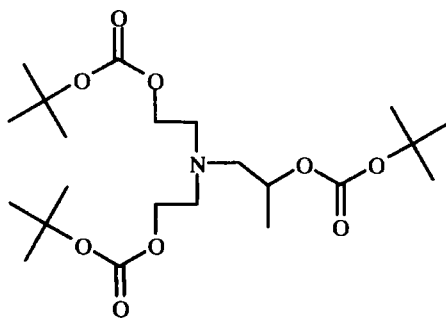
Figure 3.10 Second generation homo- and heterodendrons

To synthesise dendrons **BG2OH (CC)** and **BG2OH (UC)** the preparation of the first generation dendron with carbonate functional groups **BG1OH (C)** was required (*Figure 3.11*, overleaf).



*Figure 3.11 Synthesis of first generation carbonate-linked dendron*

The synthesis involved the addition of 0.5 equivalents of the branching unit containing two primary alcohol functions and one secondary alcohol function, *i.e.* **HEAP**, to a stirred solution of **BG0IM**, under basic conditions (potassium hydroxide, KOH). A reaction temperature of 75°C and a reaction time of 2 days were required compared to the lower temperature of 60°C and shorter time of 1 day for a urethane forming process. The harsher reaction conditions were necessary because of the lower nucleophilicity and hence reduced reactivity of primary alcohols compared to primary amines. The addition of base was found to be essential and the concentration of the reaction mixture was also considered to have an effect. The optimum conditions were difficult to determine because of problems with the reproducibility of the reaction. The crude product was purified by silica gel chromatography, eluting with hexane:ethyl acetate 4:1, to give **BG1OH (C)** as a colourless oil of low viscosity in a yield of 54%. Purification was challenging as several side products were generated probably resulting from the high temperature, base catalysis and high concentration of the reagents. A side product, **61** (*Figure 3.12* overleaf), isolated in variable yields up to *ca.* 10%, subsequent to column chromatography, was formed by reaction of the CDI adduct at the secondary alcohol group of **HEAP** as well as at the primary alcohol functions. There has been no report or evidence in this work of the equivalent side product generated in any reaction involving the amine branching unit **AEAP**. The presence of **61** suggests the selectivity of reaction at the primary alcohol sites in the presence of a secondary alcohol group is less than for primary amine functions in the presence of a secondary alcohol function in **AEAP** reactions. This is unsurprising as basic conditions are not required for reaction of CDI adducts and primary amine functions whereas it is essential for reaction with alcohol groups. Therefore, the absence of KOH in urethane forming reactions prohibits the reaction of the CDI adduct at the secondary alcohol function.



61

Figure 3.12 Side product isolated during purification of BG1OH (C)

The second generation polycarbonate dendron **BG2OH (CC)** and the codendron **BG2OH (UC)** were synthesised from **BG1OH (C)** in one-pot reactions by consecutive addition of CDI followed by addition of either **HEAP** or **AEAP** (Figure 3.13). For similar reasons to those mentioned above, the reaction of **HEAP** with the CDI adduct required base catalysis and a higher reaction temperature. The purification of the dendrons was achieved by silica gel chromatography to give **BG2OH (CC)** and **BG2OH (UC)** as colourless oils of low viscosity in yields of 40% and 58%.

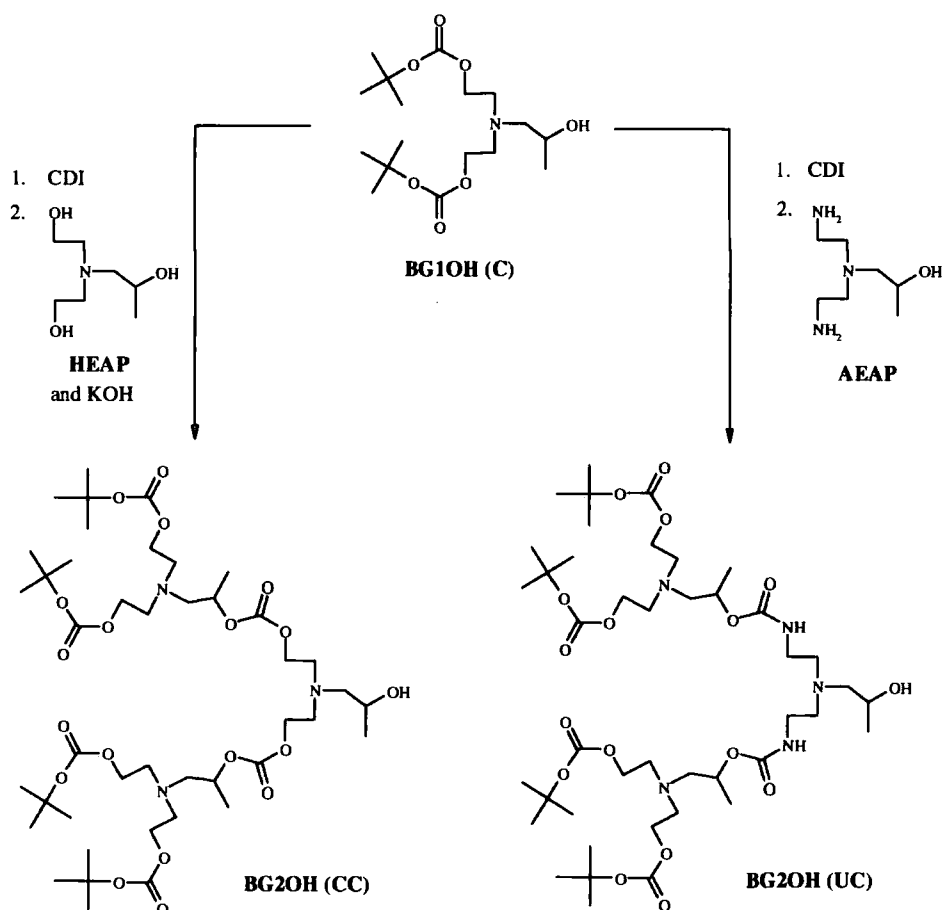


Figure 3.13 Synthesis of a polycarbonate dendron and a codendron



In an analogous way, the second generation polyurethane dendron **BG2OH** and the codendron **BG2OH (CU)** were synthesised from **BG1OH** in one-pot reactions by consecutive addition of CDI followed by addition of either **AEAP** or **HEAP** (Figure 3.14).

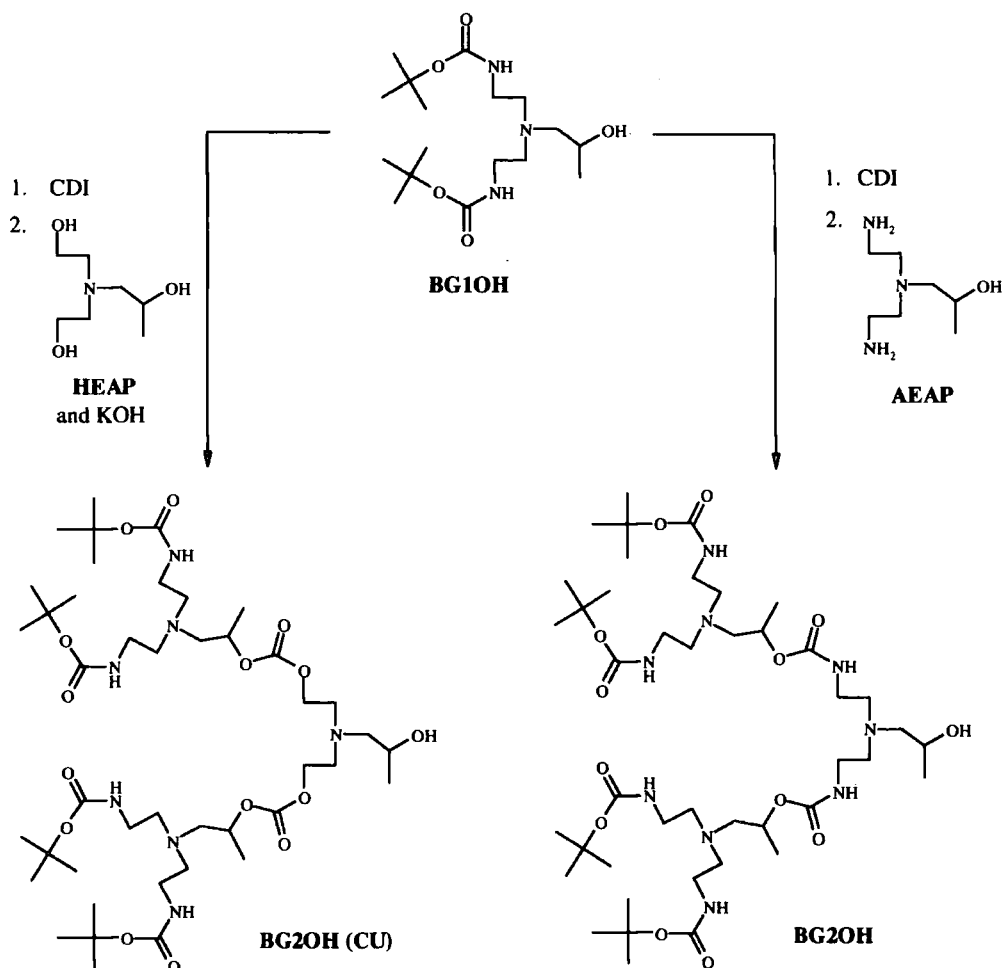


Figure 3.14 Synthesis of codendron **BG2OH (CU)** and polyurethane dendron **BG2OH**

The synthesis of **BG2OH** was reported in the previous chapter. The codendron **BG2OH (CU)** was isolated, after purification, as a sticky colourless oil in a yield of 32%.

### 3.3.4 Synthesis of Codendrimers and a Polycarbonate Dendrimer

The polycarbonate dendrimer and six codendrimers were synthesised using different combinations of the four second generation dendrons in Figure 3.10 and the trifunctional cores in Figure 3.8. The trifunctional alcohol core **TEA** introduces carbonate groups at the innermost layer of the second generation dendrimer and the amine core **TAEA** introduces urethane groups in this layer. The syntheses of all the codendrimers and the polycarbonate dendrimer follow the same method, so as an example the reaction scheme for the preparation of **BG2D (CCU)** is shown (Figure 3.15). In a one-pot reaction, the focal point of the second generation dendron **BG2OH (CU)** is activated using CDI, then reacted with the trifunctional

core **TEA**. The codendrimer was purified by silica gel chromatography and preparative gel permeation chromatography to give **BG2D (CCU)** as a sticky colourless oil. The physical state of the homo- and heterodendrimers varied from sticky oils to hard amorphous solids because of the differing glass transition temperatures of the materials. This is considered in greater detail when the thermal characterisation of the materials is discussed in chapter 4.

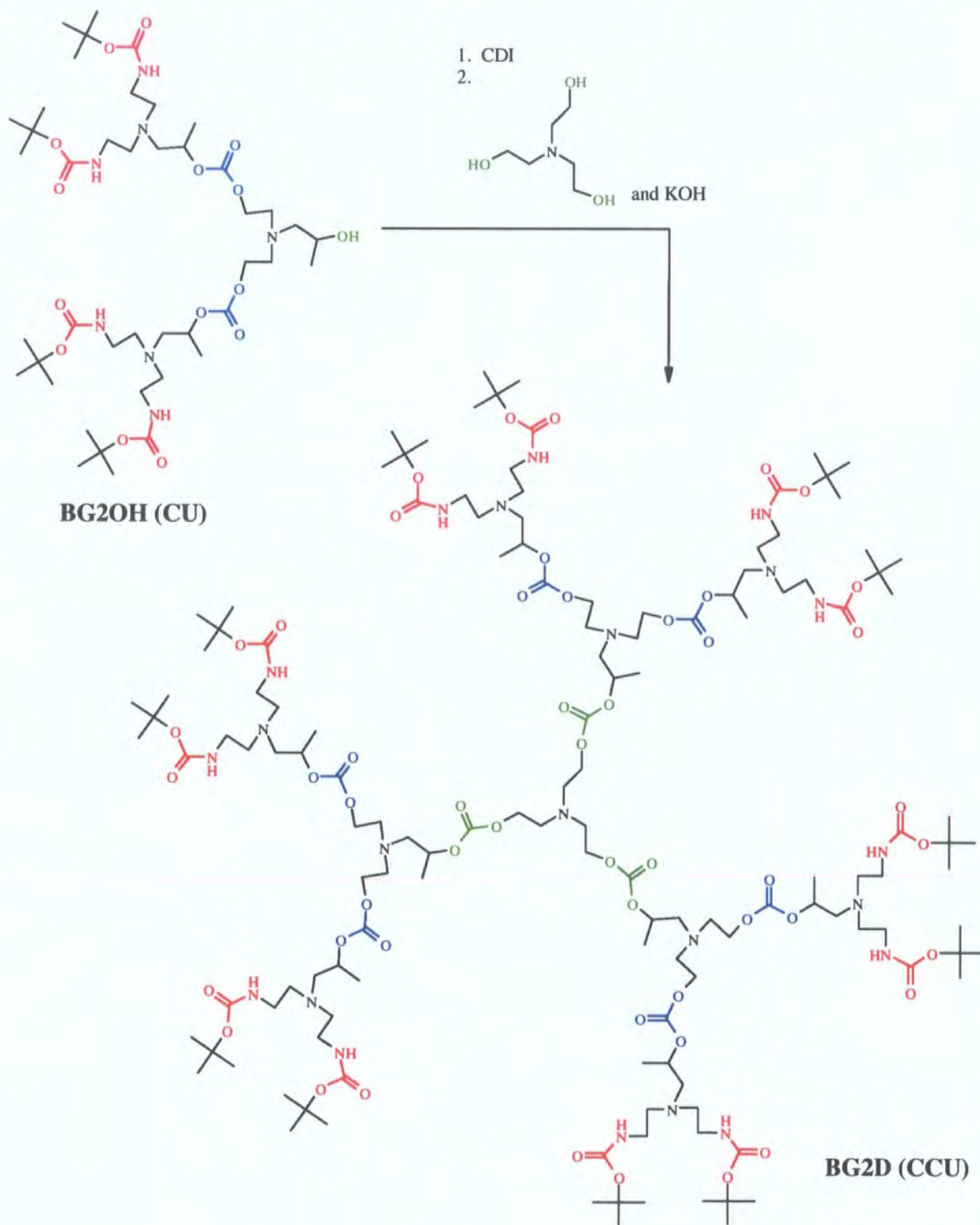
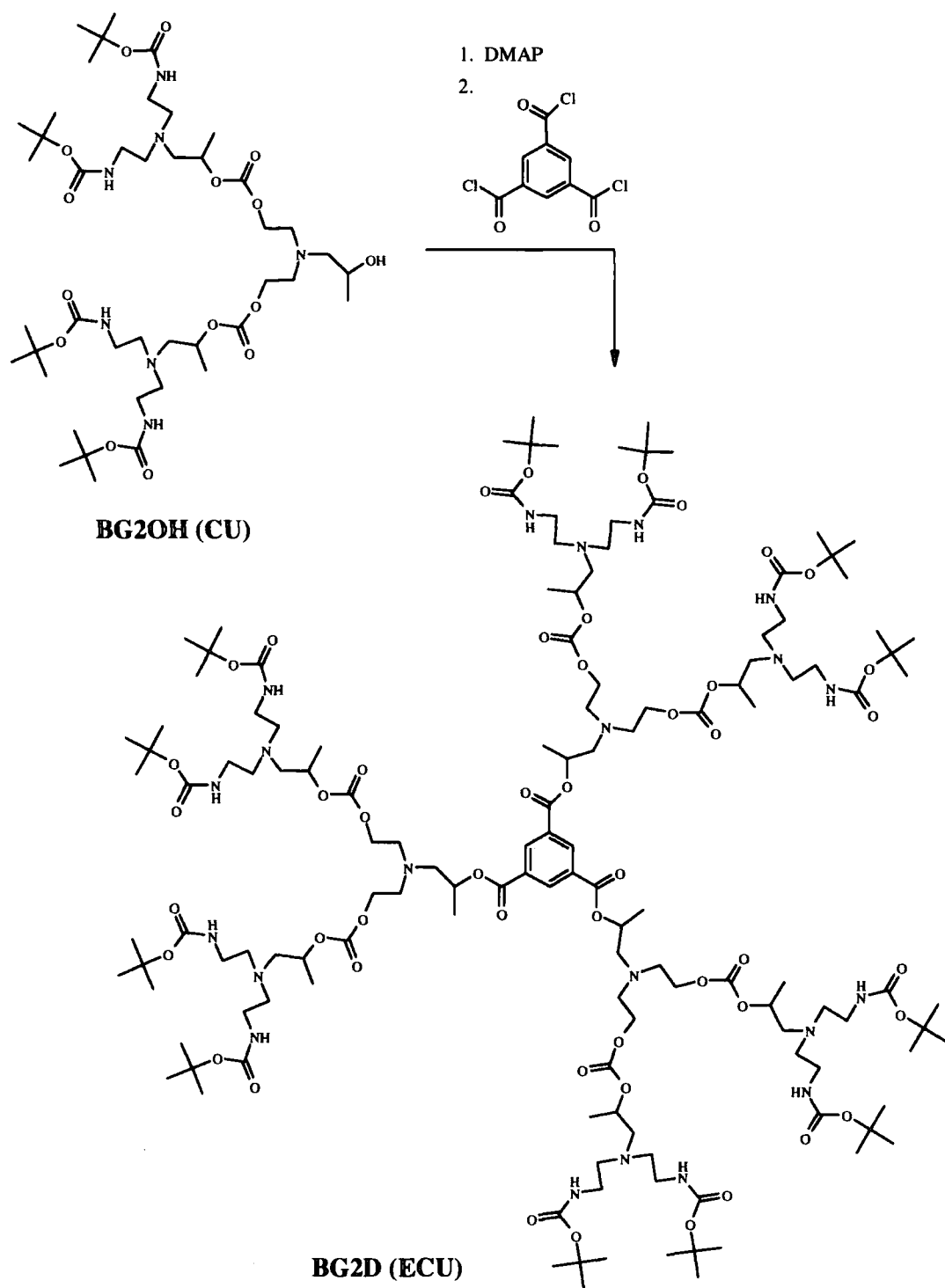


Figure 3.15 Synthesis of codendrimer **BG2D (CCU)**

An additional second generation codendrimer with three different layers was synthesised by the coupling of codendron **BG2OH (CU)** to the aromatic core unit benzene-1,3,5 tricarboxyl trichloride (see Chapter 2, page 64 for an outline of the procedure). The dendrimer contains a layer sequence of ester, carbonate and urethane functions, from the innermost to the outermost, and is represented by the code **BG2D (ECU)** (*Figure 3.16*). The dendrimer was isolated as a sticky colourless oil, subsequent to purification, in a yield of 63%.



*Figure 3.16 Synthesis of codendrimer containing ester-carbonate and urethane functions*

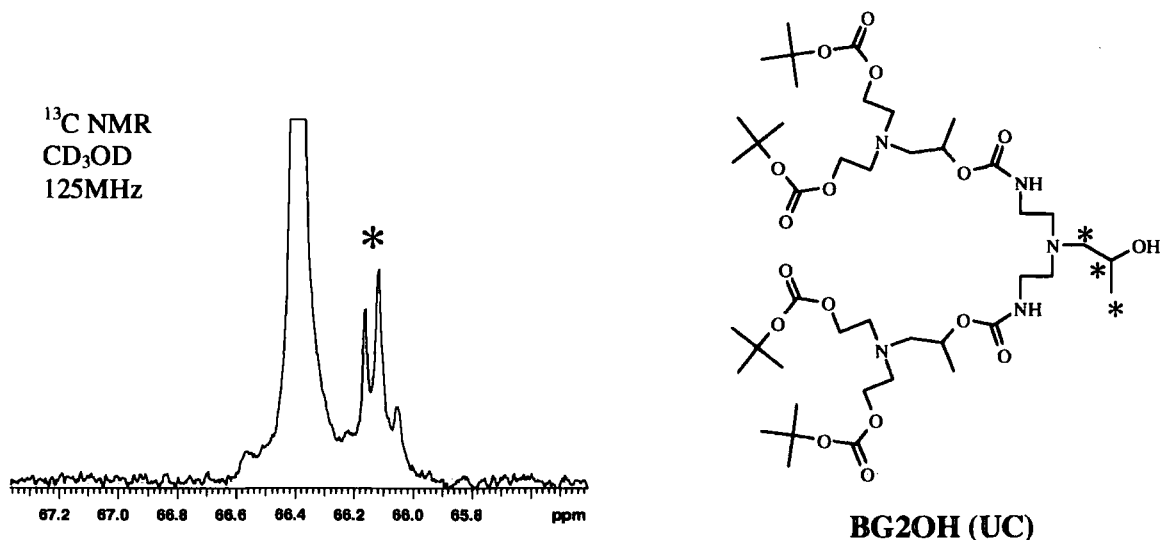
### 3.4 Characterisation of Codendrons and Codendrimers

The macromolecules synthesised were analysed by NMR spectroscopy and electrospray and/or MALDI-TOF mass spectrometry. Some pertinent details of the spectra are explained here and all spectroscopic data are recorded in the experimental section (pages 139, 140 and 149-153).

#### 3.4.1 $^{13}\text{C}$ NMR Spectroscopy

##### a) Dendrons

The  $^{13}\text{C}$  NMR spectrum of polyurethane dendron **BG2OH** indicated a mixture of three diastereoisomers as the resonance corresponding to the chiral carbon centre was split into three peaks (see Chapter 2, page 38-40). The same effect was noted in the  $^{13}\text{C}$  NMR spectra of the polycarbonate dendron **BG2OH** (CC) and codendrons **BG2OH** (UC) and **BG2OH** (CU). In the spectrum of **BG2OH** (UC) signals corresponding to the carbon at the chiral centre (\*) (see *Figure 3.17*) and the adjacent methyl group carbon (\*) (not shown here) were split into three peaks. The signal corresponding to the other adjacent carbon (\*) is also affected but the splitting is not clearly resolved into three peaks.



*Figure 3.17 Section of  $^{13}\text{C}$  NMR spectrum showing chiral centre of **BG2OH** (UC)*

To support the suggestion that some resonances are split according to the number of diastereoisomers in the mixture, the mono-substituted second generation dendron **62** was isolated and characterised by  $^{13}\text{C}$  NMR spectroscopy (*Figures 3.18 and 3.19*, overleaf). The molecule contains two chiral centres and consequently the expected statistical mixture contains four different stereoisomers, RR, SS, RS and SR. The relationship between the RR and SS isomers is enantiomeric and they are diastereomeric with respect to the other enantiomeric pair, *i.e.* RS and SR. Therefore, if splitting of resonances associated with the

carbon nuclei at the focal point occurs in the NMR spectrum of **62** as expected there should be two peaks with the same integration.

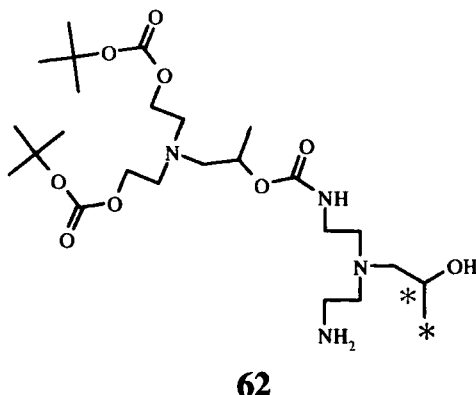


Figure 3.18 Mono-substituted second generation dendron

Two regions of the  $^{13}\text{C}$  NMR spectrum of **62** showing the resonances of the chiral centre near the focal point (\*) and the adjacent methyl carbon (\*) are shown in Figure 3.19, each is split into two peaks of the same intensity.

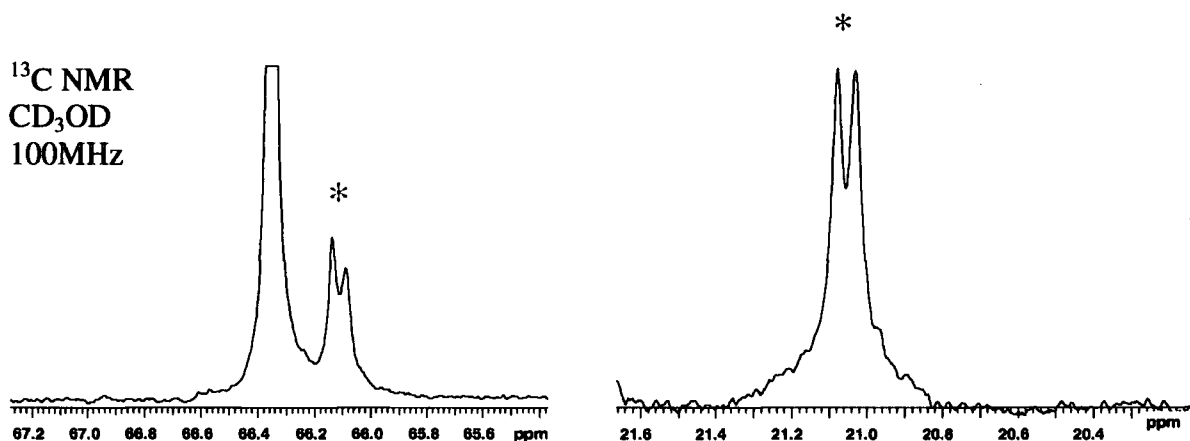


Figure 3.19 Two different regions of the  $^{13}\text{C}$  NMR spectrum of **62**

## b) Dendrimers

The second generation codendrimers and homodendrimers each have 17 distinct carbon environments and hence, in theory 17 different signals should be evident in the  $^{13}\text{C}$  NMR spectra. However, for the homodendrimer **BG2D** there are 11 distinct signals in the spectrum (125MHz) and for the equivalent carbonate structure 10 signals (63MHz). This is because of overlapping signals from carbons at comparable positions in successive layers of the dendrimer. However, the difference in layer composition of the codendrimers creates dissimilar environments for the carbons in successive layers and more of the carbon resonances are resolved into separate signals. For example, the corresponding spectra of the

six codendrimers consist of between 15 and 17 signals depending on the layer structure. The carbonyl region is distinct for each codendrimer as signals from urethane groups are observed between 158.4 ppm and 158.8 ppm and those for carbonate groups between 155.0 ppm and 156.4 ppm. For example, the carbonyl region for the codendrimer **BG2D** (UCC) has one peak at 158.5 ppm corresponding to the urethane carbonyl and two peaks at 156.2 ppm and 155.0 ppm for the carbonate carbonyls (Figure 3.20).

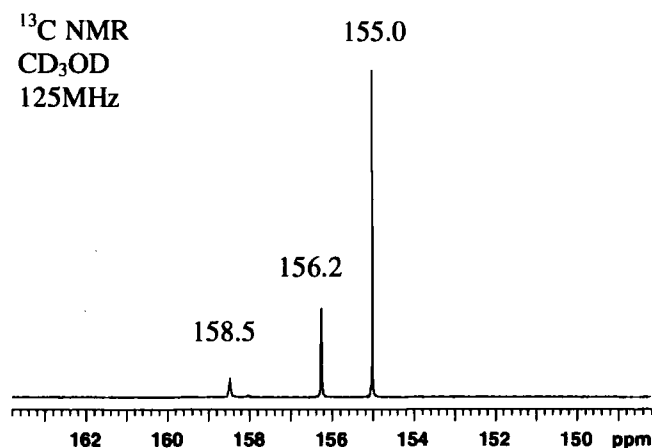


Figure 3.20 Carbonyl region of the  $^{13}\text{C}$  NMR spectrum of **BG2D** (UCC)

### 3.4.2 $^1\text{H}$ NMR Spectroscopy

#### a) Dendrons

$^1\text{H}$  NMR spectroscopy was a valuable technique for characterisation of the dendrons; however, the spectra were complicated by the presence of diastereotopic hydrogens in the molecules. For example,  $\text{H}_\alpha$  and  $\text{H}_\beta$  of the methylene group adjacent to the chiral centre in the first generation carbonate dendron **BG1OH** (C), have chemical shifts that differ by 0.29 ppm and are seen as two doublets of doublets (Figure 3.21). A similar effect was observed in the  $^1\text{H}$  NMR spectrum of the polyurethane dendron **HG1OH** (Chapter 2, pages 34-35).

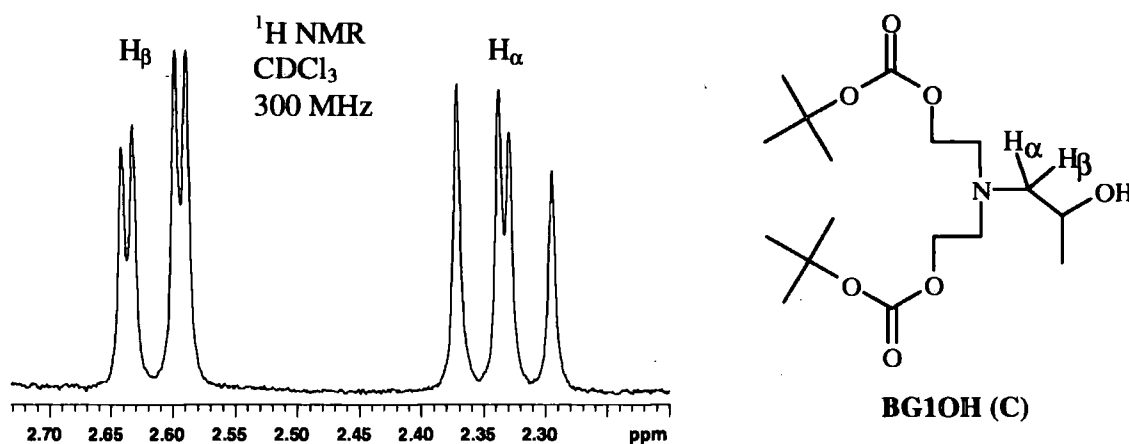
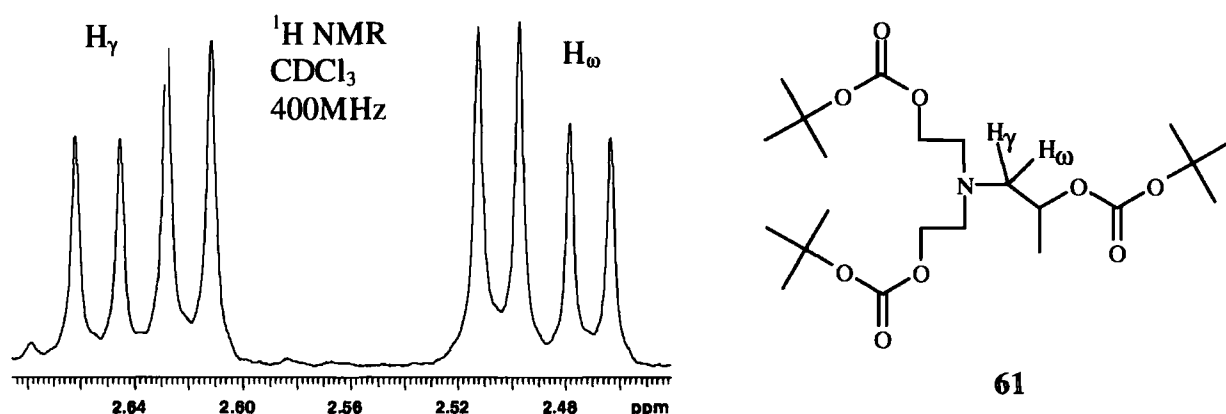


Figure 3.21 Section of  $^1\text{H}$  NMR spectrum showing the diastereotopic hydrogens adjacent to the chiral centre of **BG1OH** (C)



The hydrogens  $H_\alpha$  and  $H_\beta$  of **BG1OH (C)** couple to each other with a coupling constant ( $J$ ) of 13Hz, but couple to the hydrogen of the chiral centre with vastly different coupling constants of 10.2Hz and 2.8Hz. From the analysis of other  $^1\text{H}$  NMR data including the spectrum of side product **61**, it was evident that this difference in  $^3J$  coupling constant only occurs for dendrons with a hydroxyl group at the focal point. For example, in **16** the diastereotopic hydrogens are observed in the spectrum as two doublets of doublets, which have identical  $^3J$  couplings of 6.4Hz (*Figure 3.22*).



*Figure 3.22 Section of  $^1\text{H}$  NMR spectrum showing the diastereotopic hydrogens adjacent to the chiral centre of **61***

This spectroscopic evidence suggests that the hydroxyl group at the focal point of the dendron is hydrogen bonded to another part of the molecule, causing the structure to have a dominant conformation on the NMR timescale. One possible preferred conformation is that of a pseudo-five membered-ring formed by the hydrogen bonding of the hydroxyl group to the tertiary amine function (*Figure 3.23*, overleaf). The existence of a dominant conformation results in different dihedral angles between each of the diastereotopic hydrogens and the hydrogen of the chiral centre. Since,  $^3J$  or vicinal coupling is dependent on the dihedral angle, the coupling constants for the two hydrogens are different. For side product **61** and other compounds, hydrogen bonding cannot occur and rotation around the carbon-carbon bonds in the molecule is less restricted, resulting in similar vicinal coupling constants. A similar pattern of doublet of doublets with different vicinal couplings was noted in the  $^1\text{H}$  NMR spectrum of aspartic acid at pH 12, because the molecule adopts a preferred conformation.<sup>14</sup> At lower pH the conformation was not favoured and the vicinal couplings were of similar values.

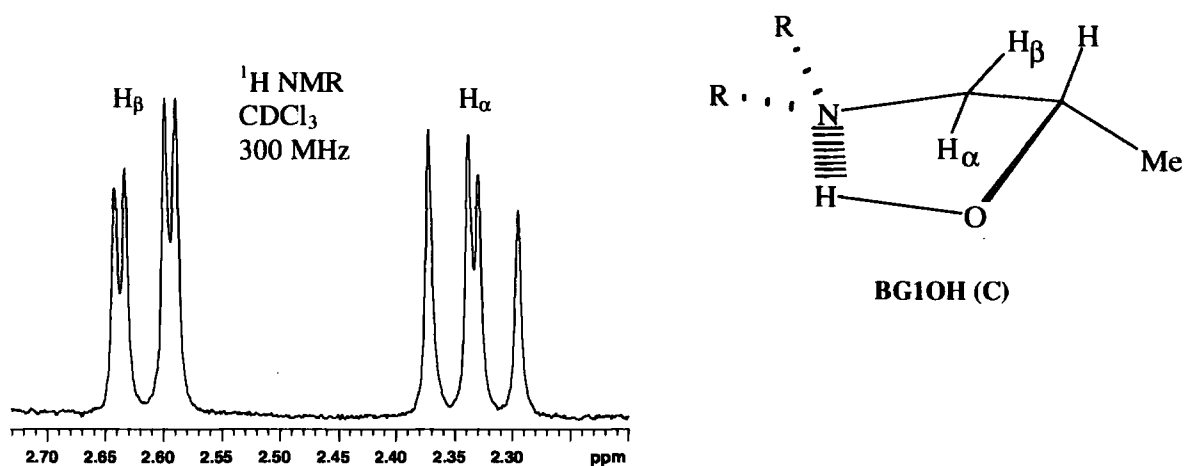


Figure 3.23 Hypothetical hydrogen bonded conformation of BG1OH (C) and part of  $^1\text{H}$  NMR spectrum showing diastereotopic hydrogens  $\text{H}_\alpha$  and  $\text{H}_\beta$ .

#### b) Dendrimers

The  $^1\text{H}$  NMR spectra for the codendrimers contain information from which the amount and type - intermolecular or intramolecular - of hydrogen bonding by the urethane functional groups can be deduced. It is well established that the chemical shift of a urethane hydrogen changes in different solvents and at different temperatures.<sup>15,16</sup> Also, the formation of the hydrogen bond has a deshielding effect on the hydrogen of the urethane group and consequently it is shifted downfield in the spectrum. In the case of intermolecular hydrogen bonding, the chemical shift depends critically on the concentration of the sample but intramolecular hydrogen bonding has less dependency on dilution.<sup>15</sup> The chemical shift difference for hydrogens of amide and urethane groups at the periphery of poly(propyleneimine) dendrimers has already been used to determine the amount and type of hydrogen bonding.<sup>17,18</sup> In these studies, a downfield shift of the N-H resonance with increasing dendrimer generation was observed. This indicated a greater amount of hydrogen bonding for the larger macromolecules, caused by the closer proximity of the amide or urethane groups. The hydrogen bonding was also concluded to be intramolecular because the chemical shift of the N-H resonances did not vary with concentration.

The chemical shifts of the N-H resonances of the codendrimers synthesised in this project were observed to vary and seemed to be dependent on the location of the urethane layers in the structure. The NMR solvent initially used for analysis of the codendrimers was  $\text{CD}_3\text{OD}$  and the chemical shifts for some of the codendrimers in this medium are shown in Table 3.2 overleaf. The first three codendrimers in the table correspond to structures with two carbonate layers and one urethane layer. For dendrimers BG2D (UCC) and BG2D (CUC), in which the urethane links are located at the innermost and middle layer of the dendrimer

respectively, the N-H resonances occur at 6.57 ppm and 6.51 ppm. However, for dendrimer **BG2D (CCU)**, in which the urethane functions are close to the end groups, the N-H resonance occurs much further upfield at 6.35 ppm. The N-H resonance of the urethane groups near the end groups of the ester-carbonate-urethane codendrimer **BG2D (ECU)** are also observed in this region of the spectrum (6.32 ppm). This upfield shift of the N-H resonance as the urethane layer moves progressively outwards to the end groups suggests the hydrogen bonding of the functions decreases in this sequence. This could be explained by the closer proximity of the urethane functions near the core of the dendrimer compared with those in the outer layers, which facilitates the formation of hydrogen bonds between the groups. The location of the urethane groups in the outermost layer (*i.e.* **BG2D (CCU)** and **BG2D (ECU)**) results in a N-H resonance occurring at a chemical shift of *considerably* lower ppm value. This positioning of the urethane groups at the termini of flexible dendritic branches may impede their close approach, even though there are an increased number of urethane groups for each molecule. In addition, the bulky nature of the *t*-butyl end groups may encumber the formation of hydrogen bonds for the outer ring of urethane functionalities.

Codendrimer	Location of Urethane Layer (s)	$\delta$ in ppm CD <sub>3</sub> OD
BG2D (UCC)	Inner (1)	6.57
BG2D (CUC)	Middle (2)	6.51
BG2D (CCU)	Outer (3)	6.35
BG2D (ECU)	Outer (3)	6.32
BG2D (UCU)	Outer (3) and Inner (1)	6.38 and 6.68

*Table 3.2 Chemical shifts of the N-H resonance in CD<sub>3</sub>OD for some codendrimers*

In the <sup>1</sup>H NMR spectrum of codendrimer **BG2D (UCU)**, which has urethane groups located in the innermost and outermost layers and a carbonate layer in between, there are two N-H resonances corresponding to the two urethane layers (*Table 3.2*). These resonances occur at 6.38 ppm and 6.68 ppm and integration of the peaks suggests that they correspond to the outer and inner urethanes respectively. This is consistent with the suggestion that the close approach of the urethane groups and hence hydrogen bonding capability is greatest for the urethane functions nearer the core of the structure. Moreover, the shift of the N-H resonances compared with those of the corresponding dendrimers **BG2D (UCC)** and **BG2D (CCU)**, which contain only one layer of urethane units, implies the hydrogen bonding of the urethane functions is enhanced in the two layers of **BG2D (UCU)**. This may be a



consequence of a constraining effect on the conformation of the dendrimer introduced by the hydrogen bonding of the groups near the core, which in turn assists the close approach and hydrogen bonding of the urethanes groups in the outer layer.

The hydrogen bonding of the molecules and consequently the position of the N-H resonances will also be affected by the nature of the NMR solvent. In the above experiments the protic solvent, deuterated methanol, itself capable of hydrogen bonding was used. It has been presumed that at these low concentrations the solvent was present in large excess and could be considered a constant factor for the experiments. Therefore, the observed differences in chemical shift can be attributed to changes in the amount of hydrogen bonding between urethane functions rather than between urethane functions and solvent. However, to affirm the trend in hydrogen bonding the  $^1\text{H}$  NMR spectra of some codendrimers using deuterated chloroform as a solvent were obtained and the relative position of the N-H resonances analysed (Table 3.3). Also, the approximate concentration of the NMR experiments in  $\text{CDCl}_3$  was constant for each dendrimer studied (20 mM) and variation of the sample concentration (between 10 mM – 175 mM) was observed not to effect the position of the N-H resonance. This information implies that the hydrogen bonding is intramolecular and not intermolecular, which is the same conclusion reached from previous NMR data (Chapter 2, page 55).

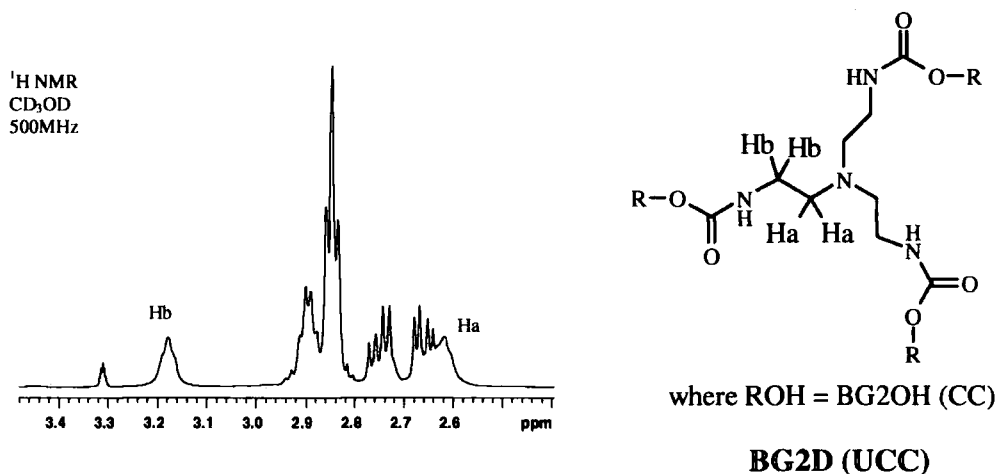
Codendrimer	Location of Urethane layer	Concentration mM	$\delta$ in ppm $\text{CDCl}_3$
BG2D (UCC)	Inner (1)	20	5.34 <sup>a</sup>
BG2D (CUC)	Middle (2)	20	5.33 <sup>a</sup>
BG2D (CCU)	Outer (3)	20	5.20
BG2D (CCU)	Outer (3)	10	5.20
BG2D (CCU)	Outer (3)	175	5.20

<sup>a</sup> The chemical shift of the N-H resonance was not observed to vary with concentration

Table 3.3 Chemical shift of urethane hydrogen for codendrimers in  $\text{CDCl}_3$

The trend in the position of the N-H resonances of codendrimers **BG2D (UCC)**, **BG2D (CUC)** and **BG2D (CCU)** in  $\text{CDCl}_3$  is similar to that observed in  $\text{CD}_3\text{OD}$ . The N-H resonance of the latter dendrimer, which consists of a urethane layer close to the terminal units occurs further downfield than the N-H resonances of the other dendrimers. The same assumption, that the hydrogen bonding is dependent on the propinquity of the urethane groups, can be made.

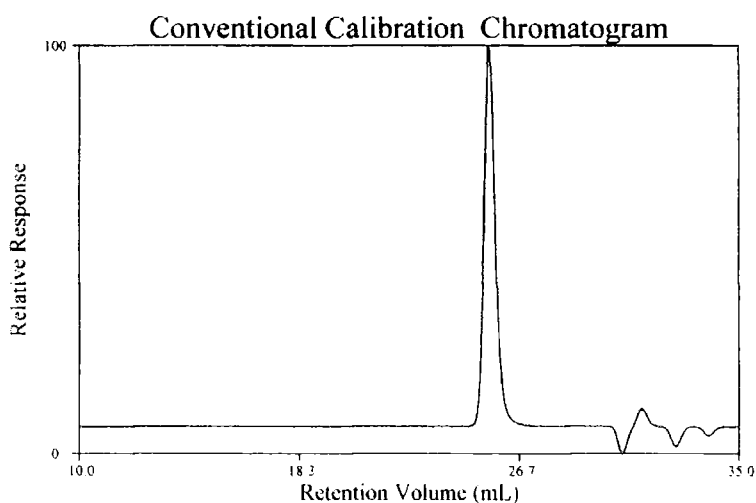
The conclusions about hydrogen bonding in these structures, which have been deduced from the location of the N-H resonance, is substantiated by observations in other regions of the  $^1\text{H}$  NMR spectrum of **BG2D** (UCC) (*Figure 3.24*). The downfield shift of the N-H resonance implies the greater hydrogen bonding of the urethanes in the inner layer and the broadness of the signals corresponding to hydrogens attached to the aliphatic portion of the core unit confirms this. These signals are considerably broader than the peaks corresponding to the aliphatic portions of the outer branching units, which is consistent with their reduced mobility.



*Figure 3.24 Part of  $^1\text{H}$  NMR spectrum showing hydrogens at the core of **BG2D** (UCC)*

### 3.4.3 Gel Permeation Chromatography (GPC)

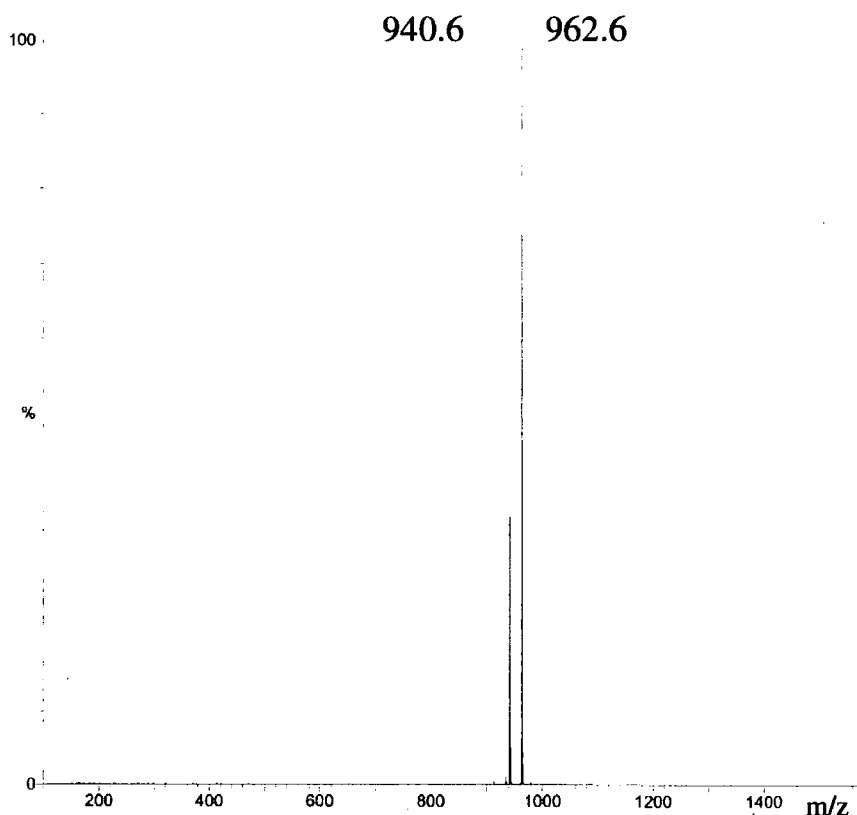
The second generation dendrons and dendrimers were analysed by gel permeation chromatography and this technique gave a useful indication of the purity of the macromolecules. For example, after purification of a dendrimer the presence of a small amount of residual second generation dendron not detectable by NMR could be observed in the GPC trace as an extra peak of low intensity at a higher retention time. The GPC trace of **BG2D** (UCU) after purification is shown opposite (*Figure 3.25*).



*Figure 3.25 GPC trace of **BG2D** (UCU)*

### 3.4.4 Mass Spectrometry

The second generation dendrons were characterised by electrospray (ES) mass spectrometry and peaks corresponding to the protonated molecular ion and those cationised by Na and K were observed. The mass values obtained were extremely accurate; for example, the calculated mass for the protonated molecular ion of dendron **BG2OH** (UC) is 940.6 Da and this is in excellent agreement with the experimental  $[M+H]^+$  at an  $m/z$  value of 940.6 from the ES mass spectrum (*Figure 3.26*). The ion cationised with sodium,  $[M+Na]^+$ , is also evident at an  $m/z$  value of 962.6.



*Figure 3.26 ES mass spectrum of codendron **BG2OH** (UC)*

Mass spectrometry data for the codendrimers was difficult to obtain because of the *t*-butyl end groups (*cf.* Chapter 2, pages 42-43). Electrospray mass spectrometry was the only effective method for the analysis of the second generation dendrimers as MALDI-TOF (Voyager) mass spectrometry did not yield any results. The ES mass spectrum of **BG2D** (CCU) that has a calculated molecular weight of 3064.6 Da is shown below (*Figure 3.27*, overleaf). The molecular ion cationised with sodium is observed at an  $m/z$  value of 3063.8 and the corresponding doubly charged species at 1543.5.



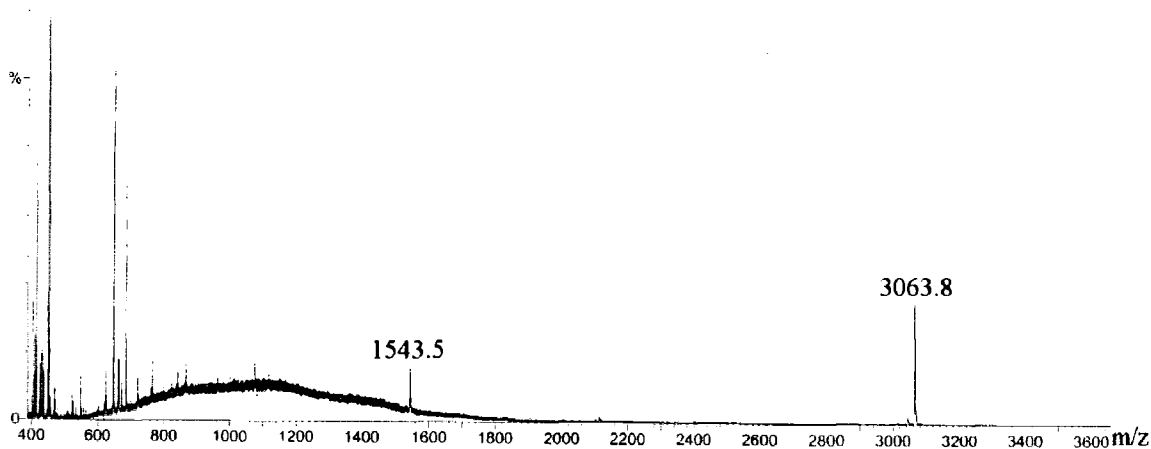


Figure 3.27 ES mass spectrum of second generation codendrimer BG2D (CCU)

### 3.5 Conclusions

A family of second generation layer codendrimers and the corresponding polycarbonate dendrimer have been synthesised using the selective chemistry of CDI and a variety of reagents possessing either primary amine functions or primary alcohol functions. The reactions involved in the introduction of carbonate groups were less selective in nature than the urethane forming reactions owing to the basic catalysis required for the former procedures. The codendrons and codendrimers were characterised by NMR spectroscopy, GPC and ES mass spectrometry and interpretation of the  $^1\text{H}$  NMR spectra of some codendrimers lead to two interesting conclusions concerning the hydrogen bonding of the compounds in solution. Firstly, the nearer the layer of urethane groups to the core of the dendrimer, the greater their degree of hydrogen bonding; secondly, the hydrogen bonding is intramolecular. The physical states of the second generation codendrimers, polyurethane dendrimer and polycarbonate dendrimer vary from viscous oils to amorphous solids and this observation is developed in a section of the following chapter.

### 3.6 References

- (1) Fréchet, J. M. J.; Hawker, C. J. *Synthesis and Properties of Dendrimers and Hyperbranched Polymers*, in *Comprehensive Polymer Science*, 2<sup>nd</sup> Suppl. 1996, p71.

- (2) Hawker, C. J.; Fréchet, J. M. J. *J. Am. Chem. Soc.* **1992**, *114*, 8405.
- (3) Kremers, J. A.; Meijer, E. W. *J. Org. Chem.* **1994**, *59*, 4262.
- (4) Hawker, C. J.; Fréchet, J. M. J. *Macromolecules* **1990**, *23*, 4726.
- (5) Wooley, K. L.; Hawker, C. J.; Fréchet, J. M. J. *J. Chem. Soc. Perkin Trans. I* **1991**, 1059.
- (6) Aoi, K.; Itoh, K.; Okada, M. *Macromolecules* **1997**, *30*, 8072.
- (7) Grayson, S.; Fréchet, J. M. J. *J. Am. Chem. Soc.* **2000**, *122*, 10335.
- (8) Newkome, G. R.; Yao, Z.; Baker, G. R.; Gupta, V. K. *J. Org. Chem.* **1985**, *50*, 2003.
- (9) Peerlings, H. W. I.; van Benthem, R. A. T. M.; Meijer, E. W. *J. Polym. Sci., Part A: Polym. Chem.* **2001**, *39*, 3112.
- (10) Hawker, C. J.; Fréchet, J. M. J. *J. Am. Chem. Soc.* **1990**, *112*, 7638.
- (11) Wooley, K. L.; Hawker, C. J.; Fréchet, J. M. J. *J. Am. Chem. Soc.* **1993**, *115*, 11496.
- (12) Hawker, C. J.; Wooley, K. L.; Fréchet, J. M. J. *J. Chem. Soc. Perkin Trans. I* **1993**, 1287.
- (13) Pesak, D. J.; Moore, J. S. *Tetrahedron* **1997**, *53*, 15331.
- (14) Sanders, J. K. M.; Hunter, B. K. *Modern NMR Spectroscopy*, 2nd ed.; O. U. P.: Oxford, 1987.
- (15) Abraham, R. J.; Fisher, J.; Loftus, P. *Introduction to NMR spectroscopy*, 2nd ed.; Wiley & Sons: New York, 1988.
- (16) Akitt, J. W. *NMR and Chemistry*, 3rd ed.; Chapman and Hall: London, 1992.
- (17) Stevelmans, S.; van Hest, J. C. M.; Jansen, J. F. G. A.; van Boxtel, D. A. F. J.; de Brabander-van den Berg, E. M. M.; Meijer, E. W. *J. Am. Chem. Soc.* **1996**, *118*, 7398.
- (18) Bosman, A. W.; Bruining, M. J.; Kooijman, H.; Spek, A. L.; Janssen, R. A. J.; Meijer, E. W. *J. Am. Chem. Soc.* **1998**, *120*, 8547.

## Chapter 4

# Thermal Properties of Dendritic Systems

### 4.1 Introduction

One characteristic of polymers, which has promoted their widespread industrial use, is the tuneable thermal properties of the materials. Consequently, understanding the thermal behaviour of a polymer is a crucial factor in defining its potential for different applications. In this chapter, the main features in the thermal transitions of linear polymers will be introduced, including the concept of the glass transition temperature ( $T_g$ ). Secondly, literature examples of investigations into the thermal properties of different dendrimer families and hyperbranched polymers will be summarised. This is followed by experimental data obtained from the thermal analysis of the dendritic molecules prepared in this study, the syntheses of which have been described in Chapters 2 and 3. A preliminary investigation of the thermal behaviour of blends of these polymers has also been undertaken. Analysis of the results leads to conclusions which develop the current understanding of how the chemical compositions of the three main architectural areas of a dendrimer, *i.e.* the core unit, interior branching units and end groups, influence the thermal properties of the macromolecules.

## 4.2 The Glass Transition Temperature

### 4.2.1 Background

On heating, a thermoplastic polymer that has both crystalline and amorphous areas will go through two thermally induced transitions.<sup>1</sup> These transitions are reversible if no degradation has occurred and are called the glass transition temperature ( $T_g$ ) and the melting temperature ( $T_m$ ). Phenomenologically, the glass transition is the temperature at which the amorphous regions of the partially crystalline polymer change from being a hard rigid solid to a soft rubber-like material. This change of state is accompanied by changes in other physical properties, for example the modulus decreases and heat capacity increases. The melting temperature, which is a first-order thermodynamic transition, corresponds to the loss of three-dimensional order in the crystalline portions of the polymer to form a viscous liquid. As the material passes through  $T_g$  the heat capacity increase indicates that the molecular chains have more degrees of freedom; however, unlike the melting transition, there is no latent heat associated with the process, consequently the  $T_g$  is described as a second order transition. If the polymer is completely amorphous in the solid state, which is true for most dendrimers and hyperbranched polymers then a glass transition is observed but no melting transition.

On a molecular level, the glass transition is considered as the temperature at which the polymer chains have sufficient space and energy to move in a certain way. The movement of the polymer chains is assumed not to be translational because of chain entanglement, but is instead described as long-range segmental motion. The unoccupied space in an amorphous polymer, which has to be available for such motion to occur, results from inefficient packing of the molecules. This empty space in the material is given the term free volume and its magnitude is temperature dependent. In the liquid or rubber-like state, the free volume is sufficient to enable the chains to move in the manner described, but as the sample is cooled, the free volume decreases until there is insufficient room to allow movement of the chains. This is the glass transition and below this critical temperature no long-range segmental motion occurs resulting in the chains being locked in the conformation they were in when the  $T_g$  was reached. However, bond vibrations and some rotations may occur below the glass transition.

### 4.2.2 Factors that affect the $T_g$ of a Linear Polymer

The glass transition temperature of a linear polymer is affected by factors including the chain flexibility and the number average molecular weight ( $M_n$ ) and some details are mentioned in this section.<sup>1,2</sup> In addition, the method of measuring the  $T_g$  of a polymer and the

thermal history of the sample affects the experimental value obtained within a range of 10-20°C. If the polymer is crosslinked, the  $T_g$  increases because the density of the material increases resulting in a reduction of the free volume.

#### a) Flexibility of Chain

The flexibility of the polymer backbone is considered to have the most influence on the  $T_g$  of the material. For example, the  $T_g$  of poly(phenylene oxide) (83°C) is 206°C higher than that of polyethylene (-83°C) as its rigid conformation requires more thermal energy to induce motion of the polymer chains.<sup>1</sup> Also, the presence of bulky pendant groups on the main chain increases the  $T_g$ . The increase is related to the molar volume of the group, increasing as the volume increases.

#### b) Molecular Weight

The correlation of  $T_g$  with molecular weight for a linear polymer can be divided into three regions which correspond to polymeric material above a critical molecular weight (Region 1), shorter polymer chains (Region 2) and oligomeric material (Region 3).<sup>1</sup> This is illustrated by a schematic graph of  $T_g$  against  $\log x$ , where  $x$  is of the number of atoms or bonds in the polymer backbone (Figure 4.1).<sup>1,3</sup> The value of  $x$  is proportional to the molecular weight of linear homopolymers, so the plot represents the relationship between  $T_g$  and molecular weight.

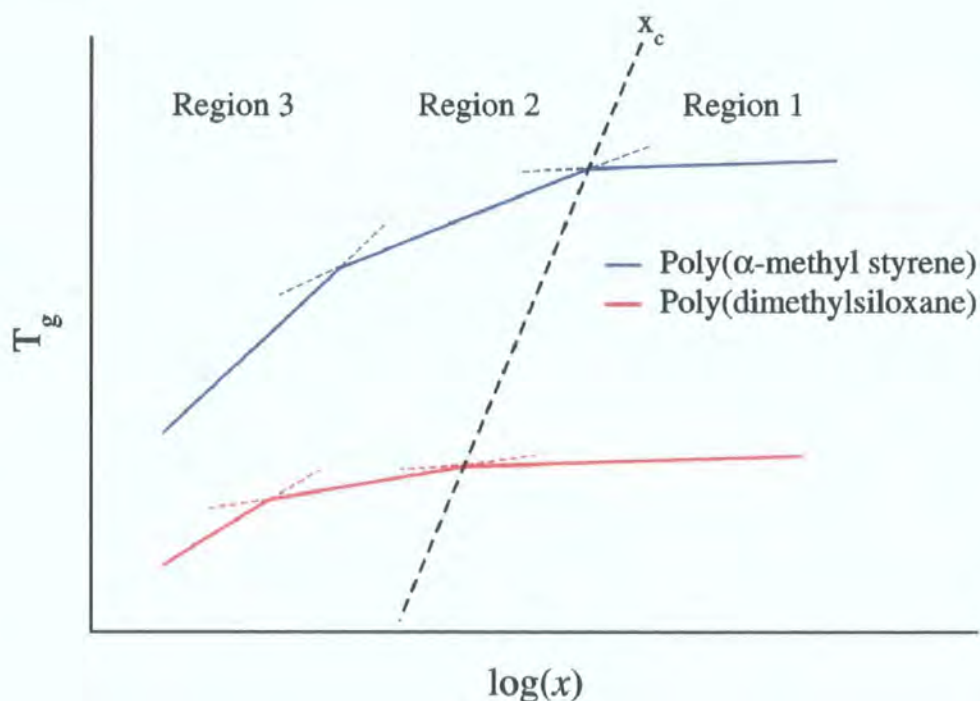


Figure 4.1 Schematic plot to show the relationship between  $T_g$  and chain length<sup>3</sup>

In Region 1, at high molecular weight, the  $T_g$  is constant and the critical molecular weight at which this occurs increases with the rigidity of the polymer chain. For example, poly( $\alpha$ -methyl styrene) is considerably more rigid than poly(dimethylsiloxane) and the onset of maximum  $T_g$  occurs at a chain length of approximately 600 bonds compared to a chain length of about 90 bonds for the less rigid polymer. Below the onset of this maximum value, in regions 2 and 3, the  $T_g$  rises with increasing molecular weight. This relationship can be explained by considering the unoccupied space in the polymer sample and is called free volume theory. The movement of the two ends of a polymer chain is less constrained compared to the movement of the inner segments and therefore the chain ends have more free volume. As the size of the polymer increases, the ends become a smaller proportion of the chain and therefore have less of an effect and the  $T_g$  of the material increases. The difference in the rate of increase of  $T_g$  with chain length in Regions 3 and 2 corresponds to the change from oligomers to polymer chains of lengths sufficiently long to entangle. The value for this entanglement length varies with polymer structure, *e.g.* for poly( $\alpha$ -methyl styrene) it is approximately 30 bonds and for poly(dimethylsiloxane) it is approximately 13 bonds. As the molecular weight increases further, a point is reached where the chain end effects become insignificant and the  $T_g$  approaches a maximum value. This value is determined by the composition of the backbone of the polymer and represents the  $T_g$  at infinite molecular weight ( $T_{g\infty}$ ).

This relationship of glass transition temperature with the number average molecular weight  $M_n$  for linear polymers is summarised by equation 1 where  $T_{g\infty}$  is the  $T_g$  at infinite molecular weight,  $\rho$  is the density of the polymer,  $N$  is Avogadro's number,  $\theta$  represents the free volume per chain end,  $\alpha$  is the free volume expansion coefficient and the integer 2 signifies the number of chain ends.<sup>4</sup> The equation can be simplified to equation 2 where  $K$  is a constant. Therefore, a graph of  $T_g$  versus  $1/M_n$  gives the values of  $T_{g\infty}$  and  $K$  for a linear polymer as the y-intercept and gradient of the line respectively.

$$T_g = T_{g\infty} - \left( \frac{2\rho N\theta}{\alpha} \right) \left( \frac{1}{M_n} \right) \quad (1)$$

$$T_g = T_{g\infty} - \frac{K}{M_n} \quad (2)$$



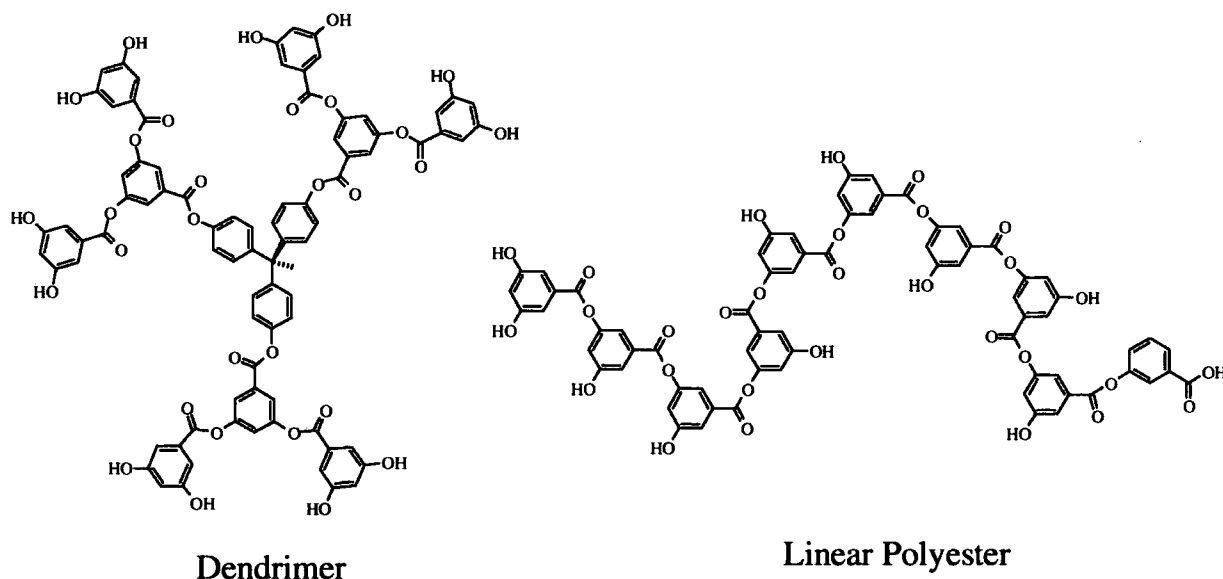


### 4.2.3 Copolymers and Blends<sup>1</sup>

A random linear copolymer and blends of compatible polymers show a single glass transition temperature that, in most cases, lies between those of the separate homopolymers. However, different  $T_g$ s are observed for block copolymers that phase separate into incompatible regions and for blends of incompatible polymers. If the different blocks mix by a significant amount the temperatures of the glass transitions may not be identical to the  $T_g$  values observed experimentally for the separate homopolymers.

### 4.3 The Glass Transition Temperature of Dendrimers and Hyperbranched Polymers

An investigation into the thermal properties of dendrimers, hyperbranched and linear polyesters composed of identical building blocks, resulted in the observation of glass transitions at temperatures which were equivalent for all three families, within experimental error.<sup>5</sup> These structures were based on the building block 3,5-dihydroxybenzoic acid and a low generation dendrimer in the series and the linear polymer are depicted in *Figure 4.2*. The dendrimer with 48 phenolic end groups, the hyperbranched polymer analogue and the linear polymer analogue were all observed to have  $T_g$ s in the region of 200°C.



*Figure 4.2 Polyester dendrimer and linear polymer<sup>5</sup>*

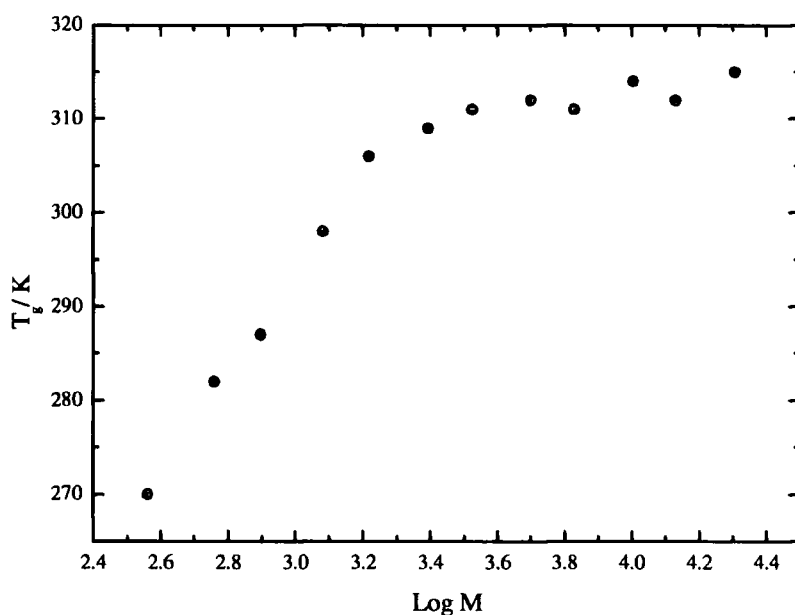
As a consequence of this observation for the polyesters it has been proposed that the glass transition temperature is independent of molecular topology, *i.e.* linear or branched.<sup>5</sup> Hyperbranched poly(ether ketones) with differing degrees of branching were also found to have similar  $T_g$ s,<sup>6</sup> which confirmed this suggestion and a theoretical study of the glass

transition of dendritic polymers also reached the same conclusion.<sup>6,7</sup> However, it is unlikely that explanations given for the thermal behaviour of linear polymers can be applied to dendrimers and hyperbranched polymers. Some reasons for this statement are the increasing number of end groups with molecular weight and the possibility of differing conformations and density for macromolecules of successive generations. Therefore, the thermal properties of dendrimers remain poorly understood despite the analysis of several different series of macromolecules within the last decade.<sup>8,9</sup>

In the following sections investigations from the literature into the  $T_g$  of dendritic polymers will be summarised. The adaptation of equations 1 and 2 for the dendritic structures will be briefly explained and the application and authenticity of the new equations discussed. Principally the  $T_g$  of dendrimers will be considered, though some reference to hyperbranched polymers will be included.

#### 4.3.1 Relationship of $T_g$ and Molecular Weight

The relationship between  $T_g$  and the log of the absolute molecular weight  $M$  has been explored for poly(benzyl ether) dendrimers (*Figure 4.3*). At high molecular weights, the glass transition temperature of the dendrimers reaches a limiting value *i.e.*  $T_{g\infty}$ .



*Figure 4.3 Plot of  $T_g$  versus  $\log M$  for poly(benzyl ether) dendrimers*

This relationship between  $T_g$  and molecular weight is similar to that observed for linear polymers for which the entanglement of the chains and the reduction of chain end effects are given as explanations for the constant value. These reasons cannot be valid for dendritic systems as the number of chain ends increases with molecular weight. Also,

generally it is assumed the larger macromolecules adopt a spherical conformation with a crowded surface, which is less capable of entangling. These changes result in an increase in density of the dendrimer with increasing generation number, which has been concluded from the study of the intrinsic viscosity of dendritic molecules and is described in more detail in Chapter 1, pages 7-8.<sup>10</sup> Interestingly, the critical molecular weight at which the constant value of  $T_g$  is reached for the poly(benzyl ether) dendrimers is approximately the same point at which the maximum in the intrinsic viscosity versus  $M$  plot was observed. For other families of dendrimers and hyperbranched polymers a similar relationship between  $T_g$  and molecular weight has been observed and a limiting value of  $T_g$  reached at high molecular weight.<sup>9,11</sup>

#### 4.3.2 Derivation of Equations for Dendritic System

The relationship between  $T_g$  and molecular weight for dendritic polymers cannot be represented by equations 1 and 2 as they rely on the number of chain ends remaining constant. This was realised by Fréchet *et al.* and the derivation of equation 1 was repeated taking into consideration the continuous increase in the number of end groups for a growing dendritic system. This adapted derivation resulted in equation 3, where  $n_e$  is the number of end groups and  $M$  is the absolute molecular weight of the dendrimer. Equation 3 was simplified to equation 4 where  $K'$  is a constant. The authors acknowledged that  $K'$  may include terms which are not constant, for example the density,  $\rho$ , of the dendrimer.

$$T_g = T_{g\infty} - \left( \frac{\rho N \theta}{\alpha} \right) \left( \frac{n_e}{M} \right) \quad (3)$$

$$T_g = T_{g\infty} - K' \left( \frac{n_e}{M} \right) \quad (4)$$

For linear polymers, the value of  $n_e/M$  (*i.e.*  $2/M$ ) approaches zero at high molecular weights, but for dendritic polymers  $n_e/M$  approaches a constant value. Therefore, a plot of  $T_g$  versus  $n_e/M$  for dendritic polymers will not give the value of  $T_{g\infty}$  as the y-intercept of the graph. However, if the limiting value of  $n_e/M$  at infinite molecular weight, or  $(n_e/M)_\infty$ , is subtracted from the  $n_e/M$  term, to give equation 5 (overleaf) then it follows that the value of  $T_{g\infty}$  is the y-intercept of a plot of  $T_g$  versus  $[(n_e/M) - (n_e/M)_\infty]$ . The value of  $(n_e/M)_\infty$  must be calculated for the dendritic system studied and is determined by the molecular weights of the

terminal groups, branching unit and core of the dendritic series as well as the branching multiplicity.

$$T_g = T_{g\infty} - K' \left( \frac{n_e}{M} - \left( \frac{n_e}{M} \right)_\infty \right) \quad (5)$$

In the study of the thermal properties of hyperbranched polyesters by Parker and Feast, the derivation of the equation 4 was developed following the recognition that  $n_e$  was dependent on the degree of polymerisation.<sup>12</sup> As a result, it was proved that the  $n_e/M$  term could be equated to the addition of the reciprocals of  $M$  and  $M_o$ , where  $M_o$  is the monomer mass (equation 6). This relationship made it possible to plot the graph of  $T_g$  versus  $1/M_w$  for the hyperbranched system and obtain a straight line.

$$\frac{n_e}{M} = \frac{1}{M_o} + \frac{1}{M} \quad (6)$$

The application of equation 6 without further adaptation may not be possible for most dendrimer families as the structures contain core units and terminal groups which differ from the repeat unit (which is represented in the  $M_o$  term).

### 4.3.3 Application of Derived Equations

Fréchet and coworkers proceeded to investigate the glass transition temperatures of a series of aromatic polyether dendrons, dendrimers and codendrimers containing polyester and polyether functional groups using equation 5. The polyether dendrons were synthesised from the first to sixth generation and the third generation dendron **63** is shown overleaf (*Figure 4.4*). The corresponding dendrimers were prepared by attachment of the dendrons to either difunctional or trifunctional cores to give two dendrimer series, illustrated by the third generation structures **64** and **65** respectively (*Figures 4.4*). For these third generation structures, the  $T_g$ s obtained experimentally were within 7°C of each other, however, at lower generations the glass transitions for the three series occurred over a larger temperature range. The  $T_g$  data from these materials was then used to establish if the derived equations for a dendritic system were valid and values of  $T_{g\infty}$  and  $K'$  were obtained.

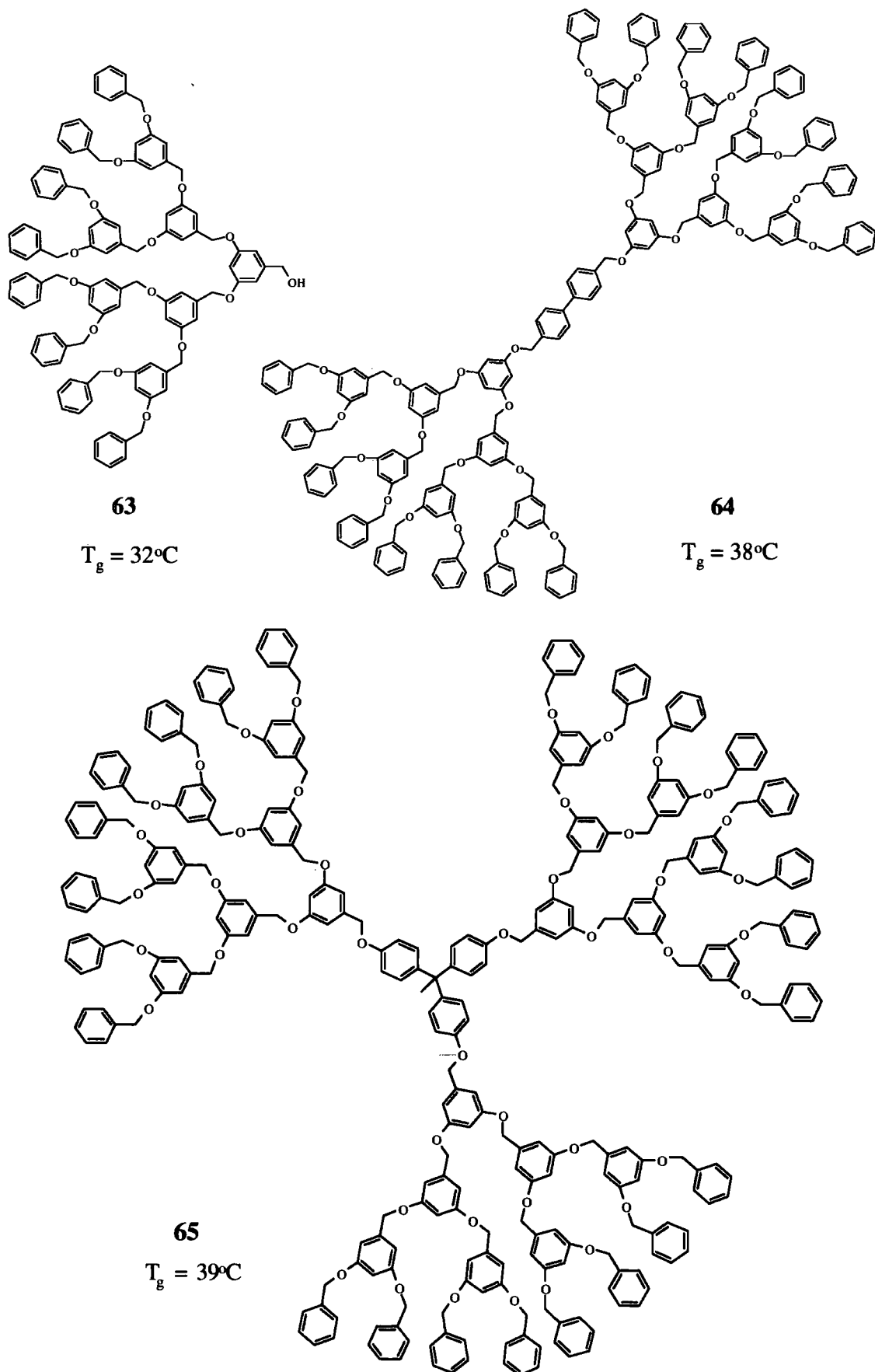
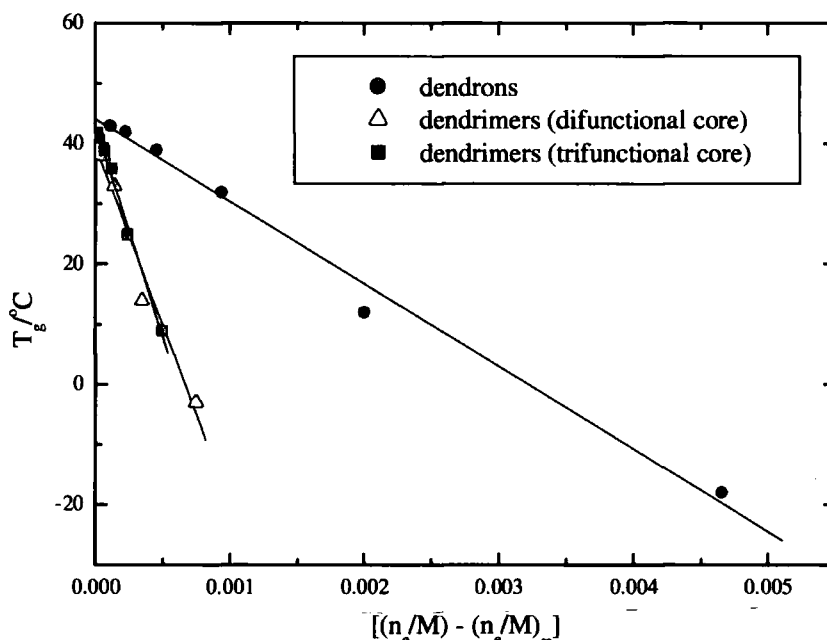


Figure 4.4 Third generation aromatic polyether dendron **63**, difunctional dendrimer **64** and trifunctional dendrimer **65**

The plots of  $T_g$  versus  $[(n_e/M) - (n_e/M)_\infty]$  for the poly(benzyl ether) dendrons and dendrimers showed a linear relationship which indicated that the terms included in  $K'$  were either constant or cancelled each other out. The  $T_{g\infty}$ s for the series of dendrons, difunctional core dendrimers and trifunctional core dendrimers were found to be the same within experimental error, with values of 44°C, 39°C and 43°C respectively. However,  $K'$  for the dendron series was 13700 which differed from the  $K'$  values obtained for the dendrimers, which were 59600 and 69900 (*Figure 4.5*). This difference in  $K'$  for the dendrons and dendrimers was explained by the presence of an additional end group at the focal point of the dendron. The extra hydroxyl end group of the dendron contributes additional free volume to the polymer and a further equation was derived to take this into account. However, it was concluded that the free volume of the hydroxyl group at the focal point was similar to that of the benzyl terminal groups or the relationship between  $T_g$  and  $[(n_e/M) - (n_e/M)_\infty]$  would not have been linear.



*Figure 4.5 Plots of  $T_g$  versus  $[(n_e/M) - (n_e/M)_\infty]$  for the poly(benzyl ether) dendrons and dendrimers*

To ascertain if the glass transition temperatures of the poly(benzyl ether) dendritic system could be represented by a linear relationship in a graph of  $T_g$  versus  $1/M$  the data was analysed by the author of this thesis (*Figure 4.6*). These graphs gave approximately linear relationships and the  $T_{g\infty}$  values, obtained from the y-intercepts, were found to be 44°C, 41°C and 43°C for the series of dendrons, difunctional core dendrimers and trifunctional core dendrimers respectively. By comparison of these values of  $T_{g\infty}$  with those obtained by



Fréchet *et al.* using the first graphical method (Figure 4.5) it is evident the two analyses are extremely similar!

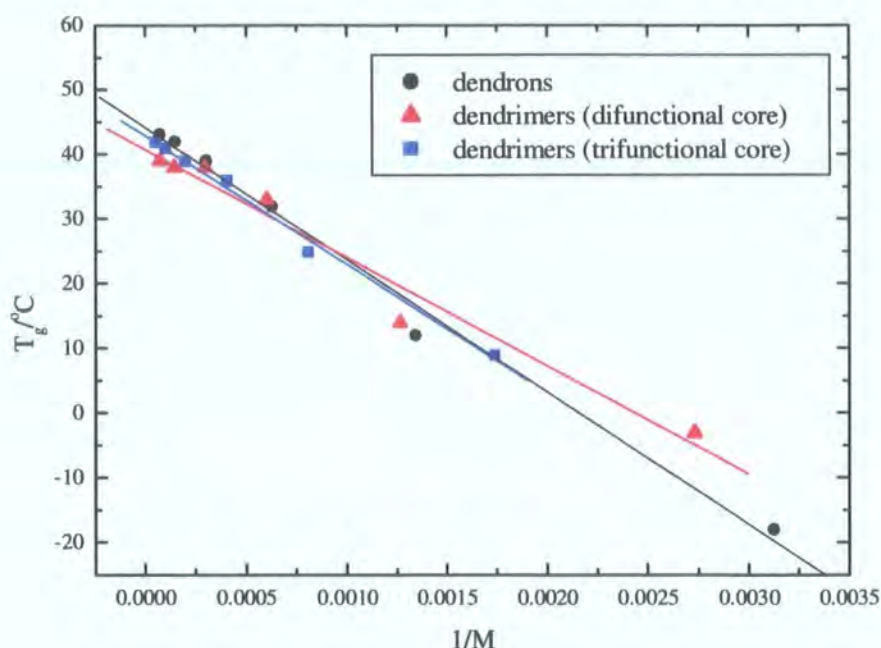


Figure 4.6 Plot of  $T_g$  versus  $1/M$  for the poly(benzyl ether) dendrons and dendrimers

#### 4.3.4 Dendritic Macromolecules with Different Terminal Groups

The nature of the chain ends of the poly(benzyl ether) dendrons was shown to affect the glass transition temperatures of the materials.<sup>8</sup> The  $T_g$  increased with the polarity of the terminal group. For example, fourth generation dendrons with hydrogen groups (*i.e.* dendron series 63, Figure 4.4, page 106), bromo groups and cyano groups at the periphery have  $T_g$ s of 42°C, 52°C and 76°C respectively and the  $T_{g\infty}$ s for the dendrimers also increased in this sequence. The values of  $K'$  were observed to increase with the larger size of the end groups, *i.e.* in the order H, CN, Br, which was attributed to either the denser arrangement of the material or the greater free volume of the chain ends.

There are other examples in the literature confirming that the chemical composition of the terminal groups affects the glass transition temperature of dendrimers and hyperbranched polymers.<sup>6,13-15</sup> In general, the increased polarity of the end groups or the more restricted their motion by steric or connectivity demands, the higher temperature at which the  $T_g$  is observed. This observation prompted Kim and Webster to suggest that the dependency of  $T_g$  on the end groups was caused by the onset of translational motion rather than segmental motion of the dendritic molecules.<sup>14</sup> However, the composition of other structural areas within the hyperbranched polymer was not varied in this study.

### 4.3.5 Dendrimers with Different Branching Units

In several reported examples there is evidence that subtle changes in the chemical composition of the dendrimers' branching units have an effect on the  $T_g$  of the materials.<sup>8,9</sup> For example, a third generation poly(benzyl ester) dendrimer has a glass transition at a higher temperature (126°C) than its poly(benzyl ether) analogue **65** (39°C).<sup>16</sup> This effect has also been noted for two different types of dendrimers comprising of benzene rings either linked by ester groups, *i.e.* **66** or  $\sigma$ -bonds, *i.e.* **67** (Figure 4.7).<sup>9,17</sup> The first generation dendrimers of these families, **66** and **67**, were found to have glass transitions at temperatures of 110°C and 126°C respectively. The comparison of higher generation dendrimers in these aromatic-linked series presented a greater difference in  $T_g$  between the two types of structures. The observation of glass transition at a lower temperature for the ester-linked dendrimers was explained by the greater flexibility and increased degrees of freedom of the macromolecules.

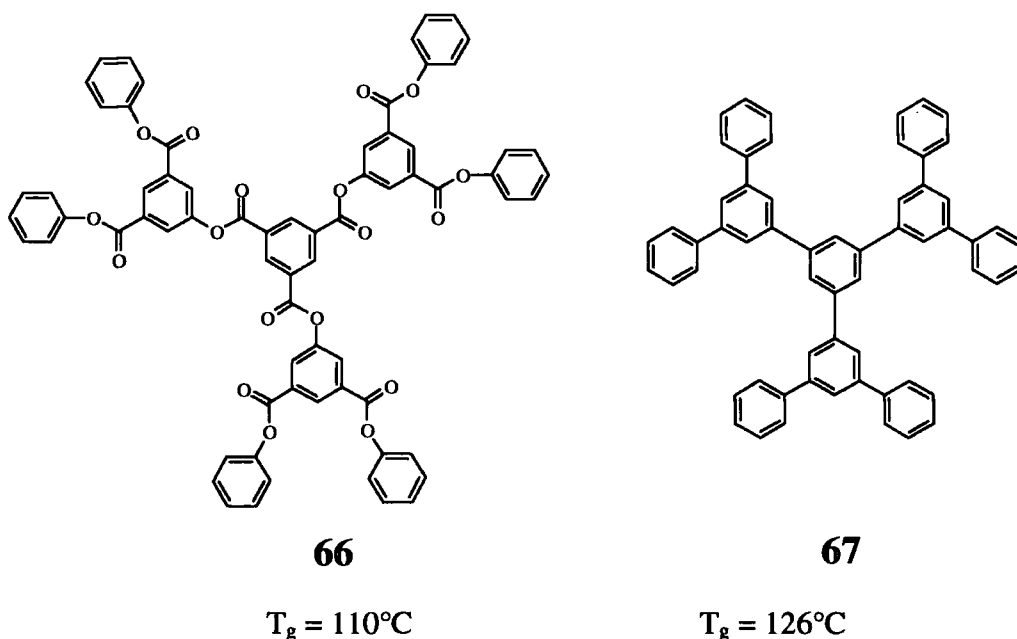
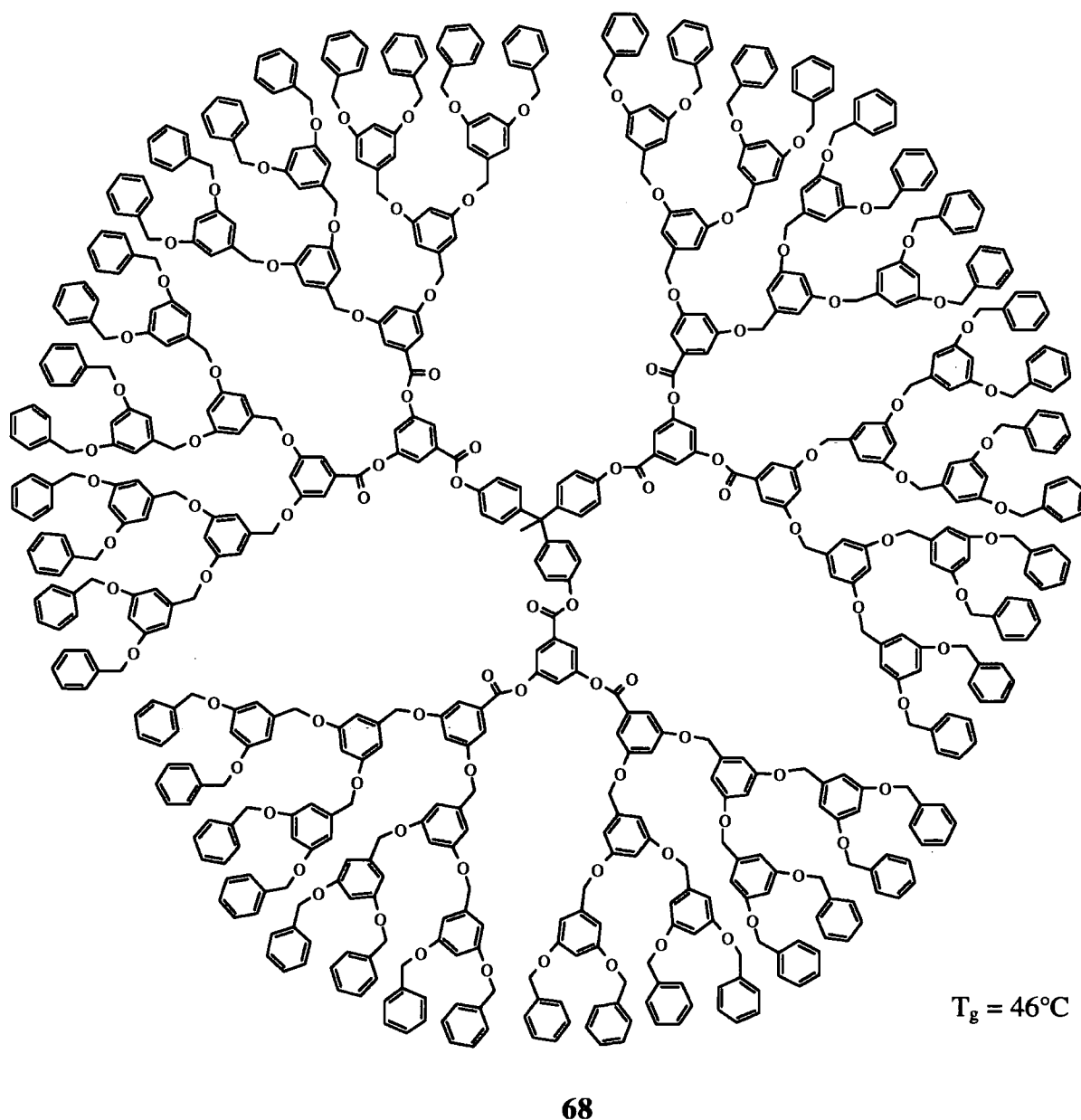


Figure 4.7  $T_g$ s of aromatic dendrimers containing different monomer units

### 4.3.6 Codendrimers

A further development of the investigation into the effect of varying the monomer units on the glass transition of a dendrimer is possible by the comparison of the thermal properties of codendrimers. The structural details and synthesis of segmental, layer and surface codendrimers by Fréchet and coworkers were outlined in Chapter 3 (pages 75-78).<sup>16</sup> The glass transition temperatures of these codendrimers were obtained experimentally and all the materials showed a single glass transition suggesting no significant phase separation had

occurred.<sup>8,16</sup> The  $T_g$ s of these heterodendrimers, consisting of a mixture of ester and ether linkages, were at temperatures intermediate between those of the homodendrimers. Also, the glass transition temperatures were found to be dependent on the proportion of ether and ester links in the structure. A fifth generation layer codendrimer **68** consisting of two concentric layers of ester linkages at the core and followed by three outer levels of ether linkages had a  $T_g$  only 7°C higher than the corresponding poly(benzyl ether) homodendrimer (*Figure 4.8*).<sup>16</sup> The authors concluded that the ether blocks were the more dominant influence owing to their large size. However, the thermal data for only a few structures with variations in their composition layering was obtained and consequently a secure correlation between structure and  $T_g$  was not possible.



*Figure 4.8 Fifth generation poly(ester-ether) layer codendrimer*



## 4.4 Thermal Properties of Polyurethane Dendrons and Dendrimers

### 4.4.1 Experimental Measurement of $T_g$

The glass transition temperatures of the polyurethane dendrons and dendrimers discussed in the following sections were determined using differential scanning calorimetry (DSC). The samples were heated from  $-180^{\circ}\text{C}$  to  $170^{\circ}\text{C}$  at a rate of  $10^{\circ}\text{C}$  per minute, cooled at a rate of  $50^{\circ}\text{C}$  per minute and heated a second time through the same temperature range at  $10^{\circ}\text{C}$  per minute. The value of  $T_g$  was taken as the midpoint of the inflection from the second heating run. The  $T_g$  values from the heating and cooling runs were usually within  $4^{\circ}\text{C}$  but in a few cases were as far apart as  $20^{\circ}\text{C}$ . This is not unusual, as the  $T_g$  of a material is known to change by as much as  $20^{\circ}\text{C}$  depending on the method of measurement and the thermal history of the sample.<sup>2</sup> The thermal analysis of the small molecules and dendritic macromolecules discussed in the following sections, with the exception of the first generation dendron **BG10H**, revealed a single glass transition. For the exception, a glass transition ( $-18.4^{\circ}\text{C}$ ) followed by a melting transition ( $61.8^{\circ}\text{C}$ ) were observed during the first heating run whereas only a glass transition ( $-5.1^{\circ}\text{C}$ ) occurred during the second heating run.

For the analysis of the poly(urethane-carbonate) codendrimers the accuracy of the  $T_g$  values was crucial, therefore the heating and cooling cycles were repeated four times to confirm the attainment of a constant value of  $T_g$ . A typical DSC trace for this procedure is shown below for the codendrimer **BG2D (UCU)** (Figure 4.9). Also, the measurement of  $T_g$  in this manner was repeated to ensure reproducibility.

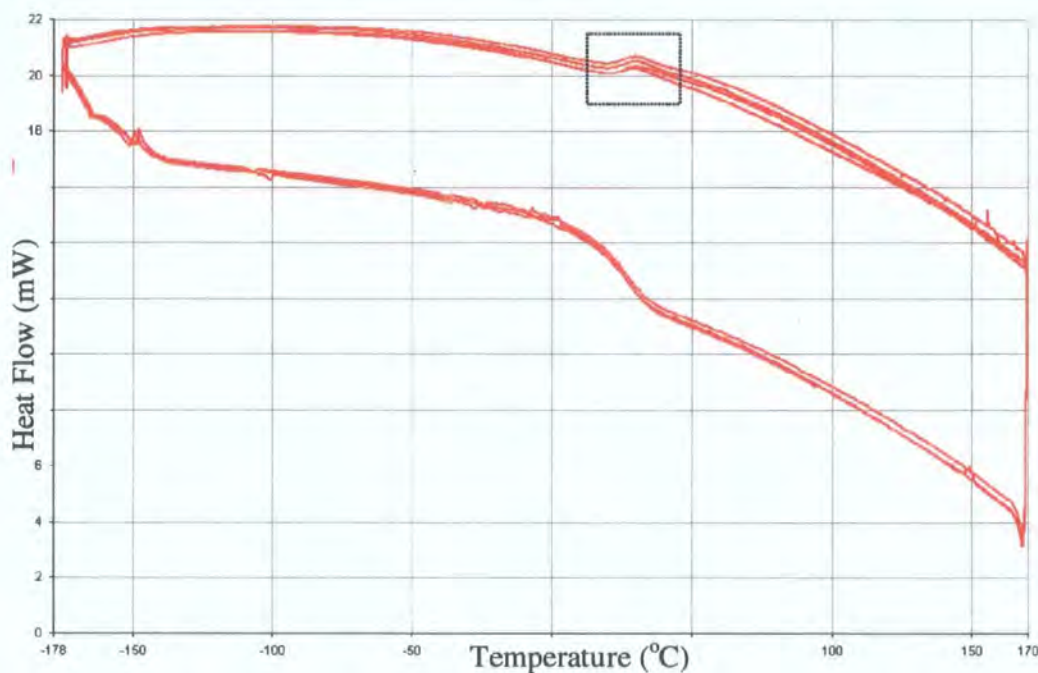


Figure 4.9 DSC trace of codendrimer **BG2D (UCU)**

Occasionally, the  $T_g$  obtained from the first heating step was different to those from latter heating and cooling runs and, in general, the glass transitions observed during these latter cycles were at similar temperatures (within  $0.5^\circ\text{C}$ ). The heating steps taken from the thermal analysis for **BG2D** (UCU) and the corresponding temperatures of the glass transitions are indicated below (Figure 4.10, this is an expansion of the highlighted area in Figure 4.9).

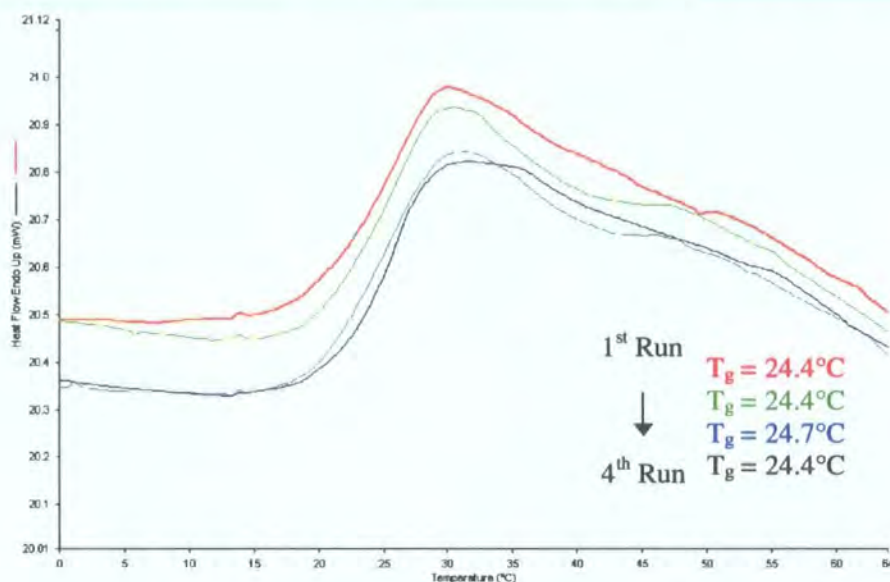


Figure 4.10 Heating runs of the DSC trace of **BG2D** (UCU)

#### 4.4.2 Effect of Molecular Weight and End Group on the $T_g$ of Polyurethane Dendrons

The relationships between  $T_g$  and the log of the molecular weight  $M$  for the polyurethane dendrons with *t*-butyl, cyclohexyl and 4-heptyl end groups, are depicted below (Figure 4.11).

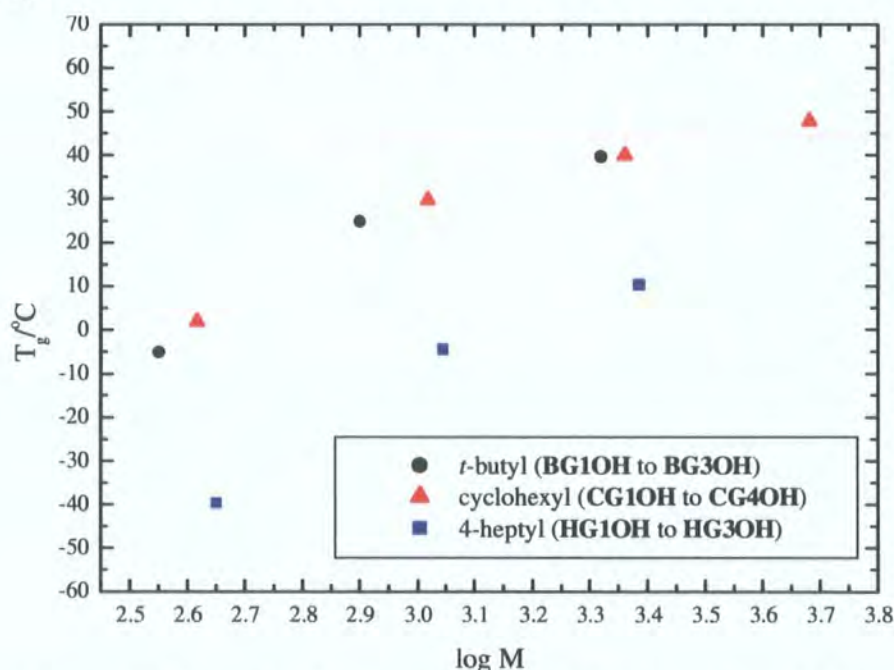


Figure 4.11 Graph of  $T_g$  versus  $\log M$  for the polyurethane dendrons

As the synthesis of dendrons has only been successful up to the third or fourth generations, there is insufficient evidence to determine if the  $T_g$  does 'level off' at high molecular weight as expected from data in the literature.<sup>8</sup> However, it appears that the rate of increase of  $T_g$  with molecular weight reduces as the generation of the polyurethane dendrons increases.

The glass transition temperatures of the polyurethane homodendrimers were plotted together with the values for the dendrons (Figure 4.12) and the attainment of a limiting  $T_g$  value at high molecular weight was substantiated. These graphs of  $T_g$  versus  $\log M$  indicate that the maximum value of  $T_g$  observed for the polyurethane dendritic molecules with the 4-heptyl end is approximately 30°C lower than for the corresponding structures with *t*-butyl and cyclohexyl end groups. This observation may be explained by the larger free volume of the flexible 4-heptyl groups resulting in a lesser amount of energy being required to induce motion and therefore, the  $T_g$  occurring at a lower temperature.

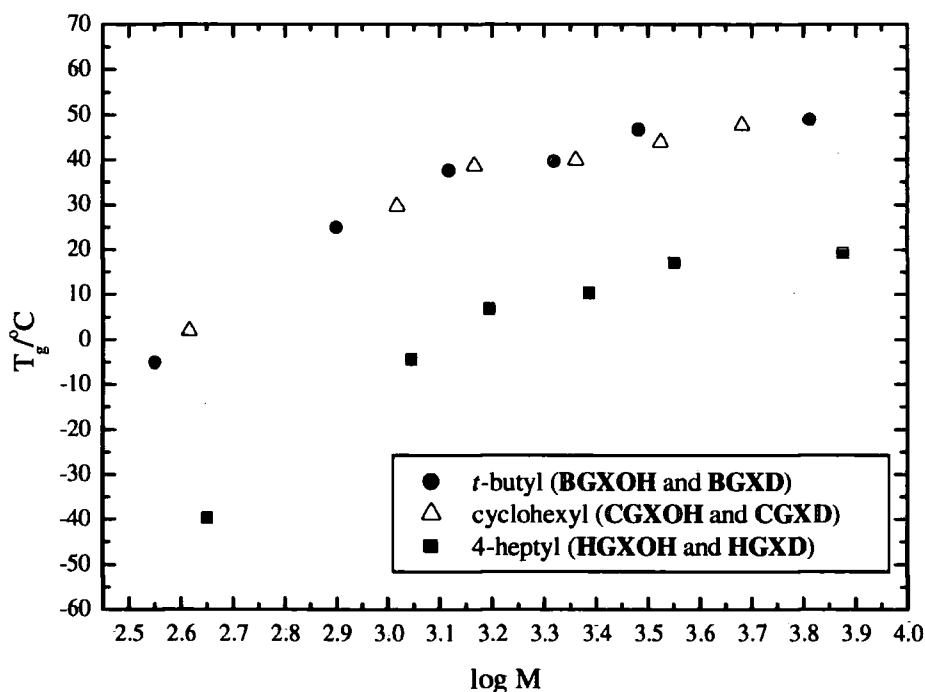


Figure 4.12 Plots of  $T_g$  versus  $\log M$  for the polyurethane dendrons and dendrimers

#### 4.4.3 Determination of $T_{g\infty}$ for Polyurethane Dendrons

In the previous section it was demonstrated that the glass transition temperatures of the polyurethane macromolecules reached limiting values at high molecular weight which were dependent on the nature of the terminal groups. In an attempt to determine these values of  $T_{g\infty}$  for the three different dendron series the thermal data obtained were analysed using two graphical methods. Firstly, the equations introduced by Fréchet *et al.* (pages 104-105) were applied and the glass transition temperatures of the polyurethane dendrons were plotted



on a graph of  $T_g$  versus  $[(n_e/M) - (n_e/M)_\infty]$  (Figure 4.13). In each case a linear relationship was observed and  $r$ , the correlation coefficient, is indicated on the graph. The values of  $T_{g\infty}$  for the *t*-butyl, cyclohexyl and 4-heptyl terminated structures were obtained from the y-intercepts of the graph and are listed in Table 4.1. The  $T_{g\infty}$  for the 4-heptyl dendron series was found to be 30.2°C and 33.5°C lower than for the *t*-butyl- and cyclohexyl-terminated series respectively. The term  $(n_e/M)_\infty$ , which had to be calculated for each different dendron series so as to obtain the necessary values to plot the graph is also included in Table 4.1.

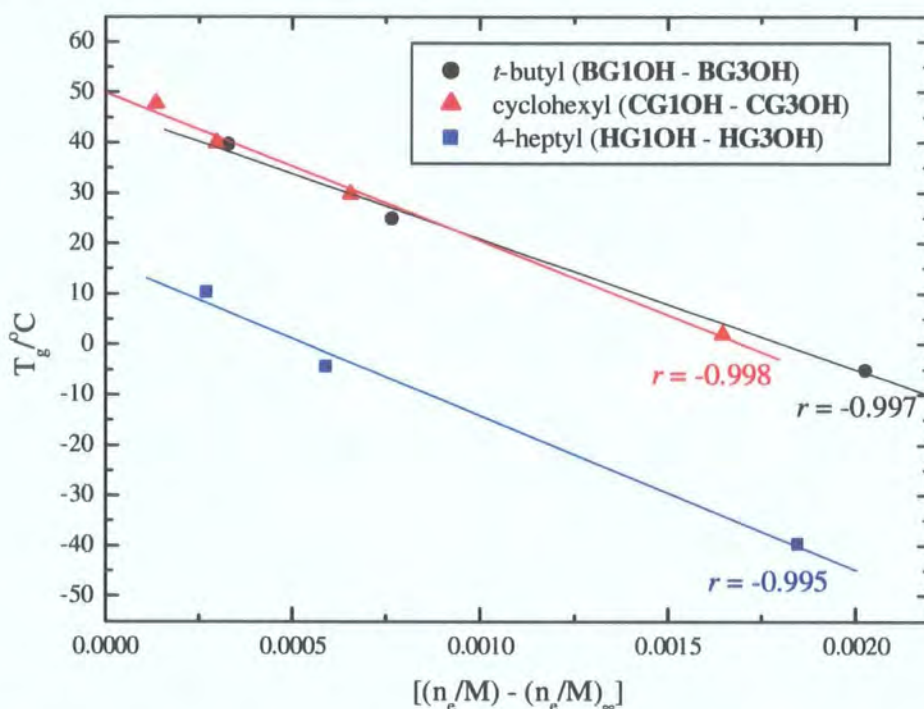


Figure 4.13 Plots of  $T_g$  versus  $[(n_e/M) - (n_e/M)_\infty]$  for the polyurethane dendrons

Dendron Series	$T_{g\infty}/^\circ\text{C}$	$(n_e/M)_\infty$
<b>BGXOH</b>	46.7	0.0035075
<b>CGXOH</b>	50.0	0.0030355
<b>HGXOH</b>	16.5	0.0031909

Table 4.1 Data for the polyurethane dendrons

Secondly, values of  $T_{g\infty}$  for the three dendrons series were obtained from the y-intercept of the plots of  $T_g$  versus  $1/M$  (Figure 4.14, overleaf). These values for the *t*-butyl, cyclohexyl and 4-heptyl dendrons were found to be 47.4°C, 50.2°C and 21.1°C, which are approximately in agreement with those obtained from the previous graphical method (Table 4.1), with only the 4-heptyl series showing a significant difference.

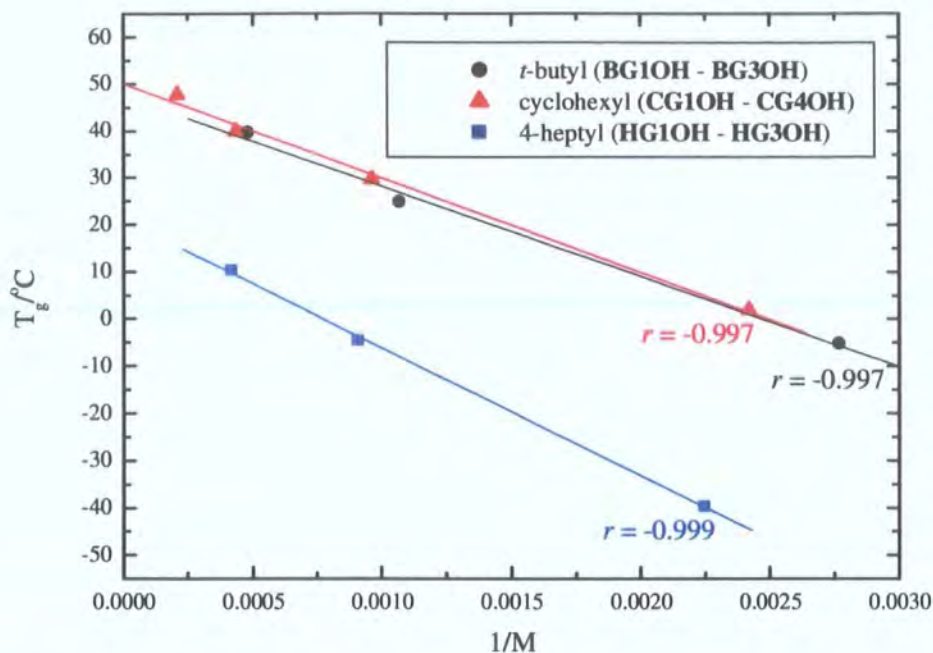


Figure 4.14 Plots of  $T_g$  versus  $1/M$  for the polyurethane dendrons

#### 4.4.4 Determination of $T_{g\infty}$ for Polyurethane Dendrimers

Analogous graphical interpretations of the glass transitions were carried out for the polyurethane dendrimers and the plots of  $T_g$  versus  $[(n_e/M) - (n_e/M)_\infty]$  for the *t*-butyl- and 4-heptyl-terminated structures are depicted in Figure 4.15. The relationships were shown to be linear and values of  $T_{g\infty}$  were found to be 52.2°C and 23.4°C for the *t*-butyl- and 4-heptyl-terminated structures respectively. Using the second method, *i.e* plotting  $T_g$  versus  $1/M$ , linear relationships were also observed and the values of  $T_{g\infty}$  were found to be 52.2°C and 23.5°C for the *t*-butyl- and 4-heptyl-terminated dendrimers.

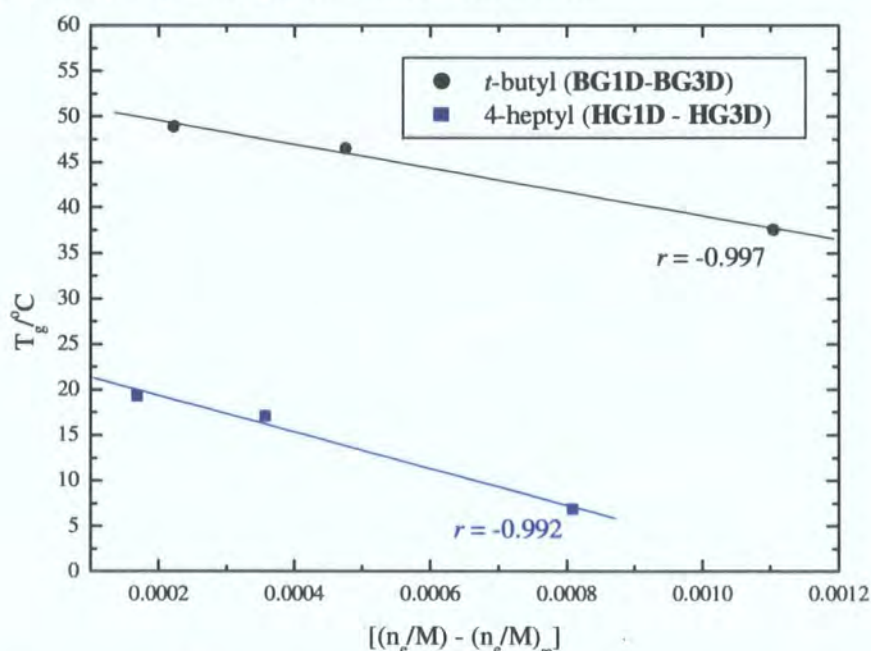


Figure 4.15 Plot of  $T_g$  versus  $[(n_e/M) - (n_e/M)_\infty]$  for the polyurethane dendrimers

#### 4.4.5 Comparison of Dendrons and Dendrimers

From the plot of  $T_g$  versus  $\log M$ , which depicted the values for the dendrons and dendrimers on the same graph (Figure 4.12), it was evident that data points corresponding to the two different structures could not be distinguished. To investigate this observation further the plots of  $T_g$  versus  $[(n_e/M) - (n_e/M)_\infty]$  for the dendrons and dendrimers were overlaid on the same graph (Figure 4.16) and the corresponding values of  $T_{g\infty}$  have been listed in Table 4.2.

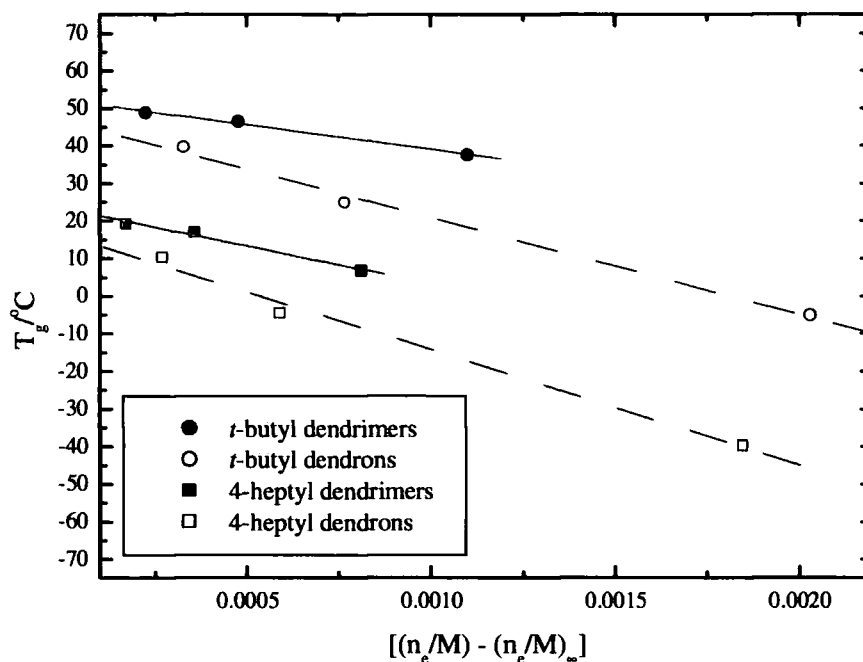


Figure 4.16 Graph of  $T_g$  versus  $[(n_e/M) - (n_e/M)_\infty]$  for the polyurethane dendrimers and dendrons

Terminal groups	Type of Series (Code)	$T_{g\infty}/^\circ\text{C}$
t-butyl	Dendron (BGXOH)	46.7
	Dendrimer (BGXD)	52.2
4-heptyl	Dendron (HGXOH)	16.5
	Dendrimer (HGXD)	23.4

Table 4.2  $T_g$  for the polyurethane dendrons and dendrimers with different terminal groups

From the graph it is evident that the  $T_g$ s of the two different types of dendritic molecules approach similar values at high molecular weight. The values of  $T_{g\infty}$  obtained graphically for the different sets of dendritic molecules (Table 4.2) indicate that for structures with the same terminal groups, there is only a small difference in  $T_{g\infty}$ . This observation may be rationalised by the fact that at high generations the focal point of the dendron becomes a

smaller proportion of the macromolecule and essentially a dendron becomes a dendrimer with a difunctional core. Therefore, dendrons and dendrimers of similar molecular weight would be expected to have similar values of  $T_g$ . The slope of the lines (*i.e.*  $K'$ ) is different for the dendrimers and dendrons within the same series and the gradient of the line and hence the value of  $K'$  was found to be greater for the polyurethane dendrons than for the dendrimers. This observation contrasts with that of Fréchet *et al.* concerning the poly(benzyl ether) dendritic systems, where the dendrimers displayed a steeper slope than the dendrons. The explanation given by Fréchet for his observation of differing gradients was the presence of an additional chain end at the focal point of the dendron. An explanation for the current results could be that the hydroxyl group at the focal point of the polyurethane dendrons hydrogen bonds to the urethane links in the dendritic wedge and therefore has less free volume than would be expected for a free focal point. Additionally, within the term  $K'$  or the gradient of the line there are a few terms which may vary between the dendrons and dendrimers, perhaps most likely is the density  $\rho$ .

#### 4.4.6 Dendrimers with Aromatic-ester Core

In this section the glass transition temperatures of dendrimers, which differ by the structure of their core units will be investigated. Firstly, in order to compare the polyurethane homodendrimers (**BG1D** – **BG3D**) and the aromatic-ester core dendrimers (**BG1DAC** – **BG3DAC**), the relevant  $T_g$ s have been depicted on a plot of  $T_g$  versus  $1/M$  (*Figure 4.17*, overleaf). The  $T_g$ s of the second and third generation dendrimers ( $G = 2$  and  $3$ ) were evidently not affected by the composition of the core, whereas the first generation structures had  $T_g$ s of slightly differing values ( $2.5^\circ\text{C}$ ). However, an equivalent analysis of the structures with cyclohexyl end groups indicated that some of these observations were not reproducible (*Figure 4.18*, overleaf). In this case the first generation dendrimer with the aromatic-ester core unit had a slightly higher  $T_g$  than the corresponding amine core structure and the glass transitions of the second generation dendrimers were dissimilar. However, if a linear relationship was assumed for the **CGXDAC** series, the  $T_{g\infty}$  ( $52.5^\circ\text{C}$ ) was found to be approximately equal to the  $T_{g\infty}$  obtained for the polyurethane *dendrons* with cyclohexyl termini ( $50.2^\circ\text{C}$ ). This similarity in the limiting value of  $T_g$  for the dendrons and dendrimers suggests that at high molecular weight the structure of the core and the architecture of the dendritic species (*i.e.* dendron or dendrimer) does not affect the  $T_g$ . However, for the lower generations it is impossible to determine and rationalise the effect a more rigid aromatic core has on the  $T_g$  from the data available.

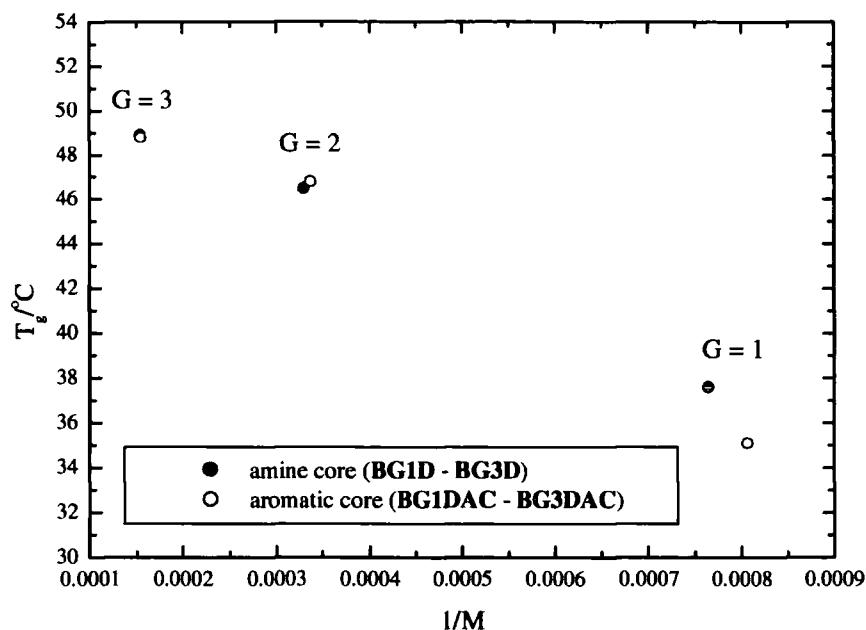


Figure 4.17 Graph of  $T_g$  versus  $1/M$  for dendrimers with differing core units

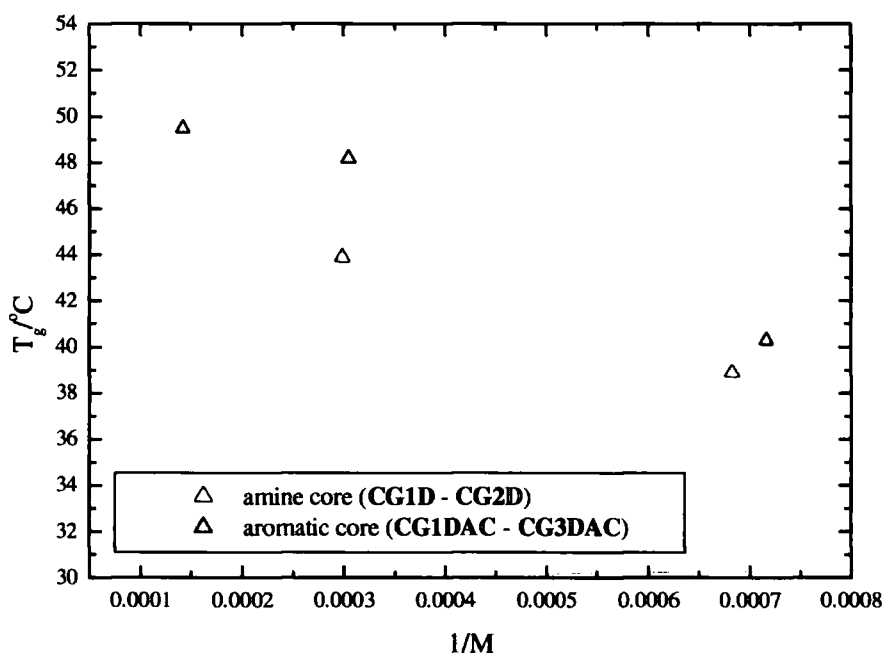


Figure 4.18 Graph of  $T_g$  versus  $1/M$  for cyclohexyl-terminated dendrimer series

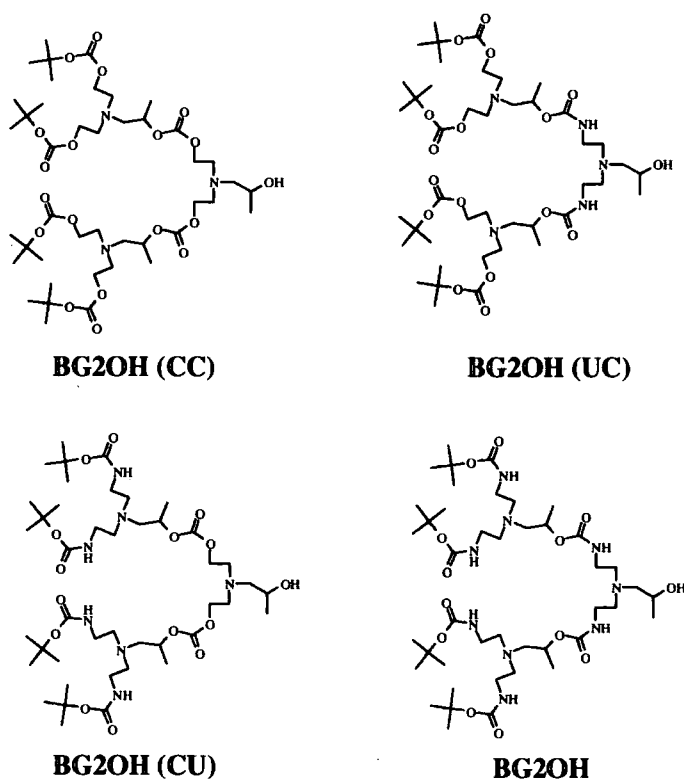
#### 4.4.7 Layer Codendrimers

The polycarbonate analogue **BG2D** (CCC) of the polyurethane second generation dendrimer **BG2D** is a viscous oil whereas the urethane-linked structure is a hard amorphous solid. Therefore, prior to the measurement of the  $T_g$  of the materials it was evident that different values would be obtained. This was confirmed experimentally as the glass transition for the carbonate and urethane dendrimers were found to occur at temperatures of  $-14.0^\circ\text{C}$



and 46.7°C. This observation could be explained by the ability of the urethane groups to form strong hydrogen bonds whereas the carbonate groups are not capable of interacting with each other in this manner. Consequently, the carbonate branches of the dendrimer are more flexible than the 'locked' urethane branches, less energy is required for long-range segmental motion within the molecules to occur and the  $T_g$  is observed at a lower value. In addition, the glass transition temperatures of codendrimers comprising a mixture of urethane and carbonate groups were found experimentally with the purpose of investigating the relationship between  $T_g$  and the location and number of urethane and carbonate groups in the structures. The synthesis of this set of six layer codendrimers, with different proportions of urethane and carbonate groups, was outlined in Chapter 3 (pages 79-86). For all the codendritic molecules investigated in this study a single glass transition was observed experimentally. This is in agreement with the thermal analysis of poly(ether-ester) codendrimers, as only one glass transition occurred for these structures of mixed functionality.<sup>8</sup> However, a literature example of a surface-block fourth generation polyether codendrimer with one region of termini comprising acid functions and another comprising benzyl-ether groups was observed to have two glass transitions.<sup>18</sup>

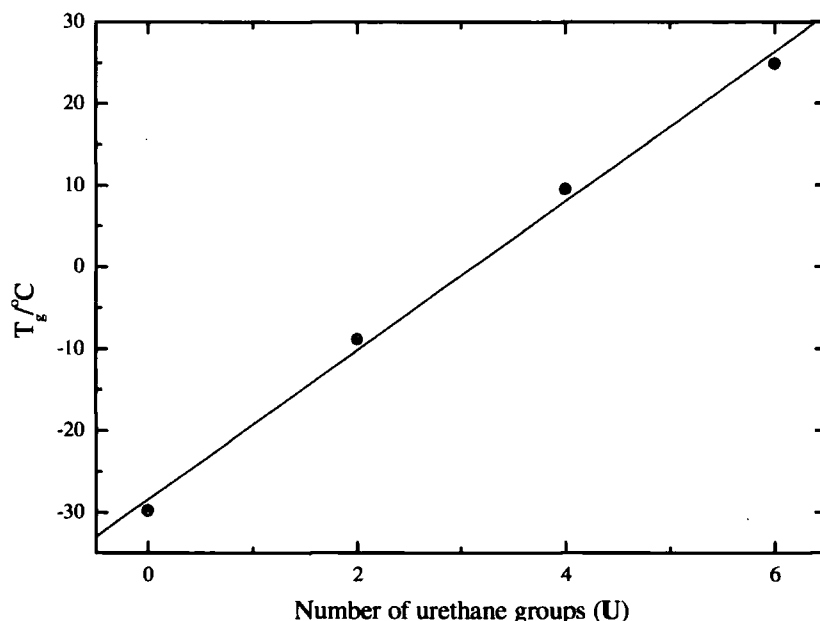
Firstly, the glass transition temperatures of the second generation dendrons with varying proportions of carbonate and urethane groups were compared to determine the effect of the relative proportions of the two functions on the  $T_g$  of small molecules (*Figure 4.19*).



*Figure 4.19 Second generation dendrons*



The  $T_g$ s of the second generation dendrons were found to be dependent on the number of urethane links in the molecule and the relationship was shown to be linear (*Figure 4.20*). Since the dendrons are effectively model compounds of the codendrimers this analysis showing that their  $T_g$ s can be correlated with the number of urethane groups will be useful in our analysis of the codendrimers.



*Figure 4.20 Plot of  $T_g$  versus number of urethane groups (U) for second generation codendrons*

The layer codendrimers were formed by the reaction of the second generation dendrons with either a trifunctional amine or alcohol core unit and are identified by a code which describes the composition of the concentric linking groups in the structure (See Chapter 3, page 80 for a full explanation). To summarise this code, a carbonate link is represented by C, a urethane link by U and the layers are described from the interior to the exterior of the dendrimer. For example **BG2D (UCU)** has a urethane link at the core, a carbonate link in the middle and another urethane link near the end groups. The glass transition temperatures of the codendrimers were obtained experimentally by DSC and are shown in the table below together with those of the polyurethane and polycarbonate homodendrimers (*Figure 4.21* and *Table 4.3*). The number of urethane groups (Number of U) for each second generation dendrimer is given in the table, as this factor must be taken into consideration.

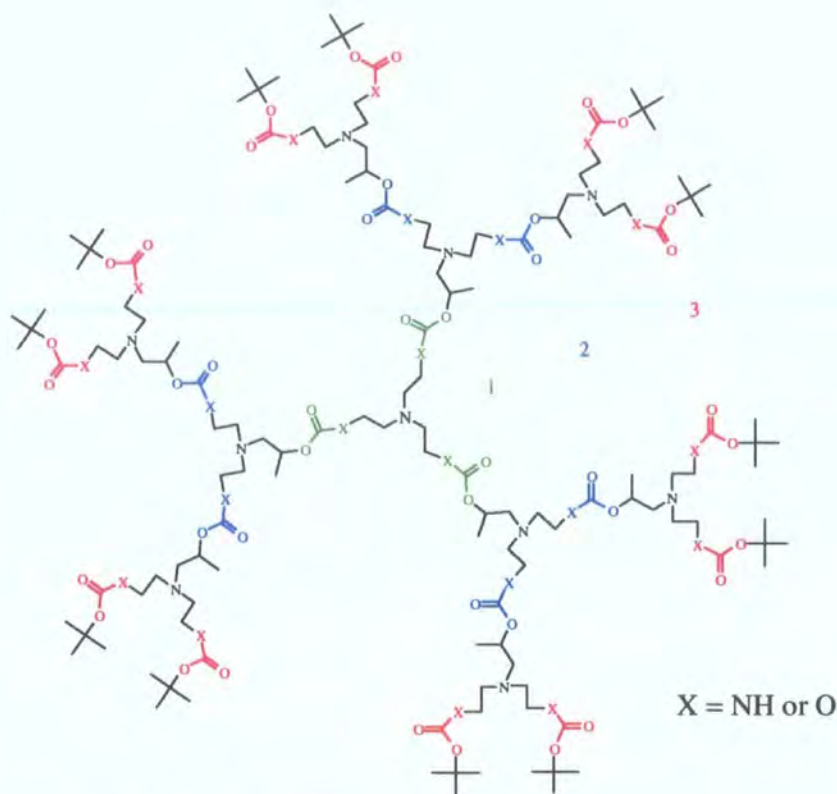


Figure 4.21 Schematic of second generation homo- or codendrimers

	Dendrimer Code	1	2	3	T <sub>g</sub> /°C	Number of U
Region 1	BG2D (CCC)	C	C	C	-14.0	0
	BG2D (UCC)	U	C	C	-8.5	3
Region 2	BG2D (CUC)	C	U	C	1.9	6
	BG2D (UUC)	U	U	C	9.4	9
	BG2D (CCU)	C	C	U	16.8	12
	BG2D (UCU)	U	C	U	24.4	15
Region 3	BG2D (CUU)	C	U	U	38.3	18
	BG2D	U	U	U	46.7	21

Table 4.3 T<sub>g</sub>s of second generation homo- or codendrimers

The glass transition temperature data for the dendrimers included in Table 4.3 has been represented in a plot of T<sub>g</sub> against number of urethane units (Figure 4.22, overleaf). The code of the dendrimer is also given on the x-axis and the graph has been divided into three regions to assist with discussion of the data. The differences between the T<sub>g</sub>s of consecutive dendrimers in the series, which will be discussed later in the text, are also included in the appropriate positions on the graph. For Region 2 the average difference in T<sub>g</sub> between the successive dendrimers in the series is quoted (7.6°C).

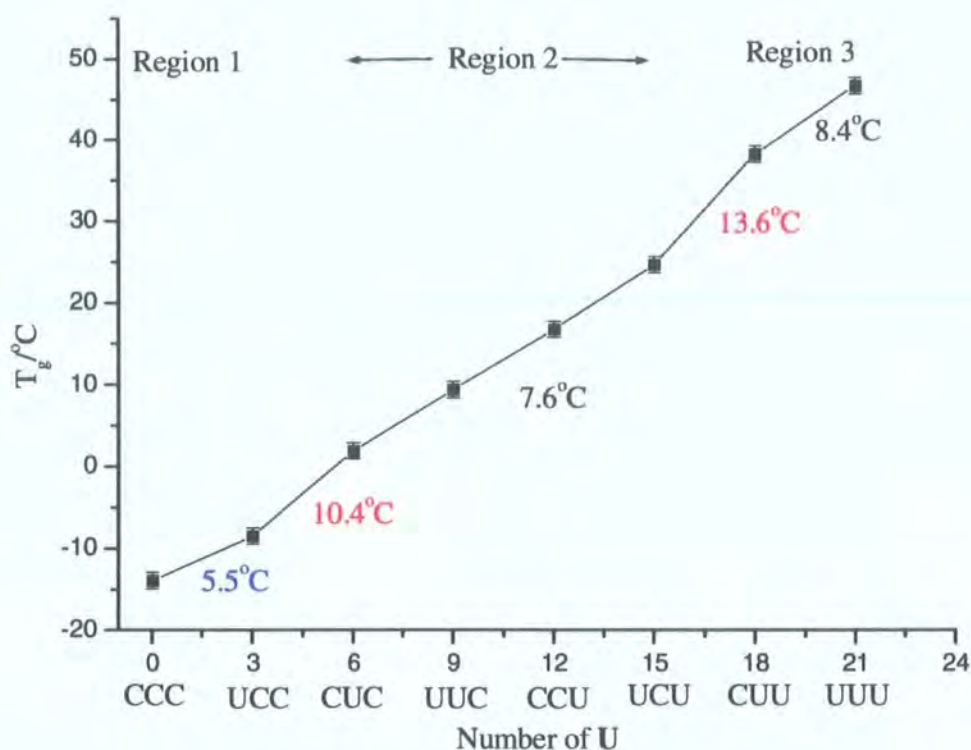
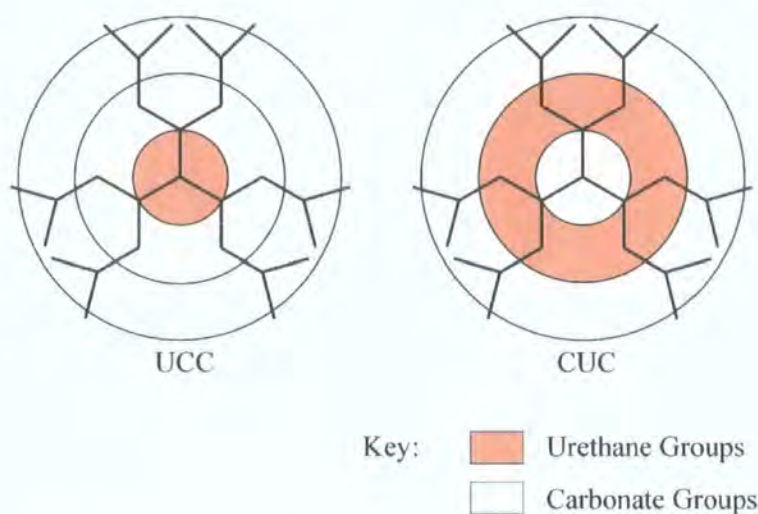


Figure 4.22 Plot of  $T_g$  against the number of urethane groups for homo- and codendrimers

From the graph it is evident that the relationship between  $T_g$  and the number of urethane groups is not linear contrary to the observation for the second generation dendrons (Figure 4.20). There are irregularities in the graph associated with increases in glass transition temperature that are greater or lesser than expected from the uniform addition of three urethane groups within the series of molecules. This suggests the glass transition temperature is not solely dependent on the proportion of urethane and carbonate groups but also on their relative location in the dendrimer. The two greatest differences in  $T_g$  between consecutive dendrimers in the series occur between **BG2D (UCC)** and **BG2D (CUC)**, and **BG2D (UCU)** and **BG2D (CUU)**. The differences in  $T_g$  between these pairs of dendrimers are  $10.4^\circ\text{C}$  and  $13.6^\circ\text{C}$  respectively. In both cases the location of a urethane layer changes from being situated at the innermost layer of the first dendrimer of the pair to being situated at the middle layer. In the following diagrams the second generation dendrimers will be represented schematically with shaded urethane-linked regions and white carbonate-linked regions (Figures 4.23 and 4.24, overleaf). It should be emphasized that the shaded areas of the structure contain functions capable of hydrogen bonding and therefore some amount of induced rigidity is present in these layers. In addition, for the codendrimers the presence of a mixture of urethane and carbonate functions, means that the carbonate groups are capable of hydrogen bonding with the urethane groups, although this will be a less pronounced effect.



The first irregularity to be considered in the relationship between  $T_g$  and the number of urethane groups in the macromolecules is between dendrimers **BG2D (UCC)** and **BG2D (CUC)** (*Figure 4.23*). The difference in  $T_g$  for these codendrimers ( $10.4^\circ\text{C}$ ) is larger than observed for codendrimers within *Region 2* ( $7.6^\circ\text{C}$ ) and is brought about by a lower  $T_g$  than expected for **BG2D (UCC)**. The  $T_g$  for dendrimer **BG2D (UCC)**, which contains carbonate layers with the exception of a urethane layer near the core, is only  $5.5^\circ\text{C}$  higher than the  $T_g$  of the entirely carbonate-linked dendrimer, **BG2D (CCC)** (see *Figure 4.22*). This observation suggests that the inclusion of a urethane layer at the core has only a small increasing effect on the  $T_g$ . This is unsurprising as the dendrimer **BG2D (UCC)** has flexible carbonate dendrons attached to a 'hydrogen bonded' core and segmental motion of the carbonate branches will occur with greater ease than if urethane functions were present in the branches. However, in dendrimer **BG2D (CUC)** a urethane layer is located in the middle of the structure, which inhibits movement of the branches compared to the dendrimer **BG2D (UCC)** (*Figure 4.23*).



*Figure 4.23 Schematic of codendrimers **BG2D (UCC)** and **BG2D (CUC)***

The second irregularity occurs between dendrimers **BG2D (UCU)** and **BG2D (CUU)** and analogous with the previous irregularity, urethane groups moves from the inner layer to the middle layer of the structure (*Figure 4.24*, overleaf). However, in this case the difference in glass transition temperature between the pair of dendrimers is greater, at a value of  $13.6^\circ\text{C}$ . This higher than expected value for the  $T_g$  of **BG2D (CUU)**, considering the uniform addition of three urethane groups within the series of molecules, could be explained by the positioning of two urethane layers consecutively in the dendrimer. This arrangement results in one large 'block' of urethane functions within which the cumulative effects of hydrogen bonding may result in a greater degree of rigidity and therefore, a higher  $T_g$  than expected on a simple



additivity basis. Moreover, carbonate groups are located solely in the centre of the structure and consequently their otherwise enhanced flexibility compared to the urethane groups, maybe quashed by the rigid outer layers of urethane functions. In comparison, if the carbonate functions are situated in the middle of the structure, *i.e.* **BG2D (UCU)** the flexible nature of these portions of the branches results in increased overall movement of the macromolecule.

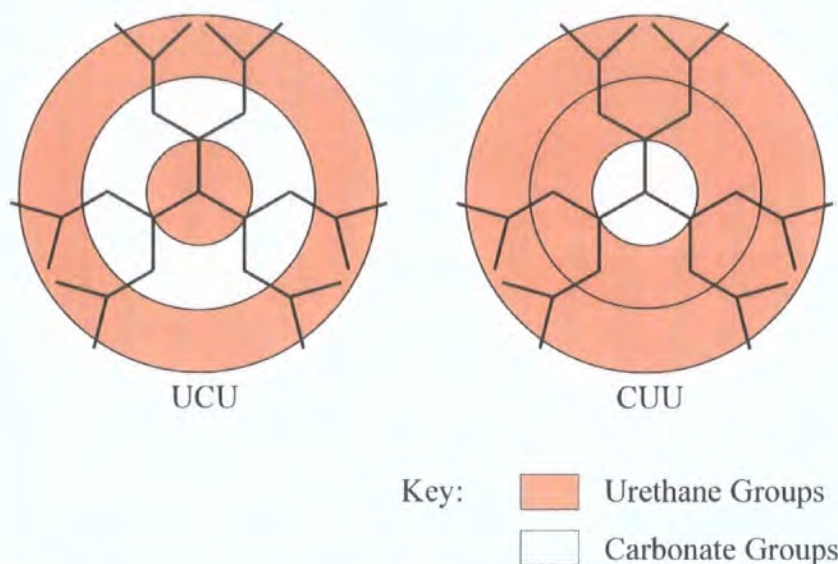


Figure 4.24 Codendrimers **BG2D (UUC)** and **BG2D (CCU)**

There are several other interesting conclusions that can be drawn from the graph. Firstly, a difference in  $T_g$  of  $8.4^\circ\text{C}$  between **BG2D (CUU)** and the polyurethane homodendrimer **BG2D** is at first glance surprising as the groups changing their composition are located near the core of the structure. From the previous example **BG2D (UCC)**, it was concluded that the introduction of a urethane group near the core had little effect on the glass transition temperature of the dendrimer. However, in this case the inclusion of three urethane groups close to the core has an increasing effect on the  $T_g$ . To explain this observation, the analysis of  $^1\text{H}$  NMR spectroscopic data of some codendrimers will be recalled (Chapter 3, pages 91-94). The results from the  $^1\text{H}$  NMR spectroscopy study implied that the closer the layer of urethane groups to the core of the codendrimer the greater the degree of hydrogen bonding, probably because of the closer proximity of the functions. Using this information, the difference in  $T_g$  between **BG2D (CUU)** and **BG2D** could be explained by the central urethane bonds 'locking' the conformation of the structure, enabling the closer approach of urethane functions in two successive layers. However, this rationalisation has to be treated with some caution since we are contrasting solid state and solution data. In general, the more effective packing of the dendrimer because of the entirely urethane-linked nature of the

macromolecule may result in the observed difference in  $T_g$  between **BG2D** (CCU) and **BG2D**.

#### 4.4.8 $T_g$ of Dendrimer Blends

The thermal properties of equimolar mixtures or blends of two different second generation dendrimers have been the subject of a preliminary investigation. These results are included here because they appear to have interesting implications regarding the nature of the  $T_g$  process in these systems. Three blends of differing dendrimer composition were made, each incorporating the codendrimer **BG2D** (CCU) and one of **BG2D**, **CG2D** or **HG2D**, to give *Blend A*, *Blend B* and *Blend C* respectively (*Table 4.4*) (see Experimental, page 130 for method). For all the blends prepared and analysed a single glass transition was observed. However, the location of the  $T_g$  of the blend relative to the  $T_g$ s of the separate, parent dendrimers were not consistent (*Table 4.4*).

<i>Blend</i>	$T_g$ of Blend/ $^{\circ}\text{C}$	Dendrimers	Separate $T_g$ s/ $^{\circ}\text{C}$
<i>Blend A</i>	33.9	<b>BG2D</b> and <b>BG2D</b> (CCU)	46.7 and 16.8
<i>Blend B</i>	35.1	<b>CG2D</b> and <b>BG2D</b> (CCU)	43.9 and 16.8
<i>Blend C</i>	21.1	<b>HG2D</b> and <b>BG2D</b> (CCU)	17.2 and 16.8

*Table 4.4  $T_g$  of blends of two different second generation dendrimers*

For *Blend A*, the glass transition occurred at  $33.9^{\circ}\text{C}$  which is approximately halfway between the values of the  $T_g$ s for the two separate dendrimers, **BG2D** (CCU) ( $16.8^{\circ}\text{C}$ ) and **BG2D** ( $46.7^{\circ}\text{C}$ ). For *Blend B*, the glass transition was also observed to lie between those of the separate dendrimers, but was closer in temperature to the glass transition of the cyclohexyl-terminated structure. In contrast, for *Blend C*, comprised of the dendrimers **BG2D** (CCU) and **HG2D**, the glass transition temperature was observed at  $21.1^{\circ}\text{C}$ , a value which is slightly higher than both glass transition temperatures for the parent polymers ( $T_g$ s of **BG2D** (CCU) and **HG2D** are at  $16.8^{\circ}\text{C}$  and  $17.2^{\circ}\text{C}$ ). This observation for the  $T_g$  of *Blend C* is unexpected and time did not allow confirmation of the result. However, the presence of a single glass transition for mixtures of the dendrimers is a reproducible phenomenon from which conclusions may be drawn. If we presume that there is no interpenetration between the two dendrimers in the blends then the result indicates that the process is characteristic of the whole assembly of molecules rather than an individual molecule characteristic. That is to say, if the  $T_g$  process was a molecular characteristic we should have seen two  $T_g$ s in the analysis of the blends. In contrast, if there were some degree of intermolecular interactions or



interpenetration of the molecules then the occurrence of segmental motion of portions of the dendrimer rather than translational movement of the molecules would be more likely at  $T_g$ . The opinion of the author is that the latter process, involving the segmental motion of partially interpenetrated molecules, is the process associated with the glass transitions of these dendrimers. The limited data set in *Table 4.4* offers some support for this concept of partial interpenetration in as much as, *Blend A*, where both components have *t*-butyl termini will have least interpenetration whereas *Blends B* and *C* with cyclohexyl and 4-heptyl termini have progressively more interpenetration with bigger consequences. These comments are entirely speculative but the author believes the observations merit further study.

#### 4.5 Conclusions

From the analysis of the thermal data of the polyurethane dendrons and dendrimers several conclusions can be drawn. Firstly, the structure of the end groups has an effect on the  $T_g$  of the macromolecules, as structures consisting of 4-heptyl termini had considerably lower  $T_g$ s than their equivalent *t*-butyl- and cyclohexyl-terminated analogues. In addition, a study of the  $T_g$ s of the poly(urethane-carbonate) codendrimers indicated that the composition of the interior branching units affected the glass transition temperature of the materials. Primarily, the proportion of urethane and carbonate links in the structure governed the  $T_g$ s in this series; however, the relative location of the urethane functions was also of importance.

Using equations from the literature, the values of  $T_g$  at infinite molecular weight were obtained for the polyurethane dendrons and dendrimers and the values from the two different methods employed were in approximate agreement. Also, it was apparent that the specific architecture of the dendritic molecule, *i.e.* dendron or dendrimer, had little effect on the glass transition temperature but that the molecular weight was the crucial factor for determining the  $T_g$  of macromolecules composed of alike termini and branching units.

Some preliminary observations concerning the glass transition process in dendrimer blends raises fundamental questions about the nature of the  $T_g$  process in this family of dendrimers.

## 4.6 References

- (1) Cowie, J. M. G. *Polymers: Chemistry and Physics of Modern Materials*, 2nd ed.; Blackie A & P: London, 1997.
- (2) Mark, H. F.; Bikales, N. M.; Overberger, C. G.; Menges, G. In *Encyclopedia of Polymer Science and Engineering*; Kroschwitz, J. I., 2nd ed.; John Wiley & Sons: New York, 1987; Vol. 7, p 531.
- (3) Cowie, J. M. G. *Europ. Polym. J.* **1974**, *11*, 297.
- (4) Fox, T. G.; Flory, P. J. *J. Appl. Phys.* **1950**, *21*, 581.
- (5) Wooley, K. L.; Fréchet, J. M. J.; Hawker, C. J. *Polymer* **1994**, *35*, 4489.
- (6) Hawker, C. J.; Chu, F. *Macromolecules* **1996**, *29*, 4370.
- (7) Stutz, H. J. *Polym. Sci., Part B: Polym. Phys.* **1995**, *33*, 333.
- (8) Wooley, K. L.; Hawker, C. J.; Pochan, J. M.; Fréchet, J. M. J. *Macromolecules* **1993**, *26*, 1514.
- (9) Milller, T. M.; Kwock, E. W.; Neenan, T. X. *Macromolecules* **1992**, *25*, 3143.
- (10) Mourey, T. M.; Turner, S. R.; Rubinstein, M.; Fréchet, J. M. J.; Hawker, C. J.; Wooley, K. L. *Macromolecules* **1992**, *25*, 2401.
- (11) Parker, D.; Feast, W. J. *Macromolecules* **2001**, *34*, 5792.
- (12) Parker, D.; Feast, W. J. *Macromolecules* **2001**, *34*, 2048.
- (13) Ihre, H.; Hult, A.; Fréchet, J. M. J.; Gitsov, I. *Macromolecules* **1998**, *31*, 4061.
- (14) Kim, Y. H.; Webster, O. W. *Macromolecules* **1992**, *25*, 5561.
- (15) Jansen, J. F. G. A.; de Brabander-van den Berg, E. M. M.; Meijer, E. W. *Science* **1994**, *266*, 1226.
- (16) Hawker, C. J.; Fréchet, J. M. J. *J. Am. Chem. Soc.* **1992**, *114*, 8405.
- (17) Miller, T. M.; Neenan, T. X.; Zayas, R.; Bair, H. E. *J. Am. Chem. Soc.* **1992**, *114*, 1018.
- (18) Hawker, C. J.; Wooley, K. L.; Fréchet, J. M. J. *J. Chem. Soc. Perkin Trans. 1* **1993**, 1287.

# Chapter 5

## Experimental

### 5.1 General Information

#### 5.1.1 Chemicals

Starting materials were purchased from Aldrich, Acros, Lancaster and Raylo Chemicals, Canada (CDI) and used without further purification. Toluene and benzene used as solvent for the reactions were analytical grade and were used as received. The ethanol used was general purposed solvent grade. All reactions were performed under an atmosphere of N<sub>2</sub>, unless stated otherwise. Silica gel used for column chromatography was supplied from Aldrich (70-270 mesh, 60Å) or Fluorochem (40-63u, 60Å). For preparative gel permeation chromatography, BioBeads®, S-X1 Beads purchased from Bio-Rad were used in a column mode.

#### 5.1.2 Characterisation

##### *Elemental Analysis*

Elemental analysis data was obtained from an Exeter Analyser CE-440.

## *NMR Spectroscopy*

NMR spectra were recorded using either a Varian Mercury-200 ( $^1\text{H}$  at 200 MHz and  $^{13}\text{C}$  at 50.2 MHz), a Bruker AM-250 ( $^1\text{H}$  at 250.1 MHz and  $^{13}\text{C}$  at 62.9 MHz), a Varian Unity-300 ( $^1\text{H}$  at 299.9 MHz and  $^{13}\text{C}$  at 75.4 MHz), a Varian Mercury 400 ( $^1\text{H}$  at 400 MHz and  $^{13}\text{C}$  at 100 MHz) or a Varian Inova-500 ( $^1\text{H}$  at 500 MHz and  $^{13}\text{C}$  at 125 MHz). Deuterated solvents were used as supplied from Aldrich ( $\text{CDCl}_3$  and  $\text{D}_2\text{O}$ ) and Cambridge Isotope Laboratories ( $\text{CD}_3\text{OD}$  and  $(\text{CD}_3)_2\text{SO}$ ). Chemical shifts ( $\delta$ ) are reported in parts per million (ppm) with respect to an internal reference of tetramethylsilane (TMS) using residual solvent signals as secondary references. Coupling constants (J) are reported in Hertz and the error in the values is  $\pm 0.3$  Hz because of the digital resolution of the method.

## *Mass Spectrometry*

For gas chromatography electron ionisation (GC EI) and gas chromatography chemical ionisation (GC CI) Micromass Autospec instruments were used.

Electrospray mass spectra (ES MS) were obtained on a Micromass LCT instrument. A solution of the sample in dichloromethane of concentration of 1 mg/mL was diluted in methanol, to give a solution of 10  $\mu\text{g}/\mu\text{L}$ . This solution was injected using a syringe pump at a flow rate of 10  $\mu\text{L}/\text{min}$ .

Two different MALDI-TOF mass spectrometers were used in the characterisation of some of the macromolecules. Firstly, a Kratos MALDI-IV MALDI-TOF mass spectrometer, represented by the term 'MALDI-TOF (Kratos)' in the text, and secondly, a Voyager-DE STR MALDI-TOF mass spectrometer, represented by the term 'MALDI-TOF (Voyager)' in the text. For the MALDI-TOF (Kratos) mass spectrometer the sample preparation and other details were as follows: the matrix used was trans-3-indole acrylic acid and the concentration of the matrix solution (in THF) was 10 mg/mL. The concentration of the dendritic solution was 1 mg/mL to 3 mg/mL. The dendritic and matrix solutions were mixed in a ratio of 1:1 by volume and this dendritic/matrix solution was deposited into a well on the slide. The MALDI-TOF (Kratos) mass spectra were obtained in linear mode using polyethylene oxide (Polymer Labs) as an external calibrant. For the MALDI-TOF Voyager mass spectrometer the sample preparation and other details were as follows: the matrix used was trans-3-indole acrylic acid and the concentration of the matrix solution (in MeOH, or THF for **XGXDAC** dendrimer series) was 10 mg/mL. The concentrations of the dendritic solutions (in MeOH, or THF for **XGXDAC** dendrimer series) varied in the range of 1 mg/mL to 3 mg/mL. Initially, the matrix solution was deposited on the slide, followed by the dendritic solution. The MALDI-TOF (Voyager) mass spectra were obtained in reflection mode using polyethylene

oxide (Polymer Labs) as external calibrants. Some spectra were obtained in linear mode for comparison.

### *Gel Permeation Chromatography (GPC)*

Analysis by GPC was achieved using tetrahydrofuran (THF) as eluent using a flow rate of 1 mL/min at 30°C. Columns comprised of 2 x 'mixed B' columns containing PL-gel beads. The columns were calibrated with polystyrene standards (Polymer Laboratories) and samples analysed using conventional calibration with all data collected from a refractive index detector.

### *Thermal Analysis*

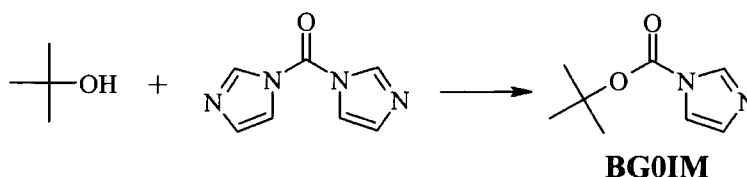
For thermogravimetric analysis (TGA) a Perkin Elmer Pyris 1 TGA was used and the sample was contained under an atmosphere of N<sub>2</sub> using a heating rate of 10°C/min from room temperature to 1000°C. For differential scanning calorimetry (DSC) a Perkin Elmer Pyris 1 DSC was used and the machine was calibrated using 99.9% cyclohexane and Indium metal. Melting points were obtained using an Electrothermal IA9200 series digital melting apparatus.

The blends were prepared using the following method: two different dendrimers (12 mg of each) were dissolved in CH<sub>2</sub>Cl<sub>2</sub> (*ca.* 2 mL) in a glass vial. A few drops of the solution was pipetted into the DSC pan and the solvent allowed to evaporate. This procedure was repeated four times and then the DSC pan was placed in a clean glass vial (with no lid) and left in the vacuum oven for 16 hrs.

## **5.2 Procedures for the Synthesis of the First to Fourth Generation Polyurethane Dendrons**

### **5.2.1 Compounds of the Zeroth and First Generation**

#### *Synthesis of BG0IM*



In a round bottom, glass flask with a reflux condenser attached, a solution of *t*-butanol (6.38 g, 86.1 mmol) in toluene (100 mL) was prepared at room temperature. To this stirred solution

was added CDI (16.7 g, 103.1 mmol) and the reaction mixture was heated at 60°C for 6 hrs. The solvent was removed using the rotary evaporator and the oil obtained redissolved in CH<sub>2</sub>Cl<sub>2</sub> (200 mL). The organic phase was washed with water (3 x 200 mL), dried over MgSO<sub>4</sub>, filtered and the solvent removed *in vacuo*. The product was dried under vacuum (10<sup>-1</sup> mbar) for 1 day, to give **BG0IM** as a white crystalline solid (13.7 g, 95%). Found C, 56.89; H, 7.16; N, 16.58%. Calculated for C<sub>8</sub>H<sub>12</sub>N<sub>2</sub>O<sub>2</sub>, C, 57.13; H, 7.19; N, 16.66%. <sup>13</sup>C NMR (62.9 MHz, CDCl<sub>3</sub>) δ 27.6, 85.33, 116.9, 130.0, 136.8, 146.9. <sup>1</sup>H NMR (300 MHz, CDCl<sub>3</sub>) δ 1.64 (s, 9H), 7.07 (s, 1H), 7.4 (s, 1H), 8.13 (s, 1H). T<sub>m</sub> = 51°C, lit. value = 56°C.<sup>1</sup>

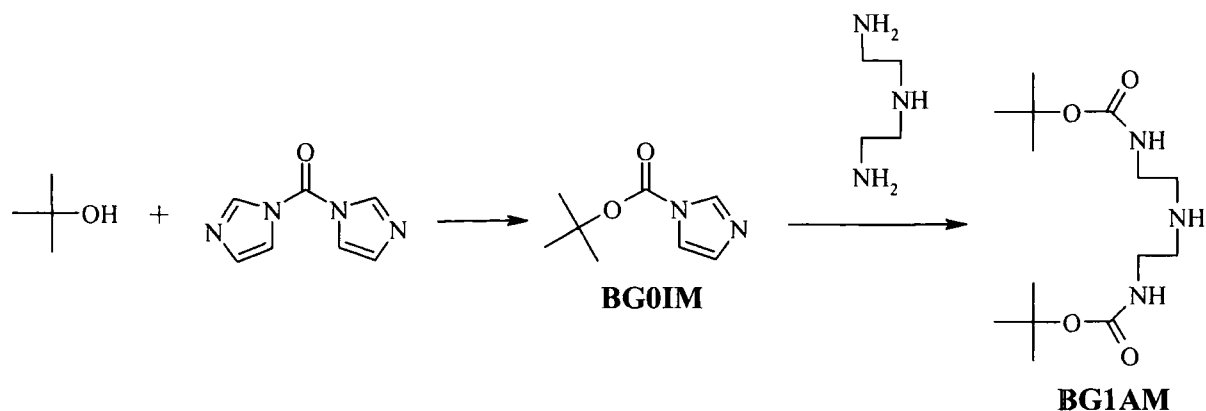
**Synthesis of HG0IM:** The procedure was as described for the synthesis of **BG0IM**, using 4-heptanol as the alcohol reagent, to give *compound HG0IM* as a pale yellow oil (93%). Found C, 62.49; H, 8.60; N 13.23%. C<sub>11</sub>H<sub>18</sub>N<sub>2</sub>O<sub>2</sub> requires, C, 62.83; H, 8.63; N, 13.32%. <sup>13</sup>C NMR (62.8 MHz, CDCl<sub>3</sub>) δ 13.0, 18.4, 36.0, 79.7, 117.1, 130.3, 137.0, 149.0. <sup>1</sup>H NMR (300 MHz, CDCl<sub>3</sub>) δ 0.95 (t, J=7.2Hz, 6H), 1.41 (m, 4H), 1.69 (m, 4H), 5.11 (qn, J=6.2Hz, 1H), 7.08 (m, 1H), 7.43 (t, J=1.2Hz, 1H), 8.15 (s, 1H). *m/z* (GC, EI) 210 [M+H]<sup>+</sup>, calculated M<sub>w</sub> = 210.27.

**Synthesis of CG0IM:** The procedure was as described for the synthesis of **BG0IM**, using cyclohexanol as the alcohol reagent, to give *compound CG0IM* as a white crystalline solid (88%). Found C, 61.83; H, 7.33; N, 14.32%. C<sub>10</sub>H<sub>14</sub>N<sub>2</sub>O<sub>2</sub> requires, C, 61.84; H, 7.26; N, 14.42%. <sup>13</sup>C NMR (62.9 MHz, CDCl<sub>3</sub>) δ 23.4, 25.0, 31.2, 77.7, 117.1, 130.0, 136.9, 147.9. <sup>1</sup>H NMR (200 MHz, CDCl<sub>3</sub>) δ 1.39-1.65 (m, 6H), 1.79 (m, 2H), 1.98 (m, 2H), 5.01 (m, 1H), 7.08 (s, 1H), 7.44 (s, 1H), 8.15 (s, 1H). *m/z* (GC, EI) 194 [M+H]<sup>+</sup>, calculated M<sub>w</sub> = 194.23.

**Synthesis of BHG0IM:** The procedure was as described for the synthesis of **BG0IM**, using benzhydrol as the alcohol reagent, to give *compound BHG0IM* as a white crystalline solid (96%). T<sub>m</sub> = 128°C (*cf.* T<sub>m</sub> = 126°C from measurement by DSC). Found C, 73.30; H, 4.99; N, 10.14%. C<sub>17</sub>H<sub>14</sub>O<sub>2</sub>N<sub>2</sub> requires, C, 73.37; H, 5.07; N, 10.07%. <sup>13</sup>C NMR (63 MHz, CDCl<sub>3</sub>) δ 81.2, 117.2, 127.1, 128.7, 128.8, 130.8, 137.1, 138.3, 148.0. <sup>1</sup>H NMR (200 MHz, CDCl<sub>3</sub>) δ 7.06 (s, 1H), 7.10 (m, 1H), 7.33-7.42 (m, 10H), 7.50 (t, J=1.2Hz, 1H), 8.23 (t, J=1.2Hz, 1H).



### Synthesis of **BG1AM**:



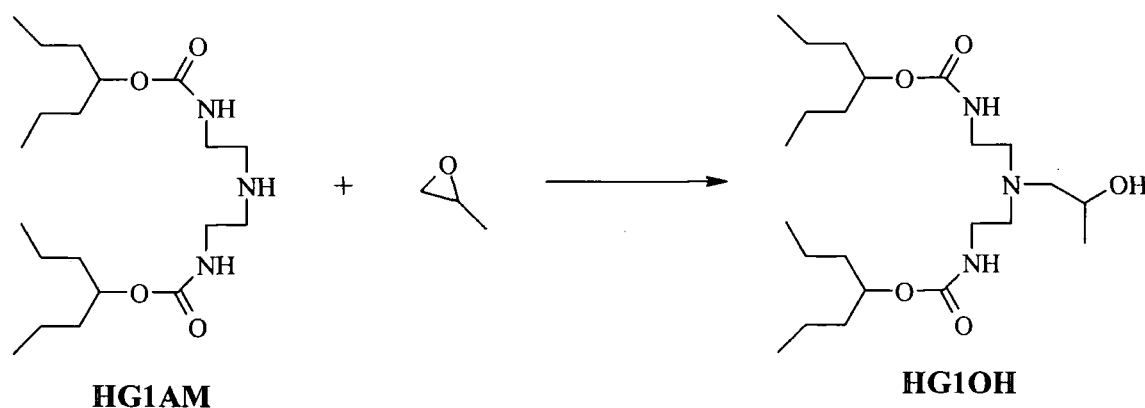
CDI (163.3 g, 1.01 mol) was added to a stirred solution of *t*-butanol (143.0 g, 1.93 mol) in toluene (1200 mL) at room temperature and the reaction mixture heated at 60°C for 6 hrs. Diethylenetriamine (54.57 g, 0.53 mol) was added dropwise and the reaction mixture heated at 60°C for 18 hrs. The solvent was removed under reduced pressure and the mixture redissolved in CH<sub>2</sub>Cl<sub>2</sub> (800 mL). The organic phase was washed with water (3 x 800 mL), dried over MgSO<sub>4</sub>. After filtration, the solvent was removed using the rotary evaporator. The product was dried under vacuum (10<sup>-1</sup> mbar) to give **BG1AM** as a white crystalline solid (118.0 g, 77%). Found C, 54.63; H, 9.52; N, 13.34%. Calculated for C<sub>14</sub>H<sub>29</sub>N<sub>3</sub>O<sub>4</sub>, C, 55.42; H, 9.63; N, 13.85%. <sup>13</sup>C NMR (62.9 MHz, CDCl<sub>3</sub>) δ 28.4, 40.3, 48.8, 79.7, 156.1. <sup>1</sup>H NMR (300 MHz, CDCl<sub>3</sub>) δ 1.35 (s, br, CH<sub>2</sub>NHCH<sub>2</sub>), 1.43 (s, 18H), 2.71 (t, J=5.7Hz, 4H), 3.20 (m, 4H), 4.99 (s, br, O(CO)NHCH<sub>2</sub>); on addition of a drop of D<sub>2</sub>O the signals corresponding to the N-H resonances of the urethane and secondary amine functions disappear. *m/z* (ES MS) 304 [M+H]<sup>+</sup>, 326 [M+Na]<sup>+</sup>, dimer 629 [2M+Na]<sup>+</sup>, calculated M<sub>w</sub> = 303.40. T<sub>m</sub> = 71°C.

**Synthesis of **HG1AM**:** **HG0IM** (33.0 g, 156.9 mmol) was dissolved in toluene (250 mL) and diethylenetriamine (9.32 g, 90.3 mmol) added to the solution. The mixture was stirred and heated at 60°C for 16 hrs. The solvent was removed under reduced pressure and the mixture redissolved in CH<sub>2</sub>Cl<sub>2</sub> (150 mL). The organic phase was washed with distilled water (4 x 150 mL), dried over MgSO<sub>4</sub> and after filtration the solvent was removed *in vacuo*. The colorless oil obtained was dried under vacuum (10<sup>-1</sup> mbar) to give *compound* **HG1AM** as a white waxy solid (26.2 g, 86%). Found C, 61.82; H, 10.72; N, 10.65%. C<sub>20</sub>H<sub>41</sub>N<sub>3</sub>O<sub>4</sub> requires, C, 61.98; H, 10.66; N, 10.84%. <sup>13</sup>C NMR (100 MHz, CDCl<sub>3</sub>) 14.0, 18.5, 36.6, 40.6, 48.8, 74.4, 157.0. <sup>1</sup>H NMR (400 MHz, CDCl<sub>3</sub>) δ 0.91 (t, J=7.2Hz, 12H), 1.40 (m, 8H), 1.48 (m, 8H), 2.76 (t, J=5.2Hz, 4H), 3.27 (m, 4H), 4.77 (qn, J=5.6Hz, 2H), 5.01 (s, br, O(CO)NHCH<sub>2</sub>). *m/z* (GC, EI) 388 [M+H]<sup>+</sup>, calculated M<sub>w</sub> = 387.56.

**Synthesis of CG1AM:** The procedure was as described for the synthesis of **HG1AM**, using **CG0IM** as the starting material, to give **CG1AM** as a white crystalline solid (76%).  $T_m = 58^\circ\text{C}$ . Found C, 60.32; H, 9.37; N, 11.71%.  $\text{C}_{18}\text{H}_{33}\text{N}_3\text{O}_4$  requires, C, 60.82; H, 9.36; N, 11.82%.  $^{13}\text{C}$  NMR (100 MHz,  $\text{CDCl}_3$ )  $\delta$  23.9, 25.3, 32.0, 40.5, 48.7, 73.0, 156.5.  $^1\text{H}$  NMR (400 MHz,  $\text{CDCl}_3$ )  $\delta$  1.23-1.56 (m, 12H), 1.71 (m, 4H), 1.87 (m, 4H), 2.76 (t,  $J=6\text{Hz}$ , 4H), 3.27 (m, 4H), 4.63 (m, 2H), 5.05 (s, br,  $\text{O}(\text{CO})\text{NHCH}_2$ ).  $m/z$  (ES MS) 356  $[\text{M}+\text{H}]^+$ , 378  $[\text{M}+\text{Na}]^+$ , dimers 711  $[2\text{M}+\text{H}]^+$ , 733  $[2\text{M}+\text{Na}]^+$ , calculated  $M_w = 355.47$ .

**Synthesis of BHG1AM:** The procedure was similar to that described for the synthesis of **HG1AM**, but using **BHG0IM** as the starting material. After aqueous work-up, the yellow oil was purified by silica gel chromatography using EtOAc as eluent to give the compound **BHG1AM** as a white crystalline solid (72%). Found C, 73.18; H, 6.38; N, 8.03%.  $\text{C}_{32}\text{H}_{33}\text{O}_4\text{N}_3$  requires, C, 73.40; H, 6.35; N, 8.02%.  $^{13}\text{C}$  NMR (75.4 MHz,  $\text{CDCl}_3$ )  $\delta$  40.5, 48.3, 77.2, 126.8, 127.6, 128.2, 140.5, 155.8.  $^1\text{H}$  NMR (200 MHz,  $\text{CDCl}_3$ )  $\delta$  1.36 (s, br,  $\text{CH}_2\text{CH}_2\text{NH}$ ), 2.71 (t,  $J=5.4\text{Hz}$ , 4H), 3.25 (m, 4H), 5.23 (s, br,  $\text{OCONHCH}_2$ ), 6.79 (s, 2H), 7.32 (m, 20H).  $m/z$  (CI) 524  $[\text{M}+\text{H}]^+$ , 690  $[\text{M}+\text{KI}]^+$ , calculated  $M_w = 523.62$ .

#### Synthesis of HG1OH:



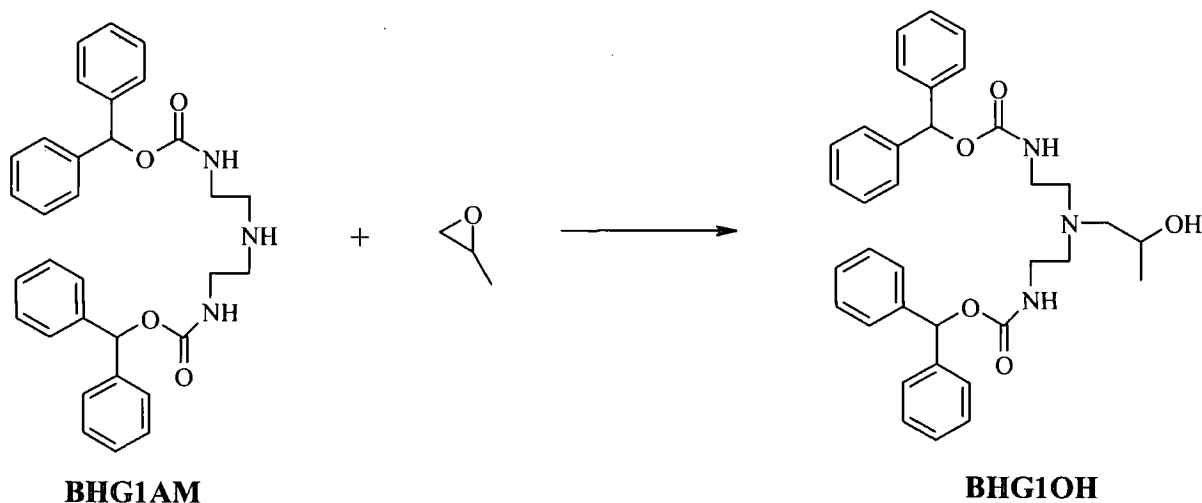
To a stirred solution of **HG1AM** (26.2 g, 67.5 mmol) in ethanol (200 mL) propylene oxide (11.8 g, 202 mmol) was added and the mixture heated at  $30^\circ\text{C}$  for 20 hrs. The solvent was removed using the rotary evaporator and the oil dried under vacuum ( $10^{-1}$  mbar) for 1 day. Purification by column chromatography (silica gel, eluting with EtOAc) gave compound **HG1OH** as a colourless oil (23.8 g, 91%).  $T_g = -39.5^\circ\text{C}$ . Found C, 61.90; H, 10.61; N, 9.43%.  $\text{C}_{23}\text{H}_{47}\text{N}_3\text{O}_5$  requires, C, 61.99; H, 10.63; N, 9.43%.  $^{13}\text{C}$  NMR (62.9 MHz,  $\text{CDCl}_3$ )  $\delta$  14.0, 18.5, 20.0, 36.7, 39.2, 55.1, 63.2, 64.1, 74.4, 157.2.  $^1\text{H}$  NMR (300 MHz,  $\text{CDCl}_3$ )  $\delta$  0.91 (t,  $J=7.2\text{Hz}$ , 12H), 1.12 (d,  $J=6.3\text{Hz}$ , 3H), 1.33 (m, 8H), 1.47 (m, 8H), 1.63 (s, br, OH), 2.34

(dd,  $J=12.9\text{Hz}$ ,  $J=9.9\text{Hz}$ , 1H), 2.46 (dd,  $J=13.2\text{Hz}$ ,  $J=3\text{Hz}$ , 1H), 2.56 (dt,  $J=13.2\text{Hz}$ ,  $J=5.4\text{Hz}$ , 2H), 2.67 (m, 2H), 3.23 (m, 4H), 3.73 (m, 1H), 4.76 (qn,  $J=6\text{Hz}$ , 2H), 5.07 (s, br,  $\text{O}(\text{CO})\text{NHCH}_2$ ) (see text pages 34-35).  $m/z$  (GC, EI) 446  $[\text{M}+\text{H}]^+$ , calculated  $M_w = 445.64$ .

**Synthesis of CG1OH:** The procedure was as described for the synthesis of **HG1OH**, but using **CG1AM** as the starting material, to give *compound CG1OH* as a sticky colourless oil (86%).  $T_g = 2.0^\circ\text{C}$ . Found C, 60.15; H 9.42; N, 9.67%.  $\text{C}_{21}\text{H}_{39}\text{N}_3\text{O}_5$  requires, C, 60.99; H, 9.51; N, 10.16%.  $^{13}\text{C}$  NMR (62.9 MHz,  $\text{CDCl}_3$ )  $\delta$  19.8, 23.6, 25.2, 31.8, 39.2, 54.9, 63.1, 63.9, 72.7, 156.7.  $^1\text{H}$  NMR (300 MHz,  $\text{CDCl}_3$ )  $\delta$  1.12 (d,  $J=6.4\text{Hz}$ , 3H), 1.25 (m, 10H), 1.52 (m, 2H), 1.72 (m, 4H), 1.86 (m, 4H), 2.33 (dd,  $J=12.9\text{Hz}$ ,  $J=9.3\text{Hz}$ , 2H), 2.42 (dd,  $J=13.1\text{Hz}$ ,  $J=3\text{Hz}$ , 2H), 2.52 (dt,  $J=13.2\text{Hz}$ ,  $J=4.8\text{Hz}$ , 2H), 2.69 (m, 2H), 3.22 (m, 4H), 3.72 (m, 1H), 4.62 (m, 2H), 5.17 (s, br,  $\text{O}(\text{CO})\text{NHCH}_2$ ).  $m/z$  (GC CI) 414  $[\text{M}+\text{H}]^+$ , calculated  $M_w = 413.55$ .

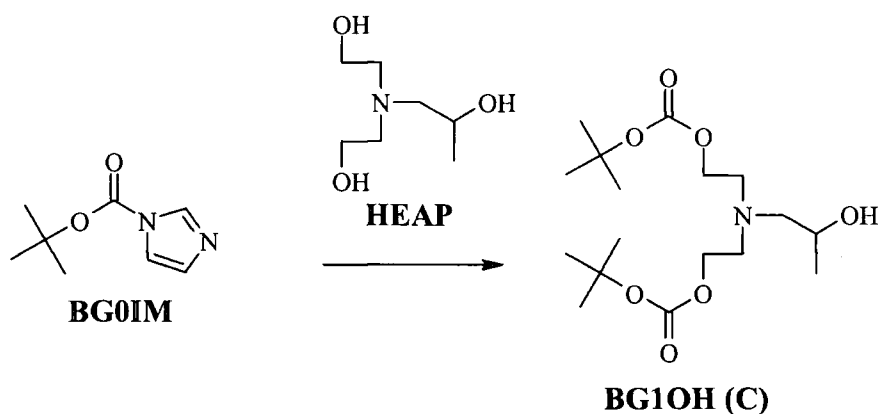
**Synthesis of BG1OH:** The procedure was as described for the synthesis of **HG1OH**, but using **BG1AM** as the starting material, to give *compound BG1OH* as a white crystalline solid (89%).  $T_g = -18.4^\circ\text{C}$ ,  $T_m = 61.8^\circ\text{C}$  from first heating run.  $T_g = -5.1^\circ\text{C}$  from second heating run. Found C, 56.21; H, 9.82; N, 11.57%.  $\text{C}_{17}\text{H}_{35}\text{N}_3\text{O}_5$  requires, C, 56.49; H, 9.76; N, 11.62%.  $^{13}\text{C}$  NMR (62.9 MHz,  $\text{CDCl}_3$ )  $\delta$  20.0, 28.3, 38.7, 55.1, 63.0, 63.9, 79.3, 156.5.  $^1\text{H}$  NMR (300 MHz,  $\text{CDCl}_3$ )  $\delta$  1.12 (d,  $J=6.3\text{Hz}$ , 3H), 1.46 (s, 18H), 2.37 (m, 2H), 2.50 (dt,  $J=13.2\text{Hz}$ ,  $J=4.5\text{Hz}$ , 2H), 2.68 (m, 2H), 3.19 (m, 4H), 3.76 (m, 1H), 5.13 (s, br,  $\text{O}(\text{CO})\text{NHCH}_2$ ).  $m/z$  (GC, EI) 361  $[\text{M}+\text{H}]^+$ , calculated  $M_w = 361.48$ .

**Synthesis of BHG1OH:**



To a solution of **BHG1AM** (3.81 g, 7.28 mmol) in ethanol (50 mL), propylene oxide (1.69 g, 29.1 mmol) was added. The reaction mixture was stirred at 30°C for 1 day and a white suspension was formed. The mixture was heated to 55°C and stirred until the suspension had dissolved. The solution was left to cool to room temperature (unstirred) and the white crystals formed were isolated by filtration and washed with cold ethanol (25 mL). The crystals were dried in a vacuum oven for 2 days to give *compound BHG1OH* as a white crystalline solid (3.17 g, 75%).  $T_m = 125.5^\circ\text{C}$  from first heating run.  $T_g = 20.2^\circ\text{C}$  from second heating run. Found C, 72.09; H, 6.80; N, 7.25%.  $\text{C}_{35}\text{H}_{39}\text{O}_5\text{N}_3$  requires, C, 72.27; H, 6.76; N, 7.22%.  $^{13}\text{C}$  NMR (62.9 MHz,  $\text{CDCl}_3$ )  $\delta$  19.9, 39.3, 54.9, 62.9, 64.1, 77.2, 126.9 (split), 127.5, 128.2, 140.5 (split), 156.1.  $^1\text{H}$  NMR (200 MHz,  $\text{CDCl}_3$ )  $\delta$  1.05 (d,  $J=4\text{Hz}$ , 3H), 2.21-2.37 (m, 2H), 2.58 (m, 4H), 3.15 (m, 4H), 3.64 (m, 1H), 5.36 (s, br,  $\text{O}(\text{CO})\text{NHCH}_2$ ), 6.78 (s, 2H), 7.29 (m, 1H).  $m/z$  (GC, CI) 582  $[\text{M}+\text{H}]^+$ , calculated  $M_w = 581.70$ .

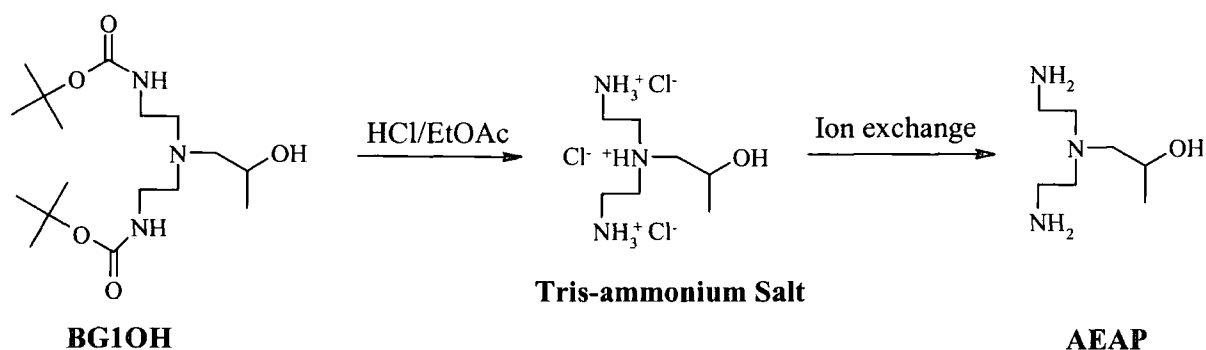
#### Synthesis of **BG1OH (C)**:



To a solution of **BG0IM** (8.25 g, 49.1 mmol) in toluene (60 mL) was added **HEAP** (4.0 g, 24.5 mmol) and KOH (approx. 50 mg). The mixture was then stirred and heated at 80°C for 2 days. The reaction mixture was analysed by  $^1\text{H}$  NMR spectroscopy and interpretation of the spectrum indicated there was no evidence of **BG0IM**. The reaction mixture was concentrated *in vacuo* and redissolved in  $\text{CH}_2\text{Cl}_2$  (200 mL). The organic phase was subsequently washed with water (3 x 300 mL), dried over  $\text{MgSO}_4$  and the solvent removed using the rotary evaporator. The yellow oil was purified by column chromatography (silica gel, eluting with  $\text{EtOAc}:\text{C}_6\text{H}_{12}$  1:4) and the colourless oil obtained was dried under vacuum ( $10^{-1}$  mbar) to give *compound BG1OH (C)* as a colourless oil (4.8 g, 54%). Found C, 55.93; H, 9.04; N, 3.71%.  $\text{C}_{17}\text{H}_{33}\text{N}_1\text{O}_7$  requires, C, 56.18; H, 9.15; N, 3.85%.  $^{13}\text{C}$  NMR (62.9 MHz,  $\text{CDCl}_3$ )  $\delta$  19.6, 27.7, 53.3, 63.1, 63.6, 64.4, 82.1, 153.5.  $^1\text{H}$  NMR (200 MHz,  $\text{CDCl}_3$ )  $\delta$  1.11 (d,  $J=6\text{Hz}$ , 3H), 1.48 (s, 18H), 2.33 (dd,  $J=13\text{Hz}$ ,  $J=10.2\text{Hz}$ , 1H), 2.62 (dd,  $J=13\text{Hz}$ ,  $J=2.8\text{Hz}$ , 1H), 2.81 (dt,  $J=14.1\text{Hz}$ ,  $J=5.4\text{Hz}$ , 2H), 2.91 (dt,  $J=14.1\text{Hz}$ ,  $J=6.6\text{Hz}$ , 2H), 3.23 (s, br,  $\text{CH}_2\text{CH}(\text{OH})\text{CH}_3$ ),

3.73 (m, 1H), 4.12 (m, 4H).  $m/z$  (ES MS) 364  $[M+H]^+$ , 386  $[M+Na]^+$ , calculated  $M_w = 363.45$ .

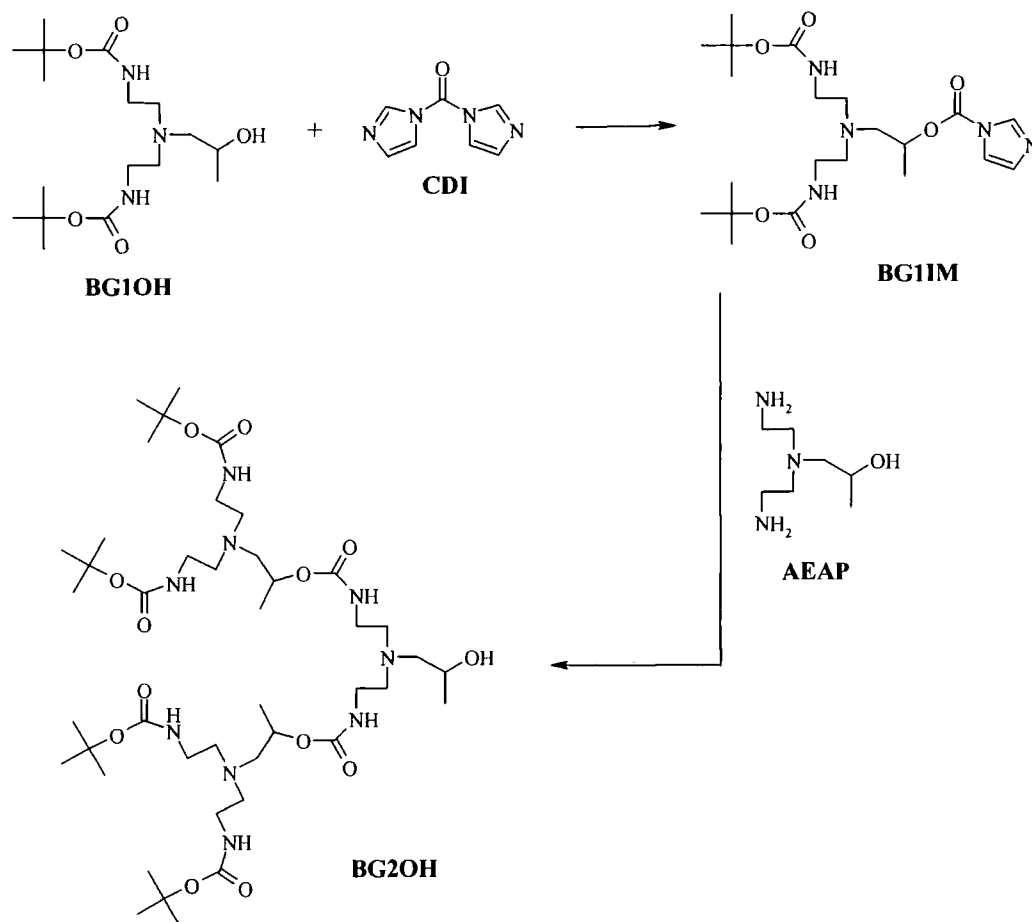
**Synthesis of 1-[N, N-bis(2-aminoethyl)amino]-2-propanol (AEAP):** The following reaction was not performed under an atmosphere of  $N_2$ .



4M HCl/EtOAc (250 mL) was added to a stirred solution of **BG1OH** (55.0 g, 152.3 mmol) in EtOAc (100 mL) at room temperature. On addition of the acid the reaction mixture effervesced and the white suspension formed was stirred for 3 hrs. The mixture was concentrated *in vacuo* and the orange oil obtained was dried under vacuum to give the **tris-ammonium salt** as a pale yellow solid. The tris-ammonium salt was characterized by  $^1H$  and  $^{13}C$  NMR spectroscopy;  $^{13}C$  NMR (62.9 MHz,  $D_2O$ ) 22.6, 36.5, 53.4, 62.7, 64.5 and  $^1H$  NMR (200MHz,  $D_2O$ ) 1.26 (d,  $J=6.4\text{Hz}$ , 3H), 3.21 (dd,  $J=13.6\text{Hz}$ ,  $J=10.4\text{Hz}$ , 1H), 3.35 (dd,  $J=13.6\text{Hz}$ ,  $J=3\text{Hz}$ , 1H), 3.48 (m, 4H), 3.62 (m, 4H), 4.23 (m, 1H). For the second step, the activation of Amberlite® ion exchange beads (700g) was achieved by stirring the beads in a 2M KOH solution in distilled water (300 mL) for 1 hr. The beads were subsequently isolated by filtration and washed with distilled water (1 L). The **tris-ammonium salt** was dissolved in distilled water (150 mL) and added to a beaker (1 L) containing activated ion exchange beads in distilled water. The beads and solution were stirred for 4 hours and the mixture filtered. The filtrate was concentrated using the rotary evaporator and the oil obtained was stirred and dried under vacuum to give a pale yellow solid. It was necessary to repeat the ion exchange process, so after the reactivation of the beads the procedure was repeated using the pale yellow solid. After this second ion exchange process, a yellow oil was isolated. The oil was purified by vacuum distillation ( $10^{-1}$  mbar,  $160^\circ\text{C}$ ) to give **compound AEAP** as a colourless oil (15.7 g, 64%).  $^{13}C$  NMR (62.9 MHz,  $CDCl_3$ ) 19.9, 39.8, 57.8, 62.8, 64.8.  $^1H$  NMR (300MHz,  $CDCl_3$ ) 1.10 (d,  $J=6.3\text{Hz}$ , 3H), 2.32 (dd,  $J=13.2\text{Hz}$ ,  $J=9.9\text{Hz}$ , 1H), 2.44 (dd,  $J=13.2\text{Hz}$ ,  $J=2.7\text{Hz}$ , 1H), 2.58 (m, 4H), 2.76 (m, 4H), 3.79 (m, 1H).  $m/z$  (GC, EI) 162.6  $[M+H]^+$ , calculated  $M_w = 161.25$ .

### 5.3 Procedures for the Synthesis of the Second Generation Dendrons (*i.e.* XG2OH)

#### Synthesis of **BG2OH**:



CDI (4.55 g, 28.1 mmol) was added to a stirred solution of **BG1OH** (8.82 g, 24.4 mmol) in toluene (100 mL). The mixture was heated at 60°C for 6 hrs. Subsequently, the reaction mixture was analysed by  $^1\text{H}$  NMR spectroscopy and interpretation of the spectrum indicated there was no evidence of the starting materials (**BG1OH** or CDI). The branching unit **AEAP** (2.17 g, 13.4 mmol) was added and the solution was heated for 20 hrs. The reaction mixture was concentrated *in vacuo* and redissolved in  $\text{CH}_2\text{Cl}_2$  (200 mL). The organic phase was subsequently washed with water (3 x 250 mL), dried over  $\text{MgSO}_4$  and the solvent removed using the rotary evaporator. The resulting pale yellow oil was purified by column chromatography (silica gel, eluting with  $\text{EtOAc}:\text{C}_6\text{H}_{12}$  3:2) and the colourless oil obtained was dried under vacuum ( $10^{-1}$  mbar) to give compound **BG2OH** as a colourless amorphous solid (5.7 g, 50%).  $T_g = 24.9^\circ\text{C}$ . Found C, 54.62; H, 9.14; N, 13.50%.  $\text{C}_{43}\text{H}_{85}\text{N}_9\text{O}_{13}$  requires, C, 55.17; H, 9.15; N, 13.47%.  $^{13}\text{C}$  NMR (400 MHz,  $\text{CD}_3\text{OD}$ ,  $50^\circ\text{C}$ )  $\delta$  18.9, 21.0, 28.9, 39.9, 40.2, 55.7, 56.0, 61.1, 64.1, 66.2, 71.0, 80.1, 158.3, 158.8. The signal at 66.2 is split into three peaks – 66.25, 66.18, 66.12 – with the relative intensities 1: 2.0: 0.8 (see text 37-40).  $^1\text{H}$  NMR (500 MHz,  $\text{CD}_3\text{OD}$ )  $\delta$  1.12 (d,  $J=6.0\text{Hz}$ , 3H,  $\text{CH}_2\text{CH}(\text{OH})\text{CH}_3$ ), 1.19 (d,  $J=6.5\text{Hz}$ , 6H,  $\text{C}(\text{H})(\text{CH}_3)\text{OC}(\text{O})\text{N}(\text{H})$ ), 1.40 (s, 36H,  $\text{C}(\text{O})\text{C}(\text{CH}_3)$ ), 2.41 (m, 2H,  $\text{NCH}_2\text{CH}(\text{CH}_3)(\text{OH})$ ),



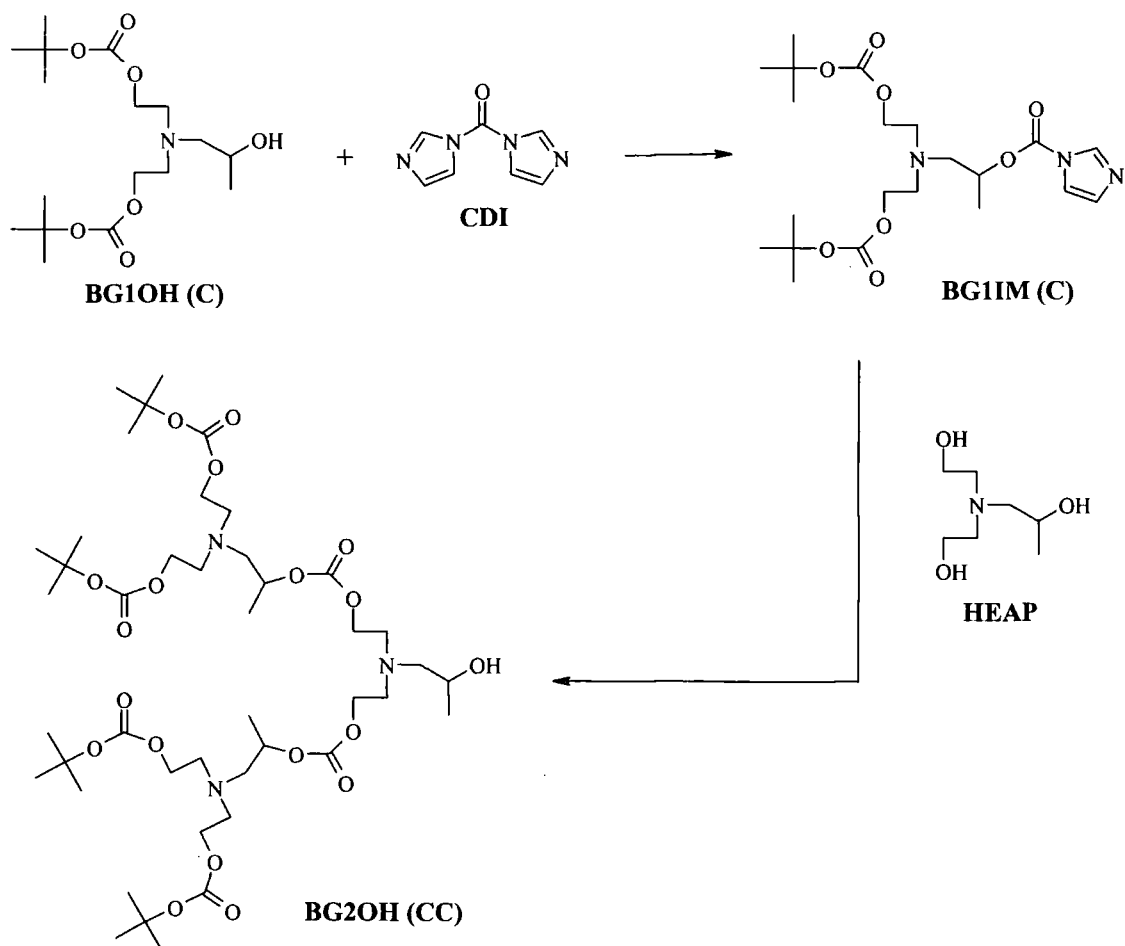
2.49 and 2.66 (m, 4H,  $\text{NCH}_2\text{C}(\text{H})(\text{CH}_3)\text{OC}(\text{O})\text{N}(\text{H})$ ), 2.58 (m, 12H,  $\text{O}(\text{CO})\text{N}(\text{H})\text{CH}_2\text{CH}_2$ ), 3.08 (m, 12H,  $\text{O}(\text{CO})\text{N}(\text{H})\text{CH}_2\text{CH}_2$ ), 3.22 (m, 4H,  $\text{O}(\text{CO})\text{NHCH}_2\text{CH}_2$  – closer to focal point), 3.78 (m, 1H,  $\text{CH}_2\text{CH}(\text{CH}_3)(\text{OH})$ ), 4.85 (m, obscured by water peak, 2H,  $\text{CH}_2\text{C}(\text{H})(\text{CH}_3)\text{OC}(\text{O})\text{N}(\text{H})$ ), 6.43 (s, br,  $\text{O}(\text{CO})\text{NHCH}_2$ ), 6.88 (s, br, 2H,  $\text{O}(\text{CO})\text{NHCH}_2$ ).  $m/z$  (ES MS) 936  $[\text{M}+\text{H}]^+$ , 958  $[\text{M}+\text{Na}]^+$ , 974  $[\text{M}+\text{K}]^+$ , 469  $[\text{M}+2\text{H}]^{2+}$ , 480  $[\text{M}+\text{H}+\text{Na}]^{2+}$ , 488  $[\text{M}+\text{H}+\text{K}]^{2+}$ , 491  $[\text{M}+2\text{Na}]^{2+}$ , calculated  $M_w = 936.19$ . GPC;  $M_w = 1120$ ,  $\text{Pd} = 1.02$ .

**Synthesis of HG2OH:** The procedure was similar to that described for the synthesis of **BG2OH**, but using **HG1OH** as the starting material. The purification step was achieved by column chromatography (silica gel, eluting with  $\text{EtOAc}:\text{C}_6\text{H}_{12}$  1:2) to give *compound HG2OH* as a sticky colourless oil (49%).  $T_g = -4.3^\circ\text{C}$ . Found C, 59.54; H, 9.91; N, 11.20%.  $\text{C}_{55}\text{H}_{109}\text{N}_9\text{O}_{13}$  requires, C, 59.81; H, 9.95; N, 11.41%.  $^{13}\text{C}$  NMR (62.9 MHz,  $\text{CD}_3\text{OD}$ )  $\delta$  14.5, 18.9, 19.5, 20.9, 37.8, 39.9 (resonances from two distinct carbons overlap), 55.5, 55.9, 60.9, 64.0, 65.8 (split into 3 peaks), 70.6, 74.9, 158.6, 158.9.  $^1\text{H}$  NMR (400 MHz,  $\text{CD}_3\text{OD}$ )  $\delta$  0.92 (t,  $J=7.2\text{Hz}$ , 24H), 1.12 (d,  $J=6.4\text{Hz}$ , 3H), 1.19 (d,  $J=6.4\text{Hz}$ , 6H), 1.30-1.41 (m, 16H), 1.47-1.54 (m, 16H), 2.38-2.68 (m, 18H), 3.09-3.28 (m, 12H), 3.77 (m, 1H), 4.73 (m, 4H), 4.85 (m, 2H), 6.67 (s, br,  $\text{O}(\text{CO})\text{NHCH}_2\text{CH}_2$ ), 6.89 (s, br,  $\text{O}(\text{CO})\text{NHCH}_2\text{CH}_2$ ).  $m/z$  (ES MS) 1105  $[\text{M}+\text{H}]^+$ , 1127  $[\text{M}+\text{Na}]^+$ , 1143  $[\text{M}+\text{K}]^+$ , 553  $[\text{M}+2\text{H}]^{2+}$ , 564  $[\text{M}+\text{H}+\text{Na}]^{2+}$ , 575  $[\text{M}+2\text{Na}]^{2+}$ .  $m/z$  (MALDI-TOF (Kratos) MS) 1105  $[\text{M}+\text{H}]^+$ , 1127  $[\text{M}+\text{Na}]^+$ , calculated  $M_w = 1104.51$ . GPC;  $M_w = 1180$ ,  $\text{Pd} = 1.00$ .

**Synthesis of CG2OH:** The reaction and purification procedures were as described for the synthesis of **BG2OH**, using **CG1OH** as the starting material, to give *compound CG2OH* as a colourless oil (42%).  $T_g = 29.8^\circ\text{C}$ . Found C, 58.62; H, 8.97; N, 11.98%.  $\text{C}_{51}\text{H}_{93}\text{N}_9\text{O}_{13}$  requires, C, 58.88; H, 9.01; N, 12.12%.  $^{13}\text{C}$  NMR (62.8 MHz,  $\text{CD}_3\text{OD}$ )  $\delta$  18.9, 21.0, 24.8, 26.5, 33.1, 39.9 (resonances from two distinct carbons overlap), 55.5, 55.9, 60.9, 64.0, 66.0 (split into 3 peaks), 70.7, 74.0, 158.6, 158.8.  $^1\text{H}$  NMR (400 MHz,  $\text{CD}_3\text{OD}$ )  $\delta$  1.12 (d,  $J=6\text{Hz}$ , 3H), 1.18 (d,  $J=6\text{Hz}$ , 6H), 1.21-1.45 (m, 20H), 1.56 (m, 4H), 1.74 (m, 8H), 1.85 (m, 8H), 2.40-2.70 (m, 18H), 3.08-3.27 (m, 12H), 3.78 (m, 1H), 4.56 (m, 4H), 4.84 (m, 2H), 6.61 (s, br,  $\text{O}(\text{CO})\text{NHCH}_2\text{CH}_2$ ), 6.88 (s, br,  $\text{O}(\text{CO})\text{NHCH}_2\text{CH}_2$ ).  $m/z$  (ES MS) 1040.4  $[\text{M}+\text{H}]^+$ , 1062.4  $[\text{M}+\text{Na}]^+$ , 1078  $[\text{M}+\text{K}]^+$ , 521  $[\text{M}+2\text{H}]^{2+}$ , 532  $[\text{M}+\text{H}+\text{Na}]^{2+}$ , 539  $[\text{M}+\text{H}+\text{K}]^{2+}$ , 543  $[\text{M}+2\text{Na}]^{2+}$ .  $m/z$  (MALDI-TOF (Kratos) MS) 1041  $[\text{M}+\text{H}]^+$ , 1063  $[\text{M}+\text{Na}]^+$ , 1079  $[\text{M}+\text{K}]^+$ , calculated  $M_w = 1040.34$ . GPC;  $M_w = 970$ ,  $\text{Pd} = 1.02$ .

**Synthesis of BG2OH (UC):** The procedure was similar to that described for the synthesis of **BG2OH**, but using **BG1OH (C)** as the starting material. The purification step was achieved by column chromatography (silica gel, eluting with EtOAc:C<sub>6</sub>H<sub>12</sub> 1:3, increasing to EtOAc) and the colourless oil obtained dried under vacuum (10<sup>-1</sup> mbar) to give *compound* **BG2OH (UC)** as a colourless oil (58%). *T<sub>g</sub>* = -9.6°C. Found C, 54.78; H, 8.72; N, 7.70%. C<sub>43</sub>H<sub>81</sub>O<sub>17</sub>N<sub>5</sub> requires, C, 54.94; H, 8.68; N, 7.45%. <sup>13</sup>C NMR (125 MHz, CD<sub>3</sub>OD) δ 18.8, 21.0 (split into 3 peaks), 28.1, 40.1, 54.9, 56.0, 61.1, 64.1 (split but not well resolved), 66.1 (split into 3 peaks), 66.4, 71.0, 82.7, 155.1, 158.7. <sup>1</sup>H NMR (500 MHz, CD<sub>3</sub>OD) δ 1.12 (d, *J*=6.0Hz, 3H), 1.20 (d, *J*=6.5Hz, 6H), 1.46 (s, 36H), 2.40 (dd, *J*=13 Hz, *J*=8.5Hz, 1H), 2.45 (dd, *J*=13Hz, *J*=4Hz, 1H), 2.56-2.66 (m, 6H), 2.71 (dd, *J*=4Hz, *J*=6.5Hz, 2H), 2.84 (m, 8H), 3.18 (m, 4H), 3.78 (m, 1H), 4.09 (m, 8H), 4.82 (m, 2H), 6.77 (s, br, O(CO)NHCH<sub>2</sub>CH<sub>2</sub>). *m/z* (ES MS) 940.6 [M+H]<sup>+</sup>, 962.6 [M+Na]<sup>+</sup>, 977 [M+K]<sup>+</sup>. *m/z* (MALDI TOF (Voyager) MS) 940.5 [M+H]<sup>+</sup>, 962.5 [M+Na]<sup>+</sup>, 978.4 [M+K]<sup>+</sup> and four sets of similar peaks at 100 mass intervals, see Appendix, page XVII, calculated *M<sub>w</sub>* = 940.13. GPC; *M<sub>w</sub>* = 1100, *Pd* = 1.00.

**Synthesis of BG2OH (CC):**

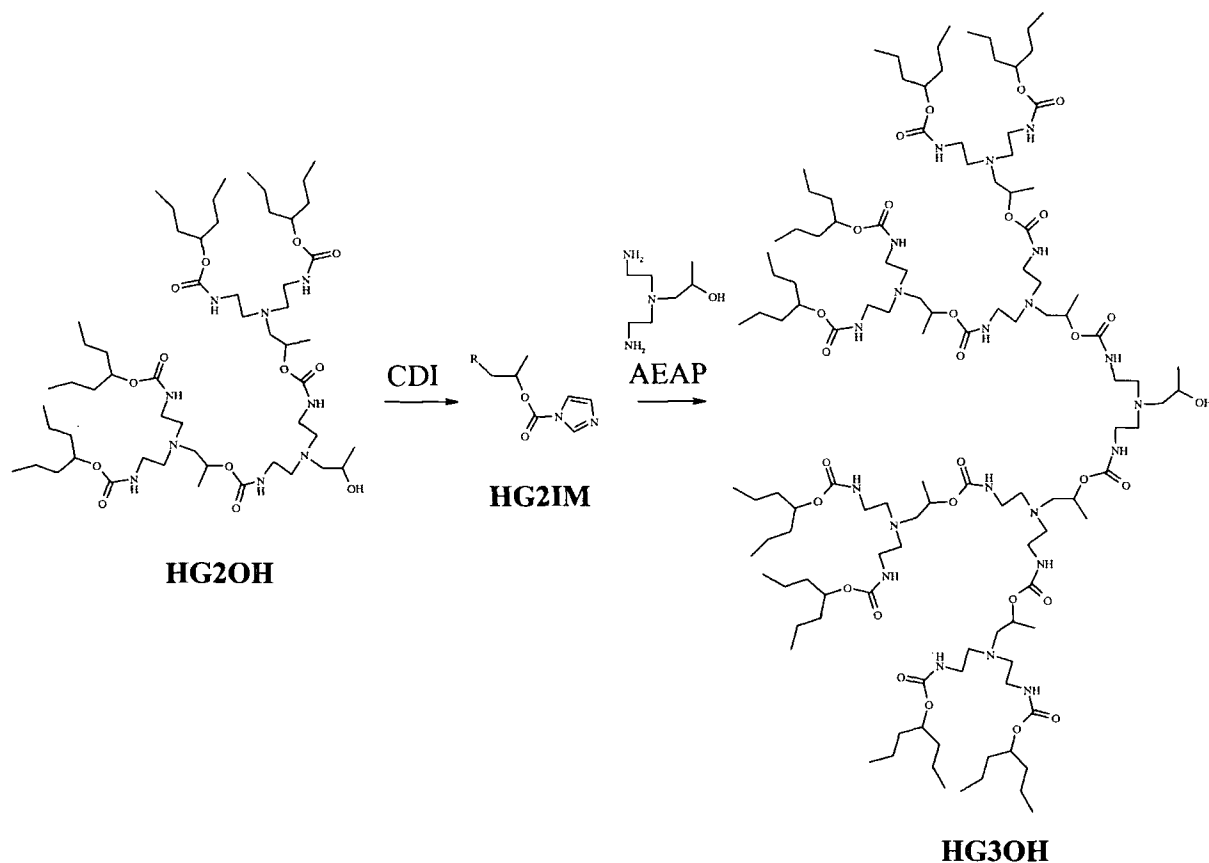


CDI (1.42 g, 8.77 mmol) was added to a stirred solution of **BG1OH (C)** (2.66 g, 7.33 mmol) in toluene (50 mL). The mixture was heated at 60°C for 4 hours. Subsequently, the reaction mixture was analysed by  $^1\text{H}$  NMR spectroscopy and interpretation of the spectrum indicated there was no evidence of the starting materials (*i.e.* **BG1OH (C)** or CDI). **HEAP** (0.59 g, 3.66 mmol) and KOH (70 mg) were added and the solution was heated for 2 days at 75°C. The reaction mixture was concentrated *in vacuo* and redissolved in  $\text{CH}_2\text{Cl}_2$  (100 mL). The organic phase was subsequently washed with water (3 x 100 mL), dried over  $\text{MgSO}_4$  and the solvent removed using the rotary evaporator. The resulting pale yellow oil was purified by column chromatography (silica gel,  $\text{EtOAc}:\text{C}_6\text{H}_{12}$  1:3 increasing to  $\text{EtOAc}:\text{C}_6\text{H}_{12}$  1:2) and the colourless oil obtained dried under vacuum ( $10^{-1}$  mbar) to give *compound* **BG2OH (CC)** as a colourless oil (1.4 g, 40%).  $T_g = -29.8^\circ\text{C}$ . Found C, 54.54; H, 8.34; N, 4.54%.  $\text{C}_{43}\text{H}_{79}\text{O}_{19}\text{N}_3$  requires, C, 54.82; H, 8.45; N, 4.46%.  $^{13}\text{C}$  NMR (500 MHz,  $\text{CD}_3\text{OD}$ )  $\delta$  18.3, 20.8, 28.1, 54.8, 54.9, 61.0, 64.1, 66.1 (split into 3 peaks), 66.3, 66.9, 74.8, 82.6, 155.0, 156.3.  $^1\text{H}$  NMR (500 MHz,  $\text{CD}_3\text{OD}$ )  $\delta$  1.16 (d,  $J=6.0$  Hz, 3H), 1.29 (d,  $J=6.0$  Hz, 6H), 1.51 (s, 36H), 2.52 (dd,  $J=13\text{Hz}$ ,  $J=8\text{Hz}$ , 1H), 2.60 (dd,  $J=13$  Hz,  $J=4$  Hz, 1H), 2.70 (dd,  $J=13.75$  Hz, 5.5 Hz, 2H), 2.78 (dd,  $J=13.75$  Hz, 7 Hz, 2H), 2.88 (t,  $J=6\text{Hz}$ , 8H), 2.92 (m, 4H), 3.82 (m, 1H), 4.13 (m, 8H), 4.23 (t,  $J=6\text{Hz}$ , 4H), 4.84 (m, 2H).  $m/z$  (ES MS) 941.5  $[\text{M}+\text{H}]^+$ , 963.4  $[\text{M}+\text{Na}]^+$ , calculated  $M_w = 942.10$ . GPC;  $M_w = 1390$ ,  $\text{Pd} = 1.00$ .

**Synthesis of BG2OH (CU):** The procedure was similar to that described for the synthesis of **BG2OH (CC)**, but using **BG1OH** as the starting material. The purification step was achieved by column chromatography (silica gel,  $\text{EtOAc}:\text{C}_6\text{H}_{12}$  3:1) and the colourless oil obtained dried under vacuum ( $10^{-1}$  mbar) to give *compound* **BG2OH (CU)** as a colourless oil (32%).  $T_g = 9.5^\circ\text{C}$ . Found C, 54.78; H, 8.91; N, 10.40%.  $\text{C}_{43}\text{H}_{83}\text{O}_{15}\text{N}_7$  requires, C, 55.05; H, 8.92; N, 10.45%.  $^{13}\text{C}$  NMR (62.9 MHz,  $\text{CD}_3\text{OD}$ )  $\delta$  18.5, 20.8, 28.9, 39.6, 54.7, 55.6, 60.6, 64.0, 66.1 (split into 3 peaks), 66.9, 74.7, 79.9, 156.4, 158.3.  $^1\text{H}$  NMR (250 MHz,  $\text{CD}_3\text{OD}$ )  $\delta$  1.15 (d,  $J=6.3\text{Hz}$ , 3H), 1.28 (d,  $J=6.3\text{Hz}$ , 6H), 1.47 (s, 36H), 2.45-2.72 (m, 14H), 2.91 (m, 4H), 3.12 (m, 8H), 3.79 (m, 1H), 4.22 (m, 4H), 4.83 (m, obscured by water peak, 2H), 6.40 (s, br,  $\text{OCONH}_2\text{CH}_2$ ).  $m/z$  (MALDI TOF (Kratos) MS) 939  $[\text{M}+\text{H}]^+$ , 961  $[\text{M}+\text{Na}]^+$ , 977  $[\text{M}+\text{K}]^+$ .  $m/z$  (ES MS) 938.5  $[\text{M}+\text{H}]^+$ , 960.3  $[\text{M}+\text{Na}]^+$ , calculated  $M_w = 938.16$ . GPC;  $M_w = 1100$ ,  $\text{Pd} = 1.00$ .

## 5.4 Procedures for the Synthesis of Third and Fourth Generation Dendrons (i.e. **HG3OH** and **CG4OH**)

### Synthesis of **HG3OH**:



CDI (0.75 g, 4.62 mmol) was added to a stirred solution of **HG2OH** (4.3 g, 3.89 mmol) in toluene (50 mL). The mixture was heated at 60°C for 4 hrs. Subsequently, the reaction mixture was analysed by  $^1\text{H}$  NMR spectroscopy and interpretation of the spectrum indicated there was no evidence of the starting materials (i.e. **HG2OH** or CDI). The branching unit **AEAP** (0.31 g, 1.95 mmol) was added and the solution was heated for 1 day at 60°C. The reaction mixture was concentrated *in vacuo* and redissolved in  $\text{CH}_2\text{Cl}_2$  (100 mL). The organic phase was subsequently washed with water (3 x 100 mL), dried over  $\text{MgSO}_4$  and the solvent removed using the rotary evaporator. The resulting pale yellow oil was purified by column chromatography (silica gel, eluting with EtOAc increasing to EtOAc:MeOH 100:5) and the colourless oil obtained was dried under vacuum ( $10^{-1}$  mbar) to give compound **HG3OH** as a colourless oil (2.1 g, 44%).  $T_g = 10.5^\circ\text{C}$ . Found C, 59.08; H, 9.72; N, 12.02%.

$\text{C}_{119}\text{H}_{233}\text{O}_{29}\text{N}_{21}$  requires, C, 59.01; H, 9.70; N, 12.14%.  $^{13}\text{C}$  NMR (62.9 MHz,  $\text{CD}_3\text{OD}$ )  $\delta$  14.5, 19.0, 19.6, 21.0, 37.9, 40.1, 55.6, 61.0, 64.1, 66.1, 70.7, 75.2, 158.7, 159.2.  $^1\text{H}$  NMR (250 MHz,  $\text{CD}_3\text{OD}$ )  $\delta$  0.92 (t,  $J=7\text{Hz}$ , 48H), 1.12 (d,  $J=6\text{Hz}$ , 3H), 1.20 (d,  $J=6\text{Hz}$ , 18H), 1.36 (m, 32H), 1.49 (m, 32H), 2.45-2.62 (m, 42H), 3.10-3.27 (m, 28H), 3.78 (m, 1H), 4.73 (m, 8H), 4.81 (m, obscured by water peak, 6H), 6.64 (s, br,  $\text{O}(\text{CO})\text{NHCH}_2\text{CH}_2$ ), 6.71 (s, br,

O(CO)NHCH<sub>2</sub>CH<sub>2</sub>), 6.85 (s, br, O(CO)NHCH<sub>2</sub>CH<sub>2</sub>). *m/z* (MALDI TOF (Voyager) MS) 2423.6 [M+H]<sup>+</sup>, 2445.2 [M+Na]<sup>+</sup>, 2461.2 [M+K]<sup>+</sup>, calculated M<sub>w</sub> = 2422.25. GPC; M<sub>w</sub> = 2830, Pd = 1.00.

**Synthesis of CG3OH:** The procedure was similar to that described for the synthesis of **HG3OH**, but using **CG2OH** as the starting material. The colourless oil obtained after silica gel chromatography (eluting with EtOAc increasing to EtOAc:MeOH 100:5) was purified further by preparative GPC (Biobeads, eluting with toluene) to give *compound CG3OH* as a colourless amorphous solid (28%). T<sub>g</sub> = 40.0°C. Found C, 58.05; H, 8.85; N, 12.69%. C<sub>111</sub>H<sub>201</sub>O<sub>29</sub>N<sub>21</sub> requires, C, 58.12; H, 8.83; N, 12.82%. <sup>13</sup>C NMR (100 MHz, CD<sub>3</sub>OD) δ 19.0, 21.0, 24.9, 26.6, 33.2, 39.9, 40.1, 40.5, 55.5, 55.7, 55.9, 60.9, 64.1, 66.0, 70.7, 73.9, 157.6, 157.7, 157.8. <sup>1</sup>H NMR (400 MHz, CD<sub>3</sub>OD) δ 1.12 (d, J=6.4Hz, 3H), 1.45 (d, J=5.6Hz, 18H), 1.25-1.42 (m, 40H), 1.56 (m, 8H), 1.75 (m, 16H), 1.85 (m, 16H), 2.42-2.69 (m, 42H), 3.15-3.25 (m, 28H), 3.78 (m, 1H), 4.57 (m, 8H), 4.84 (m, obscured by water peak, 6H), 6.59 (s, br, O(CO)NHCH<sub>2</sub>CH<sub>2</sub>), 6.71 (s, br, O(CO)NHCH<sub>2</sub>CH<sub>2</sub>), 6.86 (s, br, O(CO)NHCH<sub>2</sub>CH<sub>2</sub>). *m/z* (MALDI TOF (Voyager) MS) 2294.0 [M+H]<sup>+</sup>, 2316.2 [M+Na]<sup>+</sup>, 2331.2 [M+K]<sup>+</sup>, calculated M<sub>w</sub> = 2293.91. GPC; M<sub>w</sub> = 2440, Pd = 1.00.

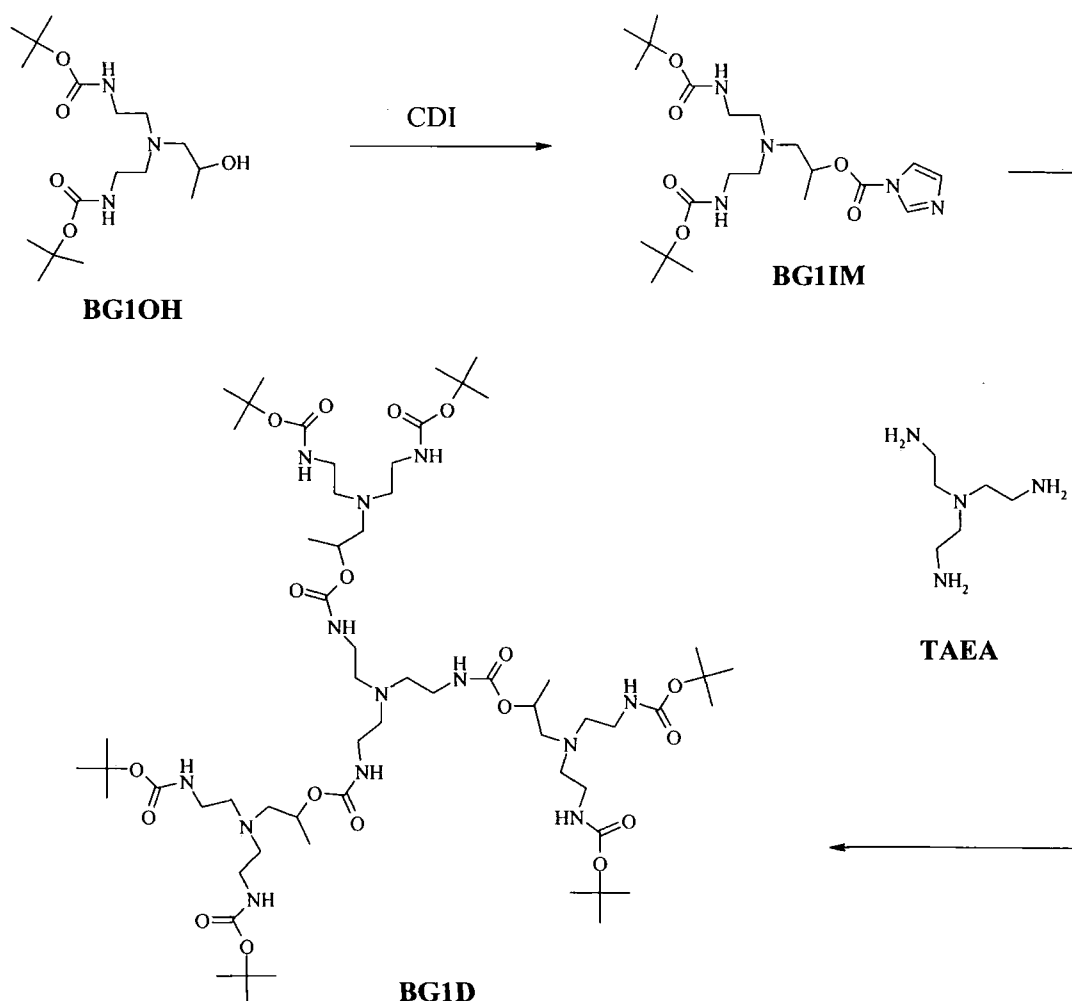
**Synthesis of BG3OH:** The procedure was similar to that described for the synthesis of **HG3OH**, but using **BG2OH** as the starting material. The oil obtained was purified by column chromatography (silica gel, eluting with EtOAc increasing to EtOAc:MeOH, 100:5) and then purified by preparative GPC (Biobeads, eluting with toluene) to give *compound BG3OH* as a colourless amorphous solid (48%). T<sub>g</sub> = 40.0°C. Found C, 54.16; H, 9.08; N, 13.83%. C<sub>95</sub>H<sub>185</sub>O<sub>29</sub>N<sub>21</sub> requires, C, 54.71; H, 8.94; N, 14.10%. <sup>13</sup>C NMR (62.9 MHz, CD<sub>3</sub>OD) δ 19.0, 21.0, 28.9, 39.6, 40.0, 55.6, 55.9, 61.0, 64.0, 66.0, 70.7, 79.9, 158.3, 158.7, 158.8. <sup>1</sup>H NMR (400 MHz, CD<sub>3</sub>OD) δ 1.12 (d, J=6Hz, 3H), 1.20 (d, J=6.4Hz, 18H), 1.44 (s, 72H), 2.41-2.64 (m, 42H), 3.04-3.24 (m, 28H), 3.78 (m, 1H), 4.85 (m, obscured by water peak, 6H), 6.42 (s, br, O(CO)NHCH<sub>2</sub>CH<sub>2</sub>), 6.71 (s, br, O(CO)NHCH<sub>2</sub>CH<sub>2</sub>), 6.85 (s, br, O(CO)NHCH<sub>2</sub>CH<sub>2</sub>). *m/z* (ES MS) 2108.2 [M+Na]<sup>+</sup>, 1054.4 [M+2H]<sup>2+</sup>, 1065.4 [M+H+Na]<sup>2+</sup>. *m/z* (MALDI TOF (Voyager) MS) 2086 [M+H]<sup>+</sup>, 2108 [M+Na]<sup>+</sup>, 2124 [M+K]<sup>+</sup> – and sets of similar peaks at 100 mass intervals below the molecular ion, calculated M<sub>w</sub> = 2085.61. GPC; M<sub>w</sub> = 2300, Pd = 1.00.

**Synthesis of CG4OH:** The procedure was similar to that described for the synthesis of **HG3OH**, but using **CG3OH** as the starting material. The crude product obtained was

purified by column chromatography (silica gel, eluting with EtOAc:MeOH, 100:5) and the colourless solid obtained was purified by preparative GPC (Biobeads, eluting with toluene) to give **compound CG40H** as a colourless amorphous solid (14%).  $T_g = 47.8^\circ\text{C}$ . Found C, 56.95; H, 8.66; N, 12.57%.  $\text{C}_{231}\text{H}_{417}\text{O}_{61}\text{N}_{45}$  requires, C, 57.79; H, 8.75; N, 13.13%.  $^{13}\text{C}$  NMR (100 MHz,  $\text{CD}_3\text{OD}$ )  $\delta$  19.0, 19.1, 21.1, 24.9, 26.6, 33.2, 39.9, 40.1, 40.4, 40.5, 55.5, 55.7, 60.9, 64.1, 66.0, 70.7, 74.0, 158.6, 158.7, 158.8.  $^1\text{H}$  NMR (400 MHz,  $\text{CD}_3\text{OD}$ )  $\delta$  1.12 (d,  $J=6\text{Hz}$ , 3H), 1.19-1.45 (m, 122H), 1.56 (m, 16H), 1.74 (m, 36H), 1.85 (m, 36H), 2.44-2.68 (m, 88H), 3.11-3.20 (m, 60H), 3.78 (m, 1H), 4.57 (m, 16H), 4.84 (m, 14H), 6.59 (s, br,  $\text{O}(\text{CO})\text{NHCH}_2\text{CH}_2$ ), 6.70 (s, br,  $\text{O}(\text{CO})\text{NHCH}_2\text{CH}_2$ ), 6.85 (s, br,  $\text{O}(\text{CO})\text{NHCH}_2\text{CH}_2$ ).  $m/z$  (MALDI TOF (Voyager) MS) 4801.4  $[\text{M}+\text{H}]^+$ , 4823.4  $[\text{M}+\text{Na}]^+$ , 4839.3  $[\text{M}+\text{K}]^+$ , calculated  $M_w = 4801.05$ . GPC;  $M_w = 4190$ ,  $\text{Pd} = 1.02$ .

## 5.5 General Procedure for the Synthesis of First Generation Dendrimers with Amine core units (*i.e.* XG1D).

### Synthesis of BG1D:





CDI (5.5 g, 33.9 mmol) was added to a stirred solution of **BG1OH** (10.2 g, 28.3 mmol) in toluene (150 mL). The mixture was heated at 60°C for 4 hrs. Subsequently, the reaction mixture was analysed by  $^1\text{H}$  NMR spectroscopy and interpretation of the spectrum indicated there was no evidence of the starting materials (*i.e.* **BG1OH** or CDI). Tris(2-aminoethyl)amine **TAEA** (1.38 g, 9.42 mmol) was added and the solution was heated at 60°C for 24 hrs. The reaction mixture was concentrated *in vacuo* and redissolved in  $\text{CH}_2\text{Cl}_2$  (150 mL). The organic phase was subsequently washed with water (3 x 150 mL), dried over  $\text{MgSO}_4$  and the solvent removed using the rotary evaporator. The crude product was purified by column chromatography (silica gel, eluting with eluting with  $\text{EtOAc}:\text{C}_6\text{H}_{12}$ , 1:1 increasing to  $\text{EtOAc}$ ) to give the compound **BG1D** as a colourless amorphous solid (3.7 g, 30%).  $T_g = 37.6^\circ\text{C}$ . Found C, 55.72; H, 8.96; N, 13.37%.  $\text{C}_{60}\text{H}_{117}\text{O}_{18}\text{N}_{13}$  requires, C, 55.07; H, 9.01; N, 13.91%.  $^{13}\text{C}$  NMR (100 MHz,  $\text{CD}_3\text{OD}$  at 50°C)  $\delta$  19.0, 28.9, 39.7, 40.1, 55.2, 55.6, 61.0, 70.7, 79.8, 158.1, 158.5.  $^1\text{H}$  NMR (400 MHz,  $\text{CD}_3\text{OD}$ )  $\delta$  1.20 (d,  $J=6.4\text{Hz}$ , 9H), 1.44 (s, 54H), 2.50 (dd,  $J=13.6\text{Hz}$ ,  $J=4.8\text{Hz}$ , 3H), 2.57-2.63 (m, 21H), 3.04-3.25 (m, 18H), 4.85 (m, 3H) 6.43 (s, br,  $\text{O}(\text{CO})\text{NHCH}_2\text{CH}_2$ ), 6.79 (s, br,  $\text{O}(\text{CO})\text{NHCH}_2\text{CH}_2$ ).  $m/z$  (TOF MS ES) 1307  $[\text{M}+\text{H}]^+$ , 1313  $[\text{M}+\text{Li}]^+$ , 1329  $[\text{M}+\text{Na}]^+$ , 676  $[\text{M}+2\text{Na}]^{2+}$ .  $m/z$  (MALDI TOF (Kratos) MS) 1307  $[\text{M}+\text{H}]^+$ , 1330  $[\text{M}+\text{Na}]^+$ , 1346  $[\text{M}+\text{K}]^+$ , calculated  $M_w = 1308.65$ . GPC;  $M_w = 1780$ ,  $\text{Pd} = 1.00$ .

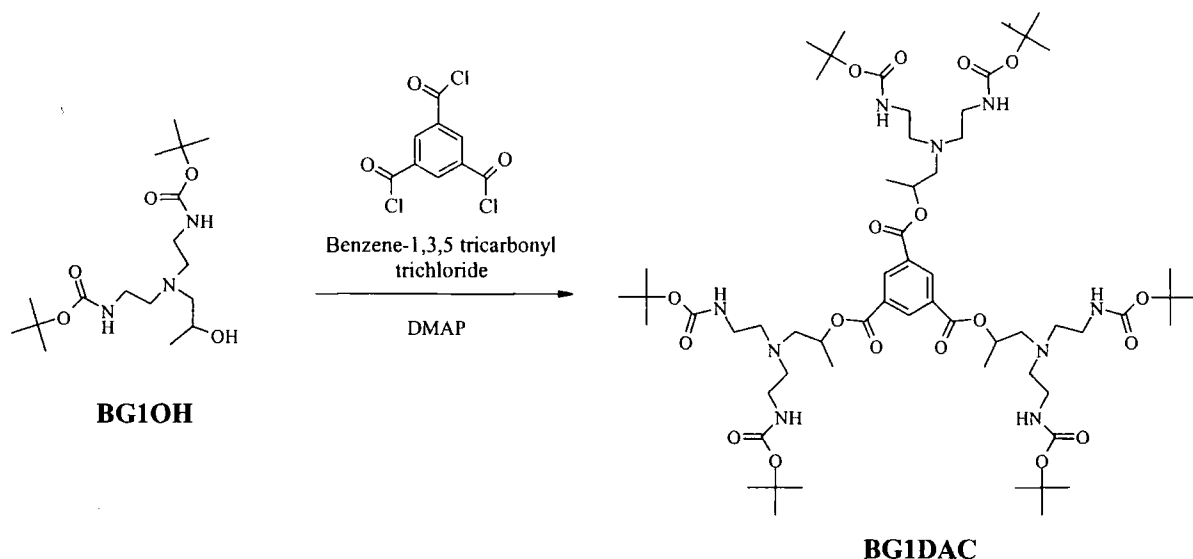
**Synthesis of HG1D:** The procedure was similar to that described for the synthesis of **BG1D**, but using **HG1OH** as the starting material. The crude product was purified by column chromatography (silica gel, eluting with  $\text{EtOAc}:\text{C}_6\text{H}_{12}$ , 3:1 increasing to  $\text{EtOAc}$ ) to give compound **HG1D** as a colourless solid (32%).  $T_g = 6.9^\circ\text{C}$ . Found C, 59.78; H, 9.91; N, 11.73%.  $\text{C}_{78}\text{H}_{153}\text{O}_{18}\text{N}_{13}$  requires, C, 60.01; H, 9.88; N, 11.66%.  $^{13}\text{C}$  NMR (62.9 MHz,  $\text{CD}_3\text{OD}$ )  $\delta$  14.5, 19.0, 19.6, 37.9, 40.0, 55.3, 55.6, 61.0, 70.7, 75.2, 158.7, 159.2.  $^1\text{H}$  NMR (400 MHz,  $\text{CD}_3\text{OD}$ )  $\delta$  0.92 (t,  $J=7.2\text{Hz}$ , 36H), 1.20 (d,  $J=6\text{Hz}$ , 9H), 1.36 (m, 24H), 1.50 (m, 24H), 2.50-2.63 (m, 24H), 3.10-3.21 (m, 18H), 4.73 (m, 6H), 4.86 (m, obscured by water peak, 3H), 6.66 (s, br,  $\text{O}(\text{CO})\text{NHCH}_2\text{CH}_2$ ), 6.79 (s, br,  $\text{O}(\text{CO})\text{NHCH}_2\text{CH}_2$ ).  $m/z$  (ES MS) 1561.1  $[\text{M}+\text{H}]^+$ , 1583.0  $[\text{M}+\text{Na}]^+$ , 781.3  $[\text{M}+2\text{H}]^{2+}$ , 792.3  $[\text{M}+\text{H}+\text{Na}]^{2+}$ , 803.3  $[\text{M}+2\text{Na}]^{2+}$ .  $m/z$  (MALDI TOF (Voyager) MS) 1561.2  $[\text{M}+\text{H}]^+$ , 1583.1  $[\text{M}+\text{Na}]^+$ .  $m/z$  (MALDI TOF (Kratos) MS) 1557  $[\text{M}+\text{H}]^+$ , 1580  $[\text{M}+\text{Na}]^+$ , calculated  $M_w = 1561.13$ . GPC;  $M_w = 1740$ ,  $\text{Pd} = 1.02$ .

**Synthesis of CG1D:** The procedure was similar to that described for the synthesis of **BG1D**, but using **CG1OH** as the starting material. The crude product was purified by column

chromatography (silica gel, eluting with EtOAc increasing to EtOAc:MeOH 100:5) to give compound **CG1D** as a colourless solid (32%).  $T_g = 38.9^\circ\text{C}$ . Found C, 58.30; H, 8.73; N, 12.06%.  $\text{C}_{72}\text{H}_{129}\text{O}_{18}\text{N}_{13}$  requires, C, 59.03; H, 8.88; N, 12.43%.  $^{13}\text{C}$  NMR (62.9 MHz,  $\text{CD}_3\text{OD}$ )  $\delta$  19.0, 24.9, 26.6, 33.2, 40.0, 55.3, 55.5, 61.0, 70.8, 74.0, 158.7, 158.9.  $^1\text{H}$  NMR (400 MHz,  $\text{CD}_3\text{OD}$ )  $\delta$  1.19 (d,  $J=4.8\text{Hz}$ , 9H), 1.28-1.40 (m, 30H), 1.54 (m, 6H), 1.75 (m, 12H), 1.85 (m, 12H), 2.49-2.61 (m, 24H), 3.16 (m, 18H), 4.56 (m, 6H), 4.85 (m, obscured by water peak, 3H), 6.60 (s, br,  $\text{O}(\text{CO})\text{NHCH}_2\text{CH}_2$ ), 6.77 (s, br,  $\text{O}(\text{CO})\text{NHCH}_2\text{CH}_2$ ).  $m/z$  (ES MS) 1464.8  $[\text{M}+\text{H}]^+$ , 1486.7  $[\text{M}+\text{Na}]^+$ , 732.9  $[\text{M}/2+\text{H}]^+$ , 743.9  $[\text{M}/2+\text{Na}]^+$ , 755.4  $[\text{M}/2+\text{K}]^+$ .  $m/z$  (MALDI TOF (Voyager) MS) 1464.9  $[\text{M}+\text{H}]^+$ , 1486.9  $[\text{M}+\text{Na}]^+$ , 1502.9  $[\text{M}+\text{K}]^+$ , calculated  $M_w = 1464.87$ . GPC;  $M_w = 1350$ ,  $\text{Pd} = 1.02$ .

## 5.6 General Procedure for the Synthesis of First and Second Generation Dendrimers with Aromatic-ester core units (i.e. XGXDAC).

### Synthesis of **BG1DAC**:



A solution of **BG1OH** (2.0 g, 5.54 mmol) and 4-dimethylaminopyridine **DMAP** (1.8 g, 14.8 mmol) in benzene (100 mL) was refluxed for 3 hrs with a Dean-Stark trap filled with molecular sieves attached. The mixture was cooled to room temperature and 1,3,5-benzenetricarbonyl trichloride (0.45 g, 1.70 mmol) was added. The reaction mixture was stirred heated at  $40^\circ\text{C}$  for 3 hrs and then concentrated *in vacuo*. The crude product obtained was purified by column chromatography (silica gel, eluting with EtOAc: $\text{C}_6\text{H}_{12}$ , 5:1) to give compound **BG1DAC** as a white amorphous solid (1.75 g, 83%).  $T_g = 35.1^\circ\text{C}$ . Found C, 57.08; H, 8.45; N, 9.86%.  $\text{C}_{60}\text{H}_{105}\text{O}_{18}\text{N}_9$  requires, C, 58.09; H, 8.53; N, 10.16%.  $^{13}\text{C}$  NMR (62.9 MHz,  $\text{CDCl}_3$ )  $\delta$  18.1, 28.3, 38.3, 54.6, 59.2, 70.8, 78.9, 131.5, 134.3, 156.1, 164.4.  $^1\text{H}$  NMR (250 MHz,  $\text{CDCl}_3$ )  $\delta$  1.32-1.36 (m, 63H), 2.58-2.79 (m, 18H), 3.04-3.25 (m, 12H), 5.18

(s, br, OC(O)NHCH<sub>2</sub>), 5.21 (m, 3H), 8.78 (s, 3H). *m/z* (MALDI TOF (Kratos) MS) 1240 [M+H]<sup>+</sup>, 1263 [M+Na]<sup>+</sup>, 1280 [M+K]<sup>+</sup>, calculated *M<sub>w</sub>* = 1240.53. GPC; *M<sub>w</sub>* = 1320, Pd = 1.00.

**Synthesis of HG1DAC:** The procedure was similar to that described for the synthesis of **BG1DAC**, but using **HG1OH** as the starting material. The crude product was purified by column chromatography (silica gel, eluting with EtOAc:C<sub>6</sub>H<sub>12</sub>, 3:2) to give *compound HG1DAC* as a waxy white solid (75%). *T<sub>g</sub>* = -1.71°C. Found C, 62.53; H, 9.61; N, 8.33%. C<sub>78</sub>H<sub>141</sub>O<sub>18</sub>N<sub>9</sub> requires, C, 62.75; H, 9.52; N, 8.44%. <sup>13</sup>C NMR (62.9 MHz, CD<sub>3</sub>OD) δ 14.5, 18.6, 19.6, 37.9, 39.9, 55.5, 60.7, 72.2, 75.2, 133.1, 135.3, 159.1, 165.7. <sup>1</sup>H NMR (250 MHz, CD<sub>3</sub>OD) δ 0.90 (t, J=7Hz, 36H), 1.25-1.47 (m, 57H), 2.65-2.91 (m, 18H), 3.18 (m, 12H), 4.68 (m, 6H), 5.23 (m, 3H), 6.53 (s, br, OC(O)NHCH<sub>2</sub>), 8.83 (s, 3H). *m/z* (MALDI TOF (Kratos) MS) 1490 [M+H]<sup>+</sup>. *m/z* (MALDI TOF (Voyager) MS) 1493.2 [M+H]<sup>+</sup>, 1515.2 [M+Na]<sup>+</sup>, 1531.0 [M+K]<sup>+</sup>, calculated *M<sub>w</sub>* = 1493.00. GPC; *M<sub>w</sub>* = 1720, Pd = 1.00.

**Synthesis of CG1DAC:** The procedure was similar to that described for the synthesis of **BG1DAC**, but using **CG1OH** as the starting material. The crude product was purified by column chromatography (silica gel, EtOAc:C<sub>6</sub>H<sub>12</sub>, 3:1) to give *compound CG1DAC* as a white amorphous solid (78%). *T<sub>g</sub>* = 40.3°C. Found C, 61.67; H, 8.42; N, 8.87%. C<sub>72</sub>H<sub>117</sub>O<sub>18</sub>N<sub>9</sub> requires, C, 61.91; H, 8.44; N, 9.03%. <sup>13</sup>C NMR (62.9 MHz, CDCl<sub>3</sub>) δ 18.1, 23.7, 25.3, 31.8, 38.6, 54.4, 59.2, 70.7, 72.7, 131.4, 134.3, 156.4, 164.4. <sup>1</sup>H NMR (250 MHz, CDCl<sub>3</sub>) δ 1.29-1.39 (m, 39H), 1.53 (m, 6H), 1.64 (m, 12H), 1.82 (m, 12H), 2.68-2.90 (m, 18H), 3.22 (m, 12H), 4.58 (m, 6H), 5.20 (s, br, OC(O)NHCH<sub>2</sub>), 5.26 (m, 3H), 8.81 (s, 3H). *m/z* (MALDI TOF (Voyager) MS) 1396.8 [M+H]<sup>+</sup>, 1418.8 [M+Na]<sup>+</sup>, 1434.8 [M+K]<sup>+</sup>. *m/z* (MALDI TOF (Kratos) MS) 1395 [M+H]<sup>+</sup>, 1417 [M+Na]<sup>+</sup>, 1433 [M+K]<sup>+</sup>, calculated *M<sub>w</sub>* = 1396.75. GPC; *M<sub>w</sub>* = 1320, Pd = 1.00.

**Synthesis of BHG1DAC:** The procedure was similar to that described for the synthesis of **BG1DAC**, but using **BHG1OH** as the starting material. The crude product was purified by column chromatography (silica gel, EtOAc:C<sub>6</sub>H<sub>12</sub>, 3:2) to give *compound BHG1DAC* as a white amorphous solid (75%). *T<sub>g</sub>* = 63.4°C. Found C, 71.73; H, 6.13; N, 6.56%. C<sub>114</sub>H<sub>117</sub>O<sub>9</sub>N<sub>18</sub> requires, C, 72.02; H, 6.20; N, 6.63%. <sup>13</sup>C NMR (62.9 MHz, CDCl<sub>3</sub>) δ 17.9, 39.0, 54.6, 58.9, 70.9, 77.2, 126.9, 127.6, 128.3, 131.5, 134.3, 140.7, 156.0, 164.4. <sup>1</sup>H NMR (400 MHz, (CD<sub>3</sub>)<sub>2</sub>SO) δ 1.17 (d, J=4Hz, 9H), 2.51-2.66 (m, 18H), 2.96-3.16 (m, 12H), 5.06

(m, 3H), 6.63 (s, 6H), 7.20-7.34 (m, 60H), 8.60 (s, 3H).  $m/z$  (MALDI TOF (Voyager) MS) 1923.8  $[M+Na]^+$ , 1939.6  $[M+K]^+$ , calculated  $M_w = 1901.20$ . GPC;  $M_w = 1730$ , Pd = 1.00.

**Synthesis of CG2DAC:** The procedure was similar to that described for the synthesis of **BG1DAC**, but using **CG2OH** as the starting material and a reaction temperature of 50°C for 16 hrs. The crude mixture obtained was purified by column chromatography (silica gel, eluting with EtOAc increasing to EtOAc:MeOH 100:5) and by preparative GPC (Biobeads, eluting with toluene) to give *compound CG2DAC* as a white amorphous solid (65%).  $T_g = 31.7^\circ\text{C}$ . Found C, 58.45; H, 8.70; N, 11.33%.  $C_{162}H_{279}O_{42}N_{27}$  requires, C, 59.37; H, 8.58; N, 11.54%.  $^{13}\text{C}$  NMR (62.9 MHz,  $\text{CD}_3\text{OD}$ )  $\delta$  18.7, 19.0, 24.9, 26.6, 33.2, 40.0, 55.6, 61.0, 70.7, 72.4, 74.0, 133.1, 135.3, 158.7, 165.7.  $^1\text{H}$  NMR (400 MHz,  $\text{CD}_3\text{OD}$ )  $\delta$  1.11-1.44 (m, 87H), 1.55 (m, 12H), 1.73 (m, 24H), 1.84 (m, 24H), 2.48-2.87 (m, 54H), 3.10-3.23 (m, 36H), 4.55 (m, 12H), 4.82 (m, 6H), 5.28 (m, 3H), 6.58 (s, br,  $\text{OC}(\text{O})\text{NHCH}_2$ ), 8.81 (s, 3H).  $m/z$  (MALDI TOF (Voyager) MS) 3278.9  $[M+H]^+$ , 3297.8  $[M+Na]^+$ , 3315.7  $[M+K]^+$ .  $m/z$  (MALDI TOF (Kratos) MS) 3270  $[M+H]^+$ , 3293  $[M+Na]^+$ , 3310  $[M+K]^+$ , calculated  $M_w = 3277.11$ . GPC;  $M_w = 2790$ , Pd = 1.00.

**Synthesis of BG2DAC:** The procedure was similar to that described for the synthesis of **BG1DAC**, but using **BG2OH** as the starting material and a reaction temperature of 50°C for 16 hrs. The crude mixture obtained was purified by column chromatography (silica gel, eluting with EtOAc increasing to EtOAc:MeOH 100:5) and by preparative GPC (Biobeads, eluting with toluene) to give *compound BG2DAC* as a white amorphous solid (63%).  $T_g = 46.8^\circ\text{C}$ . Found C, 55.19; H, 8.58; N, 12.45%.  $C_{138}H_{255}O_{42}N_{27}$  requires, C, 55.91; H, 8.67; N, 12.76%.  $^{13}\text{C}$  NMR (62.9 MHz,  $\text{CD}_3\text{OD}$ )  $\delta$  18.7, 19.0, 28.9, 39.7, 40.0, 55.6, 61.0, 70.7, 72.3, 79.9, 133.1, 135.3, 158.4, 158.6, 165.7.  $^1\text{H}$  NMR (250 MHz,  $\text{CD}_3\text{OD}$ )  $\delta$  1.14-1.7 (m, 18H), 1.39-1.43 (m, 117H), 2.49-2.86 (m, 54H), 3.09-3.22 (m, 36H), 4.80 (m, obscured by water peak, 6H), 5.29 (m, 3H), 6.39 (s, br,  $\text{OC}(\text{O})\text{NHCH}_2$ ), 6.69 (s, br,  $\text{OC}(\text{O})\text{NHCH}_2$ ) 8.81 (s, 3H).  $m/z$  (MALDI TOF (Kratos) MS) 2982  $[M+Na]^+$ , calculated  $M_w = 2964.66$ . GPC;  $M_w = 3250$ , Pd = 1.00.

**Synthesis of HG2DAC:** The procedure was similar to that described for the synthesis of **BG1DAC**, but using **HG2OH** as the starting material and using a reaction temperature of 50°C for 20 hrs. The crude mixture obtained was purified by column chromatography (silica gel, eluting with EtOAc increasing to EtOAc:MeOH 100:5) and by preparative GPC (Biobeads, eluting with toluene) to give *compound HG2DAC* as a sticky colourless oil (56%).

Found C, 59.95; H, 9.43; N, 10.81%.  $C_{174}H_{327}O_{42}N_{27}$  requires, C, 60.23; H, 9.50; N, 10.90%.  $^{13}C$  NMR (100 MHz,  $CD_3OD$ )  $\delta$  14.5, 18.8, 19.0, 19.7, 38.0, 40.1, 55.6, 61.0, 70.7, 72.3, 75.2, 133.1, 135.3, 158.7, 159.2, 165.7.  $^1H$  NMR (400 MHz,  $CD_3OD$ )  $\delta$  0.91 (t,  $J=7.2$ Hz, 72H), 1.16 (m, 18H), 1.30-1.40 (m, 57H), 1.49 (m, 48H), 2.51-2.86 (m, 54H), 3.15 (m, 36H), 4.72 (qn,  $J=5.2$ Hz, 12H), 4.83 (m, obscured by water peak, 6H), 5.29 (m, 3H), 6.63 (s, br,  $OC(O)NHCH_2$ ), 8.82 (s, 3H).  $m/z$  (MALDI TOF (Voyager) MS) 3468.6  $[M+H]^+$ , 3490.6  $[M+Na]^+$ , 3506.4  $[M+K]^+$ .  $m/z$  (MALDI TOF (Kratos) MS – inaccurate calibration) 3447  $[M+H]^+$ , 3470  $[M+Na]^+$ , calculated  $M_w = 3469.61$ . GPC;  $M_w = 3590$ ,  $Pd = 1.03$ .

## 5.7 General Procedure for the Synthesis of Second Generation Dendrimers with Amine core units

### 5.7.1. Polyurethane Homodendrimers (*i.e.* **XG2D**).

**Synthesis of HG2D:** CDI (0.52 g, 3.21 mmol) was added to a stirred solution of **HG2OH** (3.2 g, 2.90 mmol) in toluene (100 mL). The mixture was heated at 60°C for 4 hrs. Subsequently, the reaction mixture was analysed by  $^1H$  NMR spectroscopy and interpretation of the spectrum indicated there was no evidence of the starting materials (*i.e.* **HG2OH** or CDI). Tris(2-aminoethyl)amine **TAEA** (0.14 g, 0.96 mmol) was added and the solution was heated for 20 hrs at 60°C. The reaction mixture was concentrated *in vacuo* and redissolved in  $CH_2Cl_2$  (150 mL). The organic phase was subsequently washed with water (3 x 150 mL), dried over  $MgSO_4$  and the solvent removed using the rotary evaporator. The crude product was purified by column chromatography (silica gel, eluting with EtOAc increasing to EtOAc:MeOH 100:5) and the colourless oil obtained was purified further by preparative GPC (Biobeads, eluting with toluene) to give *compound* **HG2D** as a sticky colourless oil (0.86 g, 24%).  $T_g = 17.2^\circ C$ . Found C, 58.38; H, 9.55; N, 12.15%.  $C_{174}H_{339}O_{42}N_{31}$  requires, C, 59.07; H, 9.66; N, 12.27%.  $^{13}C$  NMR (62.9 MHz,  $CD_3OD$ )  $\delta$  14.5, 19.1, 19.6, 37.9, 40.0, 55.2, 55.6, 60.9, 70.7, 75.1, 158.6, 159.1.  $^1H$  NMR (400 MHz,  $CD_3OD$ )  $\delta$  0.92 (t,  $J=7.2$ Hz, 72H), 1.20 (d,  $J=6$ Hz, 27H), 1.36 (m, 48H), 1.50 (m, 48H), 2.50-2.62 (m, 60H), 3.16 (m, 42H), 4.73 (m, 12H), 4.86 (m, 9H), 6.65 (s, br,  $OC(O)NHCH_2$ ), 6.76 (s, br,  $OC(O)NHCH_2$ ).  $m/z$  (ES MS) 3558.5  $[M+Na]^+$ , 1791.5  $[M+2Na]^{2+}$ .  $m/z$  (MALDI TOF (Kratos) MS) 3558  $[M+Na]^+$ , calculated  $M_w = 3537.74$ . GPC;  $M_w = 3680$ ,  $Pd = 1.00$ .

**Synthesis of CG2D:** The procedure was similar to that described for the synthesis of **HG2D** but **CG2OH** was used as the starting material. The purification step was achieved by column chromatography (silica gel, eluting with EtOAc increasing to EtOAc:MeOH 100:5) and the

oil obtained was purified further by preparative GPC (Biobeads, eluting with toluene) to give compound **CG2D** as a colourless amorphous solid (41%).  $T_g = 43.9^\circ\text{C}$ . Found C, 57.43; H, 8.70; N, 12.75%.  $\text{C}_{162}\text{H}_{291}\text{O}_{42}\text{N}_{31}$  requires, C, 58.16; H, 8.77; N, 12.98%.  $^{13}\text{C}$  NMR (62.9 MHz,  $\text{CD}_3\text{OD}$ )  $\delta$  19.0, 24.8, 26.5, 33.1, 39.9, 55.5, 60.9, 70.7, 73.9, 158.57, 158.62, 158.7.  $^1\text{H}$  NMR (250 MHz,  $\text{CD}_3\text{OD}$ )  $\delta$  1.19 (d,  $J=5.5\text{Hz}$ , 27H), 1.39 (m, 60H), 1.55 (m, 12H), 1.75 (m, 24H), 1.85 (m, 24H), 2.48-2.61 (m, 60H), 3.16 (m, 42H), 4.57 (m, 12H), 4.84 (m, obscured by water peak, 9H), 6.58 (s, br,  $\text{OC}(\text{O})\text{NHCH}_2$ ), 6.70 (s, br,  $\text{OC}(\text{O})\text{NHCH}_2$ ).  $m/z$  (MALDI TOF (Voyager) MS) 3370.2  $[\text{M}+\text{Na}]^+$ , 3386.1  $[\text{M}+\text{K}]^+$ , calculated  $M_w = 3345.23$ . GPC;  $M_w = 2780$ ,  $\text{Pd} = 1.05$ .

**Synthesis of BG2D:** The procedure was the same as that described for the synthesis and purification of **HG2D** but **BG2OH** was used as the starting material to give compound **BG2D** as colourless oil (32%).  $T_g = 46.7^\circ\text{C}$ . Found C, 55.11; H, 8.79; N, 13.46%.  $\text{C}_{138}\text{H}_{267}\text{O}_{42}\text{N}_{31}$  requires, C, 54.65; H, 8.87; N, 14.32%.  $^{13}\text{C}$  NMR (62.9 MHz,  $\text{CD}_3\text{OD}$ )  $\delta$  19.0, 28.9, 39.5, 40.0, 55.2, 55.7, 60.9, 70.6, 80.0, 158.4, 158.7.  $^1\text{H}$  NMR (250 MHz,  $\text{CD}_3\text{OD}$ )  $\delta$  1.21 (d,  $J=6\text{Hz}$ , 27H), 1.45 (s, 108H), 2.50-2.75 (m, 60H), 3.05-3.25 (m, 42H), 4.85 (m, obscured by water peak, 9H), 6.46 (s, br,  $\text{OC}(\text{O})\text{NHCH}_2$ ), 6.76 (s, br,  $\text{OC}(\text{O})\text{NHCH}_2$ ).  $m/z$  (ES MS) 3055.1  $[\text{M}+\text{Na}]^+$ , 1539.0  $[\text{M}/2+\text{Na}]^+$ .  $m/z$  (MALDI TOF (Kratos) MS) 3039  $[\text{M}+\text{H}]^+$ , calculated  $M_w = 3032.78$ . GPC;  $M_w = 3120$ ,  $\text{Pd} = 1.00$ .

### 5.7.2 Layer Codendrimers and Polycarbonate Homodendrimer

**Synthesis of BG2D (UCU):** CDI (0.15 g, 0.93 mmol) was added to a stirred solution of **BG2OH (CU)** (0.81 g, 0.87 mmol) in toluene (50 mL). The mixture was heated at  $60^\circ\text{C}$  for 4 hrs. Subsequently, the reaction mixture was analysed by  $^1\text{H}$  NMR spectroscopy and interpretation of the spectrum indicated there was no evidence of the starting materials (*i.e.* **BG2OH (CU)** or CDI). Tris(2-aminoethyl)amine **TAEA** (42 mg, 0.29 mmol) was added and the solution was heated for 20 hrs at  $60^\circ\text{C}$ . The reaction mixture was concentrated *in vacuo* and redissolved in  $\text{CH}_2\text{Cl}_2$  (100 mL). The organic phase was subsequently washed with water (3 x 100 mL), dried over  $\text{MgSO}_4$  and the solvent removed using the rotary evaporator. The crude product was purified by column chromatography (silica gel, eluting with EtOAc increasing to EtOAc: $\text{CH}_3\text{OH}$  100:5) and the colourless oil obtained was purified further by preparative GPC (Biobeads, eluting with toluene) to give compound **BG2D (UCU)** as a colourless amorphous solid (0.23 g, 26%).  $T_g = 24.4^\circ\text{C}$ . Found C, 53.61; H, 8.76; N, 11.38%.  $\text{C}_{138}\text{H}_{261}\text{O}_{48}\text{N}_{25}$  requires, C, 54.55; H, 8.66; N, 11.52%.  $^{13}\text{C}$  NMR (125 MHz,  $\text{CD}_3\text{OD}$  at  $50^\circ\text{C}$ )  $\delta$  18.6, 19.0, 29.0, 39.8, 40.3, 54.9, 55.4, 55.7, 60.8, 61.2, 67.4, 71.2, 74.9,



80.1, 156.4, 158.3, 158.5.  $^1\text{H}$  NMR (400 MHz,  $\text{CD}_3\text{OD}$ )  $\delta$  1.21 (m, 27H), 1.45 (s, 108H), 2.60 (m, 48H), 2.89 (m, 12H), 3.10 (m, 30H), 4.19 (m, 12H), 4.80 (m, obscured by water peak, 9H), 6.38 (s, br,  $\text{OC}(\text{O})\text{NHCH}_2$ ), 6.68 s, br,  $\text{OC}(\text{O})\text{NHCH}_2$ ).  $m/z$  (ES MS) 3058.8  $[\text{M}+\text{Na}]^+$ , 1541.9  $[\text{M}+2\text{Na}]^{2+}$ , calculated  $M_w = 3038.69$ . GPC;  $M_w = 3300$ ,  $\text{Pd} = 1.01$ .

**Synthesis of BG2D (CCU):** CDI (0.38 g, 2.35 mmol) was added to a stirred solution of **BG2OH (CU)** (1.87 g, 1.99 mmol) in toluene (70 mL). The mixture was heated at  $60^\circ\text{C}$  for 4 hrs. Subsequently, the reaction mixture was analysed by  $^1\text{H}$  NMR spectroscopy and interpretation of the spectrum indicated there was no evidence of the starting materials (*i.e.* **BG2OH (CU)** or CDI). Triethanolamine (**TEA**) (0.1 g, 0.66 mmol) and KOH (50 mg) were added and the solution was heated for 2 days at  $75^\circ\text{C}$ . The reaction mixture was concentrated *in vacuo* and redissolved in  $\text{CH}_2\text{Cl}_2$  (100 mL). The organic phase was subsequently washed with water (3 x 100 mL), dried over  $\text{MgSO}_4$  and the solvent removed using the rotary evaporator. The resulting pale yellow oil was purified by column chromatography (silica gel, eluting with  $\text{EtOAc}:\text{C}_6\text{H}_{12}$  1:2 increasing to EtOAc). The colourless oil obtained was purified further by preparative GPC (Biobeads, eluting with toluene) to give *compound BG2D (CCU)* as a sticky colourless oil (0.63 g, 31%).  $T_g = 16.8^\circ\text{C}$ . Found C, 54.37; H, 8.54; N, 9.85%.  $\text{C}_{138}\text{H}_{258}\text{O}_{51}\text{N}_{22}$  requires, C, 54.49; H, 8.55; N, 10.13%.  $^{13}\text{C}$  NMR (100 MHz,  $\text{CD}_3\text{OD}$ )  $\delta$  18.5, 18.6, 28.9, 39.6, 54.5, 54.8, 55.6, 60.6, 60.9, 67.1, 67.2, 74.6, 74.8, 80.0, 156.2, 156.4, 158.4.  $^1\text{H}$  NMR (400 MHz,  $\text{CD}_3\text{OD}$ )  $\delta$  1.25-1.27 (m, 27H), 1.45 (s, 108H), 2.51-2.80 (m, 42H), 2.90 (m, 18H), 3.04-3.15 (m, 24H), 4.11-4.27 (m, 18H), 4.81 (m, 9H), 6.35 (s, br,  $\text{OC}(\text{O})\text{NHCH}_2$ ).  $m/z$  (ES MS) 3062.8  $[\text{M}+\text{Na}]^+$ , 1543.5  $[\text{M}+2\text{Na}]^{2+}$ , calculated  $M_w = 3041.64$ . GPC;  $M_w = 3420$ ,  $\text{Pd} = 1.02$ .

**Synthesis of BG2D (CUU):** The procedure was similar to that described for the synthesis of **BG2D (CCU)**, but **BG2OH** was used as the starting material. The purification step was achieved by column chromatography (silica gel, eluting with EtOAc increasing to  $\text{EtOAc}:\text{CH}_3\text{OH}$  100:5) and the oil obtained was purified further by preparative GPC (Biobeads, eluting with toluene) to give *compound BG2D (CUU)* as colourless amorphous solid (42%).  $T_g = 38.3^\circ\text{C}$ . Found C, 53.56; H, 8.74; N, 12.63%.  $\text{C}_{138}\text{H}_{264}\text{O}_{45}\text{N}_{28}$  requires, C, 54.60; H, 8.77; N, 12.92%.  $^{13}\text{C}$  NMR (100 MHz,  $\text{CD}_3\text{OD}$ )  $\delta$  18.7, 19.1, 29.0, 39.7, 40.0, 54.5, 55.6, 61.0, 67.1, 70.8, 74.6, 80.0, 156.4, 158.5, 158.7.  $^1\text{H}$  NMR (500 MHz,  $\text{CD}_3\text{OD}$ )  $\delta$  1.22 (m, 27H), 1.45 (s, 108H), 2.59 (m, 54H), 2.91 (m, 6H), 3.10 (m, 36H), 4.19 (m, 6H), 4.59 (m, 3H), 4.81 (m, obscured by water peak, 6H).  $m/z$  (ES MS) 3056.9  $[\text{M}+\text{Na}]^+$ , calculated  $M_w = 3035.73$ . GPC;  $M_w = 3600$ ,  $\text{Pd} = 1.03$ .

**Synthesis of BG2D (UUC):** The procedure was similar to that described for the synthesis of **BG2D (UCU)**, but **BG2OH (UC)** was used as the starting material. The purification step was achieved by column chromatography (silica gel, eluting with EtOAc increasing to EtOAc:MeOH 100:5) and the oil obtained was purified further by preparative GPC (Biobeads, eluting with toluene) to give *compound BG2D (UUC)* as a colourless oil (39%).  $T_g = 9.4^\circ\text{C}$ . Found C, 53.81; H, 8.54; N, 8.68%.  $\text{C}_{138}\text{H}_{255}\text{O}_{54}\text{N}_{19}$  requires, C, 54.44; H, 8.44; N, 8.74%.  $^{13}\text{C}$  NMR (100 MHz,  $\text{CD}_3\text{OD}$ )  $\delta$  19.0, 19.1, 28.2, 40.0, 54.9, 55.3, 55.6, 61.1, 66.3, 70.8, 70.9, 82.6, 155.0, 158.5, 158.7.  $^1\text{H}$  NMR (250 MHz,  $\text{CDCl}_3$ )  $\delta$  1.19 (m, 27H), 1.47 (s, 108H), 2.5-2.74 (m, 36H), 2.84 (m, 24H), 3.18 (m, 18H), 4.08 (m, 27H), 5.48 (s, br,  $\text{OC(O)NHCH}_2$ ).  $^1\text{H}$  NMR (200 MHz,  $\text{CD}_3\text{OD}$ )  $\delta$  1.21 (d, 27H), 1.47 (s, 108H), 2.55-2.70 (m, 36H), 2.84 (m, 24H), 3.18 (m, 18H), 4.10 (m, 24H), 4.81 (m, obscured by water peak, 9H).  $m/z$  (ES MS) 3065.8  $[\text{M}+\text{Na}]^+$ , calculated  $M_w = 3044.60$ . GPC;  $M_w = 3470$ ,  $\text{Pd} = 1.01$ .

**Synthesis of BG2D (CUC):** The procedure was similar to that described for the synthesis of **BG2D (CCU)**, but **BG2OH (UC)** was used as the starting material. The purification step was achieved by column chromatography (silica gel, eluting with EtOAc: $\text{C}_6\text{H}_{12}$  1:1 increasing to EtOAc) and the oil obtained was purified further by preparative GPC (Biobeads, eluting with toluene) to give *compound BG2D (CUC)* as colourless oil (25%).  $T_g = 1.9^\circ\text{C}$ . Found C, 53.95; H, 8.29; N, 7.15%.  $\text{C}_{138}\text{H}_{252}\text{O}_{57}\text{N}_{16}$  requires, C, 54.39; H, 8.33; N, 7.35%.  $^{13}\text{C}$  NMR (125 MHz,  $\text{CD}_3\text{OD}$ )  $\delta$  18.7, 19.0, 28.2, 40.0, 54.5, 54.9, 55.7, 60.7, 61.1, 66.4, 67.1, 67.1, 71.0, 74.6, 82.7, 155.1, 156.4, 158.5.  $^1\text{H}$  NMR (500 MHz,  $\text{CD}_3\text{OD}$ )  $\delta$  1.21 (d,  $J=6.5\text{Hz}$ , 18H), 1.26 (d,  $J=6.5\text{Hz}$ , 9H), 1.47 (s, 108H), 2.58-2.74 (m, 30H), 2.80-2.92 (m, 30H), 3.16 (m, 12H), 4.10 (m, 24H), 4.20 (m, 6H), 4.82 (m, obscured by water peak, 9H), 6.51 (s, br,  $\text{OC(O)NHCH}_2$ ).  $m/z$  (ES MS) 3069.7  $[\text{M}+\text{Na}]^+$ , Calculated  $M_w = 3047.55$ . GPC;  $M_w = 3560$ ,  $\text{Pd} = 1.02$ .

**Synthesis of BG2D (UCC):** The procedure was similar to that described for the synthesis of **BG2D (UCU)**, but **BG2OH (CC)** was used as the starting material. The purification step was achieved by column chromatography (silica gel, eluting with EtOAc: $\text{C}_6\text{H}_{12}$  1:2 increasing to EtOAc) and the oil obtained was purified further by preparative GPC (Biobeads, eluting with toluene) to give *compound BG2D (UCC)* as a colourless oil (40%).  $T_g = -8.5^\circ\text{C}$ . Found C, 54.26; H, 8.42; N, 6.08%.  $\text{C}_{138}\text{H}_{249}\text{O}_{60}\text{N}_{13}$  requires, C, 54.33; H, 8.23; N, 5.97%.  $^{13}\text{C}$  NMR (125 MHz,  $\text{CD}_3\text{OD}$ )  $\delta$  18.5, 19.0, 28.2, 40.1, 54.8, 54.9, 55.3, 61.0, 61.1, 66.3, 67.2, 70.1, 74.8, 82.7, 155.0, 156.2, 158.5.  $^1\text{H}$  NMR (500 MHz,  $\text{CD}_3\text{OD}$ )  $\delta$  1.21 (d,  $J=6.4\text{Hz}$ , 9H), 1.26

(d,  $J=6.5\text{Hz}$ , 18H), 1.47 (s, 108H), 2.62 (m, br, 6H), 2.66 (dd,  $J=14\text{Hz}$ ,  $J=5.5\text{Hz}$ , 9H), 2.75 (dd,  $J=14\text{Hz}$ ,  $J=6.5\text{Hz}$ , 9H), 2.85 (m, 24H), 2.90 (m, 12H), 3.18 (m, br, 6H), 4.05-4.15 (m, 24H), 4.15-4.23 (m, 12H), 4.80 (m, 9H), 6.57 (s, br,  $\text{OC(O)NHCH}_2$ ).  $m/z$  (ES MS) 3071.4  $[\text{M}+\text{Na}]^+$ , calculated  $M_w = 3050.51$ . GPC;  $M_w = 2800$ ,  $\text{Pd} = 1.00$ .

**Synthesis of BG2D (CCC):** The procedure was similar to that described for the synthesis of **BG2D (CCU)**, but **BG2OH (CC)** was used as the starting material. The purification step was achieved by column chromatography (silica gel, eluting with  $\text{EtOAc}:\text{C}_6\text{H}_{12}$  1:3 increasing to  $\text{EtOAc}:\text{C}_6\text{H}_{12}$  1:1) and the oil obtained was purified further by preparative GPC (Biobeads, eluting with toluene) to give *compound BG2D (CCC)* as colourless oil (22%).  $T_g = -14.0^\circ\text{C}$ . Found C, 54.51; H, 8.22; N, 4.49%.  $\text{C}_{138}\text{H}_{246}\text{O}_{63}\text{N}_{10}$  requires C, 54.28; H, 8.12; N, 4.59%.  $^{13}\text{C}$  NMR (62.9 MHz,  $\text{CDCl}_3$ )  $\delta$  17.9, 27.7, 53.1, 53.5, 59.6, 64.8, 73.3, 81.8, 153.4, 154.6.  $^1\text{H}$  NMR (200 MHz,  $\text{CDCl}_3$ )  $\delta$  1.24 (d,  $J=6.2\text{Hz}$ , 27H), 1.46 (s, 108H), 2.59 (dd,  $J=13.6\text{Hz}$ ,  $J=6\text{Hz}$ , 9H), 2.75 (dd,  $J=13.6\text{Hz}$ , 6Hz, 9H), 2.84 (t,  $J=6\text{Hz}$ , 42H), 4.00-4.13 (m, 42H), 4.75 (m, 9H).  $m/z$  (ES MS) 3074.5  $[\text{M}+\text{Na}]^+$ .  $m/z$  (MALDI TOF (Kratos) MS) 3039  $[\text{M}+\text{H}]^+$ , calculated  $M_w = 3053.46$ . GPC;  $M_w = 4470$ ,  $\text{Pd} = 1.04$ .

**Synthesis of BG2D (ECU):** The procedure was similar to that described for the synthesis of **BG1DAC**, but using **BG2OH (CU)** as the starting material and a reaction temperature of  $50^\circ\text{C}$  for 16 hrs. The crude mixture obtained was purified by column chromatography (silica gel,  $\text{EtOAc}$  increasing to  $\text{EtOAc}:\text{MeOH}$ , 20:1) to give *compound BG2D (ECU)* as a sticky colourless oil (63%).  $T_g = 10.6^\circ\text{C}$ . Found C, 56.95; H, 8.67; N, 9.12%.  $\text{C}_{138}\text{H}_{249}\text{O}_{48}\text{N}_{21}$  requires, C, 55.80; H, 8.45; N, 9.90%.  $^{13}\text{C}$  NMR (125 MHz,  $\text{CD}_3\text{OD}$  at  $50^\circ\text{C}$ )  $\delta$  18.5, 28.9, 39.8, 54.9, 55.7, 60.7, 61.0, 67.2, 72.6, 74.7, 80.0, 133.1, 135.2, 156.3, 158.2, 165.7.  $^1\text{H}$  NMR (400 MHz,  $\text{CD}_3\text{OD}$ )  $\delta$  1.22 (m, 18H), 1.39 (d,  $J=6\text{Hz}$ , 9H), 1.43 (s, 108H), 2.50 (dd,  $J=13.6\text{Hz}$ ,  $J=5.2\text{Hz}$ , 12H), 2.58 (t,  $J=6\text{Hz}$ , 24H), 2.81-2.94 (m, 18H), 3.08 (m, 24H), 4.23 (m, 12H), 4.75 (m, 6H), 5.23 (m, 3H), 6.32 (s, br,  $\text{OC(O)NHCH}_2$ ), 8.80 (s, 3H).  $m/z$  (ES MS) 2991.8  $[\text{M}+\text{Na}]^+$ , calculated  $M_w = 2970.57$ . GPC;  $M_w = 3100$ ,  $\text{Pd} = 1.02$ .

## 5.8 General Procedure for the Synthesis of Third Generation Dendrimers with Amine core unit (*i.e.* XG3D)

**Synthesis of HG3D:** CDI (92 mg, 0.57 mmol) was added to a stirred solution of **HG3OH** (1.15 g, 0.47 mmol) in toluene (40 mL) and the mixture was heated at  $60^\circ\text{C}$  for 4 hours. Subsequently, the reaction mixture was analysed by  $^1\text{H}$  NMR spectroscopy and interpretation of the spectrum indicated no evidence of the presence of starting materials (*i.e.* **HG3OH** or

CDI). **AEAP** (23 mg, 0.16 mmol) was added to the solution and the mixture was heated for 1 day at 60°C. The reaction mixture was concentrated *in vacuo* and redissolved in CH<sub>2</sub>Cl<sub>2</sub> (100 mL). The organic phase was subsequently washed with water (3 x 100 mL), dried over MgSO<sub>4</sub> and the solvent removed using the rotary evaporator. The yellow oil obtained was purified by column chromatography (silica gel, eluting with EtOAc:MeOH 100:5 increasing to EtOAc:MeOH 100:10). The colourless oil obtained was purified further by preparative GPC (Biobeads, eluting with toluene) to give **compound HG3D** as an extremely sticky oil (280 mg, 24%). *T<sub>g</sub>* = 19.4°C. Found C, 57.37; H, 9.50; N, 11.88%. C<sub>366</sub>H<sub>711</sub>O<sub>90</sub>N<sub>67</sub> requires, C, 58.68; H, 9.57; N, 12.53%. <sup>13</sup>C NMR (100 MHz, CD<sub>3</sub>OD) δ 14.6, 19.1, 19.7, 40.0, 40.1, 55.7, 61.0, 70.7, 75.2, 158.7, 158.8, 159.3. <sup>1</sup>H NMR (400 MHz, CD<sub>3</sub>OD) δ 0.92 (t, J=7.2Hz, 144H), 1.20 (d, J=6Hz, 63H), 1.36 (m, 96H), 1.50 (m, 96H), 2.51-2.66 (m, 132H), 3.12-3.20 (m, 90H), 4.74 (m, 24H), 4.85 (m, obscured by water peak, 9H), 6.46 (s, br, OC(O)NHCH<sub>2</sub>), 6.76 (s, br, OC(O)NHCH<sub>2</sub>). *m/z* (ES MS) 7511.4 [M+Na]<sup>+</sup>, 7527.5 [M+K]<sup>+</sup>, calculated *M<sub>w</sub>* = 7490.96 and an impurity at 5063.6 corresponding to the two-armed dendrimer. GPC; *M<sub>w</sub>* = 6410, *Pd* = 1.01.

**Synthesis of BG3D:** The procedure was similar to that described for the synthesis of **HG3D**, but **BG3OH** was used as the starting material. After the same purification method **compound BG3D** was isolated as a white amorphous solid (20%). *T<sub>g</sub>* = 48.9°C. Found C, 54.46; H, 8.74; N, 13.41%. C<sub>294</sub>H<sub>567</sub>O<sub>90</sub>N<sub>67</sub> requires, C, 54.48; H, 8.82; N, 14.48%. <sup>13</sup>C NMR (125 MHz, CD<sub>3</sub>OD) δ 19.1, 29.0, 39.9, 40.2, 55.6, 55.7, 61.1, 70.9, 80.0, 158.3, 158.6. <sup>1</sup>H NMR (400 MHz, CD<sub>3</sub>OD) δ 1.20 (d, J=6.4Hz, 63H), 1.44 (s, 216H), 2.48-2.63 (m, 132H), 3.05-3.25 (m, 90H), 4.85 (m, obscured by water peak, 21H), 6.42 (s, br, OC(O)NHCH<sub>2</sub>), 6.71 (s, br, OC(O)NHCH<sub>2</sub>). *m/z* (ES MS) 3235.8 [M+2H]<sup>2+</sup>, 3246.9 [M+H+Na]<sup>2+</sup>, 3257.9 [M+2Na]<sup>2+</sup>. *m/z* (MALDI TOF (Kratos) MS) 6469 [M+H]<sup>+</sup>, calculated *M<sub>w</sub>* = 6481.05. GPC; *M<sub>w</sub>* = 4980, *Pd* = 1.06.

## 5.9 General Procedure for the Synthesis of Third Generation Dendrimers with Aromatic-ester core unit (*i.e.* XG3DAC)

**Synthesis of CG3DAC:** A solution of **CG3OH** (0.64 g, 0.28 mmol) and DMAP (90 mg, 0.74 mmol) in benzene (50 mL) was refluxed for 4 hrs with a Dean-Stark trap filled with molecular sieves attached. The mixture was cooled to room temperature and 1,3,5-benzenetricarbonyl trichloride (22 mg, 8.29 x 10<sup>-2</sup> mmol) was added. The reaction mixture was stirred and heated at reflux temperature (81°C) for 22 hrs and then concentrated *in vacuo*. The crude product was purified by column chromatography (silica gel, eluting with EtOAc:MeOH, 100:5) and

by preparative GPC (Biobeads, eluting with toluene) to give *compound CG3DAC* as a white amorphous solid (290 mg, 50%).  $T_g = 49.5^\circ\text{C}$ . Found C, 57.00; H, 8.52; N, 12.92%.

$\text{C}_{342}\text{H}_{603}\text{O}_{90}\text{N}_{63}$  requires, C, 58.37; H, 8.64; N, 12.54%.  $^{13}\text{C}$  NMR (100 MHz,  $\text{CD}_3\text{OD}$ )  $\delta$  18.9, 19.1, 24.9, 26.6, 33.2, 40.0, 40.5, 55.5, 55.8, 60.5, 61.0, 70.7, 72.3, 74.0, 133.1, 135.4, 158.6, 158.7, 158.8, 165.7.  $^1\text{H}$  NMR (400 MHz,  $\text{CD}_3\text{OD}$ )  $\delta$  1.19 (d,  $J=6\text{Hz}$ , 54H), 1.24-1.41 (m, 129H), 1.55 (m, 24H), 1.73 (m, 48H), 1.84 (m, 48H), 2.48-2.86 (m, 126H), 3.10-3.26 (m, 84H), 4.56 (m, 24H), 4.86 (m, obscured by water peak, 18H), 5.28 (m, 3H), 6.58 (s, br,  $\text{OC(O)NHCH}_2$ ), 6.71 (s, br,  $\text{OC(O)NHCH}_2$ ), 8.81 (s, 3H).  $m/z$  (MALDI TOF (Voyager) MS) 7064.6  $[\text{M}+\text{Na}]^+$ , 7080.5  $[\text{M}+\text{K}]^+$ , calculated  $M_w = 7037.82$ . GPC;  $M_w = 6410$ ,  $\text{Pd} = 1.01$ .

*Synthesis of BG3DAC*: The procedure was similar to that described for the synthesis of *CG3DAC*, but *BG3OH* was used as the starting material. After the same purification method the *compound BG3DAC* was isolated as a white amorphous solid (48%).  $T_g = 48.8^\circ\text{C}$ . Found C, 55.17; H, 8.67; N, 12.52%.  $\text{C}_{294}\text{H}_{555}\text{O}_{90}\text{N}_{63}$  requires, C, 55.06; H, 8.72; N, 13.76%.  $^{13}\text{C}$  NMR (100 MHz,  $\text{CD}_3\text{OD}$ )  $\delta$  18.9, 19.1, 29.0, 30.9, 40.0, 40.1, 55.7, 61.0, 70.7, 72.3, 80.0, 133.1, 135.4, 158.4, 158.7, 158.8, 165.7.  $^1\text{H}$  NMR (400 MHz,  $\text{CD}_3\text{OD}$ )  $\delta$  1.20 (d, 54H), 1.44 (m, 225H), 2.49-2.86 (m, 126H), 3.08-3.21 (m, 84H), 4.85 (m, obscured by water peak, 18H), 5.28 (m, 3H), 6.43 (s, br,  $\text{OC(O)NHCH}_2$ ), 6.73 (s, br,  $\text{OC(O)NHCH}_2$ ), 8.80 (s, 3H). GPC;  $M_w = 5650$ , calculated  $M_w = 6412.92$ ,  $\text{Pd} = 1.03$ .

## 5.10 Reference

- (1) Staab, H. A. *Angew. Chem. Int. Ed. Engl.* **1962**, *1*, 351.

## Appendix

### Contents

<sup>13</sup> C NMR Spectrum of <b>BG1OH</b>	I
<sup>1</sup> H NMR Spectrum of <b>BG1OH</b>	I
<sup>13</sup> C NMR Spectrum of <b>Trisammonium Salt</b>	II
<sup>13</sup> C NMR Spectrum of <b>AEAP</b>	II
<sup>13</sup> C NMR Spectrum of <b>BG2OH</b>	III
<sup>1</sup> H NMR Spectrum of <b>HG2OH</b>	III
GPC trace of <b>CG2OH</b>	IV
<sup>13</sup> C NMR Spectrum of <b>BG3OH</b>	IV
<sup>13</sup> C NMR Spectrum of <b>HG3OH</b>	V
<sup>13</sup> C NMR Spectrum of <b>CG4OH</b>	V
<sup>1</sup> H NMR Spectrum of <b>CG4OH</b>	VI
<sup>13</sup> C NMR Spectrum of <b>BG1D</b>	VI
<sup>13</sup> C NMR Spectrum of <b>BG2D</b>	VII
<sup>13</sup> C NMR Spectrum of <b>HG1D</b>	VII
<sup>13</sup> C NMR Spectrum of <b>HG3D</b>	VIII
<sup>1</sup> H NMR Spectrum of <b>BG1D</b>	VIII
<sup>1</sup> H NMR Spectrum of <b>BG2D</b>	IX
<sup>1</sup> H NMR Spectrum of <b>BG3D</b>	IX
<sup>1</sup> H NMR Spectrum of <b>HG1D</b>	X
<sup>1</sup> H NMR Spectrum of <b>HG2D</b>	X
<sup>1</sup> H NMR Spectrum of <b>HG3D</b>	XI
ES Mass Spectrum of <b>HG1D</b>	XI
MALDI-TOF (Voyager) mass spectrum of <b>HG1D</b>	XII
ES mass spectrum of <b>HG2D</b>	XII
GPC trace of <b>HG3D</b> before purification	XIII
GPC trace of <b>HG3D</b> (pure)	XIII
<sup>13</sup> C NMR Spectrum of <b>CG1DAC</b>	XIV
<sup>13</sup> C NMR Spectrum of <b>CG2DAC</b>	XIV
<sup>13</sup> C NMR Spectrum of <b>CG3DAC</b>	XV
<sup>13</sup> C NMR Spectrum of <b>BG1DAC</b>	XV
<sup>13</sup> C NMR Spectrum of <b>BG2DAC</b>	XVI



<sup>1</sup>H NMR Spectrum of **CG1DAC**

XVI

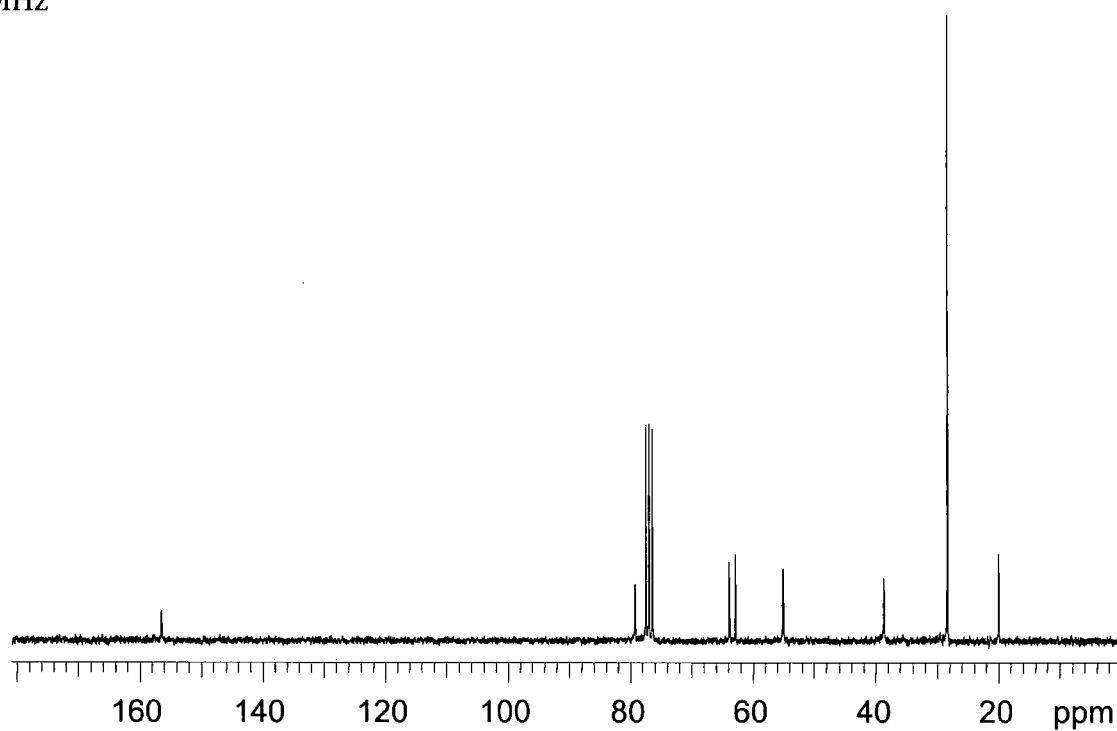
MALDI-TOF (Voyager) mass spectrum of **BG2OH (UC)**

XVII

<sup>13</sup>C NMR Spectrum of **BG1OH**

CD<sub>3</sub>OD

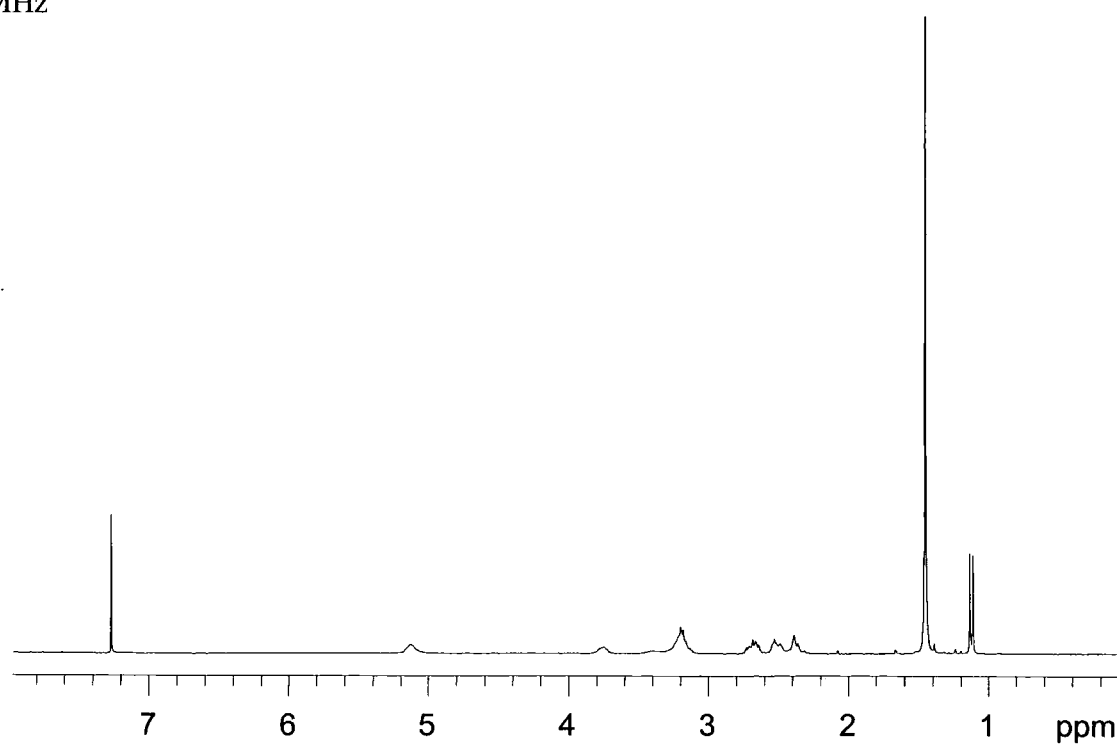
100MHz



<sup>1</sup>H NMR Spectrum of **BG1OH**

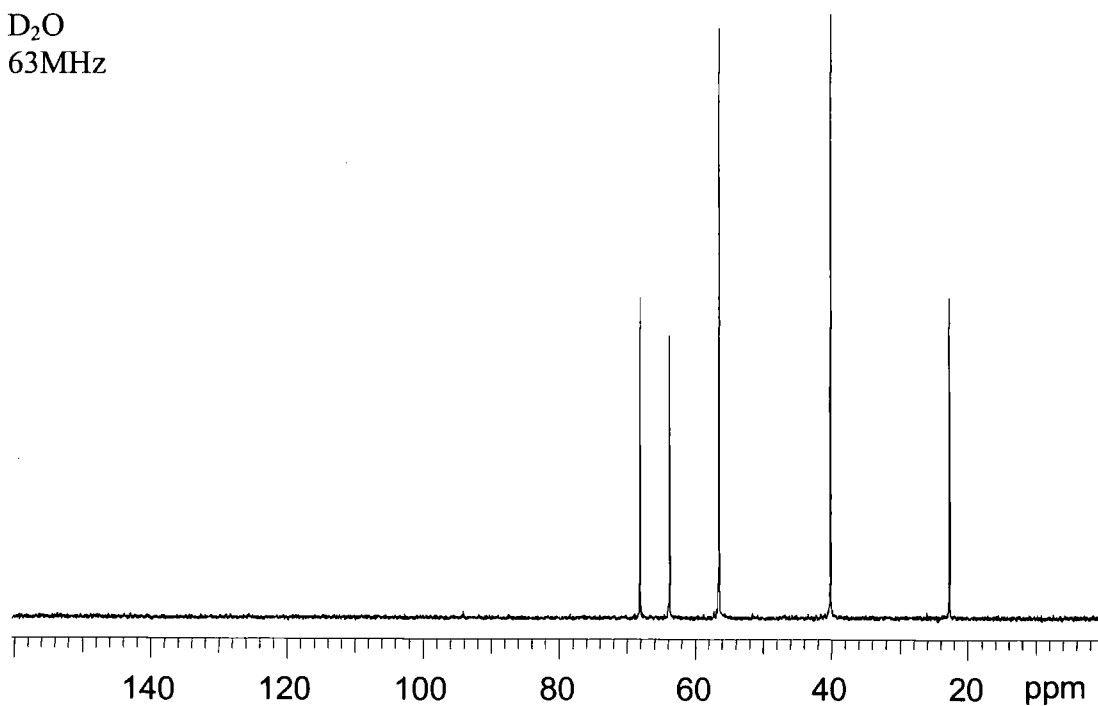
CDCl<sub>3</sub>

300MHz



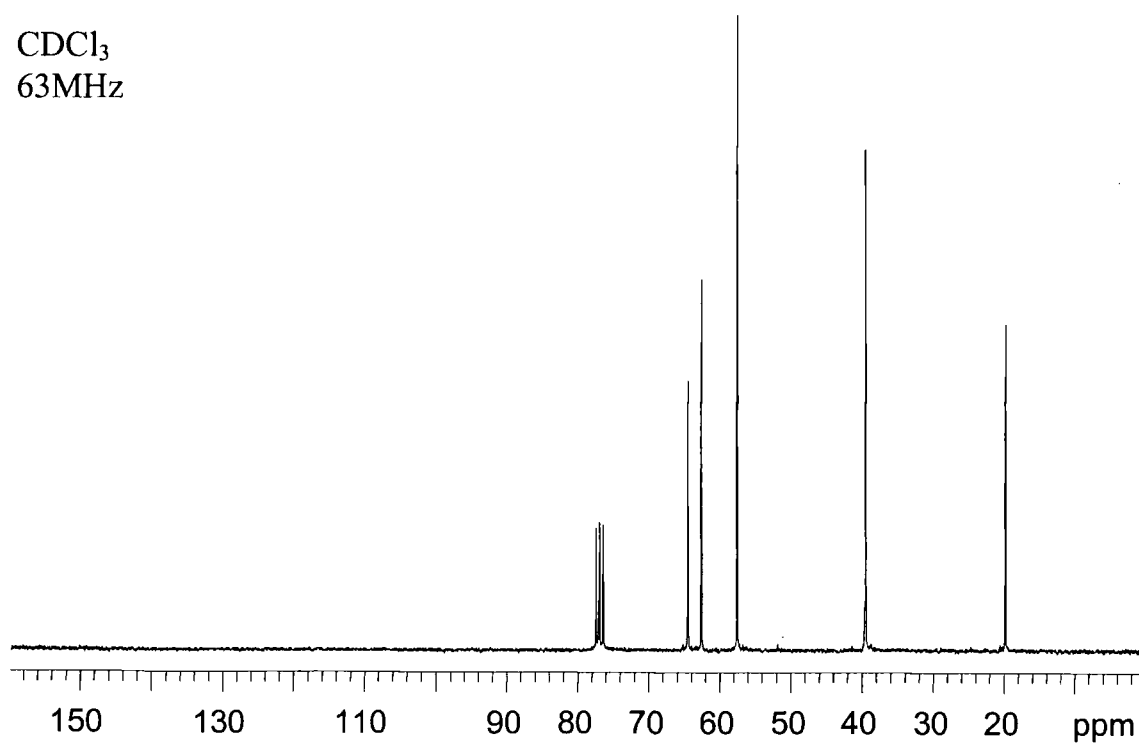
<sup>13</sup>C NMR Spectrum of **Trisammonium Salt**

D<sub>2</sub>O  
63MHz

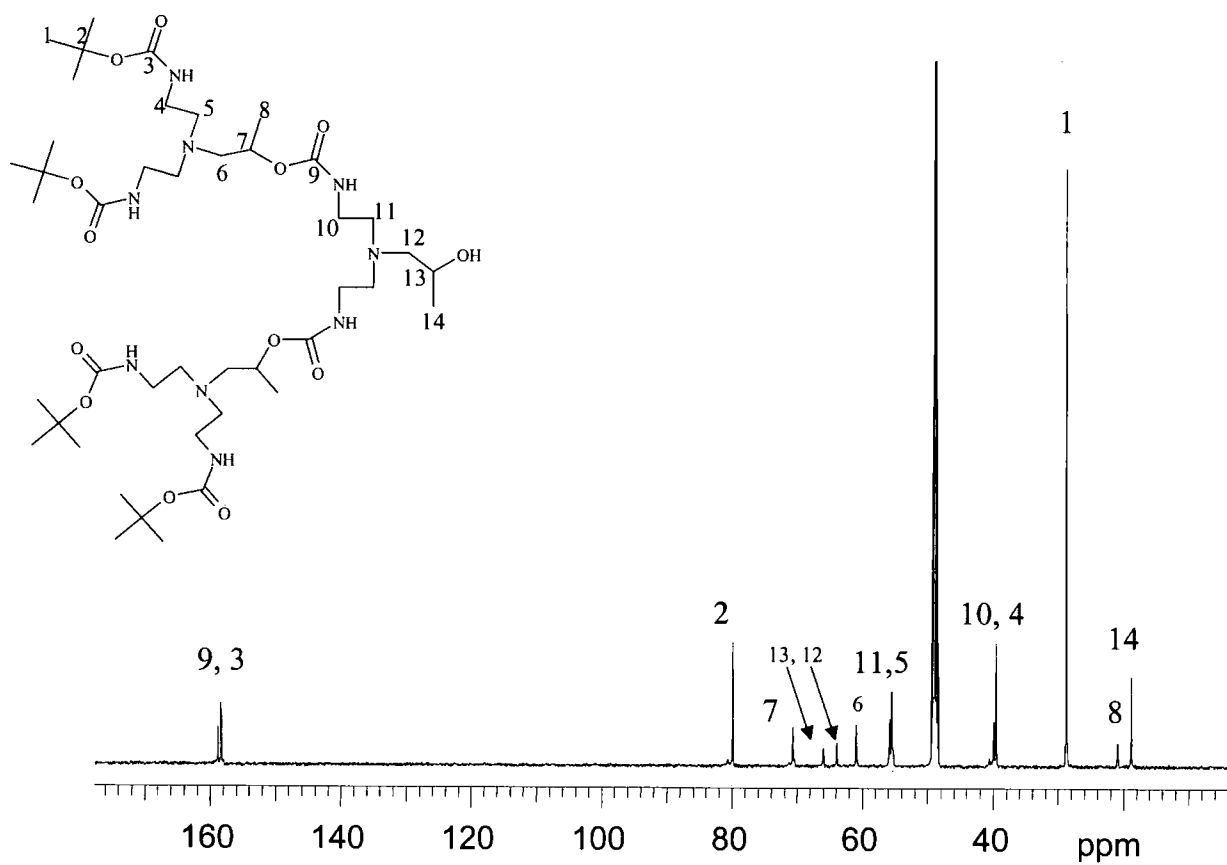


<sup>13</sup>C NMR Spectrum of **AEAP**

CDCl<sub>3</sub>  
63MHz

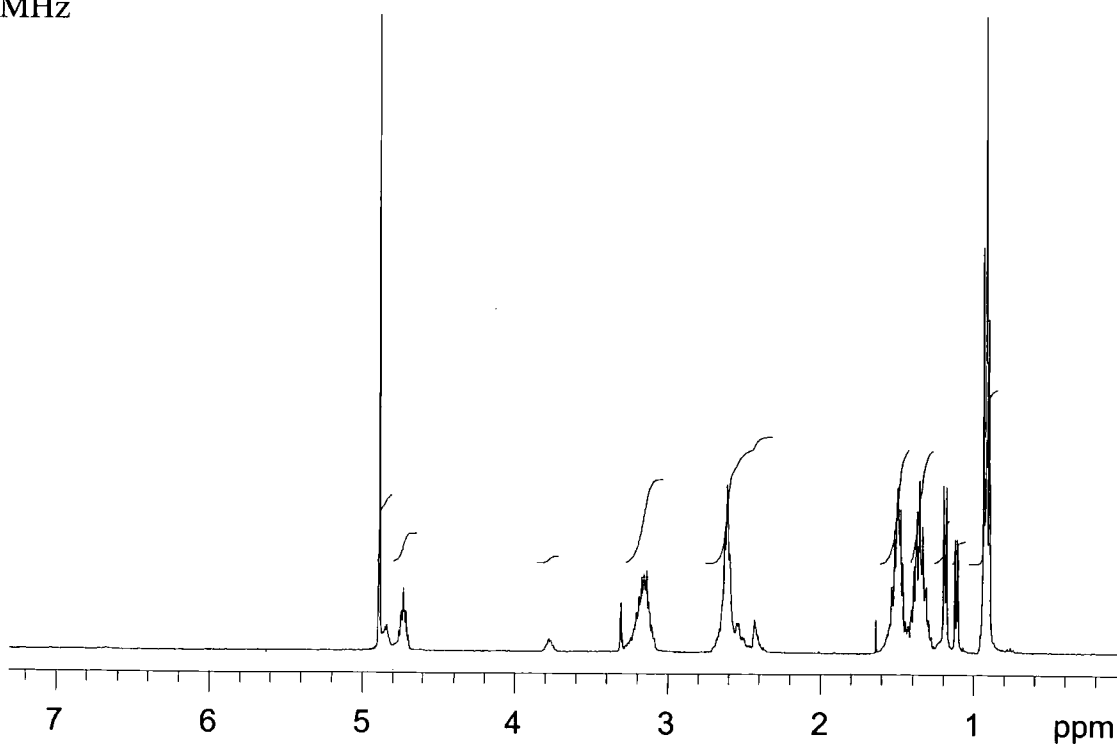


<sup>13</sup>C NMR Spectrum of **BG2OH**

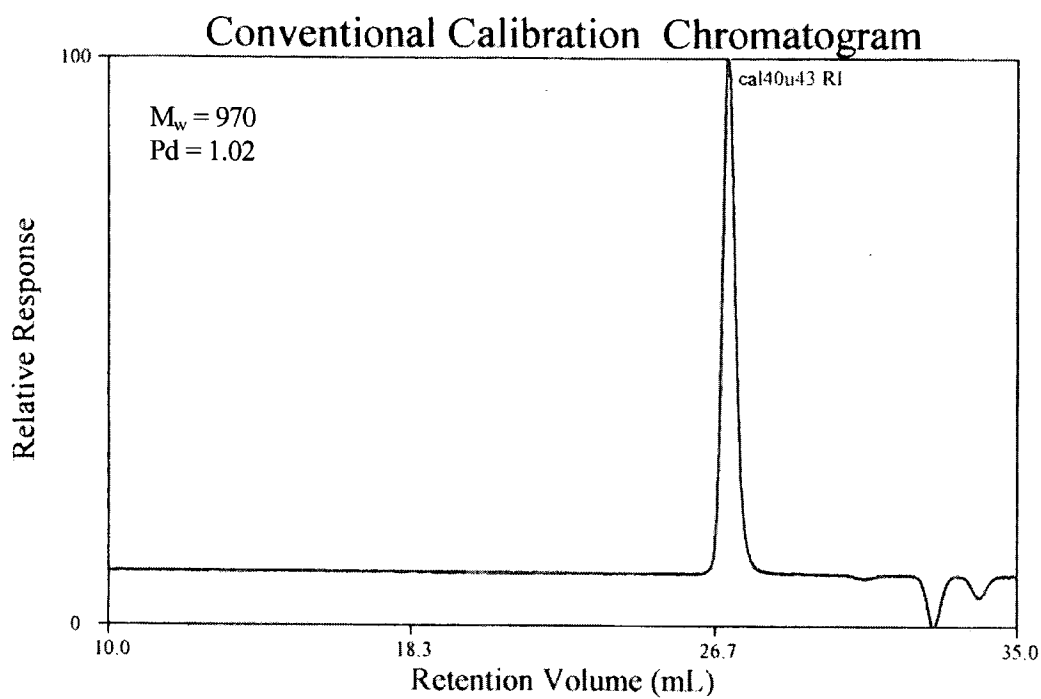


<sup>1</sup>H NMR Spectrum of **HG2OH**

CD<sub>3</sub>OD  
400 MHz

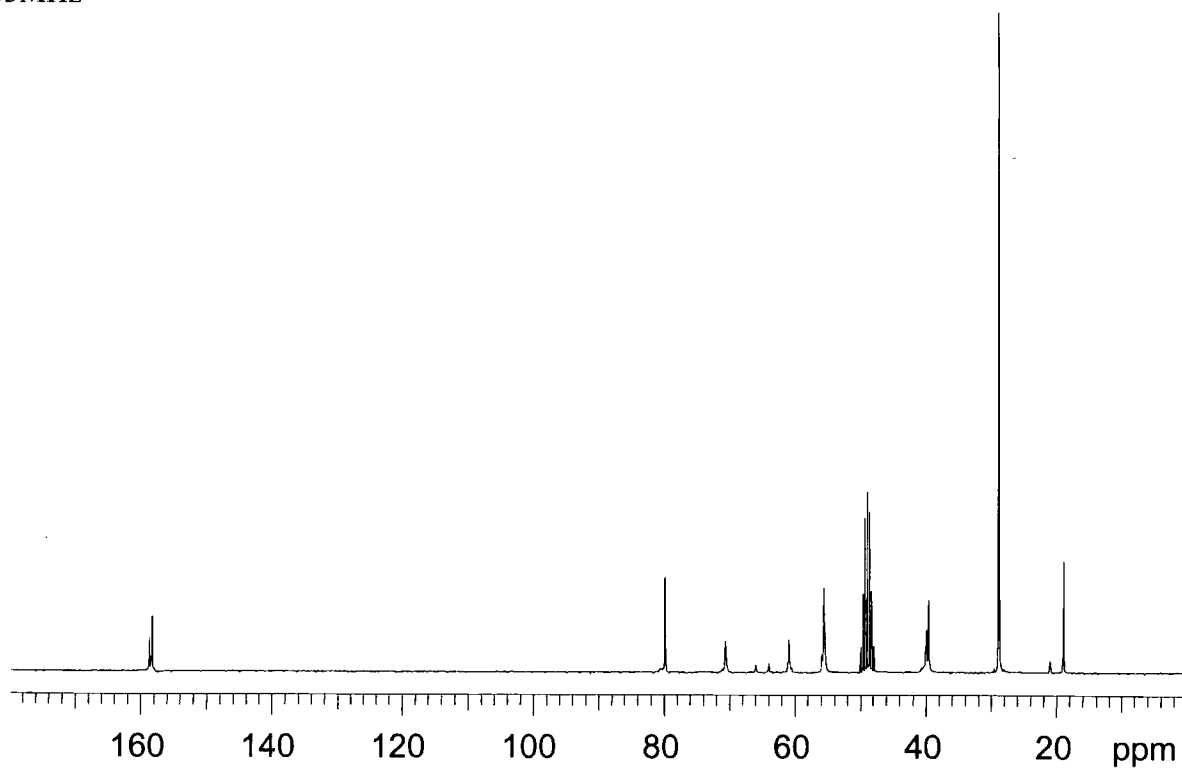


GPC trace of **CG2OH**



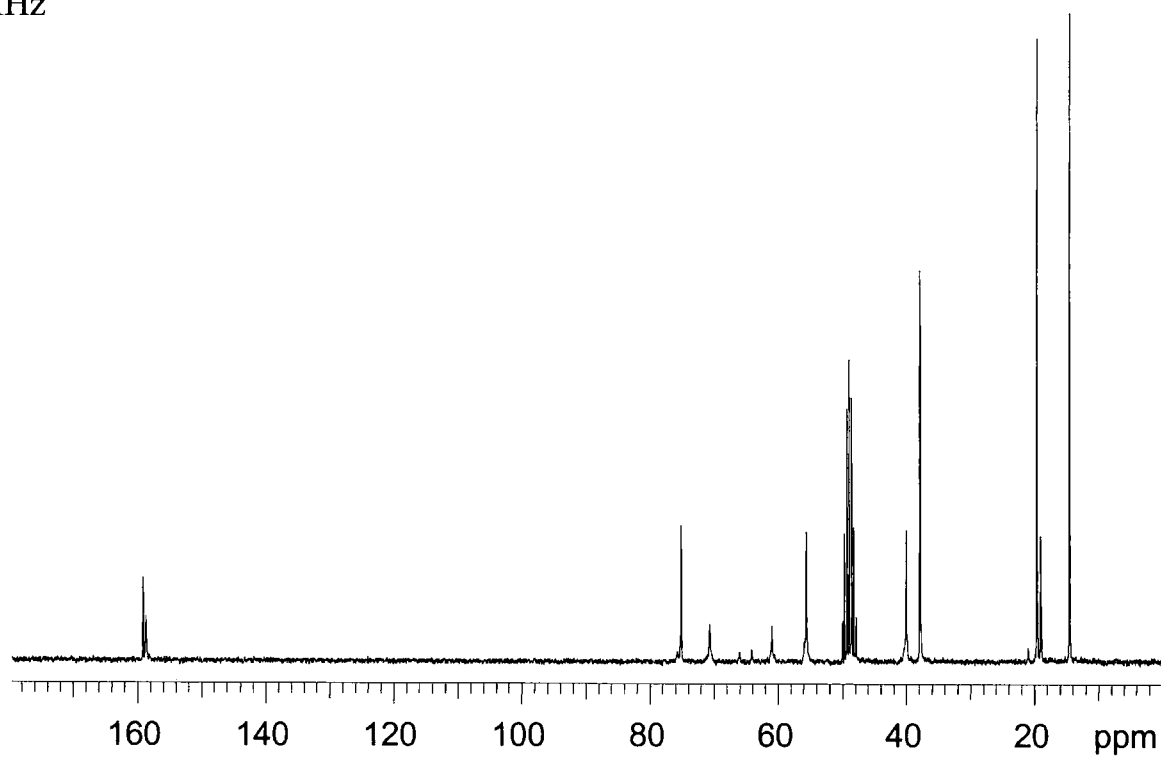
$^{13}\text{C}$  NMR spectrum of **BG3OH**

$\text{CD}_3\text{OD}$   
63MHz



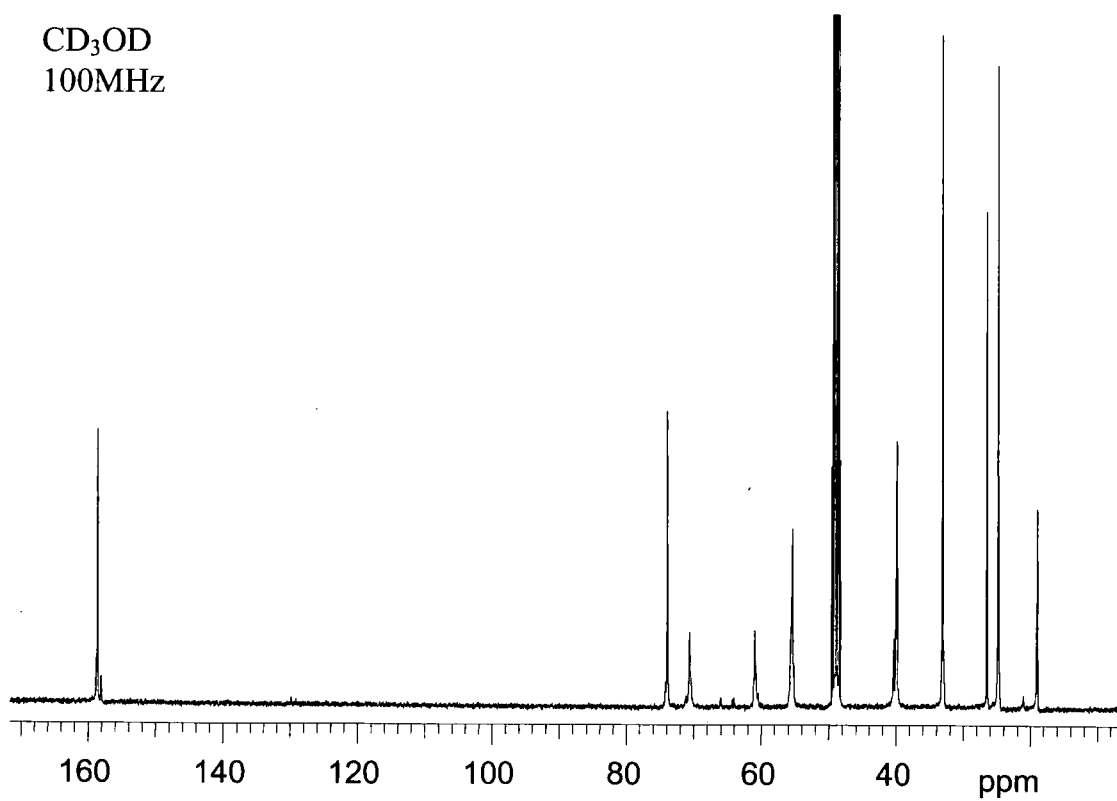
$^{13}\text{C}$  NMR spectrum of **HG3OH**

$\text{CD}_3\text{OD}$   
63MHz

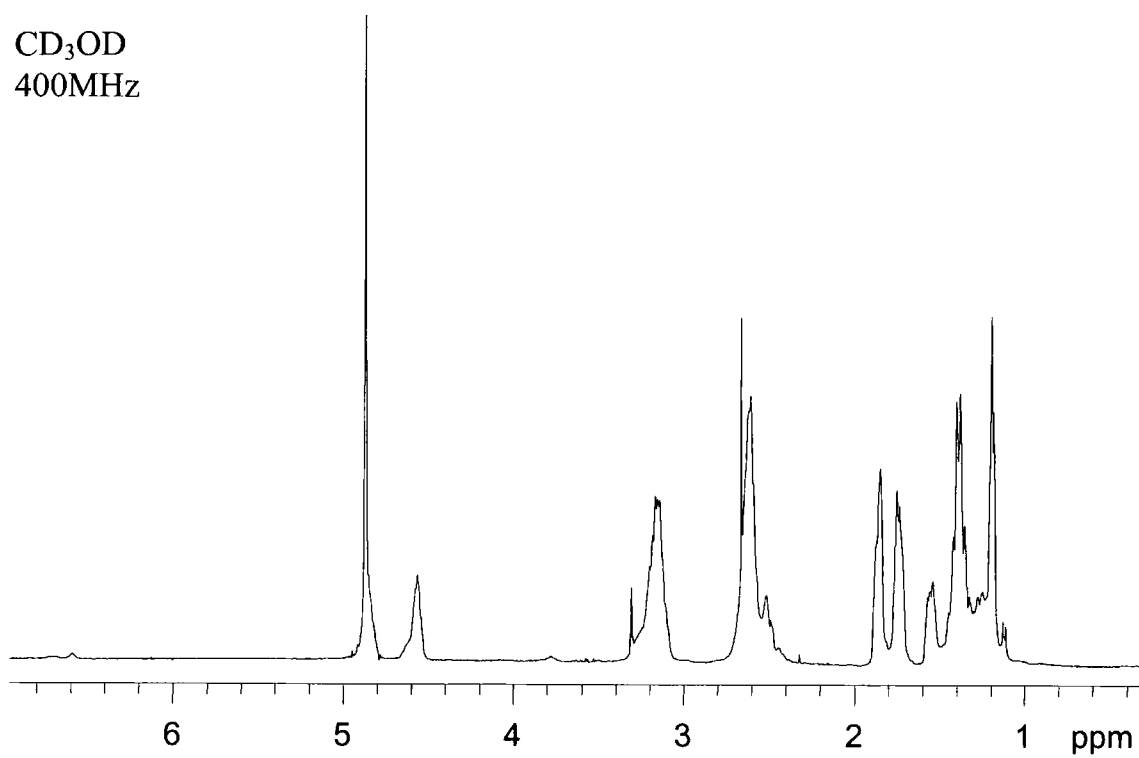


$^{13}\text{C}$  NMR spectrum of **CG4OH**

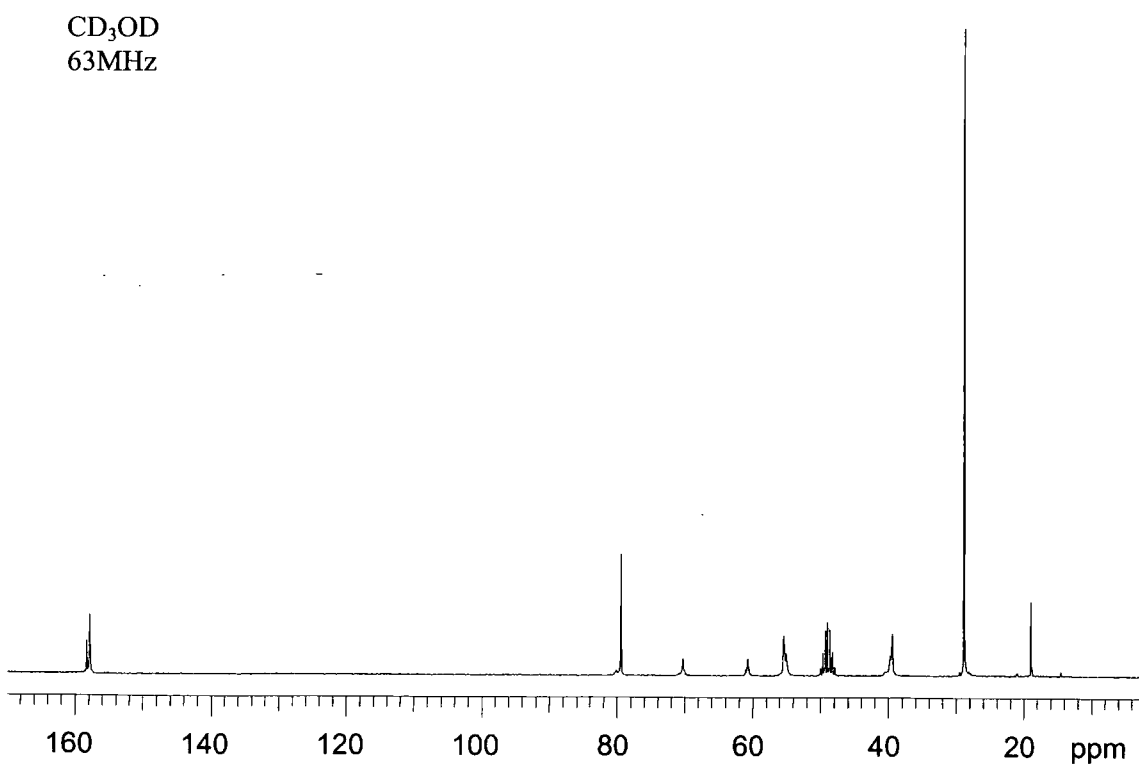
$\text{CD}_3\text{OD}$   
100MHz



$^1\text{H}$  NMR spectrum of **CG4OH**



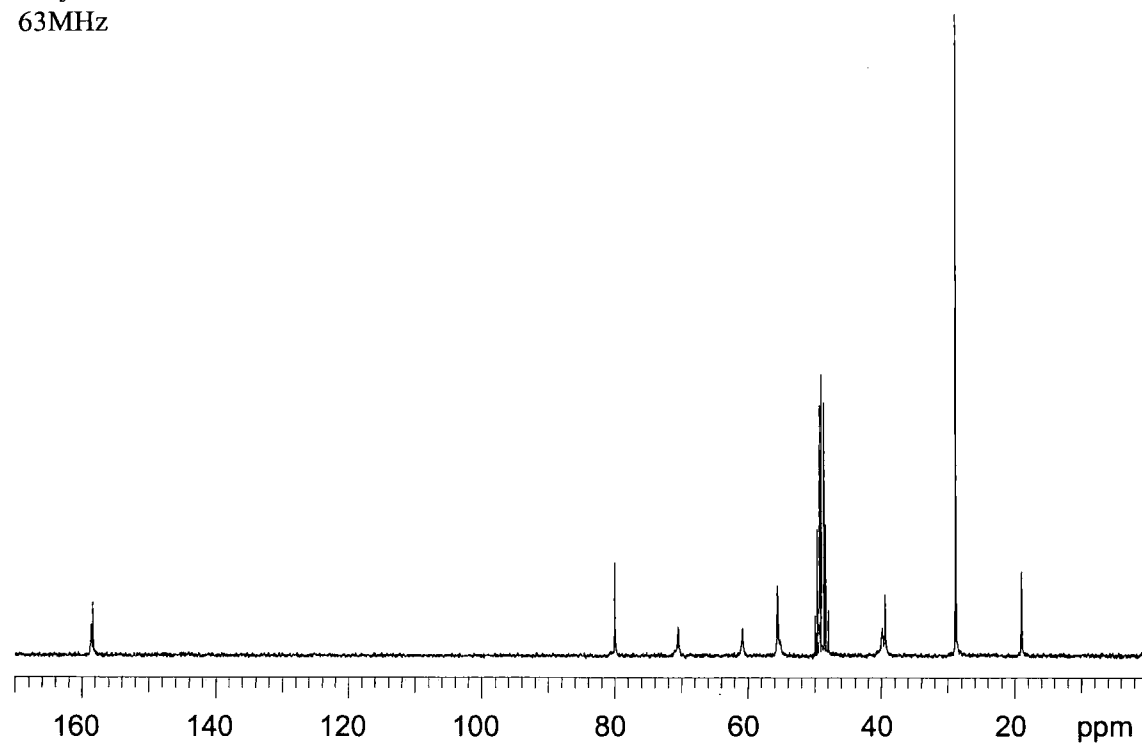
$^{13}\text{C}$  NMR spectrum of **BG1D**





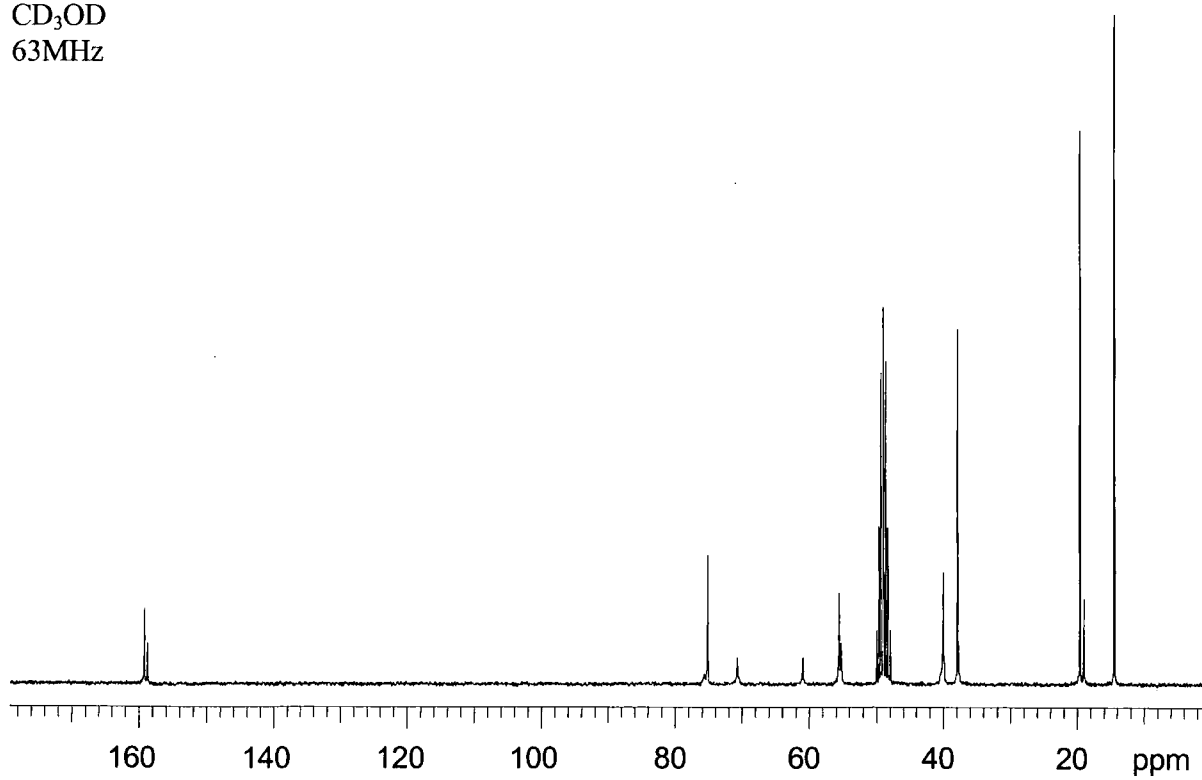
<sup>13</sup>C NMR spectrum of **BG2D**

CD<sub>3</sub>OD  
63MHz



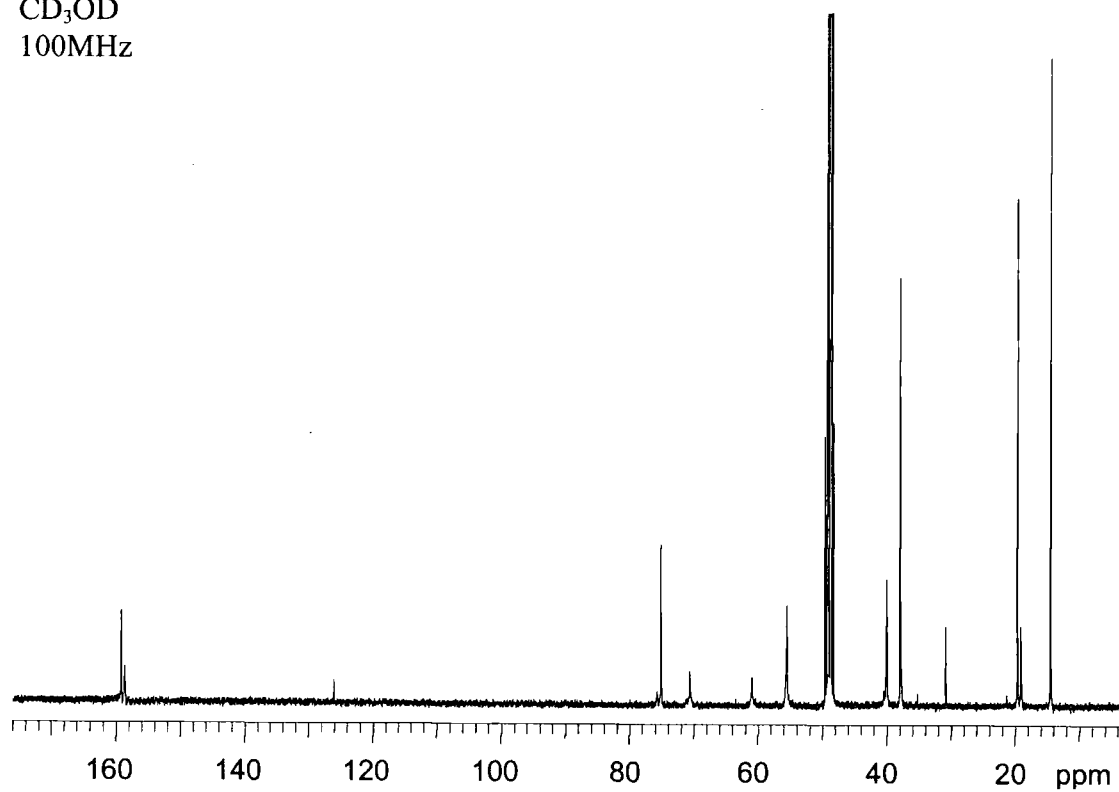
<sup>13</sup>C NMR spectrum of **HG1D**

CD<sub>3</sub>OD  
63MHz



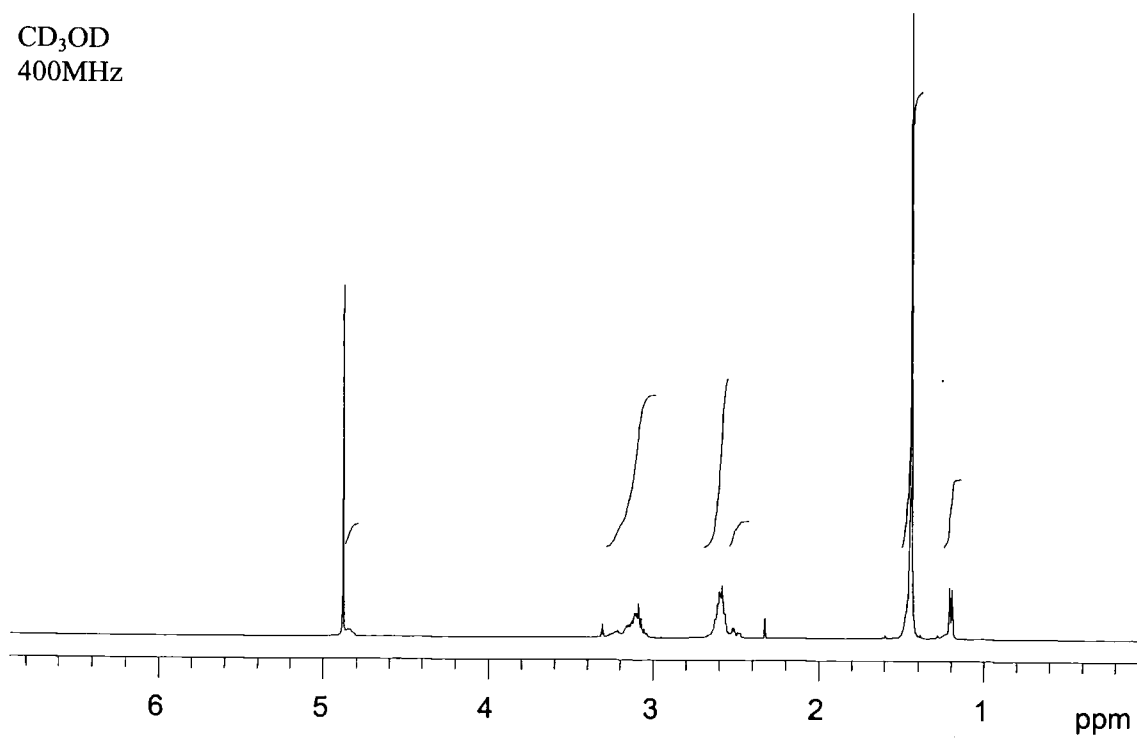
$^{13}\text{C}$  NMR spectrum of **HG3D**

$\text{CD}_3\text{OD}$   
100MHz



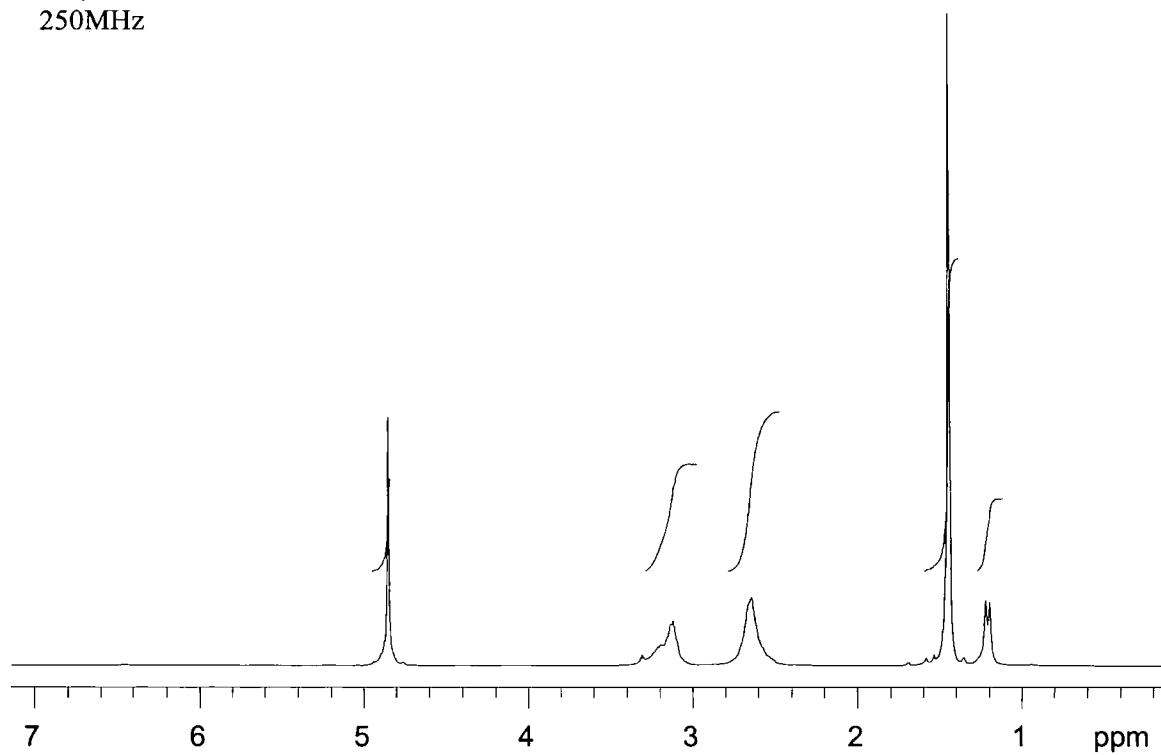
$^1\text{H}$  NMR Spectrum of **BG1D**

$\text{CD}_3\text{OD}$   
400MHz



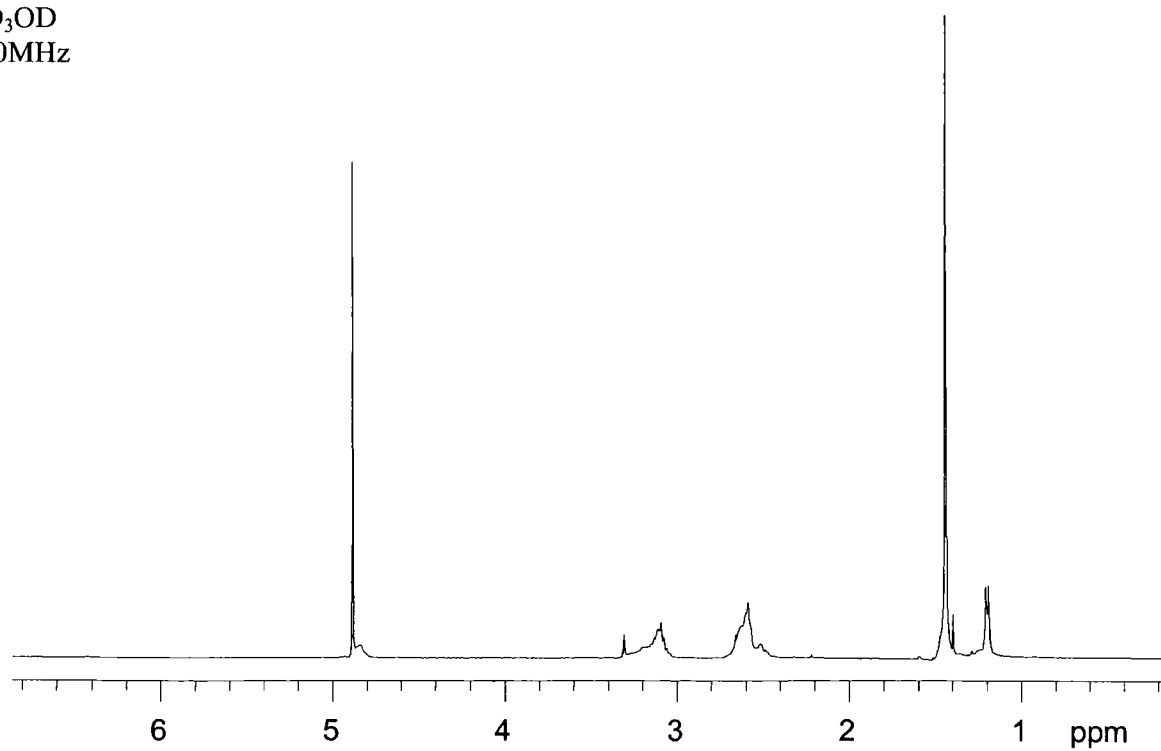
<sup>1</sup>H NMR Spectrum of **BG2D**

CD<sub>3</sub>OD  
250MHz



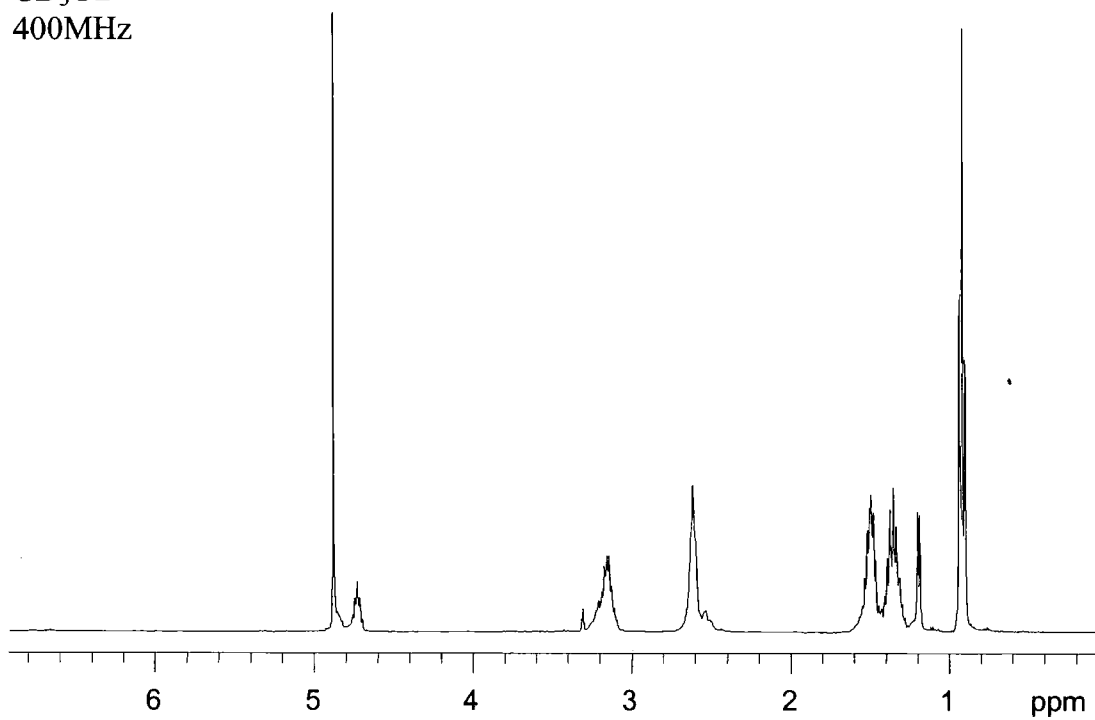
<sup>1</sup>H NMR Spectrum of **BG3D**

CD<sub>3</sub>OD  
400MHz



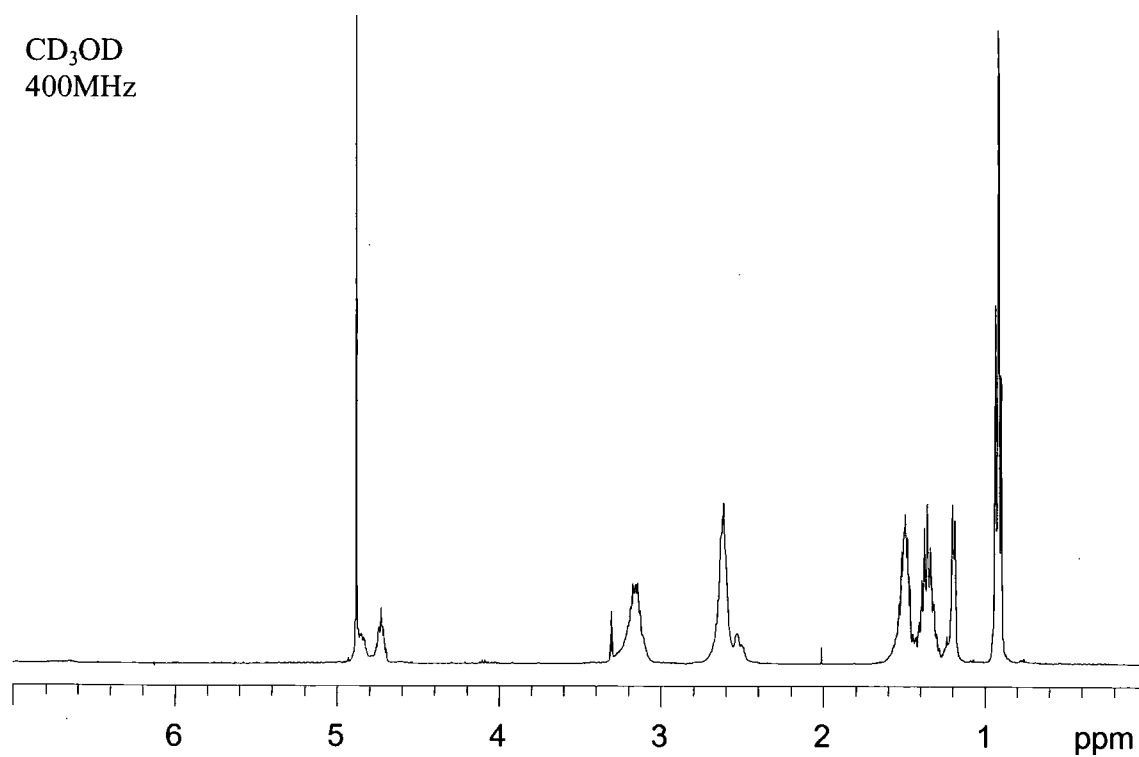
<sup>1</sup>H NMR Spectrum of **HG1D**

CD<sub>3</sub>OD  
400MHz



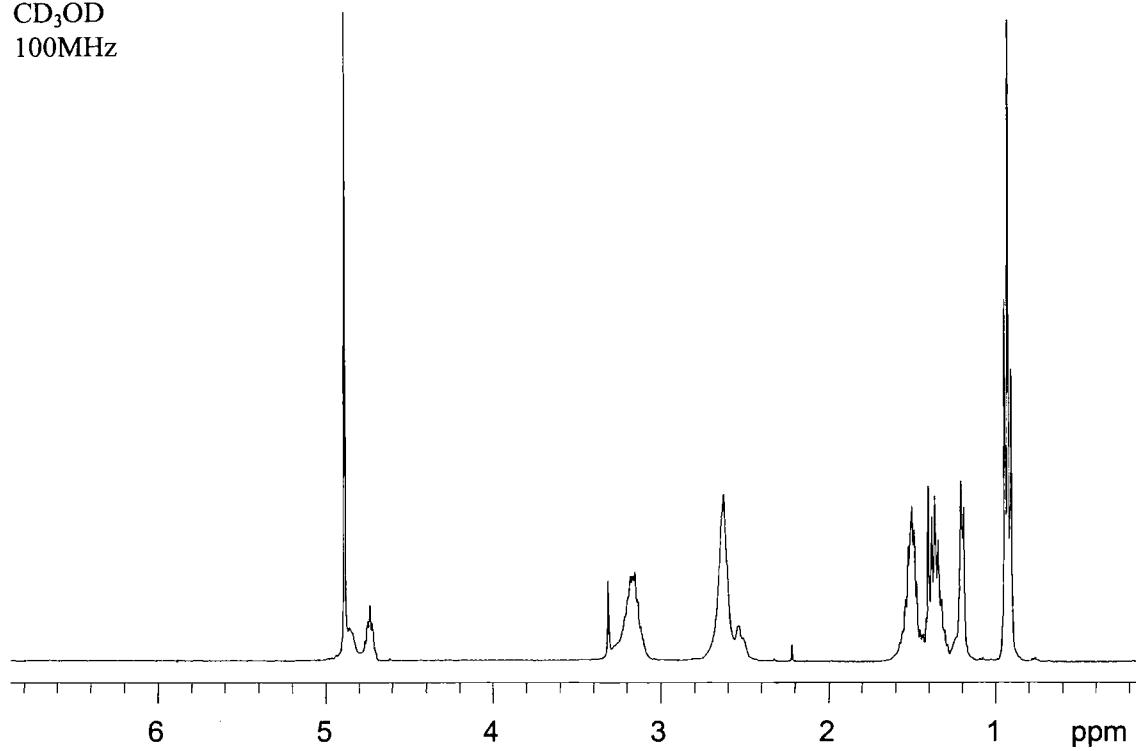
<sup>1</sup>H NMR Spectrum of **HG2D**

CD<sub>3</sub>OD  
400MHz

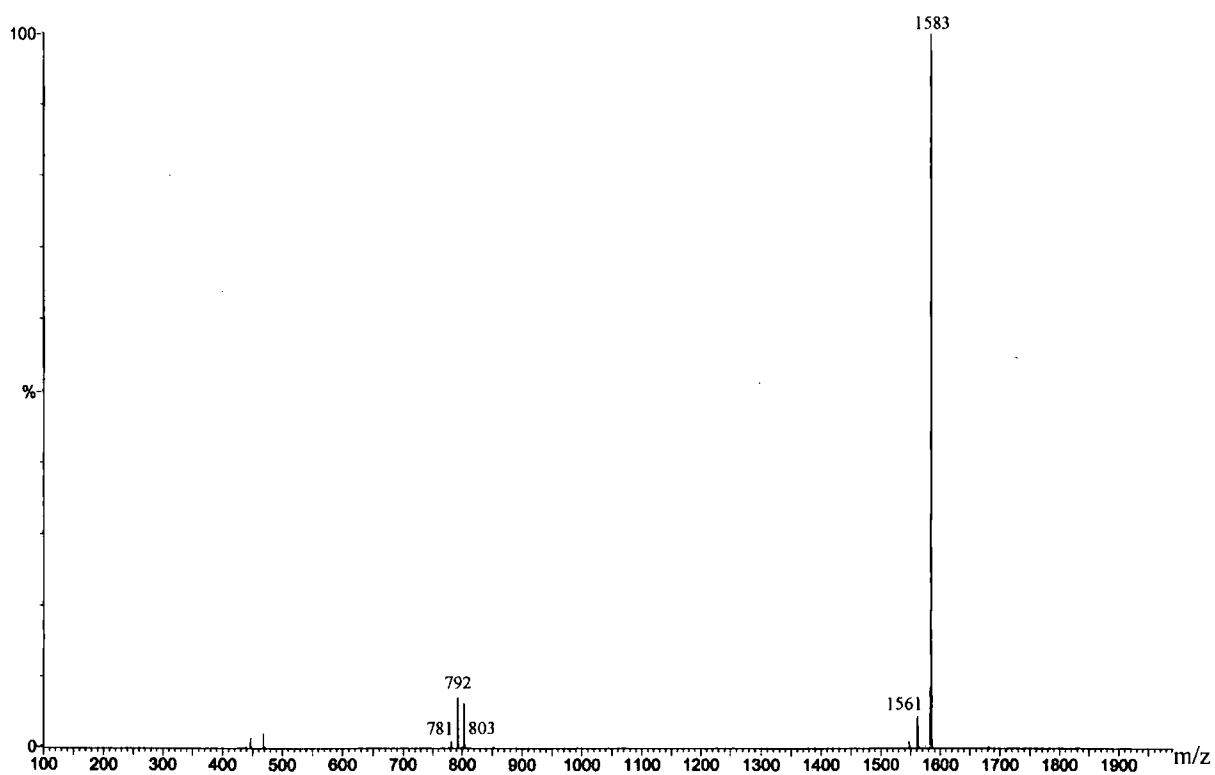


<sup>1</sup>H NMR Spectrum of **HG3D**

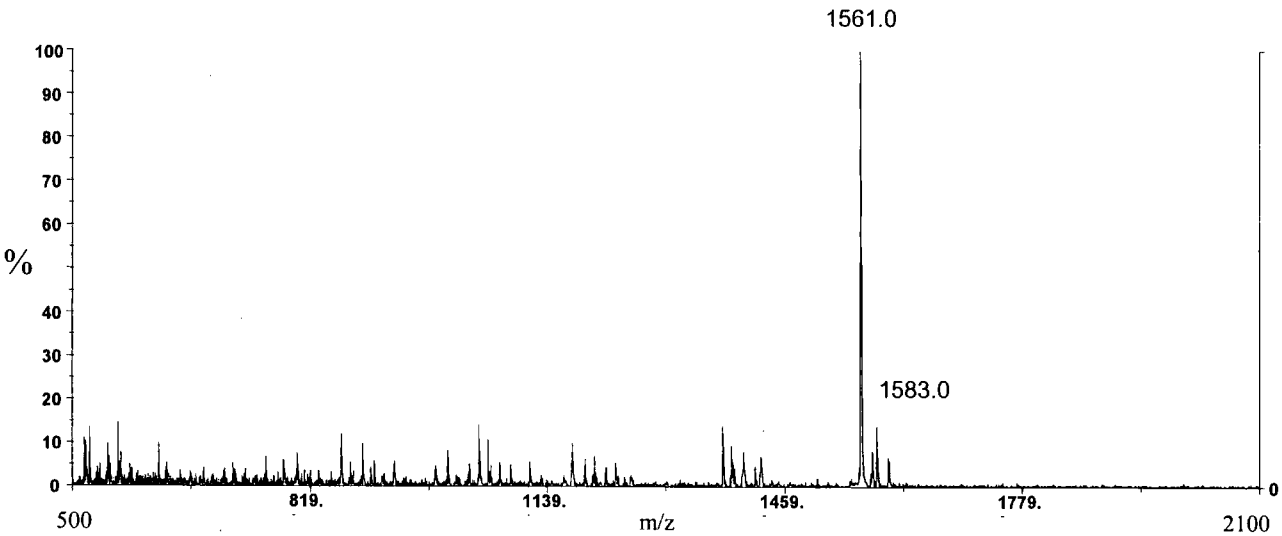
CD<sub>3</sub>OD  
100MHz



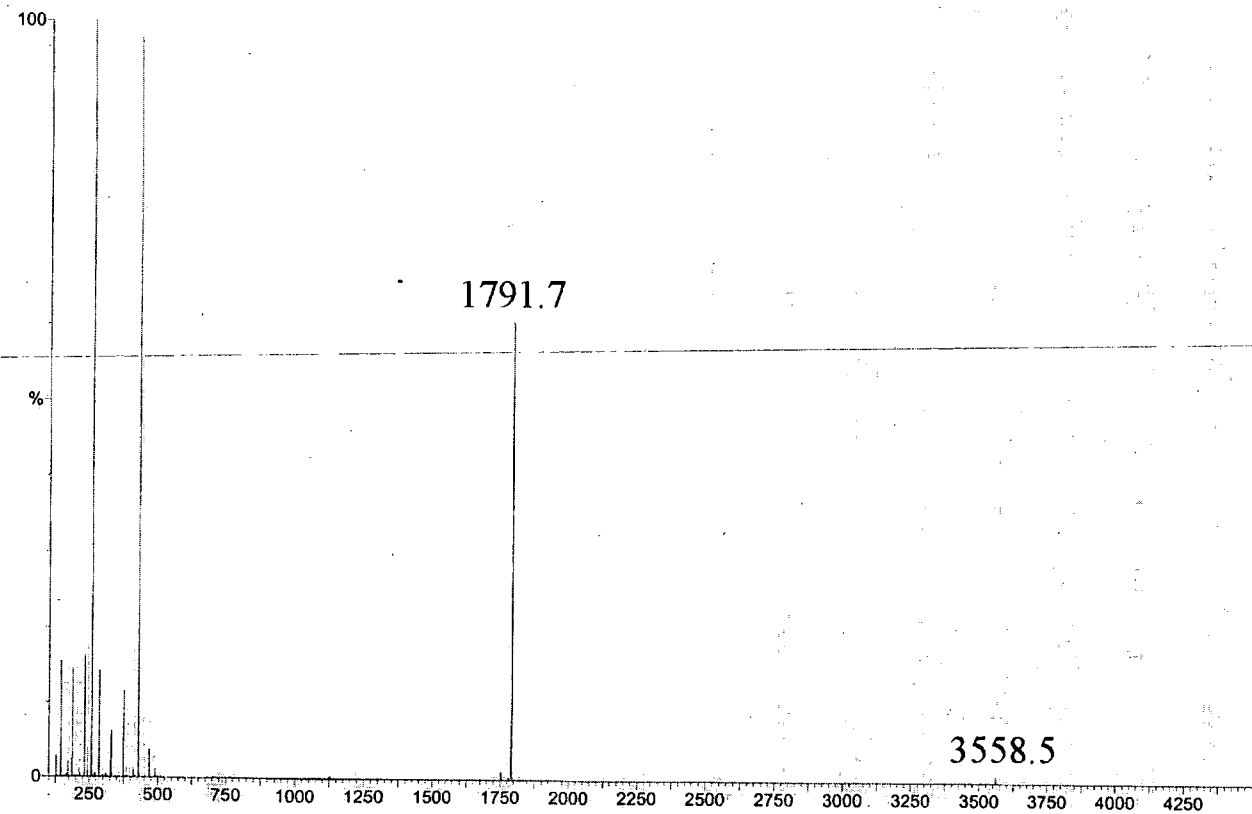
ES mass spectrum of **HG1D**



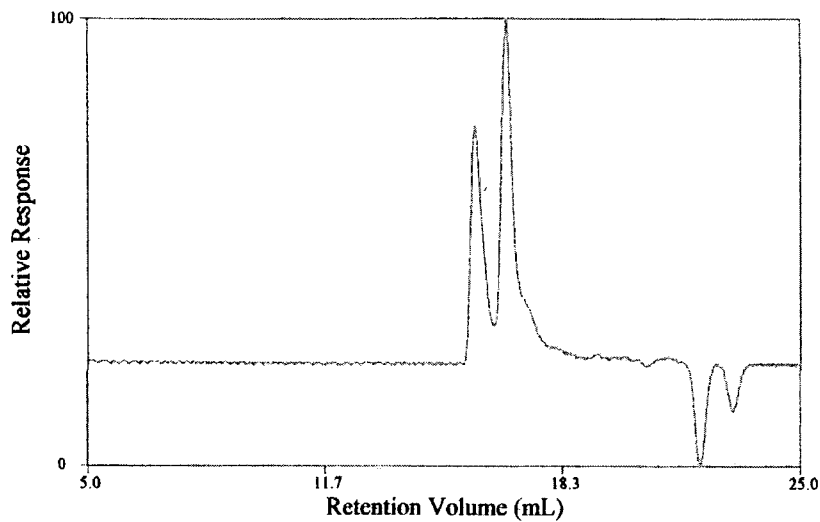
MALDI-TOF (Voyager) mass spectrum of **HG1D**



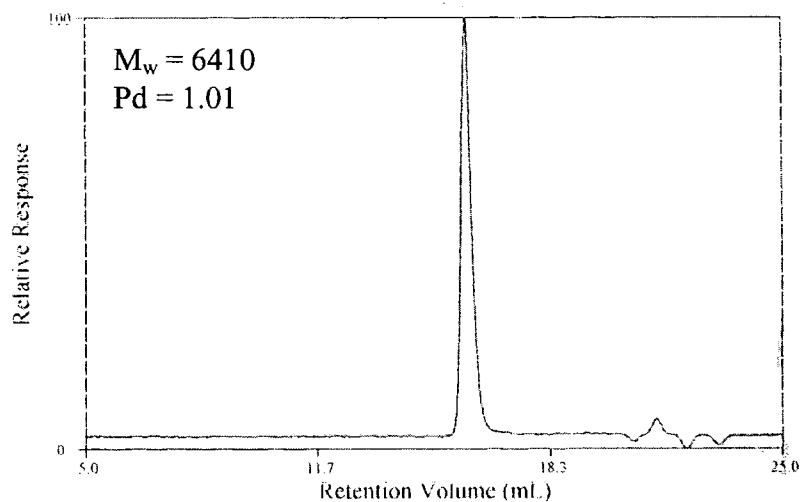
ES mass spectrum of **HG2D**



GPC trace of **HG3D** before purification by preparative GPC (Biobeads)



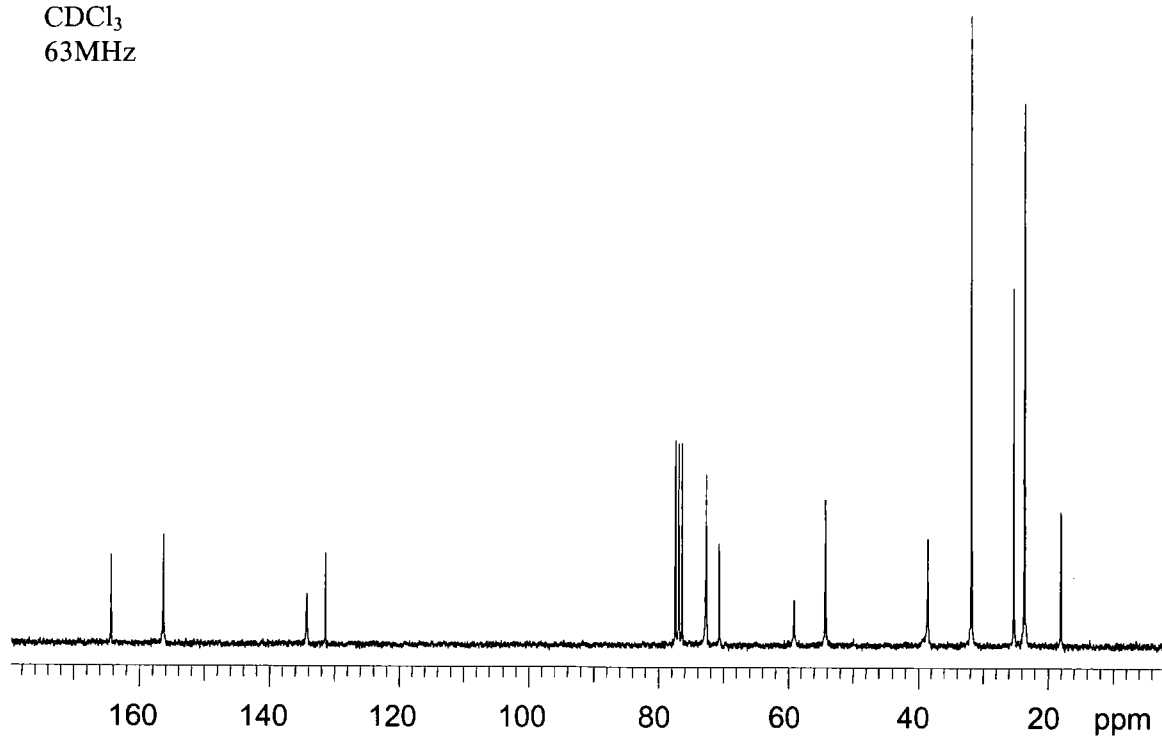
GPC trace of **HG3D**





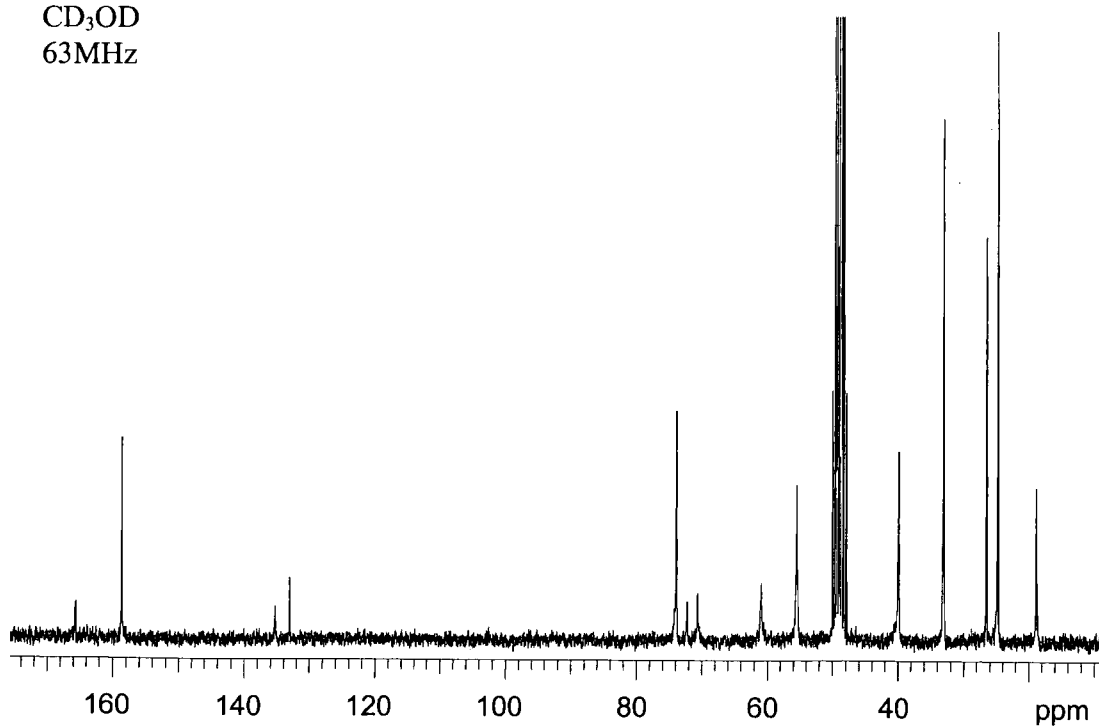
$^{13}\text{C}$  NMR spectrum of **CG1DAC**

$\text{CDCl}_3$   
63MHz



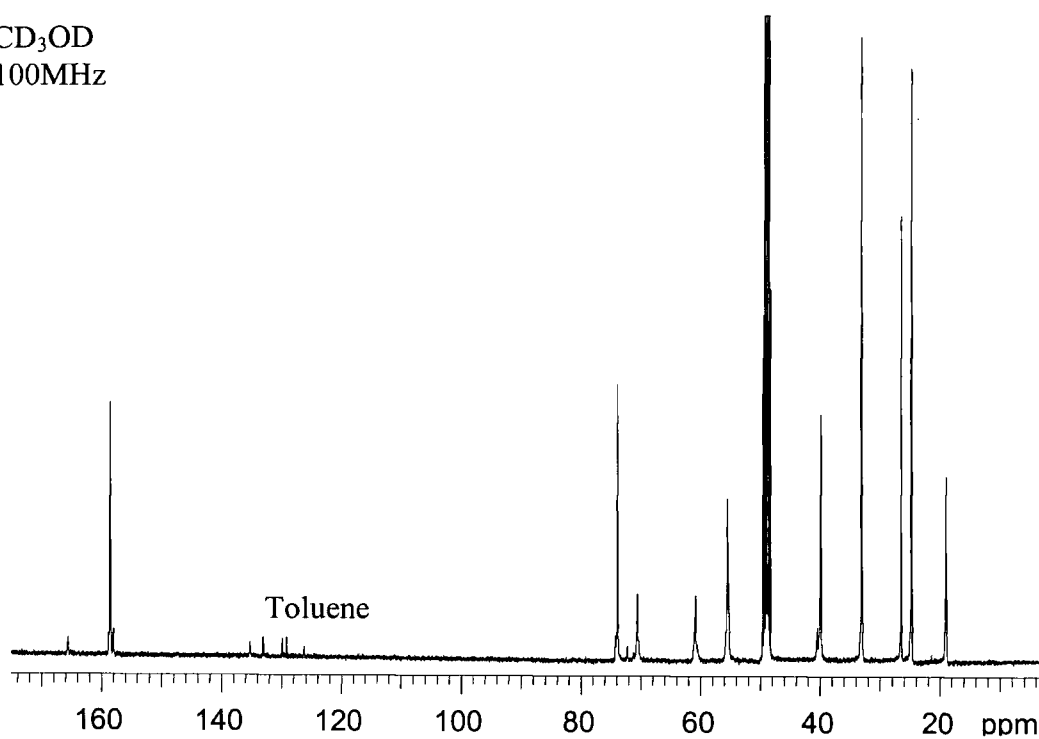
$^{13}\text{C}$  NMR spectrum of **CG2DAC**

$\text{CD}_3\text{OD}$   
63MHz



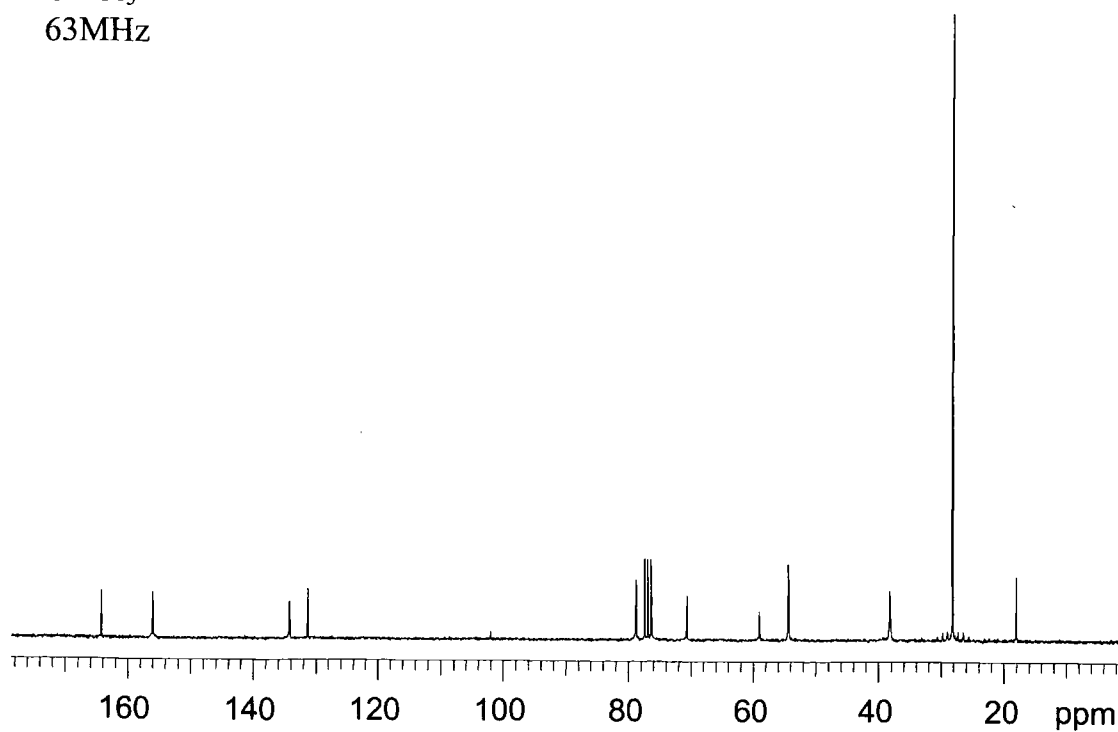
$^{13}\text{C}$  NMR spectrum of **CG3DAC**

$\text{CD}_3\text{OD}$   
100MHz

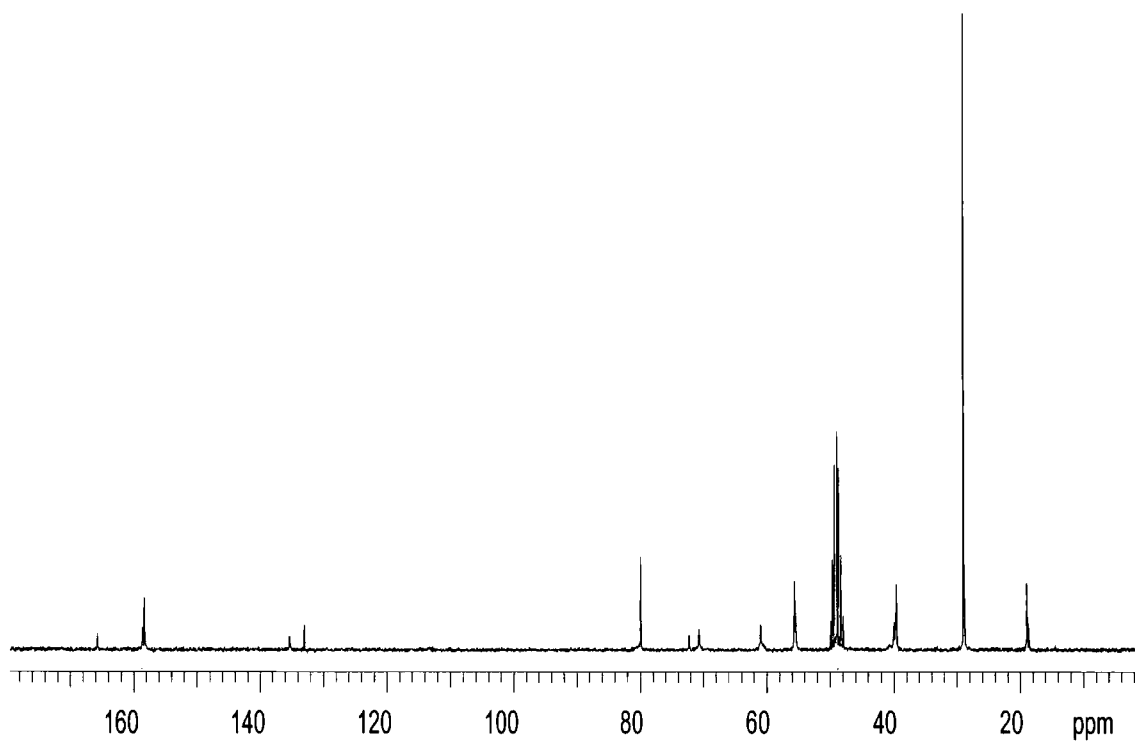


$^{13}\text{C}$  NMR spectrum of **BG1DAC**

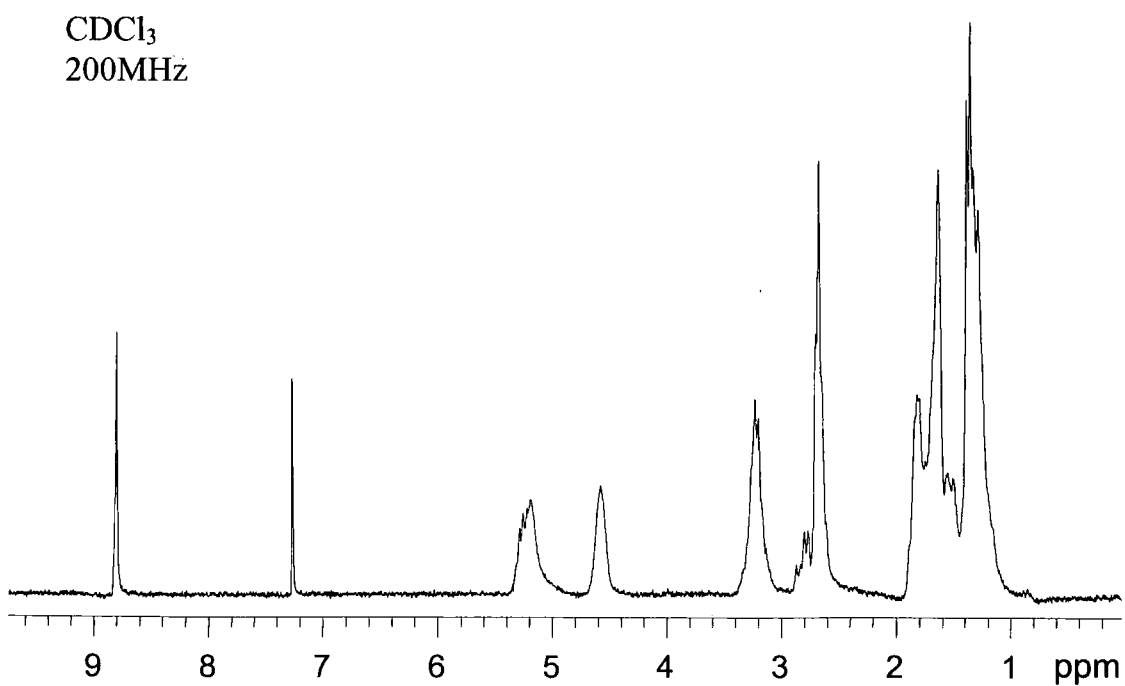
$\text{CDCl}_3$   
63MHz



$^{13}\text{C}$  NMR spectrum of **BG2DAC**



$^1\text{H}$  NMR spectrum of **CG1DAC**



MALDI-TOF (Voyager) mass spectrum of **BG2OH (UC)**

